Pressure Perturbation Calorimetry of Protein Unfolding

UNIVERSITY
of
GLASGOW

Joanna Ewa Jakus-Pol

Thesis presented for the degree of Doctor of Philosophy

Department of Chemistry
University of Glasgow

January, 2005

To my Father

ABSTRACT

Thermodynamic and structural characterisation of various interactions stabilising protein native folds is a key part of multidisciplinary research efforts to solve the problems of protein folding and binding. Amongst such interactions the hydrophobic effect has been considered for several years to be the major driving force behind protein folding and main non-covalent interaction in protein stability. The hydrophobic effect arises from solvation effects around non-polar residues that are buried inside protein interior upon protein folding. The change in heat capacity on protein unfolding (ΔC_p) is believed to be one of the "signatures" of the hydrophobic effect.

The thermal expansion coefficient (α) and protein volume change upon unfolding (ΔV) are the volumetric parameters sensitive to solvation changes and hence could be utilised in the studies of hydrophobic interactions. Both these parameters have recently become easily available with the development of the new calorimetric method called Pressure Perturbation Calorimetry (PPC).

In this research, the aqueous methanol solutions have been used as a solvent system with a modified hydrogen bonded structure in relation to water. Protein thermal unfolding has been studied in these solutions, where the solvation effects associated with exposing protein buried residues upon unfolding are diminished (the hydrophobic effect is weakened). Three small, one domain model proteins used in this study were: ubiquitin, lysozyme and ribonuclease A. ΔC_p of unfolding of those proteins in aqueous methanol solutions has been obtained by Differential Scanning Calorimetry (DSC) and ΔV of unfolding was obtained by PPC.

ΔC_p is a temperature-related thermodynamic parameter, while ΔV is a pressure-related parameter, the combined determination of both parameters allows a more comprehensive description of protein unfolding transitions to be built than merely the more routinely studied temperature-related characteristics. ΔC_p and ΔV, taken together, provide complementary data on the solvation changes during the thermal

unfolding process, therefore the effect of increasing methanol concentration on the changes in both ΔC_p and ΔV of unfolding has been investigated here.

Additionally, two other applications of PPC were investigated in this thesis. Firstly, PPC was shown to allow straightforward collection of data used to predict the structure making and structure breaking of solutes in water. Amino acids as small molecular model compound have been investigated here, and the determination of structure making and structure breaking of side-chains in amino acid model has been critically reviewed. Importantly, a serious apparent discrepancy in published data was been identified here.

Secondly, the study of another small model protein, cytochrome c conformational transitions (native to unfolded, molten globule to unfolded) has been tested here by the PPC method and the results have been shown to be in a good agreement with ones obtained from high-pressure spectroscopic studies.

In summary , PPC has been shown to be a useful technique for studying structure breaking and structure making properties of solutes, both small and macro-molecular, and for obtaining volumetric properties of protein transitions that complete the picture of already abundantly available temperature-related calorimetric data such as enthalpy, entropy and heat capacity.

ACKNOWLEDGEMENTS

I would first of all like to thank my supervisor Professor Alan Cooper for all his help and guidance throughout my PhD.

Special thanks to Margaret Nutley for all her invaluable advice over the last three years and to Diane Cameron for many useful discussions about the PPC experiments and technique. I must also thank Sharon Kelly and Tom Jess for use of the circular dichroism facility.

I would also like to thank my many colleagues who have passed through the B4-20 and C3-04 labs, in particular Nicola Meenan, Lindsay McDermott, Rachel Fleming, Cameron MacKenzie and Kevin Guthrie for . Finally, extra special thanks go to my friends, Conor, Gosia, Lukasz, Malanga, Krysia, and Paul for the support and encouragement unfailingly provide; to Slawek for coming to Scotland with me, and to my family for their unqualified love and support.

This work was funded by the University of Glasgow.

This thesis is my own work, except where stated above and in the main body of the text.

CONTENTS

ABSTRACT ..... *iii*

ACKNOWLEDGEMENTS ..... *v*

CONTENTS ..... *vi*

LIST OF FIGURES ..... *x*

LIST OF TABLES ..... *xv*

ABBREVIATIONS ..... *xvi*

***Chapter 1* Introduction** **1**

1.1 Thesis overview *3*

1.2 Thermodynamics of protein stability *5*

1.2.1 Non-covalent interactions determine protein stability 5

1.2.2 How the non-covalent interactions drive the protein folding 14

1.3 Thermodynamics of protein unfolding *17*

1.3.1 Energetic description of protein folding/unfolding transition. 17

1.3.2 Heat Capacity Changes 18

1.4 Volumetric properties – pressure-related thermodynamic parameters *21*

1.4.1 Partial molar volume (V^o) 22

1.4.2 Expansibility (E^o) and thermal expansion coefficient (α) 24

1.4.3 Hydration term in volumetric parameters interpretation 25

1.4.4 Techniques Used to Investigate Solvation 27

1.5 Protein hydration and solvation *30*

1.5.1 Water as a solvent 30

1.5.2 The solvation of molecules in water 31

1.5.3 Studying protein hydration 32

1.5.4 The effect of solutes on protein stability 36

1.6 Thesis objectives *40*

***Chapter 2* Materials and Methods** **41**

2.1 Reagents used *43*

2.1.1 Buffer Reagents 43

2.1.2 Amino acids 43

2.1.3 Proteins 43

2.1.4 Aqueous methanolic solvents 44

2.2 Protein concentration determination *45*

2.3 Circular Dichroism *46*

2.3.1 Theory 46

2.3.2 Experimental details 46

2.4 Differential scanning calorimetry (DSC) *47*

2.4.1 Introduction 47

2.4.2 Experimental details 47

2.4.3 Theory and data analysis 47

2.4.4 ΔC_p analysis from pH variation method 49

***Chapter 3* PPC – Theory and Basics of the Method 51**

3.1 Introduction *53*

3.2 Description of experimental setup - hardware *58*

3.2.1 Instrumentation 58

3.2.2 Description of a single PPC scan at constant temperature 58

3.2.3 Temperature dependence of α 61

3.3 PPC theory *64*

3.3.1 Derivation of an equation for calculating α from ΔQ and ΔP for pure liquids - for one component system in 1 cell 64

3.3.2 Derivation of an equation for calculating α from ΔQ and ΔP for dilute solutions - for 2 component system in 2 cells 66

Correcting for volume differences between the cells 70

Assumptions 72

3.4 Description of experimental setup – Software *74*

3.4.1 Equations and Unit Conversion Factors 74

3.4.2 Data Analysis in Practise 76

Step 1 – Obtaining heat values. 78

Step 2 – Obtaining thermal expansion coefficient (α) values. 80

Step 3 – Calculating the volume change. 82

3.5 Error values associated with PPC measurement *87*

3.5.1 Repeatability 87

3.5.2 Theoretical error propagation. 92

3.5.3 Error evaluation 94

***Chapter 4* Structure making and structure breaking by PPC: amino acids as model systems 98**

4.1 Introduction *100*

4.2 Structure making and structure breaking properties of solutes *101*

Pure water - two-state mixture model 101
Solute hydration in two-state mixture model of water: structure making and structure breaking properties 102
Kosmotropes and chaotropes 103
Is $(\partial C_p/\partial P)_T$ diagnostic of structure making and structure breaking properties? 103
Heat and cold thermal unfolding of proteins in two-state mixture model of water 105
How to measure solvation layer properties? 106

4.3 Amino acids structure making and structure breaking properties *107*
Differences in α between hydrophobic and hydrophilic amino acids 107
Validation of α data obtained from PPC for amino acids 114
$(\partial C_p/\partial P)_T$ obtained from α for whole amino acids and their side-chains 116
Side-chains properties obtained from tripeptides model 120
Side chains properties obtained from N-acetyl amino acid amides model 121

4.4 Amino acids in modified aqueous solvents *128*

4.5 Discussion *133*

***Chapter 5* ΔC_p of protein unfolding in methanol water mixtures 135**

5.1 Introduction *137*

5.2 Previous research on protein structure and unfolding in methanolic solutions *138*
5.2.1 Ubiquitin thermal unfolding in methanolic solutions 138
5.2.2 Ubiquitin - structural information in methanolic solutions 140
5.2.3 Lysozyme - structural information in methanolic solutions 142

5.3 Lysozyme – ΔC_p of unfolding in methanolic solutions *144*

5.4 Ribonuclease A - ΔC_p of unfolding in methanolic solutions *146*

5.5 Structural studies in methanolic solutions by circular dichroism *148*
5.5.1 Circular Dichroism spectra obtained at pH = 2 148
5.5.2 Circular Dichroism spectra obtained at pH = 7 149

5.6 Conclusions *151*

***Chapter 6* PPC of protein unfolding in methanol water mixtures 153**

6.1 Introduction *155*

6.2 Protein unfolding transition observed in PPC corresponds to the one observed in DSC *157*

6.3 Structure making and structure breaking properties of protein surface *159*

6.4 Volume changes upon unfolding (ΔV_{unf}) varies with increasing methanol concentration *164*

6.5 Conclusions *167*

Chapter 7 **PPC of cytochrome c conformational transitions** 16

7.1 Introduction 17

7.2 Comparison of thermodynamic data obtained from high pressure spectroscopy and calorimetry 17

7.3 Discussion 17

7.4 Conclusions 17

Chapter 8 **Conclusions and future work** 17

8.1 General conclusions 17

8.2 Suggested future work 18

APPENDIX A STRUCTURAL STUDIES IN METHANOLIC SOLUTIONS BY CIRCULAR DICHROISM 18

APPENDIX B PPC SCANS OF PROTEIN UNFOLDING IN WATER, METHANOLIC SOLUTIONS AND D_2O. 18

APPENDIX C PPC AND DSC SCANS OF CYTOCHROME C UNFOLDING 19

APPENDIX D CONVERSION TABLE FOR METHANOL/WATER MIXTURES CONCENTRATIONS AT 25°C 20

REFERENCES 20

LIST OF FIGURES

Figure 1.1 The partial volume of a protein in solution consists of the intrinsic volume (here represented by the van der Waals volume of the constituent atoms (vdW) and the volume of voids), the thermal volume immediately at the protein surface and the hydration volume of the solvent molecules interacting with the solute (protein here)..... 27

Figure 1.2 The coefficient of thermal expansion (α) of the partial volume of staphylococcal nuclease. Data taken from Seemann et al. (2001). 35

Figure 2.1 Typical DSC thermogram for the thermal unfolding of ribonuclease A at pH 3.0 and at a scan rate of 60°C/hr. The heat capacity (C_p) is given in kcal $mol^{-1}K^{-1}$ (1 cal = 4.184 J). 48

Figure 2.2 Example plot of unfolding enthalpy against unfolding transition temperature. Data presented in the graph is for lysozyme unfolding in 40% methanol v/v at the pH range from 2.1 to 5.0. 50

Figure 3.1 Scanning Transitiometry – a technique alternative to PPC. 56

Figure 3.2 PMC-measurement on dipalmitoylphosphatidylcholine (DPPC) with a heating rate of 0.02 K/min in a pressure range of 0.3 to 5.3 atm (Hinz 2003)..... 57

Figure 3.3 Schematic of a standard VP-DSC instrument equipped with a PPC accessory. 59

Figure 3.4 One PPC cycle comprises of decompression and compression..... 61

Figure 3.5 Temperature dependence of thermal expansion coefficient (α). The plots show the temperature unfolding of the protein ribonuclease A in 20% methanol/water at pH=2.0..... 62

Figure 3.6 Schematic representation of PPC. The black circles in the sample cell indicate the volumes occupied by the solute molecules, whereas the dotted circles in the reference cell indicate the same volumes occupied by the buffer instead. 67

Figure 3.7 Data represented in a raw file recorded by the instrument for three PPC cycles. 76

Figure 3.8 The raw data obtained upon pressure perturbation of 50 mM glycine buffer at pH = 2.0 at increasing temperature (from 5 to 80°C) at 5°C

increments. Measurements were made with buffer in the sample cell and pure water in the reference cell. Pressure perturbations of ± 5 atm were applied to the cells, and data were collected at 1-second intervals. There are 16 PPC cycles 77

Figure 3.9 An example of wrongly assigned baseline by the software algorithm: The middle peak is for compression, and the baseline correction changes the heat value from -4.64 to -7.11 μcal. The corrected value agrees with the value of decompression heat (on the left) of 7.93 μcal at the same temperature. In this example the heat calculated from integration to automatically assigned baseline would result in 35% error. 79

Figure 3.10 Second and third order polynomial fit to the buffer vs. water heat values temperature dependence 81

Figure 3.11 It is hard to define where the unfolding transition begins from the PPC measurement alone. (a) PPC of ribonuclease A unfolding at pH = 2.0 (b) PPC of lysozyme unfolding at pH=2 83

Figure 3.12 Baseline assignment and integration results for the thermal unfolding of the protein ribonuclease A in 20% methanol/water at pH=2.0. 84

Figure 3.13 Thermal unfolding of the protein ribonuclease A in 20% methanol/water at pH=2.0. Four different baselines assigned for integration resulted in four different values of fractional volume change: -0.344%, -0.287%, -0.352% and -0.319%. 85

Figure 3.14 Graphical representation of datasets for heats of water-water PPC experiment (means are indicated by solid dots) used for ANOVA test. 88

Figure 3.15 Graphical representation of datasets for heats of buffer-buffer PPC experiment (means are indicated by lines) used for ANOVA test. 89

Figure 3.16 Changes in PPC signal in dataset c. 90

Figure 3.17Changes in ΔQ in dataset c. 90

Figure 3.18 Graphical representation of datasets for heats of buffer -buffer PPC experiment (means are indicated by solid dots) used for ANOVA test. 91

Figure 3.19 The values of error in α calculated from theoretical error propagation for ribonuclease A unfolding in 30% v/v methanol solution. 95

Figure 4.1 Huge differences between hydrophilic and hydrophobic amino acid side chains observed by PPC (Lin et al. 2002). Here thermal expansion coefficient α was calculated "relative to glycine", i.e. the heats given out by glycine solution at the same concentration were subtracted from the amino acid heat, to yield the side chain only contribution to the thermal expansion coefficient. 108
Figure 4.2 Thermal expansion coefficients for the amino acid side-chains obtained from PPC. Calculated from amino acids in water "relative to glycine" as described in text and as determined in Glasgow. 111
Figure 4.3 Comparison of thermal expansion coefficient for amino acids in water obtained from PPC as a function of temperature. 113
Figure 4.4 Thermal expansion coefficient for amino acids – values obtained from PPC measurement compared to values obtained as the derivative of partial molar volume from density measurements of Kikuchi et al. (1995). 115
Figure 4.5 $(\partial C_p/\partial P)_T$ for amino acids (calculated from α obtained from the heats of whole amino acids molecules in water measured by PPC)..... 117
Figure 4.6 $(\partial C_p/\partial P)_T$ for amino acid side-chains (calculated from α obtained from the heats of amino acids in water "relative to glycine" measured by PPC)..... 119
Figure 4.7 $\alpha(T)$ derived from density measurements: (a) from DSD for tripeptides Hackel et al. (1999), (b) from isothermal densitometry for N-acetyl amino acid amides Hakin and Hedwig (2000) 123
Figure 4.8 $(\partial C_p/\partial P)_T$ for amino acid side-chains derived from density measurements: (a) from DSD for tripeptides Hackel et al. (1999), (b) from isothermal densitometry for N-acetyl amino acid amides Hakin and Hedwig (2000)..... 125
Figure 4.9 $(\partial C_p/\partial P)_T$ for methanol in water– calculated from α obtained by PPC from the heats of methanol solutions in water 129
Figure 4.10 The thermal expansion coefficient obtained by PPC for asparagine in water, D_2O, 20% and 40% (v/v) methanol solutions. 130
Figure 4.11 The thermal expansion coefficient obtained by PPC for valine in water, D_2O, 20% and 40% (v/v) methanol solutions. 131

Figure 4.12 The thermal expansion coefficient obtained by PPC for glycine in water, D_2O, 20% and 40% (v/v) methanol solutions. 131
Figure 5.1 The effect of increasing methanol concentration on the heat capacity change of ubiquitin unfolding. (Woolfson et al. 1993) 138
Figure 5.2 (top) 1H NMR spectra (500 MHz) of the native to A state transition in 40% methanol at pH 2.0; (a) N state at 288 K; (b) N and A state equally populated at 300 K; and (c) A state fully populated at 318 K. (bottom) Temperature-stability profiles (ΔG vs. T) for the N to A transition at various concentrations of methanol (20, 30, 40, and 50% v/v). Linear lines of best fit indicate ΔC_p that is close to zero for 30, 40 and 50% methanol in water (from Jourdan and Searle 2001). 139
Figure 5.3 (left) Structure of the N state of ubiquitin from the X-ray coordinates (1ubq) (Vijay-Kumar et al. 1987)); (right) model of the A state of ubiquitin in 60% methanol at low pH (Brutscher et al. 1997). (Figure adapted from Jourdan and Searle 2001) 140
Figure 5.4 CD spectra of ubiquitin collected at 290K and pH 2.0 at various concentrations of methanol (0, 10, 20, 30, 40, 50, 60, and 100% in order of increasing ellipticity at 222 nm). (Jourdan and Searle 2001) 141
Figure 5.5 Fractions of the native state conformation versus methanol concentration, obtained from 1H NMR signal intensities of several individual protons. The NMR measurements were made at pH* 1.9 and 25°C. (from Kamatari et al. 1998) 142
Figure 5.6 Fractions of the native state conformation versus methanol concentration, obtained from the ellipticity change at 222nm (circle) and 288 nm (triangle). The measurements were made at pH 1.9 (open) and pH 3.0 (filled) at 25°C. 143
Figure 5.7 Comparison of unfolding enthalpies versus temperature plots in water and 40% aqueous methanol. Lysozyme unfolding for 40% methanol was monitored by DSC in the pH range 2.0 – 4.5; ΔC_p for unfolding in water was calculated from data from Kovrigin and Potekhin (2000) 144
Figure 5.8 Change in ΔCp of lysozyme unfolding with increasing methanol concentration 145
Figure 5.9 Change in ΔCp of ribonuclease A unfolding with increasing methanol concentration 147

Figure 6.1 Ubiquitin unfolding in 10% methanol, pH=2, monitored at two different intervals in PPC: with temperature intervals of 1°C and 3°C/ 158
Figure 6.2 Ubiquitin unfolding - Changes in α in different methanol concentration, in water and in D_2O. 160
Figure 6.3 Lysozyme unfolding - Changes in α in different methanol concentration, in water and in D_2O. 161
Figure 6.4 Ribonuclease A unfolding - Changes in α in different methanol concentration, in water and in D_2O. 162
Figure 6.5 Change in ΔV_{unf} with increasing methanol concentration for ubiquitin unfolding. 164
Figure 6.6 Change in ΔV_{unf} with increasing methanol concentration for lysozyme unfolding. 165
Figure 6.7 Change in ΔV_{unf} with increasing methanol concentration for ribonuclease A unfolding. 165

LIST OF TABLES

Table 1.1 The partial molar and specific volumes of molecules in water (at 25°C). [a] (from Chalikian et al. 1996); [b] (from Squire and Himmel 1979); [c] (from Banipal et al. 1997). 23

Table 2.1 Summary of extinction coefficients used, the values were obtained from literature: [a](Ibarra-Molero et al. 1999); [b](Konishi and Scheraga 1980); [c](Aune and Tanford 1969); [d](Babul and Stellwagen 1972) 45

Table 3.1 The unit conversion factors used by the PPC data analysis software. 74

Table 3.2 Average heats, standard deviations and standard errors of the mean for water -water PPC measurements. 88

Table 3.3 Average heats, standard deviations and standard errors of the mean for buffer-buffer PPC measurements. 89

Table 3.4 Values used for calculation of error in α for ribonuclease A unfolding 95

Table 4.1 Partial specific volumes for the amino acid side chains at 25°C 110

Table 4.2 The values of $(\partial C_p/\partial P)_T$ at 25°C for the amino acids measured by PPC. 117

Table 4.3 The values of $(\partial C_p/\partial P)_T$ at 25°C for the amino acids side-chains calculated 126

Table 6.1 Average experimental scan rates in the PPC experiments. 158

Table 7.1 Comparison of volumes of unfolding (ΔH_{vH}) obtained from high pressure study([a]) by Dubins et al. (2003) and PPC of cytochrome c unfolding at the same conditions 172

Table 7.2 Comparison of enthalpies of unfolding (ΔH_{vH}) obtained from high pressure study([a]) by Dubins et al. (2003) and DSC of cytochrome c unfolding at the same conditions 173

ABBREVIATIONS

α	Coefficient of thermal expansion
α	Coefficient of thermal expansion of a solute in solution
α_0	Coefficient of thermal expansion of a pure solvent
α_{exp}	α of a solute determined differentially from the PPC experiment
$(\alpha_0)_{exp}$	α of a solvent determined differentially from the PPC experiment
α_{H_2O}	Coefficient of thermal expansion of pure water
β_S°	Coefficient of adiabatic compressibility
β_T°	Coefficient of isothermal compressibility
ϵ	Extinction coefficient
ΔC_p	Heat capacity change
ΔG	Free energy change
ΔH	Enthalpy change
ΔH_{cal}	Calorimetric enthalpy
ΔH_{vH}	van't Hoff enthalpy
ΔQ	Heat change
ΔP	Pressure change
ΔS	Entropy change
ΔV	Volume change
ΔV°	Change in partial volume (molar or specific)
ΔV_h	Hydration contribution to partial volume
ΔV_{unf}	Volume change for protein unfolding
ΔX_h	Hydration-induced change in one of the volumetric properties (X) of the solvent
A	Absorbance
A state	Expanded helical denatured state of proteins in alcohol (also known as H state)
Å	Angstroms
apoMB	apomyoglobin
ASA	Accessible surface area

atm	Atmospheres
BPTI	Basic pancreatic trypsin inhibitor
C	Protein concentration (usually in mol L^{-1})
cal	Calories
CD	Circular Dichroism
CFB	Cell feedback
C_p	Heat capacity
d	Density
DSC	Differential Scanning Calorimetry
DSD	Differential Scanning Densitometry
e	Partial specific thermal expansibility
E^o	Partial molar thermal expansibility
G	Gibb's free energy
Gdn HCl	Guanidinium hydrochloride
H	Enthalpy
H state	Expanded helical denatured state (also known as A state)
H-bonding	Hydrogen-bonding
HEW	Hen egg white
ITC	Isothermal Titration Calorimetry
I_M	Intermediate state
J	Joules
K_S°	Adiabatic compressibility
K_T^o	Isothermal compressibility
LYS	Lysozyme
m_0	Mass of a solute
m_S	Mass of solvent
MG	Molten globule
MeOH	Methanol
MW	Molecular weight
n	Number of moles
N	Native state
n_h	Hydration number (number of water molecules in hydration shell)
$(NH_4)_2SO_4$	Ammonium sulphate

NMR	Nuclear Magnetic Resonance
P	Pressure
PPC	Pressure Perturbation Calorimetry
psi	Pounds per square inch
Q	Heat
Q	Heat response of the sample cell in the PPC experiment
Q_{ref}	Heat response of the reference cell in the PPC experiment
ΔQ_{BB}	Differential heat in the buffer-buffer PPC experiment
ΔQ_{BW}	Differential heat in the buffer-water PPC experiment
ΔQ_{SB}	Differential heat in the sample-buffer PPC experiment
ΔQ_{WW}	Differential heat in the water-water PPC experiment
R	Universal gas constant
RNase A	Ribonuclease A (bovine pancreas)
S	Entropy
SAXS	Small-angle X-ray scattering
t	Time
T	Temperature
TFE	2,2,2-trifluoroethanol
UV	Ultra violet
V^o	Partial volume (molar V_m or specific V_s)
V	Volume
V_{AA}	Partial volume of amino acid molecule
V_{SC}	Partial volume of amino acid side-chain
V_0	Partial specific volume of solvent
$\overline{V}$	Partial specific volume of solute in solution
X^o	One of the partial molar volumetric properties of a solute (V^o, E^o, K_S^o and K_T^o)
X_0	One of the partial molar volumetric properties (partial molar volume, expansibility or compressibility) of the bulk solvent
X_M	Intrinsic volume, expansibility or compressibility of the solute
X_h	Average value of one of the partial molar volumetric properties of water in the solute hydration shell

Chapter 1

INTRODUCTION

Outline

Chapter 1 covers

- Thesis overview
- Thermodynamics of protein stability
- Thermodynamics of protein unfolding
- Volumetric properties
- Protein hydration and solvation
- Thesis objectives

1.1 Thesis overview

A brief overview of the content of each chapter in this thesis is provided.

1. Introduction

This chapter introduces the basic concepts in thermodynamics of protein stability. The first part focuses on the detailed description of the non-covalent forces stabilising protein folded structures, the description of energetics of the unfolding transition of proteins follows. In the second part the various experimental techniques and volumetric parameters (partial volume, expansibility and compressibility) that are used to study molecular solvation are discussed. A short review of recent literature in each field is given.

2. Materials and Methods

Details about the reagents and biophysical techniques (PPC, DSC and CD) used in this study are provided. Pressure perturbation calorimetry provides information about the solvation of molecules in solution; circular dichroism is used for structural characterisation of the studied proteins; differential scanning calorimetry is used to study thermal transitions in those proteins and for determination of ΔC_p values of unfolding through the pH variation method.

3. PPC - theory and basics of the method

PPC indirectly measures the thermal expansion coefficients (α) of molecules in solution. Chapter 3 presents the theoretical background to the method, together with derivation of the equations used for calculation of α. The instrumental setup and typical experiments are described, and the detailed data analysis procedure is presented. The chapter ends with troubleshooting of the most encountered problems with the technique and theoretical error analysis.

4. Structure making and structure breaking by PPC: amino acids as model systems

Chapter 4 describes how the measurement of a molecule's thermal expansion coefficient as a function of temperature (using PPC) can provide information about the structure of the water molecules that surround (solvate) a solute in

water. First, the theoretical considerations of the water structure are used to derive a thermodynamic parameter $(\partial C_p/\partial_P)_T$ indicative of structure making and structure breaking properties of the solutes. This parameter is later used throughout the chapter to evaluate the influence amino acids and their side-chains have on the structure of water in their hydration shell by critically comparing data derived from literature with data from PPC measurements.

5. ΔCp of protein unfolding in methanol water mixtures

This chapter describes the investigation into changes of ΔC_p of unfolding of the studied proteins (ubiquitin, lysozyme, ribonuclease A) that occur in aqueous methanolic solutions. The review of previous literature is presented, and is followed by the experimental results from determination of ΔC_p by DSC studies. Additionally, structural data on the protein folds in methanolic solutions is presented.

6. PPC of protein unfolding in methanol water mixtures

Chapter 6 describes the changes in solvation that occur in aqueous methanolic solutions around the studied proteins (ubiquitin, lysozyme, ribonuclease A) determined from the PPC measurements. ΔV of unfolding is determined at various methanol concentrations and the changes in ΔV are discussed.

7. PPC of cytochrome c conformational transitions

In this chapter PPC measurements were used to quantify the volume changes of unfolding for cytochrome c structural transitions (native to unfolded, molten globule to unfolded). The results are compared with data obtained from high-pressure spectroscopic studies.

8. Conclusions

The final chapter presents a summary of the findings of this thesis and introduces some suggestions for future work.

9. Appendices

Supplementary data for experimental chapters is presented.

1.2 Thermodynamics of protein stability

1.2.1 *Non-covalent interactions determine protein stability*

One of the most important and exciting areas of research in biochemistry is to learn what determines the three-dimensional conformation of a protein. The first question to be answered is how an unfolded polypeptide chain acquires the fold of a native protein and how the amino acid sequence of a protein encodes for its unique structure. This is called a protein folding problem. It is one of the fundamental problems in biophysical science. To attempt answering this question, protein folding kinetics and thermodynamics are extensively studied. The elucidation of the kinetic folding mechanism of a protein is the first step on the way to describe its complete folding pathway. A folding pathway is understood when all transient intermediates and the transition states between them are characterized (Kiefhaber 1995). Protein thermodynamics tries to answer the following question: What are the interactions that drive the protein folding and stabilize its final folded state?

A protein structure is the result of a subtle balance among non-covalent forces. The main interactions that determine protein stability are:

- hydrophobic interaction
- hydrogen bonding
- electrostatic forces
- van der Waals interactions
- entropic disruption of the polypeptide chain

What seems amazing at first is that proteins are only marginally stable. The free-energy difference between folded and unfolded states of a typical 100-residue protein is about 40 $kJ \cdot mol^{-1}$ (~10 $kcal \cdot mol^{-1}$). For comparison, the free energy of a typical hydrogen bond is about 20 $kJ \cdot mol^{-1}$ (5 $kcal \cdot mol^{-1}$). The average stabilization per residue is only 0.4 $kJ \cdot mol^{-1}$, which is less than random thermal energy ($RT = 2.5$ $kJ \cdot mol^{-1}$ at room temperature).

However, this only just slight stabilization of protein three-dimensional structure has its rationales. First, the protein flexibility is crucial for its action (conformational changes are essential to bind substrates, other proteins or carry out catalysis). Second, nascent proteins shouldn't fall into deep traps on their way to the native state. Third, partial unfolding enables proteins to be transported across membrane barriers. Last, but not least, proteins are constructed so that they can readily be removed.

When dealing with protein stability, all contributions are important, even the minor ones, because the unfolding free energy is small overall as a result of almost the complete cancellation of strongly stabilizing contributions (such as hydrophobic effect and hydrogen bonding) and strongly destabilizing ones (such as the conformational entropy) (Dill 1990). These various non-covalent influences sum over entire protein molecule to energies up to thousands of kilojoules per mole each. Consequently, a protein structure is the result of a subtle balance among powerful counterbalancing forces.

Short range repulsions

Repulsion between atoms and molecules takes place when they come near enough for their electron clouds to interact. Because the repulsive energy rises steeply with decreasing distance, the molecules can be considered as having definite dimensions and modelled as spheres impenetrable to other atoms defined by the van der Waals radius. This radius also defines the van der Waals surface area and volume of a molecule - for big molecules such as proteins it is not particularly relevant chemically, because there are small cavities, not accessible to other molecules, e.g. to solvent. A more practical concept of surface is the accessible surface area (ASA), the area which is defined by the solvent molecules in contact with a protein surface. The accessible surface area is generally described by the centre of a solvent molecule of radius 1.4 Å, representative of a water molecule, in van der Waals contact with a protein.

Electrostatic forces

The most fundamental non-covalent interaction comes from electrostatic attraction or repulsion between electrically charged particles. The energy of electrostatic interaction of two electric charges, q_1 and q_2, that are separated by distance r, is described by Coulomb's law:

$$\Delta E = \frac{kq_1q_2}{Dr} \qquad (1.1)$$

Here $k = 9.0 \times 10^9$ J·m·C^{-2} and D is the dielectric constant of the medium in which the charges are immersed (D = 1 for vacuum, 80 for water, and for protein interior is usually taken to be in the range 3 to 5 in analogy to dielectric constants of substances that have similar polarities). The ionic interaction varies with the first power of distance, hence it is effective over relatively large distances. Exposed charged groups and their tendencies to ionise determine pI values of a protein. They also determine variability of electrostatic interaction with changes in pH or solvent polarities (Creighton 1993).

Interactions between very close, oppositely charged groups in proteins (such as Lys, Arg, His, Asp and Glu amino acid residues plus α-amino and α-carboxyl groups) are known as salt bridges. Electrostatic interactions, even though they are strong, are believed to contribute little stability toward a protein's native structure. This is due to high free energy of solvation of two separated ions, which is about equal to the free energy of formation of the unsolvated ion pair (Voet et al. 1998).

Yet, when dealing with protein stability, even minor contributions, which are in the order of a few kJ·mol^{-1}, are important because the unfolding energy is small as a result of cancellation of strongly stabilizing contributions.

The effect of a surface salt bridge on the stability remains controversial; some reports have shown little contribution of a surface salt bridge to stability, whereas others have shown a favourable contribution. For instance it has been consistently observed that the salt bridges are more frequent in proteins from thermophiles and some theoretical studies suggested that they may contribute substantially to proteins stability in thermophiles (Sanchez-Ruiz and Makhatadze 2001).

Buried salt bridges pay large desolvation penalties caused by the difference in the dielectric properties of water versus the hydrophobic protein interior, therefore they should have little contribution to protein stability (Sanchez-Ruiz and Makhatadze 2001).

Kumar and Nussinov (1999) analysed 222 non-equivalent salt bridges derived from 36 non-homologous high-resolution monomeric protein crystal structures. They showed that the electrostatic interactions between the salt-bridging side-chains are, however, also stronger in the interior, due to the absence of solvent screening and to lower polarity of environment. Even large desolvation penalties for burying salt bridges are often more than compensated for by the electrostatic interactions between the salt-bridging side-chains.

The major finding of this work is that salt bridges can be stabilizing or destabilizing depending on their geometry. Salt bridges with favourable geometry are likely to be stabilizing anywhere in the protein structure. The most salt bridges in the dataset are stabilizing, irrespective of whether they are buried or exposed. Takano et al. (2000) attempted to estimate the contribution from charge-charge interactions to overall protein stability. The studies of systematic mutant human lysozymes demonstrated that the contributions from different salt bridges were not equal, they ranged from small for the salt bridge that was 100% accessible to the solvent to 9 $kJ \cdot mol^{-1}$ for the buried residues.

Unfolding studies of ubiquitin together with theoretical estimates of the contributions from charge-charge interactions to the ΔG of unfolding (Ibarra-Molero et al. 1999) postulated that charge-charge interactions may explain the high stability of the protein. Most of the charged residues on the ubiquitin surface were found to be stabilizing, however these residues contributed unfavourably to protein stability. The presented analysis suggested the possibility of enhancing protein thermal stability by optimising the distribution of charged residues on the protein surface by mutating these residues to neutral residues or even ones with reversed charge. This possibility was further tested by authors (Loladze et al.

1999) and showed that such mutations may indeed stabilize the protein conformation. This implies the possibility of developing a general strategy for enhancing the protein stability and design of thermostable proteins (Sanchez-Ruiz and Makhatadze 2001).

Van der Waals interactions

The non-covalent associations between electrically neutral molecules, collectively known as van der Waals forces, arise from electrostatic interactions among permanent and/or induced dipoles. These forces are responsible for many interactions of different strength between non-bonded neighbouring atoms. (The hydrogen bond, an unusual type of dipolar interaction, is described separately below.)

A molecule need not have a net charge to participate in the electrostatic interactions. It is enough if the charge is separated, so there is partial negative charge, δ- on the more electronegative atom, and partial positive charge, δ+, on the atom with smaller electronegativity. This separation of charge in a molecule determines its dipole moment (μ_D)

$$\mu_D = Z \cdot d \qquad (1.2)$$

where Z is the separated partial charge and d is the distance by which it is separated.

Interactions between permanent dipoles determine a great deal of protein structure stability, because many groups in proteins, such as carbonyl and amide groups of the peptide backbone, have permanent dipole moments. These interactions are generally much weaker than the charge-charge interactions of ion pairs and their energies vary with r^{-3} so they rapidly attenuate with distance. However, in α-helices the dipolar amide and carbonyl groups of the polypeptide backbone all point in the same direction so that their dipole moments sum up giving a significant dipole moment that is positive toward the N terminus and negative toward C terminal end of the α-helix. consequently, in the protein core of the low dielectric constant, dipole - dipole interactions are the important influence in determining protein conformations.

A permanent dipole can also modify charge distribution of a neighbouring group, and as a result attracting the induced dipole.. This interaction is however generally much weaker than dipole - dipole interactions.

Although non-polar molecules are electrically neutral, at every moment they possess transient dipole moments formed by fluctuations of electron movements. This small dipole moment polarizes neighbouring groups so that they attract each other. Forces resulting from interactions between two mutually induced dipoles (known as London dispersion forces) are extremely weak. They are only important for groups contacting within their van der Waals distances (the optimal distance for the interaction of two atoms is usually 0.3 - 0.5 Å greater than the sum of their van der Waals radii), as their association energy is proportional to r^{-6}. Nevertheless, they significantly influence protein stability as they occur among great numbers of such interatomic contacts in proteins. Quite often the latter are considered together with the water-ordering effect of non-polar residues as "the hydrophobic effect" (see below).

Hydrophobic interactions

The hydrophobic effect is believed to be a major influence in causing proteins to fold into their native conformation (Dill 1990; Kauzmann 1959). This fact has been widely accepted and is published in most of biochemistry textbooks: "Protein structures are governed primarily by hydrophobic effect and, to a lesser extent, by interactions between polar residues and other types of bonds" (Voet et al. 1998).

The hydrophobic effect results from the tendencies of non-polar molecules to interact with each other so as to minimize their contacts with water. It arises from the special properties of water as a solvent and its extensive hydrogen bonding. The understanding of hydrophobic interactions have been based on model systems. Namely, the transfer of hydrocarbon from water to a non-polar solvent resembles the transfer of a non-polar side chain from the aqueous solution to the protein interior during the folding process. If we consider the reverse process we

can estimate the magnitude of the hydrophobic effect by measuring the free energy of transfer of a non-polar molecule in the gas, liquid or solid state to water. Transferring of a solute molecule to water involves (1) creating a suitable cavity in water, (2) introducing the solute molecule into the cavity and (3) rearranging the solute and the surrounding water molecules to maximize interactions between them. The observed thermodynamics of transfer are the net effect of all these three factors and shows anomalous temperature-dependence.
At room temperature the unfavourable transfer of a non-polar molecule to water is primarily a result of the unfavourable change in entropy as the enthalpy change is approximately zero at this temperature. The unfavourable change in entropy is thought to result from increased ordering of water molecules around non-polar solute – water molecules cannot hydrogen-bond to non-polar solute so they are imagined to form hydrogen-bonded "iceberg" network among themselves around non-polar surface in a "water-ordering effect" (Creighton 1993)

As the temperature is increased, the ordered water shell around the non-polar solute tends to melt out and to become more like bulk water. This melting of ordered water produces large heat capacity (C_p) of this type of aqueous solution. This also suggests that the heat capacity change of proteins upon unfolding is positive due to the water solvating exposed non-polar residues (Privalov and Gill 1988). The heat capacity value is generally found to be proportional to the non-polar surface area of the solute molecule exposed to solvent.

The hydrophobic effect was assumed to be the dominant force stabilizing protein folded structures for several years. It results from the tendencies of non-polar molecules to interact with each other as to minimize their contacts with water. It arises from burial of polar and non-polar groups due to the special properties of water as a solvent and its extensive hydrogen bonding. There are, however, many publications that argue with the dominating role of hydrophobic interaction in stabilizing proteins. One of them recently demonstrated that tight packing of the protein interior results in strong van der Waals interactions of polar groups that together with hydrogen bonding offsets the desolvation penalty of polar group

burial - the desolvation penalty can therefore be much smaller than previously believed (Pace 2001).

One must, however, remember that the name "hydrophobic effect" is used differently by different authors. Most often the van der Waals interactions between non-polar groups and hydration effects of these groups are considered as integral entity, as they cannot be separated experimentally. Although the term "hydrophobic interactions" is widely accepted, it can lead to great misunderstanding as there are authors that mean only one of its two components, usually the one that is stipulated by water ordering by the non-polar groups, and consider the van der Waals interactions of these groups separately or do not consider them at all (Privalov and Gill 1988).

By showing that weakening the solvent ordering effect (responsible for the hydrophobic effect) by addition of methanol to water and still observing the natively folded structure of the protein studied (ubiquitin) (Jourdan and Searle 2001; Woolfson et al. 1993), Jourdan and Searle (2001) concluded that the hydrophobic effect is not a prerequisite for specific stabilization of the protein native state and that van der Waals packing of the non-polar core appears to be dominant influence for this stabilization.

Hydrogen bonds

Hydrogen bonds (D—H · · · A) are predominantly electrostatic interactions between a weakly acidic donor group (D—H) and an electronegative acceptor atom (A) that bears a lone pair of electrons. Hydrogen bonds in proteins most frequently involves the C=O and N-H groups of the peptide backbone - up to 68% of hydrogen bonds that occur in globular proteins (Pace et al. 1996). In this type of hydrogen bond H···O distance is most often 1.9 - 2.0 Å. The internal hydrogen bonds of proteins are arranged such that nearly all possible hydrogen bonds are formed. Obviously, it has a major influence on protein structures.

However, an unfolded protein makes all its hydrogen bonds with the water molecules of the aqueous solvent. Thus the free energy of stabilization of a native

protein by internal hydrogen bonds is equal to the difference in the free energy of hydrogen bonding between the native state and the unfolded state. According to the most accepted view, in a first approximation all hydrogen bonds have similar energy, so the ΔG should equal zero. "Internal hydrogen bonding cannot significantly stabilize, and, indeed, may even slightly destabilize, the structure of a native protein relative to its unfolded state" (Voet and Voet 1995).
Some scientists argue, however, with the views in biochemistry textbooks stating that hydrogen bonding plays a minor role in the stability of protein structures. It was first suggested that hydrogen bonds contribute considerably to the stabilization of protein structure by Privalov and Gill (1988).

Myers and Pace (1996) have summarized the results of series of mutant proteins with respect of hydrogen bonds and suggested that hydrogen bonding and hydrophobic effect make large but comparable contributions to protein stability. Measurements of the change in conformational stability for the mutation of a hydrogen bonded residue to one incapable of hydrogen bonding suggest a stabilization of 1.0 kcal·mol^{-1} (4.2 kJ·mol^{-1}) per hydrogen bond. If the free energy change values were corrected for differences in side-chain hydrophobicity and conformational entropy, then the estimated stabilization becomes 2.2 kcal·mol^{-1} (8.4 kJ·mol^{-1}) per hydrogen bond.

To estimate the contribution of hydrogen bonds to the conformational stability of a protein Takano et al. (1999) determined the thermodynamic parameters for denaturation of a series of mutant lysozymes. The estimation of the free energy values after removal of hydrogen bonds indicates their favourable contribution to protein stability. The net contribution of protein internal hydrogen bond was estimated to be 8.5 kJ·mol^{-1}, the intermolecular one between protein and ordered water molecule: 5.2 kJ·mol^{-1}, and the intermolecular one between ordered water molecules: 5.0 kJ·mol^{-1}, for 3Å long hydrogen bond. The net contributions of hydrogen bond to protein stability was consistent with the values published earlier (Myers and Pace 1996). The entropic cost of the introduction of a water molecule to the protein interior was estimated to be about 8 kJ·mol^{-1}. On the other hand, the statistical study has shown that a buried water in protein structures usually forms

3 - 4 hydrogen bonds, and only two hydrogen bonds with water (10.4 $kJ \cdot mol^{-1}$) are able to overcome this entropic cost (8 $kJ \cdot mol^{-1}$). Thus, a bound water in the protein structure should also contribute favourably to protein stability due to its hydrogen bonding.

Recently Nick Pace demonstrated that the burial of a polar group that can make hydrogen bonds in protein interior contribute more to protein stability than the non-polar group burial (Pace 2001). On the basis of studies of Asn to Ala mutants, the gain in stability from burying amide groups that are hydrogen bonded to peptide groups is 80 $cal \cdot mol^{-1} \cdot Å^{-3}$. On the basis of similar studies of Leu to Ala and Ile to Val mutants, the gain in stability from burying $-CH_2-$ groups is 50 $cal \cdot mol^{-1} \cdot Å^{-3}$. An amide group can be a reasonable model for a peptide group, it has a similar volume when buried in proteins and, although it can form four hydrogen bonds and a peptide group only three, the stability gained from peptide group burial should be similar, only about 10% smaller. It leads to a conclusion that peptide group burial makes a larger contribution to protein stability than non-polar side chain burial. The author argues that tight packing of the protein interior results in strong van der Waals interactions of polar groups that together with hydrogen bonding offsets the desolvation penalty of polar group burial - the desolvation penalty can therefore be much smaller than previously believed. He concludes that "perhaps we have been wrong for the past 40 years, and the burial of polar groups makes a larger contribution to protein stability than the burial of non-polar groups".

1.2.2 *How the non-covalent interactions drive the protein folding*

Recently Tsai, Maizel and Nussinov (2002) provided a new insight into the role the specific non-covalent interactions play in driving the protein folding event.

Protein cold denaturation, first described by Brandts (Brandts 1964) and Brandts and Hunt (1967) and extensively reviewed by Privalov (1990), was at first a surprising experimental observation to the protein chemists – intuitively it seemed logical to assume that decrease in temperature leads to better packing and stability

of the protein structure. This is however not the case – most proteins denature after cooling. Furthermore, the unfolding at low temperatures is accompanied by a decrease in entropy. An explanation of the decrease in entropy is a key point in the understanding of cold denaturation.

The authors based their considerations on the fluctuating two-state model of water structure to explain the thermodynamics of both heat and cold denaturation. (For the more detailed description of the two-state model of water see chapter 4).

The conclusions presented in this review are significant in understanding the protein folding problem. Namely, the authors state that while the driving force for protein folding is the hydrophobic effect, there is a second step to it, which is further stabilization of the native structure by specific interactions (Tsai et al. 2002).

Hence, protein folding is a two-step process. Starting from a high temperature unfolded state (U), the first step (driven by hydrophobic effect) in a folding leads to the molten globule-like state . It originates from change in temperature, and therefore in the structure of water. The second rearrangement step leads to specific interactions observed in the native state. Here, in the second step, the water structure plays an insignificant role as it is practically unchanged. This MG-like to native (N) step is under enthalpy control.

A two-step process does not imply that protein folding must be a three-state process (Tsai et al. 2002). The time of the hydrophobic collapse may be too short to measure experimentally, in such a case a reversible two-state folding/unfolding will be observed. Thermodynamic analysis can then be done with a strict two-step assumption. This model does not imply, however, that the two steps of protein folding are two distinctive processes, with one following the other. It could as well be a mixed process, driven by the hydrophobic effect and stabilized by specific interactions, all happening at the same time.

In other words, although the molten globule state might be a kinetic intermediate in the folding process, the population of the MG state under normal equilibrium conditions is too low to affect the 2-state assumption.

The authors conclude that both the "curious" molten globule state as well as other experimentally observed intermediate states, that occur in heat, but not in the cold denaturation fit perfectly well into such a conceptual description (Tsai et al. 2002). The model presented there is the first model providing the microscopic interpretation of the hydrophobic effect and its role in the protein folding.

1.3 Thermodynamics of protein unfolding

1.3.1 *Energetic description of protein folding/unfolding transition.*

The stability of a protein molecule is usually described by the difference in free energy between the unfolded and native states, ΔG. Using the standard convention, a positive value of ΔG indicates that the unfolding transition is unfavourable and that the native state is energetically more stable than the unfolded state.

The free energy difference, ΔG, is defined in terms of the enthalpy, ΔH, and entropy, ΔS, difference as:

$$\Delta G = \Delta H - T\Delta S \tag{1.3}$$

Both enthalpy and entropy are temperature dependent and can be related to the heat capacity changes (ΔC_p) of the system:

$$\Delta H = \Delta H_R + \int_{T_R}^{T} \Delta C_p \cdot dT \tag{1.4}$$

and

$$\Delta S = \Delta S_R + \int_{T_R}^{T} (\Delta C_p / T) \cdot dT \tag{1.5}$$

where T_R is the reference temperature, T is temperature (both temperatures in K) and ΔH_R and ΔS_R are the enthalpy and entropy changes at the reference temperature.

In the case of protein denaturation ΔC_p can be assumed to be constant and temperature independent and thus the above equations after integration can be rewritten

$$\Delta H = \Delta H_R + \Delta C_p (T - T_R) \tag{1.6}$$

and

$$\Delta S = \Delta S_R + \Delta C_p \ln(T / T_R) \tag{1.7}$$

One can easily notice that ΔH and ΔS both vary with the temperature in the same direction. If ΔC_p is positive, both ΔH and ΔS will increase with temperature and vice versa. Thus simultaneous changes in entropy and enthalpy tend to cancel each other in the free energy term. This is an example of the phenomenon called

"enthalpy-entropy compensation" (Dunitz 1995) - observed changes in ΔH and ΔS caused by changes of various experimental conditions tend to cancel out resulting in only slight changes in ΔG.

1.3.2 *Heat Capacity Changes*

In recent years analysis of heat capacity (C_p) changes has become important in understanding the thermodynamics of hydrophobic interaction and protein folding, protein-protein and protein-nucleic acid binding processes (Sharp and Madan 1997).

Nowadays sensitive and accurate calorimeters provide us with a lot of heat capacity (C_p) data for these processes:

- ITC (Isothermal Titration Calorimetry) - for binding studies
- DSC (Differential Scanning Calorimetry) - for protein folding studies
- PPC (Pressure Perturbation Calorimetry) - for protein volumetric properties studies

Furthermore, processes that involve changes in C_p can give diverse thermodynamic data as heat capacity relates the other three major thermodynamic quantities - enthalpy (H), entropy (S), and free energy (G) - to each other

$$C_p = \frac{\partial H}{\partial T} = T\frac{\partial S}{\partial T} = -T^2\frac{\partial^2 G}{\partial T^2} = \frac{\langle \Delta H^2 \rangle}{kT^2} \qquad (1.8)$$

where T is temperature, k is Boltzmann's constant, and $\langle \Delta H^2 \rangle$ is the mean squared fluctuation in enthalpy (Cooper 1976).

Changes in C_p associated with protein folding and binding come almost entirely from changes in hydration heat capacity (ΔC_p^{hyd}) due to burial (desolvation) of polar and non-polar groups. The conventional view assumes that the heat capacity changes upon unfolding (ΔC_p^{unf}) are defined only by non-polar groups exposed in the unfolded state, and the contribution of polar groups exposure to ΔC_p^{unf} can be neglected. However, the new hypothesis is becoming more established stating that because not only non-polar, but also polar groups are buried, then their exposure

to water upon unfolding should contribute to the heat capacity changes with the opposite sign to that for the transfer of non-polar groups. This was first indicated by model compound studies (Makhatadze and Privalov 1990).

Most recently, it has been argued that the changes in heat capacity do not come only from the effects of hydrophobic interactions (Cooper 2005). The other possible contributions to changes in C_p observed for biomolecular processes such as protein folding and binding could also arise from other cooperative transitions of system of weak interactions.

This would imply that the cooperative breaking of a system of hydrogen bonds, whether it is the one existing in water internal structure, or within the protein interior, could give rise to similar C_p effects as the ones traditionally associated with the exposure of hydrophobic residues to water (Cooper 2005; Cooper et al. 2001; Cooper 2000).

Similarly, the correlations of solvent accessible surface area (ASA) of proteins with the heat capacity changes for protein unfolding suggest that the exposure of the hydrophobic residues is not the only factor correlating with C_p changes, as polar residues contribute to changes in C_p to a similar extent (Murphy and Freire 1992; Robertson and Murphy 1997; Spolar et al. 1992).

Another example for the contribution of polar residues exposure to solvent to the C_p changes comes from the recent study of ubiquitin mutants, where the effect of polar to non-polar amino acid substitutions on the heat capacity change upon unfolding was measured (Loladze et al. 2001). The mutation was introduced at sites completely buried in the protein interior, so that the changed amino acid was exposed to solvent upon unfolding. The substitutions of aliphatic side chains with a polar residue lead to significant (>30%) decrease in the heat capacity change upon ubiquitin unfolding (the control substitution by an aliphatic residue did not have a considerable effect on ΔC_p^{unf}). On the other hand, the substitution of a buried polar residue to a non-polar one lead to significant (>25%) increase in ΔC_p^{unf}. Again, the control substitution had no significant effect. The changes do

not appear to be the result of significant structural perturbations as seen from the NMR spectra of the variants, thus their result indicate that the heat capacity change of burial of polar and non-polar groups has an opposite sign.

1.4 Volumetric properties – pressure-related thermodynamic parameters

There are three key thermodynamic parameters that describe volumetric properties of solutes in solutions:

- partial volume (V°) – pressure derivative of the Gibbs free energy

$$V^\circ = \left(\frac{\partial G^\circ}{\partial P}\right)_T \tag{1.9}$$

- isothermal compressibility – pressure derivative of partial volume

$$K_T^\circ = -\left(\frac{\partial V^\circ}{\partial P}\right)_T \tag{1.10}$$

- expansibility – temperature derivative of partial volume

$$E^\circ = \left(\frac{\partial V^\circ}{\partial T}\right)_P \tag{1.11}$$

The partial molar volume, V°, of a solute in solution is defined as the apparent volume occupied by one mole of a solute at infinite dilution. Both volume derivatives (compressibility and expansibility) are related to volume by the coefficients: thermal expansion coefficient (α) and isothermal coefficient of compressibility(β_T°).

$$K_T^\circ = \beta_T^\circ \cdot V^\circ \tag{1.12}$$

$$E^\circ = \alpha \cdot V^\circ \tag{1.13}$$

The thermal expansion coefficient (α), also called expansivity, describes how the partial volume of a molecule expands with temperature, the isothermal compressibility coefficient (β_T°) describes how the partial volume of a molecule changes with pressure.

- isothermal compressibility coefficient

$$\beta_T^\circ = -\frac{1}{V^\circ}\left(\frac{\partial V^\circ}{\partial P}\right)_T \tag{1.14}$$

- thermal expansion coefficient (α)

$$\alpha = \frac{1}{V^\circ}\left(\frac{\partial V^\circ}{\partial T}\right)_P \tag{1.15}$$

Isentropic (adiabatic) compressibility is also often used, as it is more accessible experimentally than the isothermal compressibility. However, these two properties are not equivalent as it is sometimes assumed in the literature. The fundamental derivations of the thermodynamic equations for partial molar volume, V^o, expansibility, E^o, isentropic (adiabatic), K_S^o, and isothermal, K_T^o, compressibilities from the macroscopic properties (such as Gibbs energy and volume) have recently been summarised in the review paper by Blendamer et al. (1999).

1.4.1 *Partial molar volume (V^o)*

The partial (molar or specific) volume of a molecule in solution is simply a measurement of how much the total volume of the solution would change if 1 mole or 1 gram of the molecule were added, see equations 1.16 and 1.17:

- Partial molar volume

$$V_m^o = \left(\frac{\partial V}{\partial n_s}\right)_{T,P,n_0} \tag{1.16}$$

- Partial specific volume

$$V_s^o = \left(\frac{\partial V}{\partial g_s}\right)_{T,P,g_0} \tag{1.17}$$

Where V is the volume of the solution; n_s and g_s are the number of moles and number of grams of solute respectively; and the subscripts T, P, n_0 and g_0 imply that that the pressure, temperature and number of moles/grams of solvent are kept constant during the measurement. The two volumes can be easily interconverted by multiplying the specific volume by the molar weight (MW) of the solvent:

$$V_m^o = V_s^o \times MW \tag{1.18}$$

In literature, the partial specific volume is often denoted with a symbol $\overline{V}$, (where bar denotes specific quality), whereas the partial molar volume is simply denoted as V^o. This nomenclature will be used throughout this thesis to distinguish between the two properties.

The partial volumes (both molar and specific) of a selection of proteins in water (and glucose as an example of small molecular solute) are listed in Table 1.1.

Solute	Partial molar volume (cm^3/mol)	Partial specific volume (cm^3/g)
Lysozyme[a]	10039	0.702
Ribonuclease A[b]	9620	0.703
Cytochrome c[b]	8855	0.715
D-Glucose[c]	111.9	0.621

Table 1.1 The partial molar and specific volumes of molecules in water (at 25°C). [(a)] (from Chalikian et al. 1996); [(b)] (from Squire and Himmel 1979); [(c)] (from Banipal et al. 1997).

Partial volumes are very sensitive to the degree of hydration of a molecule and consequently they are useful for monitoring the changes in hydration that occur when a molecule undergoes a major conformational transition. The measurement of partial volumes changes ($\Delta V°$) in protein unfolding studies is crucial, though it is experimentally difficult (Bull and Breese 1973; Chalikian and Filfil 2003; Seemann et al. 2001).

The changes in partial volume associated with protein folding/unfolding can be either positive or negative, but they are very small, being in absolute value of only 1 or 2 % of the partial volume of the native form of the protein (Chalikian 2003). This a small volume change is a result of compensation of an increase in the overall hydration of the protein, and in the thermal volume of the molecule, by the negative contribution caused by the elimination of the internal voids and the enhancement of protein hydration (Chalikian et al. 1996).

1.4.2 *Expansibility (E^o) and thermal expansion coefficient (α)*

The thermal expansion coefficient (α) is the thermodynamic property that describes how the partial volume of a molecule expands with temperature. More precisely it describes the fractional increase in the partial volume of a molecule per degree rise in temperature and it is measured in units of K^{-1}. For example: if a molecule has a thermal expansion coefficient of 0.1×10^{-3} K^{-1}, this means that the partial volume of the molecule expands by 0.01 % when heated by 1 K. The thermal expansion coefficient (α) and the molar thermal expansibility (E^o) are related through equation 1.13(earlier).

The molar thermal expansibility (E^o) similarly describes how the partial volume of a molecule changes with temperature. However, E is expressed as the partial volume expansion (in cm^3) of one mole of molecules per degree rise in temperature.

The intrinsic volumes of large and flexible macromolecules, such as proteins, often show intrinsic expansibility (E_M) through the expansion of their secondary structural elements (e.g., α-helices, β-sheets and internal voids). The intrinsic expansivity of proteins can however be estimated from temperature-dependent X-ray crystallographic measurements. For example Frauenfelder, Tilton and Young (1987) have estimated that metmyoglobin, ribonuclease A and lysozyme have intrinsic thermal expansion coefficients of 1.4×10^{-4} K^{-1}, 0.4×10^{-4} K^{-1} and 0.9×10^{-4} K^{-1} respectively: this represents approximately 15 % of the overall expansivity of a protein in solution.

Although thermal expansibilities (E^o) and expansivities (α) are extremely sensitive to solute-solvent interactions, their usefulness in hydration studies has been seriously limited by the experimental difficulties associated with their measurement. Consequently, reliable expansivity data on biological compounds are rather rare in the literature (Chalikian 2003).

Density measurements are traditionally used to calculate thermal expansibilities. The partial volume of a molecule (in solution) is measured at a series of temperatures, the partial volumes are plotted as a function of temperature and a polynomial line is fitted to the resulting data. Because the thermal expansibility of the molecule is a derivative of volume as a function of temperature, it can be obtained by analytical differentiation of the fitted polynomial. Unfortunately, large experimental errors are associated with such thermal expansibility measurements.

Recently, MicroCal has developed a new calorimetric technique called pressure perturbation calorimetry (MicroCal LCC 2000a) in order to address the problems associated with traditional expansivity measurements. PPC indirectly measures the thermal expansion coefficient of a molecule by measuring the heat that is released by the molecule (in solution) in response to a small change in pressure. By making these measurements at a series of temperatures, α can easily be determined as a function of temperature. PPC has the great advantage over densitometric techniques in that its sensitivity is higher by more than an order of magnitude (Lin et al. 2002).

1.4.3 *Hydration term in volumetric parameters interpretation*

Recently, Chalikian, in his excellent review on protein volumetric properties (Chalikian 2003), has derived a detailed description of microscopic interpretation of volumetric properties. At infinite dilution, each of the partial molar volumetric properties of a solute (V^o, E^o, K_S^o and K_T^o here denoted as X^o) can be interpreted microscopically in terms of intrinsic and hydration contributions using the general relationship (Chalikian 2003):

$$X^o = X_M + \Delta X_h \qquad (1.19)$$
$$= X_M + n_h (X_h - X_0)$$

Where X_M is the intrinsic volume, expansibility or compressibility of the solute; ΔX_h is the hydration-induced change in one of these properties of the solvent; n_h is the hydration number (the total number of water molecules within the solute's

hydration shell); X_0 is the partial molar volume, expansibility or compressibility of the bulk solvent, and X_h is the average value of the same partial molar volumetric property of water in the solute hydration shell.

(This is a simple model of solute solvation, where the assumption is made that solvent shell is discrete, and all solvating molecules have the same properties. The real situation is more complex, as the solvent perturbation effects spread far from just the direct solute surface. This is nevertheless useful for interpretation of volumetric data).

For microscopic interpretation of the partial molar volume data, the scaled particle theory was employed (Chalikian and Filfil 2003), in this representation the partial molar volume, V^o, of a solute is considered to consist of four contributions:

$$V^o = V_M + V_T + V_I + \beta_{T0}RT \qquad (1.20)$$

Where V_M is the intrinsic volume of the molecule; V_T is the 'thermal volume' – the volume of the void space that surrounds the solute molecule as a result of the mutual thermal motions of the solute and solvent molecules; V_I is the 'interaction volume' - the volume of the solvent contraction around the solute that is caused by hydrogen-bonding or electrorestriction; and β_{T0} is the coefficient of isothermal compressibility of the solvent; R is the universal gas constant; and T is the absolute temperature. The $\beta_{T0}RT$ term is an ideal term that is small for aqueous solutions (~1 cm^3/mol) and is generally neglected (Chalikian and Filfil 2003).

The intrinsic volume (V_M) can be determined from the three-dimensional structure of the molecule. The thermal volume (V_T), which is an empty space of thickness, δ ~1Å, surrounding the whole molecule, can be calculated by multiplying the molecule's solvent-accessible surface area by δ (Chalikian 2003).

By neglecting the ideal $\beta_{T0}RT$ term, the interaction volume can be established by subtracting the intrinsic and thermal volumes from the total partial volume:

$$V_I = V^o - V_M - V_T \quad (1.21)$$

The interaction volumes of proteins are highly negative, thus suggesting that the partial volume of the solvation shell surrounding a protein is smaller than that of bulk water (Chalikian 2003; Danielewicz-Ferchmin et al. 2003) . This observation is consistent with the suggestion that water molecules found in the solvation shells of proteins are approximately 10 % more dense than bulk water (Merzel and Smith 2002; Svergun et al. 1998).

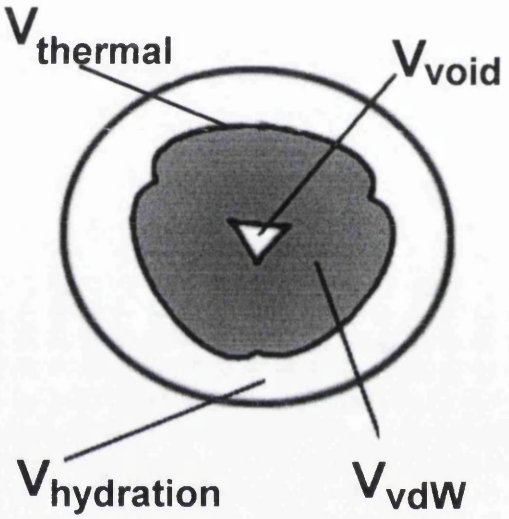

Figure 1.1 The partial volume of a protein in solution consists of the intrinsic volume (here represented by the van der Waals volume of the constituent atoms (vdW) and the volume of voids), the thermal volume immediately at the protein surface and the hydration volume of the solvent molecules interacting with the solute (protein here).

1.4.4 *Techniques Used to Investigate Solvation*

The study of molecular hydration, especially protein hydration, is currently an area of increasing interest. This is mainly because the interactions between the solvent-exposed amino acid side-chains of proteins and the surrounding solvent molecules are thought to play a major role in determining the energetics of protein stability.

As a result, more theoretical and experimental effort is now going into characterising the thermodynamic, structural and dynamic properties of hydration water (Chalikian 2003). A range of techniques can be used for studying hydration,

these include: X-ray and neutron scattering, NMR, molecular dynamics simulations, hydrodynamic techniques, and volumetric (densitometric, ultrasonic and calorimetric) techniques.

Solution scattering techniques provide information about the structure and dynamics of the water molecules directly bound to the macromolecule. Two scattering methods are used: X-ray scattering, where X-rays (photons) are scattered by electrons, and neutron scattering, where neutrons are scattered by atomic nuclei. By comparing the data obtained from both X-ray and neutron scattering techniques, information about the macromolecule's hydration shell can be obtained.

As an example, Svergun et al. (1998) performed the first direct characterization of the density of water in the hydration shell of a protein. They investigated the globular proteins lysozyme, *E. coli* thioredoxin reductase and protein R1 of *E. coli* ribonucleotide reductase by both small-angle X-ray and neutron scattering in H_2O and D_2O solutions. Their data reveal a first hydration shell that is ~3 Å thick with an average density 10% larger than that of the bulk solvent.

NMR measurements can be used to determine the number of molecules strongly and weakly bound within a solute's first hydration shell, as water molecules directly interacting with a solute's surface are characterised by an overall decrease in their tumbling rate (as compared to bulk water), and water molecules tightly bound within the interiors of proteins are even more rotationally restricted and rotate at the same rate as the protein (Shortle 1999). As the relaxation rates of magnetic nuclei (e.g., ^{17}O in H_2O) depend on the molecular motions of neighbouring atoms, NMR can therefore be used to measure the changes in rotation rates experienced by water when it leaves bulk solvent and interacts with a solute. Torres et al. (1998) have recently used this approach to determine the number of water molecules strongly and weakly bound to BSA (26.6 and 2900 respectively) and lysozyme (1.1 and 511 respectively).

Molecular dynamics (MD) simulations can provide detailed information about the structural properties of the water molecules hydrating macromolecules in solution – data that cannot be measured directly. However, the reliability of MD data depends on the suitability of the molecular models used in the simulations. Merzel and Smith (2002) have used MD simulations to investigate the density of water in the first hydration shell of lysozyme. In support of X-ray/neutron scattering experiments by Svergun et al. (1998) (discussed above), it was found that lysozyme's hydration shell was 3 Å thick and ~15 % denser than bulk water.

Hydrodynamic measurements (such as analytical ultracentrifugation) have long been used to characterise the size and shape of proteins. The experiments provide information about the molecule together with its hydration layer. In order that the size/shape of the anhydrous or hydrated molecule can be obtained, the hydration level of the protein (the grams of attached water per gram of protein – δ) and the thickness of the hydration layer must be known. Recently, the values used for these two parameters were suggested from atomic-level bead-modelling procedures, to be an average of $\delta = 0.3$ g/g and an average hydration shell thickness of ~1.2 Å for proteins (de la Torre 2001).

Pressure perturbation calorimetry (PPC), a technique recently developed by MicroCal Inc. (MicroCal LCC 2000a) and used here, provides new possibilities of studying molecules together with their hydration shell. The technique enables indirect calculations of thermal expansion coefficient (α) from the heat measurements. The basics of the method are described in detail in chapter 3.

1.5 Protein hydration and solvation

1.5.1 *Water as a solvent*

Water is an unusual solvent. It has several properties that make is unique amongst the other liquids. For example: a relatively high melting and boiling point, a high heat capacity, and the solid form is less dense than the liquid form – these properties are usually referred to as the 'anomalous' properties of water. Water's unusual properties originate from its ability to form hydrogen-bonds.

In its solid state (ice-Ih) water has an open hydrogen-bonded structure in which each water molecule is tetrahedrally surrounded by four neighbouring water molecules. When ice melts to form liquid water, the hydrogen-bonds are disrupted and occasionally break, but significant amounts of hydrogen-bonding remain in liquid water – only about 15 % of hydrogen-bonds are thought to be broken when ice melts (Ebbing 1993). After the melting of ice, water molecules become more compact, leading to a more dense liquid.

The simplest model depicts the structure of liquid water as being a mixture of two inter-convertible species: a low density, more-structured species (the iceIh-like clusters) and a high density, less-structured species, as expressed by the equilibrium (Frank and Wen 1957; Hepler 1969; Rontgen 1892):

$$(H_2O)_b \rightleftharpoons (H_2O)_d \qquad (1.22)$$

Where, $(H_2O)_b$ represents the bulky ice-like hydrogen-bonded water clusters and $(H_2O)_d$ signifies the denser bonded water molecules with lesser H-bonding structure. An increase in temperature causes the equilibrium to shift in favour of the denser less-structured species and gradually results in the breakdown of the ice-like structures. This two-state mixture model of water has been recently developed further by Robinson and co-workers (Cho et al. 2002; Urquidi et al. 1999; Vedamuthu et al. 1994) and has been successful in explaining all the physical anomalies of water as well as such biological phenomena as thermal and cold protein unfolding.

1.5.2 *The solvation of molecules in water*

In aqueous solution each solute molecule is individually surrounded by a 'co-sphere' of solvent (water), which is referred to as its solvation or hydration shell. The hydration shell should not be visualised as a rigid structure –water molecules are continually fluctuating between the 'shell' and bulk water (on a picosecond time-scale). It should instead be viewed as a time-averaged dynamic structure – the average number of water molecules perturbed by the presence of the solvent.

Inside the hydration shell the structure of water is modified to varying extents by the presence of the solute because charged, polar and hydrophobic groups form different interactions with water: water forms dipolar interactions with charged groups, hydrogen-bonds with polar groups, and something similar to clathrate structures around hydrophobic groups (Shortle 1999). Consequently, the water molecules in the solute's solvation shell have thermodynamic properties that are distinct from those of the bulk water. In particular, the water of hydration often has a different partial volume, compressibility and expansibility (Shortle 1999).

The influence on the solvation water properties depends on the nature of the solute. For example, ionic substances tend to orient water molecules in the vicinity, thus leading to the formation of a second hydration shell.

Molecules with polar groups (e.g., -OH and -NH_2 groups) can also hydrogen-bond to water. It has been suggested that the water molecules in a polar solute's first hydration shell are strongly contracted as a result of being strongly hydrogen-bonded to the solute, whereas further out in the second hydration shell the contraction effect is counterbalanced by the formation of ice-like water structures (which are of lower density than bulk water) (Frank and Wen 1957; Shortle 1999).

Water also interacts with non-polar molecules, by the so-called hydrophobic interaction where non-polar groups tend to come together in aqueous solution. The 'standard model' of hydrophobic hydration argues that water forms a cage-like 'clathrate' structure around non-polar groups (Frank and Evans 1945).

It has also been suggested that outside of the first hydration shell non-polar molecules promote the formation of denser water structure (Robinson and Cho 1999), though not by changing the hydrogen bonding distances, but by changing their angular structure. The radial/angular functions of water have recently been obtained from molecular dynamics (MD) simulations (Gallagher and Sharp 2003) that showed relative increase in the low angle population around non-polar groups.

The solvation shell for most biological macromolecules is heterogenous, as they are comprised of non-polar, polar, and charged groups. Consequently, such molecules have regions of hydrophilic and hydrophobic solvation – a mixed solvation shell.

1.5.3 *Studying protein hydration*

Much of what we know about volumetric properties of proteins comes from vibrational densitometry and ultrasonic velocimetry, which gives us information about protein partial specific volume (V°) and adiabatic compressibility (K_s°). There are many studies of proteins by this method available (Chalikian et al. 1996a; Chalikian et al. 1996b; Kharakoz and Sarvazyan 1993; Kharakoz and Bychkova 1997) and the application of this method have been revised extensively (Chalikian and Breslauer 1996).

Chalikian et al. (1996) have proposed an approach for interpreting volume and compressibility data on globular proteins that does not rely on data derived from studies on low molecular weight compounds. Using this approach, they characterized, as a function of temperature, the average hydration contributions to V° and K_s° per surface area of the charged, polar and non-polar solvent-accessible surface area (Chalikian et al. 1996b). They also described the changes in the partial specific adiabatic compressibility which accompanies protein conformational transitions upon temperature-induced, chemical and acid-induced denaturation (Chalikian and Breslauer 1996).

From compressibility studies there are indications that compression within the protein interior may not be uniform. The measurements of hydrogen bonds in basic pancreatic trypsin inhibitor (BPTI) by NMR (Li et al. 1998) show that pressure-induced shortening of the hydrogen bonds is higher for the NH groups that are externally hydrogen bonded with solvent water compared with the NH groups that are internally hydrogen bonded to carbonyls. This observation is in agreement with the compressibility of hydration waters at the protein surface being higher than the compressibility of protein interior (Chalikian et al. 1996b).

Other methods that have been used to determine protein volumetric properties involve high-pressure methods (UV,NMR and densitometry). High-pressure ultraviolet spectroscopy has been employed to study the standard volume change of unfolding for guanidinium-induced unfolding of lysozyme at high pressure (Sasahara and Nitta 1999) and at high pressure with varying temperature (Sasahara et al. 2001).

High pressure fluorescence spectroscopy was used to determine the pressure unfolding profile of staphylococcal nuclease (Prehoda et al. 1998). The authors presented the two models to derive volume changes upon unfolding, criticising the one that neglects the compressibility changes upon unfolding. They showed that this four-parameter model that is used for interpreting high-pressure spectroscopy data is insensitive to compressibility changes, and can give erroneous results if ΔK_T° is assumed to be non-zero (and that is indeed a case as was shown by NMR study presented below).

High-pressure NMR has been used by them to evaluate the standard volume change of pressure unfolding of ribonuclease A (Prehoda et al. 1998). The importance of evaluating the standard isothermal compressibility change (ΔK_T°) was emphasized as it is often assumed to be zero in analysis of pressure denaturation experiments. By analysis of NMR data the authors proved that this assumption can be incorrect and that neglecting compressibility effects can bias the interpretation of data. It must be stressed, however, that the isothermal and adiabatic (isentropic) compressibilities cannot be used interchangeably (Prehoda

et al. 1998) (the latter has been extensively studied by acoustic techniques). It is not practical to interconvert the two quantities, because doing so requires accurate values for other thermodynamic terms such as thermal expansion coefficient (α), heat capaticy (C_p) and specific partial volume(V^o) (Chalikian et al. 1994). These two quantities are related as follows (Seemann et al. 2001):

$$K_T = K_S + \frac{\alpha^2 TV}{C_p} \qquad (1.23)$$

From the analysis of experimental datasets, they found it is impractical to quantify ΔK_T^o from pressure denaturation data (such as fluorescence) that require fitting of additional terms from plateaus of the denaturation profile. However, these plateaus have known, fixed theoretical values for NMR data – thus this technique offers a practical approach for measurement of the compressibility changes for the protein pressure denaturation.

A novel technique, high-pressure densitometry was used by Seemann et al. (2001) to characterize temperature- and pressure-induced unfolding of staphylococcal nuclease. The changes in the apparent specific volume, expansion coefficient and isothermal compressibility were determined by these measurements and discussed in terms of intrinsic, hydrational and thermal contributions accompanying the unfolding transition. The measurements presented herein are the first that show isothermal compressibility changes of a protein undergoing pressure-induced unfolding (see Figure 1.2).

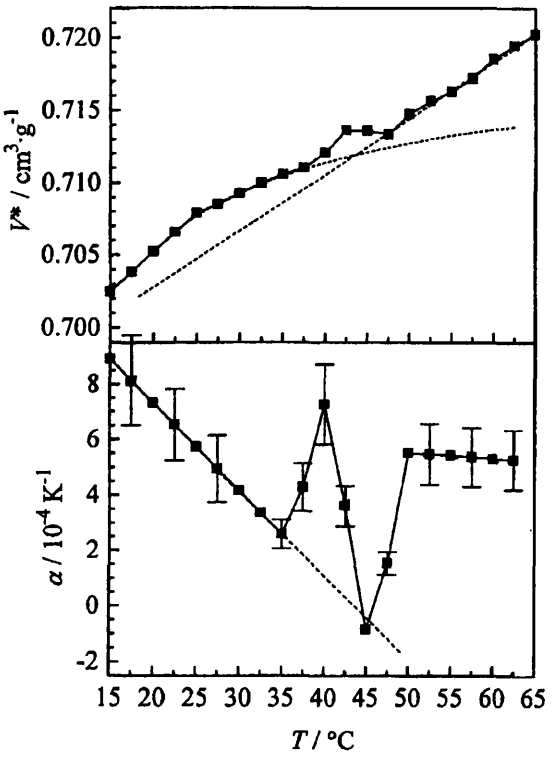

Figure 1.2 The coefficient of thermal expansion (α) of the partial volume of staphylococcal nuclease. Data taken from Seemann et al. (2001).

Though high-precision density measurements were able to detect a transition for the thermal unfolding of staphylococcal nuclease, the errors associated with the α values were of considerable magnitude. Density techniques are not sensitive enough yet to measure ΔV_{unf} for proteins and most studies before the article by Seemann et al. (2001) did not even detect any volume changes for the unfolding of ribonuclease A and lysozyme (Hinz et al. 1994; Makhatadze et al. 1990).

Conformational transitions of globular proteins are accompanied by significant alterations in protein hydration and intrinsic packing, which are reflected in corresponding changes in volume, compressibility and expansibility. The transitions between the conformational states were studied for the processes of both pressure, temperature and denaturant-induced denaturation. For the unfolding process of protein the volume change upon unfolding (ΔV_{unf}) can be defined as the change between specific partial volume of the unfolded (ΔV^{o}_{unf}) and folded states (ΔV^{o}_{fol}):

$$\Delta V_{unf} = V^{o}_{unf} - V^{o}_{fol} \quad (1.24)$$

The studies of volumes of unfolding for several small proteins were reviewed by Chalikian and Breslauer (1998). The summarized results show that ΔV_{unf} that accompany proteins at elevated pressures is always negative (the volume is decreased), whereas at atmospheric pressure the observed ΔV_{unf} can be both negative and positive, and does not correlate with the transition type.

1.5.4 *The effect of solutes on protein stability*

Different solutes have been used for a long time for specific stabilisation and destabilisation of proteins. Examples of such stabilising solutes could be trimethylamine and $(NH_4)_2SO_4$, and for destabilising urea and guanidinium salts.

The key hypothesis that all of such solutes influence protein stability indirectly by changing the amount of H-bonded structure in water has recently been shown not to be valid in all the cases (Batchelor et al. 2004), especially with the most commonly used destabilising urea and guanidinium salts, which were shown to decrease the H-bonded structure in water (structure breaking) whereas by their effect on the protein stability they were expected to increase the amount of structure in water (structure making) (Batchelor et al. 2004).

However, the description of the various solutes and cosolvents effects on the thermodynamics of folding might still provide some explanations of their mechanism of action. It may also contribute to dissecting the various energetic contributions that account for the protein stability and the folded state structure (Dill 1990; Robertson and Murphy 1997).

For example, at high concentrations (>50% v/v) alcohols have the ability to disrupt tertiary interactions while inducing non-native α-helical structure in proteins. The predominance of local secondary structure interactions over tertiary contacts in alcohol-induced states implies they may give us some understanding of the interactions present early on in the protein folding process. There is a general interest in determining the mechanism by which these various cosolvents

and denaturants control secondary structure stability and disrupt protein tertiary structure.

The order of effectiveness toward destabilization of protein tertiary structures is trifluoroethanol (TFE) > propanol > ethanol > methanol (Kamatari et al. 1996). The order is the same for effectiveness toward stabilization of the helical structures. Thus the protein transitions induced by methanol are expected to occur in a wider range of alcohol concentration than that induced by other alcohols, as methanol is the mildest denaturant.

It has been shown by theoretical studies that alcohol addition to water reorganizes ordered H-bonded structure (Graziano 1999). Such elimination of solvent ordering effect upon addition of alcohols to water should enable the study of other forces contributing to protein stability.

Methanol, amongst other alcohols, has been used to evaluate its effects on protein stability and structure in the water-alcohol mixtures. Studies of methanol –water mixtures, show that methanol changes the structure of water in an interesting way.

At low concentrations it enhances H-bonded structure in water, due to forming clathrate cages around the hydrophobic methyl group. Molecular dynamic (MD) simulations show that in the water rich region there is "high degree of ordering in water" (Laaksonen et al. 1997). Another study concluded that up to 10% v/v of methanol the structural enhancement of hydrogen bonded structure of water takes place (Sato et al. 2000).

However, at higher methanol concentrations, above 10% v/v the breakage of the clathrate hydration begins to take place due to lack of water molecules to form the clathrate cages for all methanol molecules, and above 30% v/v the abrupt breakage of the saturated hydration structure takes place (Sato et al. 2000)

A recent study of ubiquitin attempts to analyse the effects of cosolvents and denaturants on the thermodynamics of protein folding (Jourdan and Searle 2001).

Ubiquitin stability and thermodynamics was studied by Jourdan and Searle (2001) under a variety of non-physiological conditions, using the denaturants methanol and guanidinium chloride (Gdn HCl) both separately and in combination. Addition of methanol enables the decrease of the solvent ordering effect so that the hydrophobic interactions can be significantly diminished (Woolfson et al. 1993). The analysis shows that while burial of core hydrophobic residues and subsequent release of ordered water is believed to contribute to protein stability in water, this contribution is not crucial to the integrity and specificity of the folded state under the influence of both denaturants (methanol and GdnHCl).

The highly helical conformation and disrupted tertiary structure of proteins is described at high alcohol concentrations. A set of proteins (ubiquitin, ribonuclease A, α-lactalbumin, β-lactoglobulin, *Streptomyces* subtilisin inhibitor (SSI) and apomyoglobin) was investigated at 60% methanol at pH=2 to determine the structure of H state (Kamatari et al. 1999). All of the above have a helical content higher than that of the native state monitored by far-UV CD spectroscopy and no specific tertiary structure monitored by near-UV CD and NMR spectroscopy. The above proteins analysed by small-angle X-ray scattering (SAXS) (best available technique for elucidating compactness and shape of proteins) show 1.5-2.0-fold expansion with chain-like non-globular conformations. This conformation is called the A-state, A standing for the acidic conditions where it is experimentally observed.

The TFE-denatured state of lysozyme was also reported and investigated by SAXS analysis (Hoshino et al. 1997). Lysozyme in 30% TFE has similar expanded shape, what indicates that noncompact nonglobular conformation exists not only in methanol-water solvents but also in the other alcohol-water solvents. At lower alcohol concentrations cytochrome c (Kamatari et al. 1996) and apomyoglobin (Kamatari et al. 1999) are shown to exist in the intermediate state (I_M) in the methanol-induced conformational transition - their far and near-UV CD and NMR spectra at 30% methanol are quite distinct from that of native state and that found when methanol concentration is above 50%. However, there is no such an intermediate state reported for lysozyme (Kamatari et al. 1998).

The intermediate state (I_M) is a compact globular denatured state with a significant helical content, but with a disordered tertiary structure. Thus, all the available structure information indicates that the structure of the I_M for these proteins is very similar to that for well-known molten globule state (MG) induced by acid and salt.

The compact denatured state (I_M or MG) is stable under relatively mild denaturing conditions, whereas the expanded denatured state (H or A) is realized under extreme conditions of pH (large electrostatic repulsion) or high concentration of alcohol (decreased hydrophobic interactions).

In lysozyme the unfolding transition in methanol-water solvent mixture has been reported as highly cooperative (Kamatari et al. 1998; Hoshino et al. 1997; Kamatari et al. 1998), whereas in cytochrome c (Kamatari et al. 1996), β-lactoglobulin (Uversky et al. 1997) and apomyoglobin (Kamatari et al. 1999) compact denatured state can be observed. Stability of the I_M state is highly protein dependent.

1.6 Thesis objectives

The aims of my thesis are to study the solvation effects associated with the protein unfolding and other conformational changes by pressure perturbation calorimetry (PPC) and to investigate the contributions of hydrophobic interaction to protein folding energetics by changing the solvation effects usually associated with hydration. For this, the aqueous methanolic solutions are to be used, and evaluation of ΔC_p and ΔV changes associated with protein unfolding reaction is to be monitored.

This is accomplished by ΔCp analysis of differential scanning microcalorimetry (DSC) measurements and ΔV evaluation from pressure perturbation calorimetry (PPC) measurements.

Additionally, the application of PPC to other areas, such as studying solutes structure breaking and structure making properties is investigated.

Chapter 2

MATERIALS AND METHODS

Outline

Chapter 2 covers

- Reagents used
- Protein concentration determination
- Circular Dichroism
- Differential Scanning Calorimetry (DSC)
- ΔC_p analysis from pH variation method

2.1 Reagents used

2.1.1 *Buffer Reagents*

0.01M Phosphate buffer (pH 7.0): sodium dihydrogen orthophosphate dihydrate and disodium hydrogen orthophosphate (anhydrous) were purchased from BDH Laboratory Supplies.

0.01M Phosphate buffer (pH 2.0): sodium dihydrogen orthophosphate dehydrate and orthophosphoric acid (analytical grade) were purchased from BDH Laboratory Supplies and Analar respectively.

0.05M Acetate buffer (pH 3.5 - 4.5): sodium acetate and acetic acid (99.8 %) were purchased from BDH Laboratory Supplies and Riedel-de Haën respectively.

0.05M Glycine buffer (pH 2.0-3.2): glycine and hydrochloric acid (1 mol/L) were purchased from BDH Laboratory Supplies.

Potassium chloride, sodium chloride, hydrochloric acid and methanol were also purchased from BHD Laboratory Supplies. D_2O was purchased from Sigma Chemical Co.

2.1.2 *Amino acids*

L-Asparagine (Product Number A8381), L-Histidine (Product Number H8000), L-Glutamine (Product Number G3126), L-Serine (Product Number S4500), L-Alanine (Product Number A7627), and L-Valine (Product Number V0500) were purchased from Sigma Chemical Co. L-Glycine was purchased from BHD.

2.1.3 *Proteins*

Ubiquitin (bovine, Product Number U-6253), lysozyme (from chicken egg white, Product Number: L-6876), ribonuclease A (from bovine pancreas, Product Number: R-5500), and cytochrome c (from horse heart, Product Number: C-7752) were purchased from Sigma Chemical Co.

2.1.4 *Aqueous methanolic solvents*

Aqueous solutions of methanol were prepared by weight, by adding methanol into a pre-weighted amount of water and stirring immediately to minimise the methanol losses from evaporation. The methanol was added up to the required weight and transferred into the air-tight containers.

When the buffer methanolic solution had to be prepared, all the reagents were added to the required amount of water and the pH of the solution was pre-adjusted, so that after adding methanol only slight corrections to the pH are required. The methanol was then added by weight to the required concentration, pH was adjusted by using concentrated hydrochloric acid to introduce the least amount of water at this step. The prepared methanolic buffers were transferred in the air-tight containers immediately.

The concentration of methanol was not decreasing due to evaporation when stored in the air-tight containers, this was confirmed by density measurements after one month's storage. Nevertheless, the new solutions were prepared for each set of experiments or at least twice monthly, whatever was sooner.

The concentration of methanol was expressed as the volume ratio of methanol to water (% v/v). For the calculations of the weight for preparation of solutions the density of methanol of 0.7917 g cm^{-3} at 25°C was used and the density of water 0.997048 g cm^{-3} at 25°C. To facilitate the comparison with other literature on methanolic solutions, the conversion chart of methanol concentrations from % v/v to %wt (weight percentage), x (molar fraction) and molar ratio and molality (M) is presented in Appendix D

2.2 Protein concentration determination

Protein concentrations were estimated by UV-Visible spectroscopy using a Shimadzu UV160A recording spectrophotometer (Shimadzu Corp., Japan) using the Beer-Lambert Law:

$$A = \epsilon c l \qquad (2.1)$$

where ϵ is the molar extinction coefficient (M^{-1} cm^{-1}), c is the molar concentration of solute and l is the path length of the absorbance cell (cm). Quartz cuvettes with either 1cm or 0.2 cm pathlength were used.

Protein extinction coefficients were obtained from the literature, as all the proteins studied here are well characterised species. For the PPC data analysis protein concentration was expressed in mM and for DSC data analysis in mg mL^{-1}, using the extinction coefficients in the Table 2.1 below.

Protein	ϵ (mL mg^{-1} cm^{-1})	ϵ (mM^{-1} cm^{-1})
ubiquitin (280nm)[a]	0.149	1.28
ribonuclease A (280nm)[b]	0.596	8.16
lysozyme (280nm)[c]	2.65	37.932
cytochrome c (MG 400nm)[d]	9.286	115
cytochrome c (N 409nm)[d]	8.559	106

Table 2.1 Summary of extinction coefficients used, the values were obtained from literature: [a](Ibarra-Molero et al. 1999); [b](Konishi and Scheraga 1980); [c](Aune and Tanford 1969); [d](Babul and Stellwagen 1972)

2.3 Circular Dichroism

2.3.1 *Theory*

Circular Dichroism (CD) reports on the general secondary and tertiary structures of proteins by measuring the differential absorption of left- and right-handed circularly polarised light. This effect will occur when a chromophore is chiral (optically active) either intrinsically because of its structure, or by being covalently linked to chiral centre, or by being placed in an asymmetric environment. Chiral molecules interact differently with beams of left- and right-handed circularly polarised light, causing two such beams to travel at different speeds through these molecules, thereby rotating the polarised light. A CD spectrum shows the variation of this rotation with wavelength. Studies of the far-UV region (typically 240nm to 180nm) can be used to quantitatively asses the overall secondary structure content of the protein, the major absorbing group in this region being the peptide bond. In the near UV, the aromatic side chains (phenylamine, tyrosine, tryptophan) absorb in the range 250-290nm; the tertiary folding of the polypeptide chain can place these side chains in a chiral environment, giving rise to spectra which can serve as characteristic fingerprints of the native structure. The different forms of regular structure (α-helix, anti-parallel β-sheet, β-turn and irregular structure) found in peptides and proteins exhibit distinct far-UV CD spectra (Kelly and Price 1997).

2.3.2 *Experimental details*

The CD measurements were recorded with Jasco J-810 spectropolarimeter, equipped with a temperature controlled unit. The results are expressed as molar ellipticity $[\theta]$, which is defined as $[\theta] = 100\ \theta_{obs}/lc$, where θ_{obs} is the observed ellipticity in degrees, c is the molar concentration of the protein, and l is the length of the light path in centimetres. The unit of molar ellipticity is [deg cm^2 $dmol^{-1}$] or [deg m^{-1} M^{-1}]. The far-UV spectra were measured at protein concentrations of 0.1 mg/ml and with 1mm path length cuvette from 260 to 190nm. The near-UV spectra were measured at protein concentrations of 1 mg/ml and with 10mm path length cuvette from 340 to 260 nm. The measurements were carried out either at the temperature of 10°C or 80°C (additionally ubiquitin at pH = 7, 0% and 30% methanol at 95°C).

2.4 Differential scanning calorimetry (DSC)

2.4.1 *Introduction*

Differential scanning calorimetry (DSC) is an experimental technique that is used to measure the heat energy uptake that takes place in a sample solution during a controlled increase (or decrease) in temperature (Cooper 1999a). The MicroCal range of calorimeters (VP-DSC and MCS-DSC) are used to study thermally induced transitions in biological systems and can be used to determine thermal transition temperatures and thermodynamic data.

2.4.2 *Experimental details*

Experiments described in this study were carried out both using a VP-DSC or MCS-DSC microcalorimeter (Microcal, Northampton, MA) using a standard procedure (Cooper and Johnson 1994) and operating at a scan rate of 60°C per hour. The calorimetric cells were kept under an excess pressure of 28 psi during the scan to avoid bubble formation during the experiments. The heat differential between buffer in the both the sample and reference cells was recorded prior to each experiment in order to provide a baseline. Both sample and buffer solutions were degassed for 3 minutes prior to loading the calorimeter cells and protein concentrations were determined by UV-Visible spectroscopy after degassing.

2.4.3 *Theory and data analysis*

The DSC thermogram comprises three regions: the pre-transition baseline, the endothermic unfolding transition and the post-transition baseline. The pre-transition baseline represents the difference in heat capacity between the protein and the solvent it has displaced: as water has a relatively high heat capacity (C_p) in comparison to the protein, the C_p in this region is usually negative. As the protein unfolds, the C_p increases as more heat is taken up by the sample cell to denature the protein; as a result, the unfolding of the protein is characterised by a large endothermic transition. The point where the heat capacity reaches a maximum represents the mid-point temperature of the process (T_m) – the point where 50 % of the protein molecules are unfolded and the Gibb's free energy for unfolding is zero. After the unfolding transition the thermogram drops to a post-

transition baseline, which represents the relative heat capacity of the unfolded protein. Extrapolation of the pre and post transition baselines to the T_m and measurement of the difference between the two lines (at the T_m) allows the calculation of ΔC_p, the molar heat capacity change for unfolding. Figure 2.1 shows a typical DSC thermogram obtained for the thermal unfolding of the simple globular protein ribonuclease A.

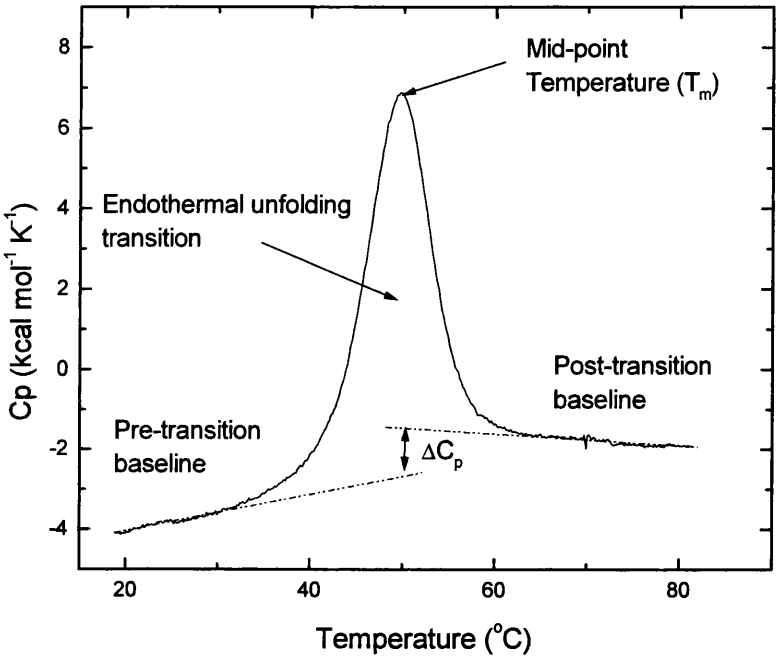

Figure 2.1 Typical DSC thermogram for the thermal unfolding of ribonuclease A at pH 3.0 and at a scan rate of 60°C/hr. The heat capacity (C_p) is given in kcal mol^{-1}K^{-1} (1 cal = 4.184 J).

The area underneath the transition peak of the DSC thermogram is a direct measure of the heat energy required to bring about the unfolding transition. This is called the calorimetric enthalpy (ΔH_{cal}). The shape of the transition can also be used to determine the van't Hoff enthalpy (ΔH_{vH}), which is an independent estimate of the enthalpy of the transition. The area underneath the C_p peak at any temperature, divided by the total area of the peak is used as a measure of the fraction or extent of unfolding that has occurred at that temperature. If a simple two-state model is assumed, the temperature variation of the fraction unfolded can

be related to the apparent enthalpy of the process using the van't Hoff equation (Cooper 1999a):

$$\left(\frac{\partial \ln K(T)}{\partial T}\right)_p = \frac{\Delta H_{vH}(T)}{RT^2} \qquad (2.2)$$

The advantage of this approach is that no information about the purity or concentration of the sample is required. Ideally, ΔH_{cal} and ΔH_{vH} should be identical in any calorimetric experiment, and comparison of them both can be quite revealing about factors such as the purity and concentration of the sample (Cooper 1999a).

In the data analysis here, the normalised excess heat capacity data were analysed in terms of both cooperative two-state and non-two-state unfolding models using Microcal Origin® v5.0 for DSC (OriginLab Corporation). Values for the van't Hoff and calorimetric enthalpies (ΔH_{vH} and ΔH_{cal}) obtained from this analysis were compared in order to evaluate the cooperativity of unfolding (Cooper 1999b).

2.4.4 ΔC_p analysis from pH variation method

Enthalpy (ΔH) is temperature dependent and can be related to the heat capacity changes (ΔC_p) by the equation:

$$\Delta H = \Delta H_R + \int_{T_R}^{T} \Delta C_p \cdot dT \qquad (2.2)$$

If ΔC_p is assumed constant and temperature independent, its relation to enthalpy can be simplified to:

$$\Delta H = \Delta H_R + \Delta C_p (T - T_R) \qquad (2.3)$$

Using this equation ΔC_p for protein unfolding can be calculated from the relationship between transition temperature (T_m) and unfolding enthalpy (ΔH) – plotting ΔH against T_m gives a straight line with gradient that is equal to ΔC_p (see Figure 2.2):

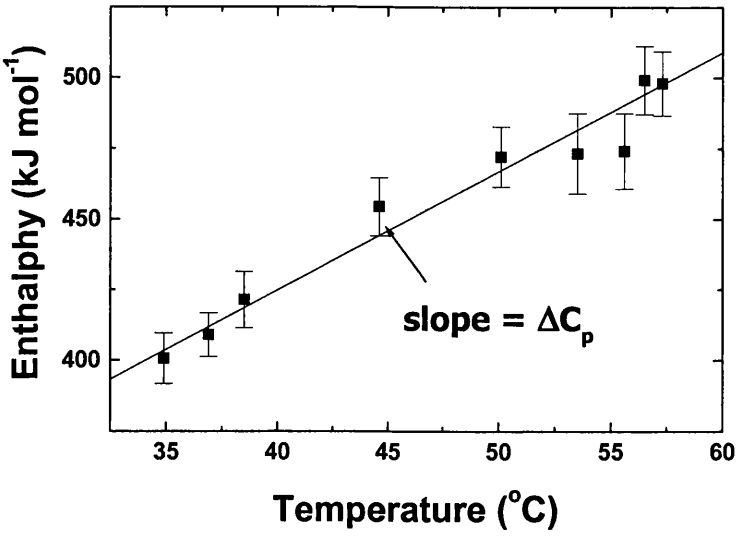

Figure 2.2 Example plot of unfolding enthalpy against unfolding transition temperature. Data presented in the graph is for lysozyme unfolding in 40% methanol v/v at the pH range from 2.1 to 5.0.

The usual way in which to achieve the variation of T_m and enthalpy of unfolding (ΔH) for the same protein is by changing the pH conditions, at which the unfolding reaction is monitored. Acquiring several data points (several DSC scans at different pH conditions resulting in different T_m) for the determination of the slope from the graph makes this method much more precise than evaluation of ΔCp from the single unfolding thermogram by calculating the difference between the pre- and post-transitional baselines C_p values.

This relies on the assumption that the changes in ΔH_{unf} arising from protonation of amino acid side-chains is negligible compared to other ΔC_p effects. This is normally valid in the acid pH range since ionisation heats for carboxylic acids (Glu, Asp) are small.

Chapter 3

PPC – THEORY AND BASICS OF THE METHOD

Outline

Chapter 3 covers

- Different calorimetric techniques enabling measurements of volumetric properties of substances
- Theoretical description of the method : the thermodynamic theory and derivation of the equations for data analysis calculations
- Description of the thermodynamics variables measured by the instrument and the ones that can be calculated and derived from the PPC measurements
- Detailed analysis of the equations used by the software
- Description of the method in practice
- Description of the hardware – how the machine works and how it is constructed
- Description of the software – how the measured data are transformed into meaningful thermodynamic qualities that can be easily interpreted
- Troubleshooting of a few theoretical considerations and problems arising in the PPC technique
- Analysis of errors associated with heat measurements and α determination

3.1 Introduction

The purpose of this chapter is to review the Pressure Perturbation Calorimetry as a calorimetric method in detail, to show how the instrument is built, how the measurements are done, and how the thermodynamic quantities are calculated from the raw data collected. The theoretical derivation of the equations used in the data analysis is also given.

At the end of 20th century there has been significant progress in commercially available instrumentation so that most of the thermodynamic quantities could be experimentally determined with high precision and accuracy, for example heat capacities using Picker type flow calorimeters, isentropic compressibilities from measurements of ultrasonic speed and densities by vibrating-tube densitometers (Reis et al. 2001).

Accurate measures of density provided a way to determine accurate partial molar volumes – volume itself is a thermodynamic quantity as it is the partial differential of the Gibbs energy with respect to pressure $(V=\partial G/\partial P)_T$. Thermal expansivity ($E^o$) is a derivative of volume with respect to temperature, hence it is a second derivative of Gibbs energy. Thermal expansion coefficient (α) is obtained by dividing expansivity by volume ($\alpha=E/V$), so it is also the second derivative of Gibbs energy.

All the volumetric properties are therefore considered to be pressure-related thermodynamic parameters. On the other hand, the parameters usually measured in calorimetric experiments (enthalpy, heat capacity) are temperature-related thermodynamic parameters. With the development of calorimetric techniques such as DSC, the temperature-related parameters have become easily available. As the volumetric parameters could so far only be obtained from densitometric methods, the information on pressure-related thermodynamic parameters was scarce.

Calculation of the thermal expansion coefficient before development of calorimetric pressure methods like PPC required measuring density as a function of temperature. Two approaches can be used: either several separate density measurements, each at constant temperature; or differential measurement of density with temperature increasing at constant rate (Differential Scanning Densitometry - DSD). The first method has been used to determine thermal expansion coefficient in a series of density measurements for thermal unfolding of protein staphylococcal nuclease (Seemann et al. 2001); the latter is in the early development, its precision still not good enough to use for applications to protein unfolding (Rosgen et al. 2002). The accuracy of densitometric measurements is generally much less than of that of calorimetric methods (Lin et al. 2002). While it is relatively easy to determine α values of pure liquids by these existing methods, their accuracy is not enough when trying to estimate α values for dissolved solutes present at low concentration in solution (MicroCal LCC 2003).

There was a need of direct calorimetric determination of isobaric expansibilities, instead of relying on densitometric measurements. In the last quarter of 20th century there have been parallel developments of instrumentation in Europe and America aimed to fulfil that need.

Although most work on biological macromolecules (including those described here) has used the MicroCal PPC system for obtaining volumetric properties such as expansibility data, it is useful to summarise some of the other calorimetric instruments now available for similar measurements.

In Europe, the development was led in the academic lab in France, starting with work on piezothermal technique, later developed into pressure-scanning and then into scanning transitiometry, the technique developed in cooperation between J.-P. Grolier at Université Pascal, Aubière, France and S. Randzio at Polish Academy of Science, Poland.

Scanning transitiometry enables simultaneous control of two of the three state variables (pressure, volume and temperature), while the third one is kept constant.

There are two contributions to the thermodynamic potential change resulting from the perturbation, and hence two outputs: thermal and mechanical, which are both measured.

For example, when the perturbation of the system is by changing the temperature under isobaric conditions, the measurement of both the heat flow and volume changes (used to keep the pressure constant) leads to the simultaneous determination of both C_p and $(\partial V/\partial T)_p$ as a function of temperature at a given pressure. In the case of the recording of both heat flow and pressure changes resulting from a volume change under isothermal conditions leads to simultaneous determination of both $(\partial S/\partial V)_T$ and $(\partial V/\partial P)_T$ (or temperature coefficient of pressure, see Maxwell relations, and isobaric compressibility) as a function of volume at a given temperature.

Simultaneous measurement of both heat flow and volume changes resulting from a pressure change under isothermal conditions leads to determination of both $(\partial S/\partial P)_T$ and $(\partial V/\partial P)_T$ (or isobaric thermal expansivity and isothermal compressibility) as a function of pressure at a given temperature." (Randzio 2000). Isobaric thermal expansivity can be converted to thermal expansion coefficient simply by dividing by the volume.

The latter corresponds to the PPC measurements where pressure is changed in isothermal mode; however the way the pressure is changed is different between the two techniques.

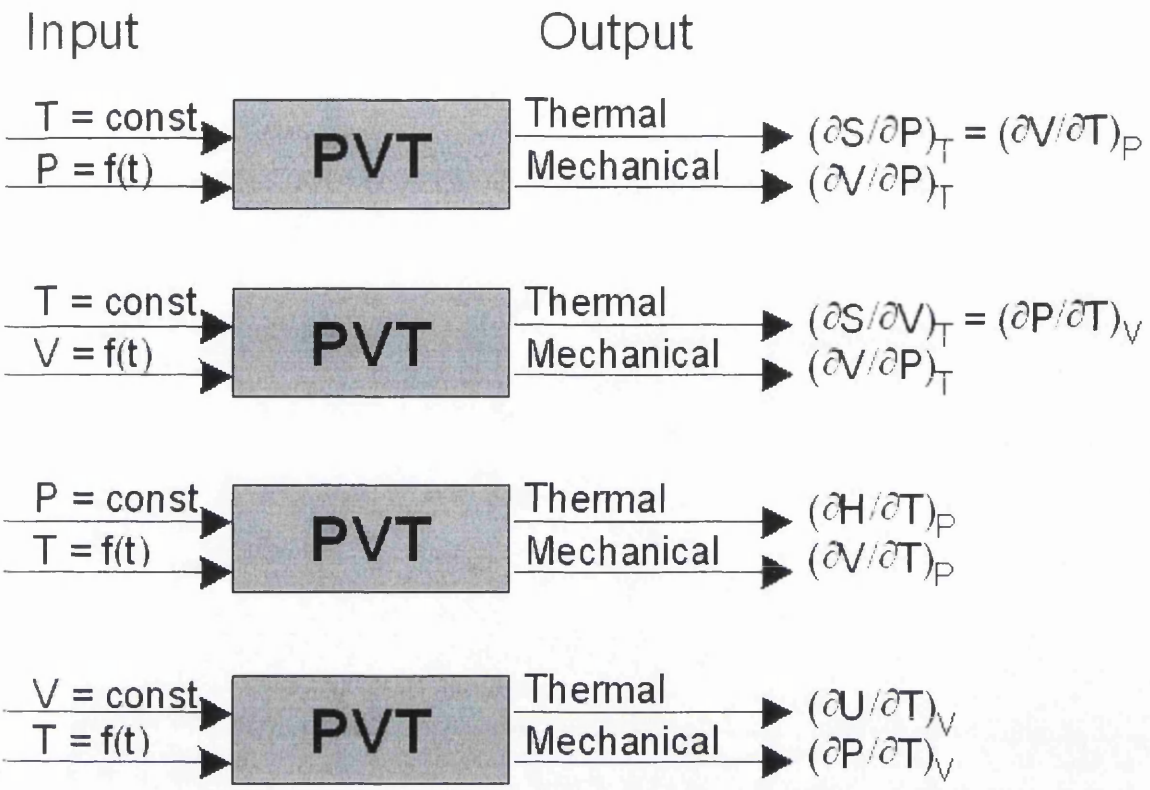

Figure 3.1 Scanning Transitiometry – a technique alternative to PPC.

The developers in Europe were mostly concerned about applications to phase transitions studies for physical chemistry and for the applications in industry, and the ones in America were concerned with applications in biocalorimetry (e.g. study of protein folding). They have been both unaware of each others developments until recently (Randzio 2003; Brandts and Lin 2004). Though they both developed calorimeters measuring the heat effects of the pressure changes, there are also substantial differences between the instruments in how the pressure is changed – in linear manner in the scanning transitiometer (up to high pressure of value about 400MPa), whereas in PPC the pressure is changed as a step-wise function of time, and pressure changes are very small, from 0.3 to 0.5 MPa, oscillating up and down to the atmospheric pressure and not increasing to any higher values of pressure.

The instruments developed in USA have been made commercially available around year 2000 and have been recently applied to several problems in biocalorimetry in research groups both in America and Europe. The scanning

transitiometer is more popular for investigating problems involving more industrial applications, and is used in several research groups in Europe, mainly in France.

Pressure Modulation Calorimetry (PMC) is a technique developed in the group of H.-J. Hinz at Westfälische Universität in Germany, which have also been used in some trial calorimetric measurements of volumetric properties of solutes. In this method the pressure changes are of the same magnitude as in PPC, up to 5 bar, but the modulation of pressure is continuous and applied during the DSC run, in contrast to PPC that uses pressure jumps to perturb the equilibrium. The other difference is that the continuous pressure oscillations are applied at the same time as the temperature increases at a constant rate, whereas in the PPC the pressure jumps are applied at the constant temperature.

Pressure modulation calorimetry has been applied to studying the lipid systems, however data analysis is still challenging due to complicated mathematical functions used to fit the experimental data (Rosgen et al. 2002) and the method has not been widely used.

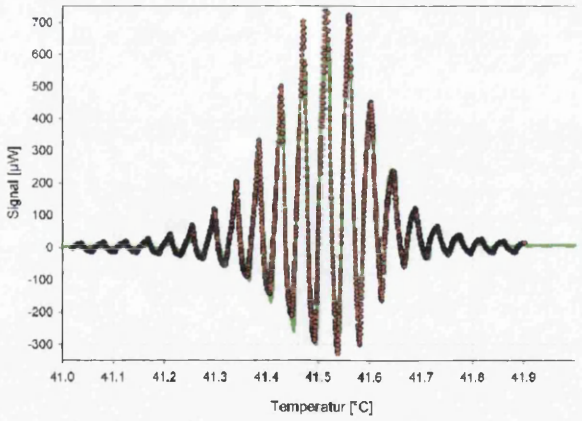

Figure 3.2 PMC-measurement on dipalmitoylphosphatidylcholine (DPPC) with a heating rate of 0.02 K/min in a pressure range of 0.3 to 5.3 atm (Hinz 2003)

3.2 Description of experimental setup - hardware

3.2.1 *Instrumentation*

Pressure Perturbation Calorimetry is a technique developed in 2000 by MicroCal™, a commercial company from USA. The company has specialised in microcalorimetry techniques for several years, and have developed PPC system based on their standard differential scanning calorimetry (VP-DSC) instrument by equipping it with the PPC accessory. The accessory is a pressurizing system, computer controlled by the software, which is an extended and modified version of DSC controlling software. The PPC accessory attaches to the DSC instrument and the cells in it are utilised for the measurement that is carried out.

There are two cells, both of equal active volume of 0.5161 ml (in the instrument used here), one for sample and one for reference solution. Any excess in heat that results from tiny differences in volumes between the cells is corrected by subtracting the heat values for solvent vs. solvent (e.g. buffer vs. buffer), in the same way as the DSC results are corrected by subtracting scans with buffer in both cells (Brandts and Lin 2004). (see the chapter 3.3.2 describing how the differences are corrected in equations used for calculating α)

3.2.2 *Description of a single PPC scan at constant temperature*

Both cells open to the same chamber with a pressure sensor. The pressure is applied to the chamber by opening the software controlled valve (in PPC accessory) connecting the chamber with a nitrogen cylinder (that is set to a required pressure value). That way both cells are pressurized to equal pressure and the pressure value is recorded by the sensor in the chamber.

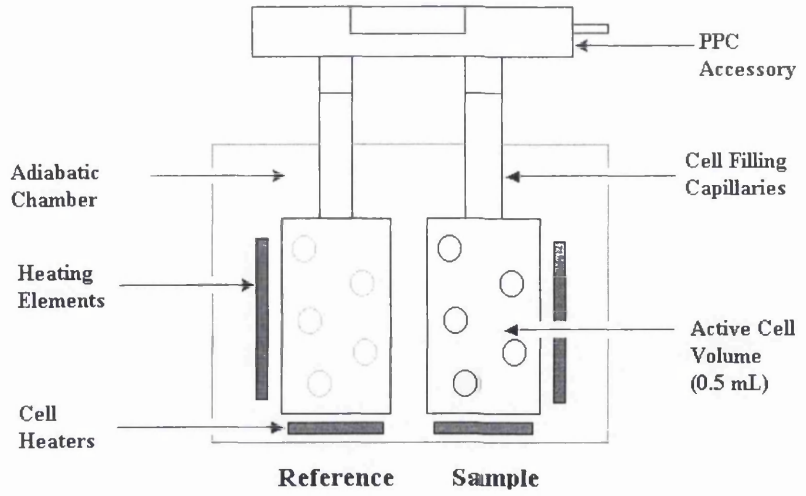

Figure 3.3 Schematic of a standard VP-DSC instrument equipped with a PPC accessory.

One PPC cycle comprises of two pressure changes at constant temperature. The cells are pre-equilibrated at constant temperature and elevated pressure of 5 bar (0.5 MPa) and the instrument is set in high feedback and low noise mode. The software initiates the first pressure change (pressure release) within a few seconds from the beginning of the isothermal scan. The pressure change causes heat release or uptake that is actively compensated by the instrument to keep the temperature of the cells constant. The differential heat changes between sample and reference cell are then recorded as a function of temperature. The compensation power returns to the baseline typically within one minute. The equilibration of the signal is automatically checked by "adjustable slope criterion" and when equilibrated, the second pressure change (compression) is applied by reconnecting the high pressure from the cylinder. The magnitude of the heat peaks should be the same value, but of the opposite sign.

This is the case for the majority of measurements, but not if the thermal properties between solvents in the sample and the reference cells are very different. For example, MicroCal has shown that for 2.8M guanidinium sulphate the heats of compressions are ca. 7% larger in magnitude than those of decompression when guanidinium sulphate solution was in the sample cell and pure water in the reference cell (MicroCal LCC 2001).

There are two possible explanations of the problem. The first one was provided by MicroCal (MicroCal LCC 2001). After investigating this lack of symmetry between compression and decompression heats the PPC manufacturers concluded that thermal properties between solvents in the sample and the reference cells are negligible and it is reasonable to assume that the average of the compression and decompression heats (after sign inversion of the decompression heats) corresponds to the true value, which would be obtained if the thermal properties did not differ (MicroCal LCC 2000b).

Another possible explanation is that compression and decompression are slightly different (they may be differently realised technically in the instrument). The compression takes a slightly longer time for the nitrogen gas to reach and compress the cells, whereas the decompression to atmospheric pressure is quicker. This may influence the differential response between the two cells in case of very different solvents.

This anomaly occurs when substantially different solvents are in the two cells and it has also been observed in my work in the case of mixed methanol-water solvents. The manufacturer of the PPC claims that this does not produce any significant problem in treating data as long as both compression heat and inverted decompression heat are used as data points at each temperature (MicroCal LCC 2000b) and I have accepted this assumption in my subsequent data analysis.

The software in the instrument records heat flow, temperature and pressure as functions of time, for both compression and decompression. This raw data is later analyzed by another software program (PPC routines in MicroCal Origin™) to yield heat changes for compression and decompression at the temperature of the scan.

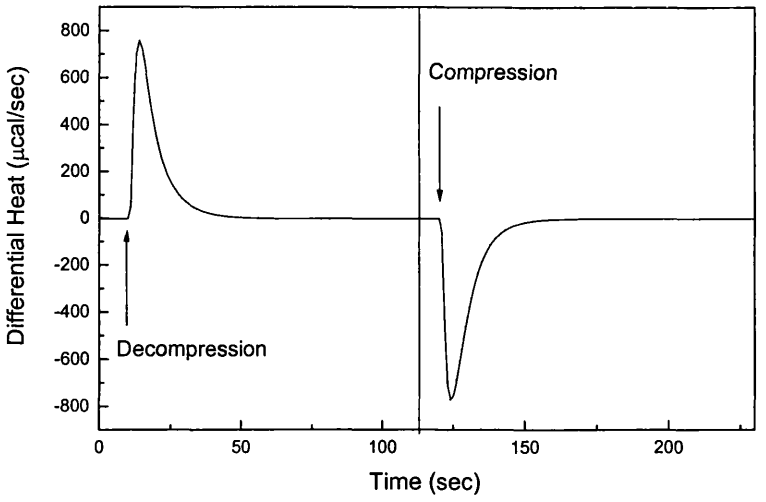

Figure 3.4 One PPC cycle comprises of decompression and compression.

3.2.3 *Temperature dependence of α*

At one particular temperature the PPC measurement yields two ΔQ data – one for compression and one for decompression, they should be the same in value but of the opposite signs.

To investigate the dependence of heats and alpha on the temperature, several such isothermal PPC cycles (scans) have to be carried out, each at different temperature. A series of ΔQ values for those temperatures is obtained and the temperature dependence of the heat values can be plotted. For each of those heats the corresponding value of α is calculated by the Data Analysis Software and its temperature dependence is plotted in the software program after carrying out the calculations.

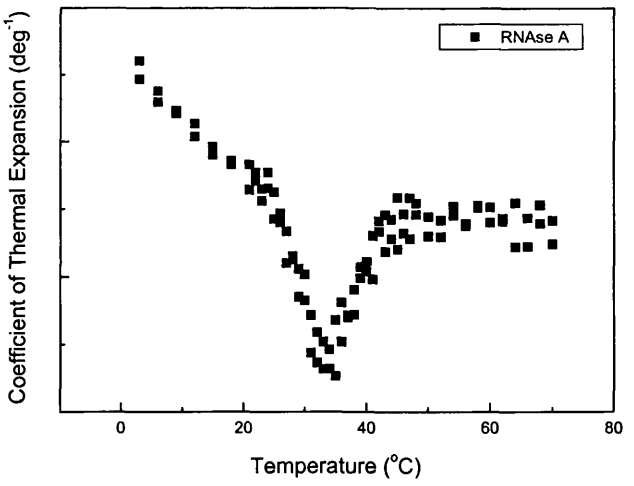

Figure 3.5 Temperature dependence of thermal expansion coefficient (α). The plot shows the temperature unfolding of the protein ribonuclease A in 20% methanol/water at pH=2.0.

The instrument software enables pre-programming the number of PPC scans and their temperatures, so that after completing one PPC cycle calorimeter heats up (or cools down) to a new desired temperature and the two pressure jumps are applied in the isothermal scan at the new temperature.

Typically, temperature is set to increase at certain intervals, for example for protein unfolding that would be every 3 or 5 degrees, but the instrument can be programmed in any way that is required. However care must be taken not to program more than 60 PPC cycles in one program, as the Data Analysis Software has difficulties to display the whole range of the scans for manual baseline corrections.

It can sometimes be confusing that the term "PPC scan" is used to mean two different things in the literature. First meaning is to describe a PPC cycle at constant temperature (sometimes referred to as an "isothermal scan"), the second one being a series of such PPC cycles, carried out at different temperatures. Such a series of PPC measurements is sometimes referred to as a "temperature scan" as its result, the temperature dependence of the heats (ΔQ) or thermal expansion

coefficients (α) can be seen as an equivalent of a DSC scan (temperature dependence of C_p).

Unlike a DSC scan, the PPC "temperature scan" is not one measurement, it is a series of isothermal PPC cycles, each comprising of decompression and compression heats of a sample.

3.3 PPC theory

The ultimate aim of PPC measurement is to determine the thermal expansion coefficient (α), which is a theoretically interesting property that can give us insight into microscopic properties of a solution. The experimentally determined properties are the differential heat (ΔQ) and pressure change (ΔP). To link with the experimentally derived properties an equation relating the differential heat (ΔQ) and the pressure change (ΔP) to the thermal expansion coefficient (α) of the molecule in solution equations had to be derived.

Thermodynamic equations used for the calculation of thermal expansion coefficient can be derived starting from general equations describing macroscopic properties of solutions such as Gibbs free energy, volume, compression and expansion. The equations that follow are adapted from the publications by Lin et al. (2002) Kujawa and Winnik (2001) and Batchelor et al. (2004).

3.3.1 *Derivation of an equation for calculating α from ΔQ and ΔP for pure liquids - for one component system in 1 cell*

Here the heat measured (ΔQ) is defined as the heat released by the pure liquid in the sample cell having a reference cell disconnected. It hence corresponds to the absolute heat measured for a pure liquid in the volume V (the active volume of the sample cell)[1].

This is given as a first part of derivation to illustrate the equation in the simpler, general form, before proceeding further in the next section to derive the equation for dilute solutions where the heat measured (ΔQ) denotes the heat difference between the sample cell and the reference cell.

From the definition of entropy it is known that the heat change dQ for a reversible process carried out at constant temperature T is related to the entropy change dS

[1] It is not practically possible to carry out such measurement with the commercial instrument; such measurements were however carried out by Lin et al. at the manufacturer's site, where such instrument modifications were possible.

$$dS = \frac{dQ}{T} \tag{3.1}$$

Differentiation of that equation with respect to pressure P at constant temperature T gives:

$$\left(\frac{\partial Q}{\partial P}\right)_T = T\left(\frac{\partial S}{\partial P}\right)_T \tag{3.2}$$

Using the Maxwell relation, $\left(\frac{\partial S}{\partial P}\right)_T = -\left(\frac{\partial V}{\partial T}\right)_P$ and substituting into Eq. 3.2 one obtains

$$\left(\frac{\partial Q}{\partial P}\right)_T = -T\left(\frac{\partial V}{\partial T}\right)_P \tag{3.3}$$

Substituting the coefficient of thermal expansion of the system that is defined as

$$\alpha = \frac{1}{V}\left(\frac{\partial V}{\partial T}\right)_P \tag{3.4}$$

into the equation 3.3 gives

$$\left(\frac{\partial Q}{\partial P}\right)_T = -TV\alpha \tag{3.5}$$

Here V is the total volume of the measured system that corresponds to the active volume of a cell in the instrument. It can be assumed that V and α are nearly invariant with a small pressure change (5 bar = 0.5 MPa). Then the integration of the Eq. 3.5, at the constant T, over a small pressure change ΔP, gives

$$\Delta Q = -TV\alpha\Delta P \tag{3.6}$$

The equation 3.6 can be rearranged to provide a working expression for calculating α:

$$\alpha = -\frac{\Delta Q}{T\Delta PV} \tag{3.7}$$

This is an equation in general form for one-component system. It describes how the coefficient of thermal expansion (α) of a pure liquid can be determined from a measurement of heat (ΔQ) released or consumed by a sample of the total volume (V). The measured heat is caused by a small pressure change (ΔP) at a constant temperature (T).

3.3.2 *Derivation of an equation for calculating α from ΔQ and ΔP for dilute solutions - for 2 component system in 2 cells*

Here ΔQ is the heat difference between sample cell containing sample solute dissolved in a solvent and the reference cell containing the pure solvent (usually water) upon the pressure changes ΔP.

To simplify this part of equation derivation the assumption is made that the active volumes of the cells are identical. In reality there are always tiny differences between the volumes of the cells, and this will be discussed at the end of this section.

When a solution is formed by dissolving a solute of mass m_S in a solvent of mass m_0 the total volume V of the solution is given by an equation

$$V = m_0 V_0 + m_S \overline{V} \qquad (3.8)$$

where $\overline{V}$ is the partial specific volume of the solute of mass m_S in solution and V_0 is the specific volume of pure solvent of mass m_0.
Assuming that the sample and the reference cells have identical active volumes, the only difference between them is that the volume occupied by the solute in the sample cell (black circles in the figure 3.3) is occupied by the solvent in the reference cell (dotted circles in the figure 3.3), i.e. the volume described by the term $m_S \overline{V}$ in the reference cell is occupied by the solvent, whereas it is occupied by the solute in the sample cell.

Hence the differential heat measured between the cells comes from different substances occupying the tiny volume $m_S \overline{V}$ as the contributions from the pure solvent volume $m_0 V_0$ cancel out between the cells.

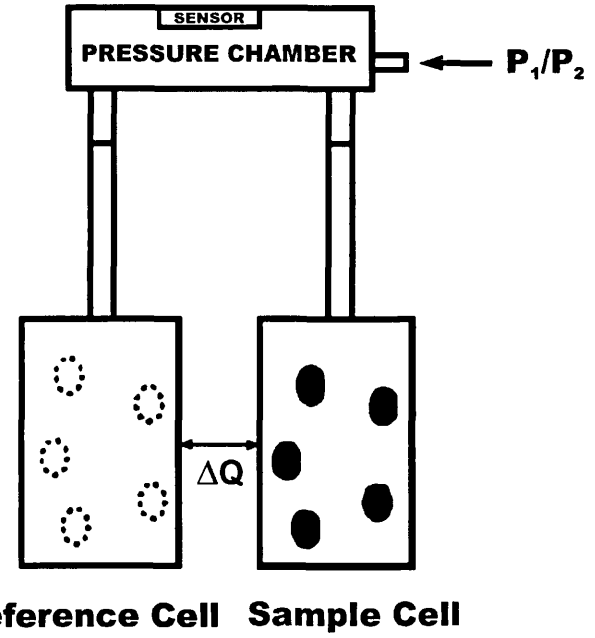

Figure 3.6 Schematic representation of PPC. The black circles in the sample cell indicate the volumes occupied by the solute molecules, whereas the dotted circles in the reference cell indicate the same volumes occupied by the buffer instead.

If we substitute the volume from which the heat differences between the cells arise ($m_S\overline{V}$) for the volume V in Eq. 3.7, the differential thermal expansion coefficient determined in the PPC experiment (α_{exp}) can be written as follows:

$$\alpha_{exp} = -\frac{\Delta Q}{T\Delta P m_S \overline{V}} \tag{3.9}$$

Below is the derivation to show how this differential thermal expansion coefficient is used to calculate the absolute thermal expansion coefficient (α) of a solute in solution.

Differentiating the equation 3.8 with respect to temperature at constant pressure gives

$$\left(\frac{\partial V}{\partial T}\right)_P = m_0\left(\frac{\partial V_0}{\partial T}\right)_P + m_S\left(\frac{\partial \overline{V}}{\partial T}\right)_P \tag{3.10}$$

After substituting the right-hand side of Eq. 3.10 into Eq. 3.3 one obtains

$$\left(\frac{\partial Q}{\partial P}\right)_T = -T\left[m_0\left(\frac{\partial V_0}{\partial T}\right)_P + m_S\left(\frac{\partial \overline{V}}{\partial T}\right)_P\right] \tag{3.11}$$

Substituting the definition of the thermal extension coefficient (Eq. 3.4) for α_0 and α into the above equation gives

$$\left(\frac{\partial Q}{\partial P}\right)_T = -T\left[m_0 V_0 \alpha_0 + m_S \overline{V} \alpha\right] \qquad (3.12)$$

where α_0 and α are the coefficients of thermal expansion of solvent and the solute, respectively.

According to Eq. 3.12, the heat arising from pressure perturbation of a solution can be viewed as the sum of heats arising from the perturbation of the solvent and from the perturbation of the solvated protein.

Two absolute heats that are the responses to the pressure perturbation of the two cells can be defined, the response of the sample cell (Q) and the response of the reference cell (Q_{ref}). In the PPC experiment, they are not measured separately, the measured heat is the differential value between the two cells ($\Delta Q = Q - Q_{ref}$).
To derive the equation describing the absolute heat (Q) resulting from the pressure perturbation of a two component solution, contained within the sample cell, the Eq. 3.12 must be integrated over a small pressure range. That gives

$$Q = -T\left[m_0 V_0 \alpha_0 + m_S \overline{V} \alpha\right]\Delta P \qquad (3.13)$$

The volume occupied by the solute in the sample cell is described by the ($m_S \overline{V}$) term. The whole volume of the reference cell is occupied by the solvent, both the volume corresponding to the volume of the solvent in the sample cell ($m_0 V_0$) and the volume corresponding to the solute volume ($m_S \overline{V}$). Hence the heat arising from the pressure perturbation in the reference cell can be written as

$$Q_R = -T\left[m_0 V_0 \alpha_0 + m_S \overline{V} \alpha_0\right]\Delta P \qquad (3.14)$$

– an equation corresponding to Eq. 3.13, the sum of heats arising from the two component volumes, but of the same substance – the solvent. It can be noticed the only difference between the two equations is that the thermal expansion

coefficient of the solute (α) is substituted with thermal expansion coefficient of the solvent (α_0) in Eq. 3.14, as the heat contribution from the volume described by factor comes from the solvent in this case, not from the solute.

In the differential calorimetric experiment both cells are subject to the same ΔP, the net heat ΔQ between cells will be equal to the difference between Eq. 3.13 for the sample cell and Eq. 3.13 for the reference cell and can be written as follows:

$$\Delta Q = Q - Q_R = -T\Delta P\left[m_S \overline{V}\alpha - m_S \overline{V}\alpha_0\right] \qquad (3.15)$$

this can be rearranged into:

$$\alpha = \alpha_0 - \frac{\Delta Q}{T\Delta P m_S \overline{V}} \qquad (3.16)$$

As the second term on the right hand side is the thermal expansion coefficient measured in the experiment (α_{exp}) (see Eq. 3.9), then the absolute thermal expansion coefficient of the solute (α) is a sum of α_{exp} and the thermal expansion coefficient of a solvent (α_0):

$$\alpha = \alpha_0 + \alpha_{exp} \qquad (3.17)$$

If the solvent is pure water, then α_0 is given by thermal expansion coefficient of water (α_{H_2O}). α_{H_2O} can be calculated from the polynomial equation E(T), previously obtained by fitting literature data (Kell 1967)

$$\alpha_{H_2O} = -\frac{E(T)}{T} \qquad (3.18)$$

where T is the absolute temperature and E(T) is the function of temperature ($E(T) = -\alpha_{H_2O} \cdot T$) that was fitted to the polynomial equation:

$$E(T) = 0.01821 - 0.00476\,T + 5.25126 \times 10^{5}\,T^2 - 6.66512 \times 10^{7}\,T^3 + 4.45806 \times 10^{9}\,T^4 - 1.265 \times 10^{11}\,T^5 \qquad (3.19)$$

If the solvent is other than water, then the absolute thermal expansion coefficient of this solvent (α_0) (for example buffer) has to be determined in the PPC experiment against water. It is the only way to determine the absolute thermal expansion coefficient α of the solute in the solvent other than water by carrying

out additional PPC experiment of that solvent against water to measure the absolute α_0 of that solvent $(\alpha_0)_{exp}$.

$$\alpha_0 = \alpha_{H_2O} + (\alpha_0)_{exp} \tag{3.20}$$

In the case of solvent against water PPC experiment (usually buffer-water), the volume that contributes to the heat effect is the whole active volume of the cell (V) so that the equation for $(\alpha_0)_{exp}$ is different than Eq. 3.9, and V is used in place of $m_S\overline{V}$:

$$(\alpha_0)_{exp} = -\frac{\Delta Q}{T\Delta PV} \tag{3.21}$$

Correcting for volume differences between the cells

There are three reference measurements that have to be conducted. They are required because the heat effects of the solvent (buffer) and water must be taken into account to accurately calculate the α value for a solute (MicroCal LCC 2001).

The three additional experiments are:
(1) buffer vs. buffer (B/B)
(2) buffer vs. water (B/W)
(3) water vs. water (W/W)

It is usual to refer to the sample cell first and then the reference cell when naming the scans, so "buffer vs. water" (or "buffer – water" or B/W) means buffer in the sample cell and water in the reference cell and "sample vs. buffer" (or "sample – buffer" or S/B) means sample in the sample cell and buffer in the reference cell.

For derivation of the equations the assumption was made that the active volumes of the sample and the reference cells are identical. In reality this is impossible to achieve technically – there will always be minor differences in volume between the cells. Thus the heats measured by PPC have to be corrected, to take into account the heat effects resulting from these volume differences. Such corrections are done in the same way as the standard procedure for DSC measurements – the

differential heats are corrected by subtracting the heats of the experiment with only the solvent in both cells (either buffer-buffer or water-water).

Taking this correction into account the equation for experimentally measured thermal expansion coefficient can be written by modifying the equation 3.9

$$\alpha_{exp} = -\frac{\Delta Q_{SB} - \Delta Q_{BB}}{T\Delta P m_S \overline{V}} \tag{3.22}$$

Where ΔQ_{SB} is the differential heat in the sample-buffer PPC experiment and ΔQ_{BB} is the differential heat in the buffer-buffer PPC experiment.

The same correction has to be applied to buffer-water PPC experiment that is carried out in order to determine the thermal expansion coefficient of the buffer (solvent) (α_0). Here the heats of water-water PPC experiment have to be subtracted:

$$\Delta Q = \Delta Q_{BW} - \Delta Q_{WW} \tag{3.23}$$

Where ΔQ_{BW} is the differential heat in the buffer-water PPC experiment and ΔQ_{WW} is the differential heat in the water-water PPC experiment.

Substituting the above equation into Eq. 3.21 and combining with Eq. 3.20 the corrected equation for calculating α_0 is obtained:

$$\alpha_0 = \alpha_{H_2O} - \frac{\Delta Q_{BW} - \Delta Q_{WW}}{T\Delta PV} \tag{3.24}$$

By substituting Eq. 3.18 for α_{H_2O} into the above equation the following equation is obtained

$$\alpha_0 = -\frac{\Delta Q_{BW} - \Delta Q_{WW} + E(T)\cdot V\cdot \Delta P}{T\cdot V\cdot \Delta P} \tag{3.25}$$

In the end the above equation is combined with Eq. 3.22 and Eq. 3.17 to obtain the final equation for calculating α of a solute in solvent other that water (usually a buffer) that is corrected for differences in volume between the cells:

$$\alpha = -\frac{\Delta Q_{SB} - \Delta Q_{BB}}{T\Delta P m_S \overline{V}} - \frac{\Delta Q_{BW} - \Delta Q_{WW} + E(T)\cdot V\cdot \Delta P}{T\cdot V\cdot \Delta P} \qquad (3.26)$$

As the mass of the solute, m_S, is obtained by multiplying its concentration (in g mL^{-1}) by the active cell volume (in mL). Then $m_S = C\cdot V$ is substituted for the mass of the solute in Eq. 3.26, where C is the concentration of the solute and V is the active volume of the cell.

After the final rearrangement of Eq. 3.26 the equation that is used in the software provided by the manufacturer can be obtained:

$$\alpha = -\frac{\Delta Q_{SB} - \Delta Q_{BB} + C\cdot \overline{V}\cdot\left(\Delta Q_{BW} - \Delta Q_{WW} + E(T)\cdot V\cdot \Delta P\right)}{T\cdot C\cdot \overline{V}\cdot V\cdot \Delta P} \qquad (3.27)$$

All the calculations are carried out by the manufacturer's software package based on MicroCal Origin ™.

Assumptions

A. Pressure - independent

For the integration of Eq. 3.5 it is assumed that volume (V) and thermal expansion coefficient (α) are almost invariant over a small pressure change. This is a good approximation for all liquids.

It was however argued by Wang (2004) that for the measurements of the phase transitions in lipids the small shifts in temperature result in large changes in α. Then in order to consider α as constant in Eq. 3.5 it should be corrected for small shifts in temperature that result from the pressure perturbation. This procedure is argued to be necessary to obtain the correct value of α. The analysis of how the precision of determination of temperature during the PPC scan influences the error of α value has been carried out in section 3.5.3 and it is shown there that such corrections are unnecessary.

Such corrections are not a standard practice and are not included in the automatic calculations done by software provided by manufacturer and were not included in this work.

B. Temperature - independent

The assumptions are made during the above derivations that the active volume of the cell (V), the partial volume of the solute ($\overline{V}$) and the solute concentration (C) are the variables that are independent of temperature.

In reality there is slight temperature dependence for those variables.

1. The changes in cell volume are related to the expansion of the cell with temperature. As the cell is made of tantalum, with thermal expansion coefficient of only $2x10^{-5}$ K^{-1}, then the changes of the cell volume in the studied temperature range 0-100°C are negligible.
2. The partial volume of the solute ($\overline{V}$) increases with temperature in accordance with its thermal expansion coefficient.
3. The solute concentration (C in moles L^{-1}) is decreasing with temperature, as the solution expands and less of it is included in the active volume of the cell.

The last two parameters work in opposite directions and tend to cancel each other. According to the instrument's manufacturer the error introduced by these parameters in the determination of α is only about 1% over the temperature range 0-100°C (MicroCal LCC 2003).

3.4 Description of experimental setup – Software

3.4.1 *Equations and Unit Conversion Factors*

The calculation of α of a solute from PPC measurements requires knowledge of the following parameters: solute concentration (C in mg/mL), pressure change (ΔP in PSI), the solute's partial specific volume ($\overline{V}$ in mL g^{-1}), and the active cell volume (V in mL). The PPC measurement yields the values of the heats of the sample vs. buffer (ΔQ_{SB}) and the values of the heats of the three reference measurements (ΔQ_{BB}, ΔQ_{BW} and ΔQ_{WW}), at exactly the same temperature as the ΔQ_{SB} value are required. Having all those experimental values available, the thermal expansion coefficient α of a solute under the study can be calculated using the equation 3.27.

However, this equation only works if all the values are in SI units. The MicroCal instrument is calibrated in non-SI units, microcalories per seconds and the integration of the raw scan data yields microcalories.

$$1\ \mu cal = 4.184 \cdot 10^{-6}\ J$$

Throughout this work data will be used in these units, but converted to Joules when necessary.

To convert the non-SI units of concentration, volume, pressure and heat into units that will cancel out and give the resulting unit for α of K^{-1} the following conversion factors are used by the software:

Variable	Input unit	Converted to unit	By multiplying by factor
C	mg/mL	g/mL	10^{-3}
V	mL	L	10^{-3}
ΔP	PSI	atm	1/14.7
$\Delta Q = V \cdot \Delta P$	L·atm	μcal	$24.2 \cdot 10^{-6}$

Table 3.1 The unit conversion factors used by the PPC data analysis software.

The software uses the equation with those conversion factors embedded, so there is no need to do separate unit conversions:

$$\alpha = -\frac{\Delta Q_{SB} - \Delta Q_{BB} + C \cdot 10^{-3} \cdot \overline{V} \cdot \left(\Delta Q_{BW} - \Delta Q_{WW} + E(T) \cdot V \cdot 10^{-3} \cdot \frac{\Delta P}{14.7} \cdot 24.2 \cdot 10^{6} \right)}{(T + 273.15) \cdot C \cdot 10^{-3} \cdot \overline{V} \cdot V \cdot 10^{-3} \cdot \frac{\Delta P}{14.7} \cdot 24.2 \cdot 10^{6}} \qquad (3.28)$$

In a given PPC measurements four data sets of ΔQ are obtained as a function of temperature: sample vs. buffer (S/B), buffer vs. buffer (B/B), buffer vs. water (B/W) and water vs. water (W/W). The three latter are the control measurements and they are each fitted to a second-order polynomial function of temperature in the form $\Delta Q(T) = A + B \cdot T + C \cdot T^2$ where T is the temperature (°C).

Below are the three equations that describe the temperature dependence of the heats of:

- buffer vs. buffer

  $\Delta Q_{BB}(T) = A_{BB} + B_{BB} \cdot T + C_{BB} \cdot T^2$ (3.29)

- buffer vs. water

  $\Delta Q_{BW}(T) = A_{BW} + B_{BW} \cdot T + C_{BW} \cdot T^2$ (3.30)

- water vs. water

  $\Delta Q_{WW}(T) = A_{WW} + B_{WW} \cdot T + C_{WW} \cdot T^2$ (3.31)

Fitting the reference measurements to the functions of temperature makes possible the calculation of the values for the heats ΔQ_{BB}, ΔQ_{BW} and ΔQ_{WW} from the polynomial fits at exactly the same temperature as the value of ΔQ_{SB} is obtained, hence making the calculation of α dependent on only two values: ΔQ_{SB} and T. All the other values in the equation 3.28 are assumed to be constant for a given PPC experiment.

3.4.2 *Data Analysis in Practice*

To obtain the easy to interpret data like that of thermal expansion coefficient, the raw data recorded by the instrument have to be analysed. The file for each PPC cycle records the heat flow (dQ/dt), temperature (T) and pressure (P) as functions of time. If the scans are repeated at different temperatures, there are several files that have to be analysed, as each of PPC cycles produces one file.

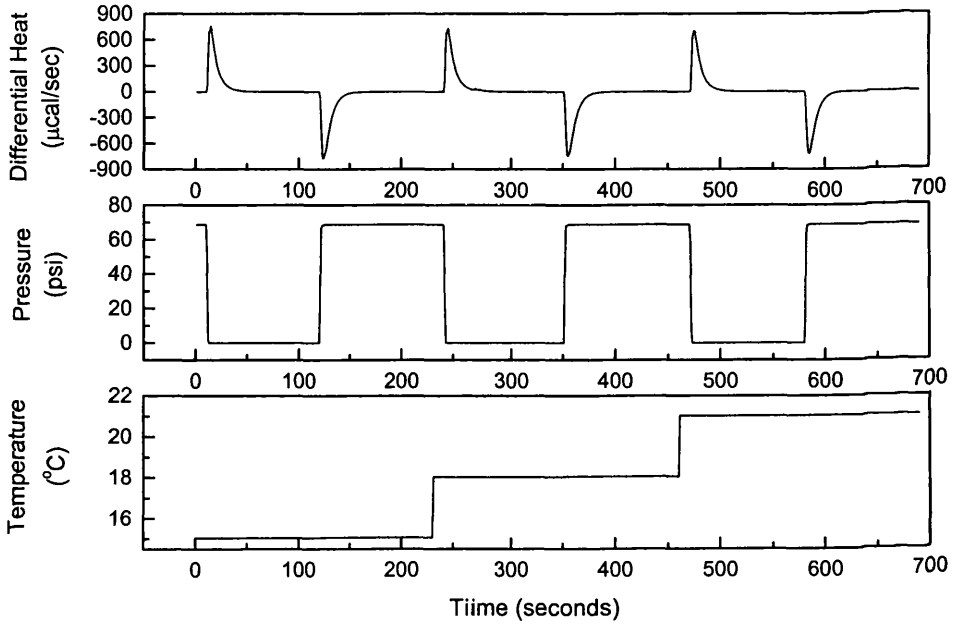

Figure 3.7 Data represented in a raw file recorded by the instrument for three PPC cycles.

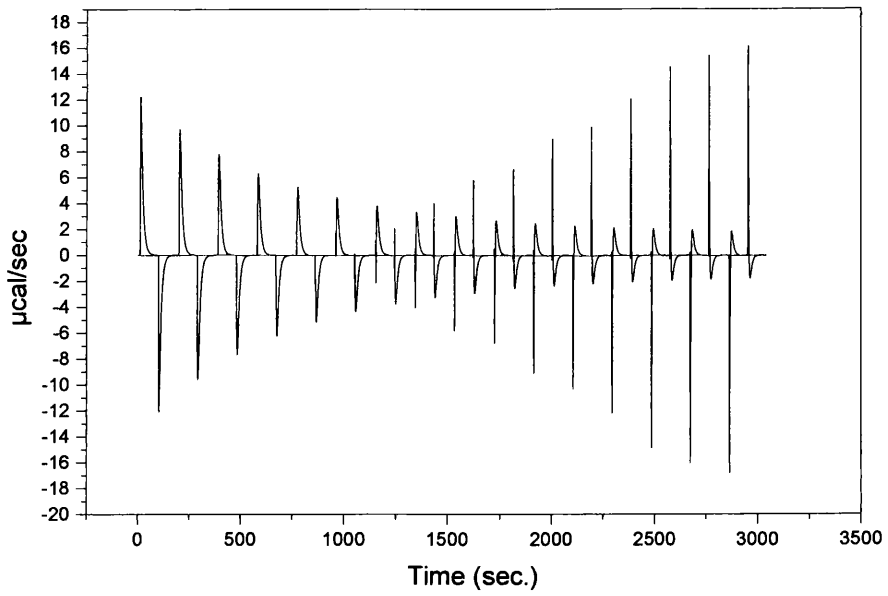

Figure 3.8 The raw data obtained upon pressure perturbation of 50 mM glycine buffer at pH = 2.0 at increasing temperature (from 5 to 80°C) at 5°C increments. Measurements were made with buffer in the sample cell and pure water in the reference cell. Pressure perturbations of ± 5 atm were applied to the cells, and data were collected at 1-second intervals. There are 16 PPC cycles

The producers of the instrument have provided data analysis software that provides automated solution to both reading and analysing several files at once. The software is based on MicroCal Origin™, which is a general purpose scientific and technical plotting and data analysis tool. Add-on routines to Origin were specifically designed by the instrument producer to deal with the analysis of PPC data. In the typical application of scanning the sample across the range of temperatures, there are 3 steps to be carried out in the data analysis process (or only 2 if there is no transition for which the volume change can be calculated):

Step 1 – Importing raw data files and obtaining heat values at different temperatures.

Step 2 – Reading the heat vs. temperature files and obtaining thermal expansion coefficient (α) values.

Step 3 – Calculating the volume change for the process taking place when the temperature is changed.

Step 1 – Obtaining heat values.

In the first step the raw data files are imported into the software. Several files recorded at different temperatures are merged and analysed one after the other automatically. The software assigns the baseline to which the integration is performed, and the result (areas under the peaks) yields the heats of compressions and decompressions. The sign for negative values is reversed, and the heat values are plotted as a function of temperature. The obtained values then have to be saved as a separate file, to be used in step 2 of the analysis. The procedure has to be carried out for both sample vs. buffer scan, as well as for the reference scans.

Troubleshooting 1: Pressure differences between scans.

One problem is that all four scans (the reference ones and the sample vs. buffer) should be carried out at the same pressure (which is set at the nitrogen tank valve). It is sometimes practically impossible, for example when the tank has to be changed to a new one and it is unattainable to set it at the exactly the same pressure. As the equation used by the software requires the heats in all datasets to come from the same pressure change (ΔP_1), the heats obtained at the different pressure (ΔP_2) can be recalculated for use at ΔP_1. Since the heat effects are directly proportional to the pressure they can be converted for use at ΔP_1 simply by multiplying the heats by $\Delta P_1/\Delta P_2$ (MicroCal LCC 2001). The software however does not provide such an utility, the user has to be aware of the pressure differences and the calculations have to be carried out manually.

Troubleshooting 2: Automatic integrations to obtain heat values.

The PPC manufacturers claim that "for reasonably good data, Origin makes a very good guess on the baseline, the range to integrate and the initialisation of the fitting parameters." (MicroCal LCC 2001) However, these factors can, and in fact should be, adjusted, or at least checked manually.

The software does a good job at assigning integration baseline automatically when the peaks are big and the signal baseline is quite flat and without much noise.
If there is any noise, or if the signal baseline is consistently dropping or rising (as happens sometimes at the region of transition in the case of protein folding), the

automatic baseline sometimes does not fit the signal baseline, and that can produce a significant and systematic error. It makes a big difference to the obtained values, the correction of the baseline can change the heat value that results from integration by 1-1.5 μcal, that is especially important when the peaks are small i.e. around 5-10 μcal. The correction of wrongly assigned baseline can prevent the error of 15% in that case. As this situation often happens where the data is most significant - at the region of the transition, it should be therefore highly recommended to check the automatic baseline assigned by the software and integrate to manually assigned baseline for the peaks where the software guess is not that accurate.

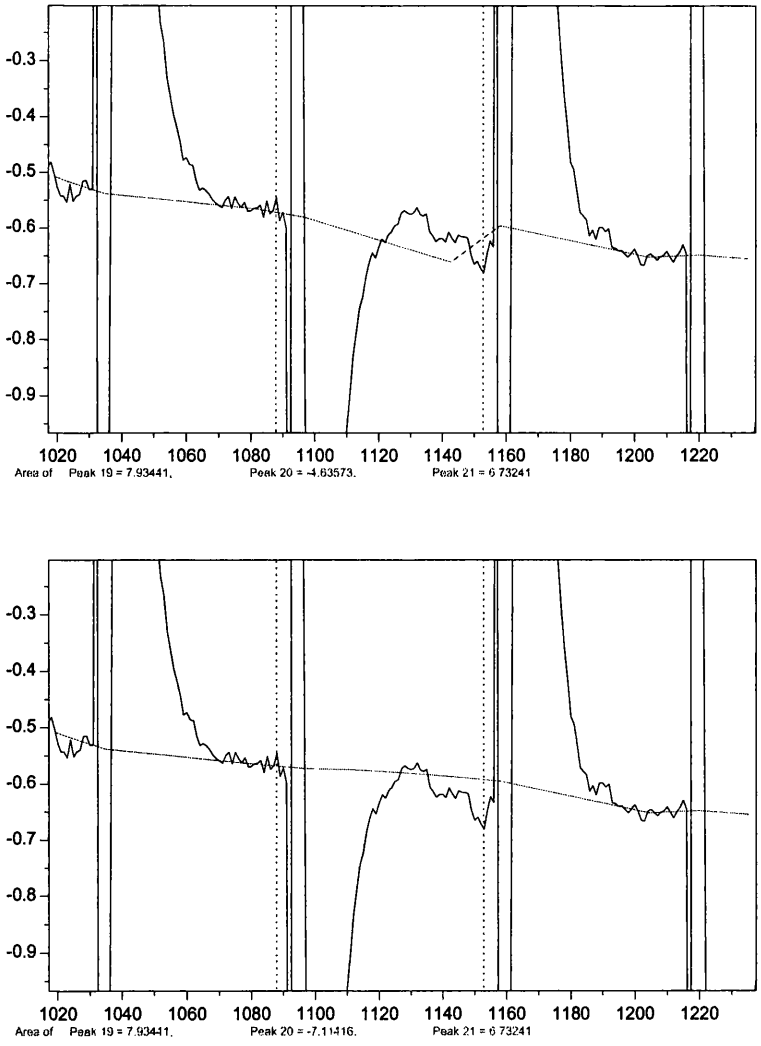

Figure 3.9 An example of wrongly assigned baseline by the software algorithm: The middle peak is for compression, and the baseline correction changes the heat value from -4.64 to -7.11 μcal. The corrected value agrees with the value of decompression heat (on the left) of 7.93 μcal at the same temperature. In this

example the heat calculated from integration to automatically assigned baseline would result in 35% error.

Step 2 – Obtaining thermal expansion coefficient (α) values.

First, the data obtained in the Step 1 must be imported, not only for the sample vs. buffer scan, but for all three reference scans, which must be taken into account during the calculations. The heats are then fed into equation 3.28 in section 3.4.1 describing how the calculations are done in the software. In order to proceed with the calculations, the reference scans must be fitted to the functions of temperature.

Troubleshooting 3: Fitting the reference scans.

Sometimes the fitting can be problematic, as often the buffer vs. water scans, the ones with biggest values and biggest influence on the final value of α, are not well described by second order polynomial function. The function curvature requires the fitting function to be a third order polynomial in order to describe the temperature dependence accurately. It was also recognized by MicroCal researchers when they have published a paper on PPC study of amino acids in water (Lin et al. 2002), there the thermal expansion coefficients of different amino acids were fitted to third order polynomials, however the PPC software provided with the instrument was developed a few years earlier and does not provide such functionality, supposedly because the authors were not yet aware that the second order fits are not suitable.

A way around this software problem that was adopted here is still using second order fits, but carrying out the calculations for lower and higher temperature regions separately. Fitting only one half of the temperature range to the second order polynomial, provides more accurate results than calculating α the reference scan fitted to one function across the whole temperature range. Ideally the routines in the software should be rewritten to enable fitting the heats of the reference measurements with higher accuracy of the 3rd order polynomial fits. The inaccuracy in fitting the second order polynomial function to the buffer water heats is especially profound for the buffers that are very different than water, and

which are characterized by the big heat values relative to the sample buffer heat values.

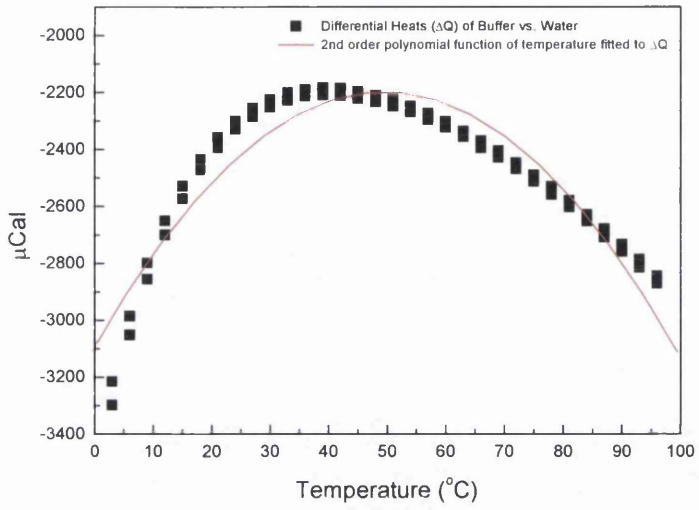

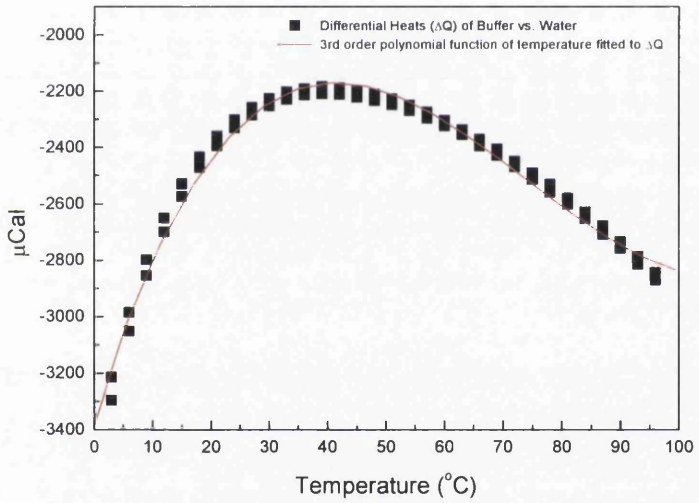

Figure 3.10 Second and third order polynomial fit to the buffer vs. water heat values temperature dependence

After fitting the polynomial functions to the reference heat values, the calculation can be carried out. Prior to starting the calculation, the software brings the dialog box to confirm, edit or input the conditions of the experiment that were saved in the raw data files when the experiment was run:

- solute concentration C [mg/mL]
- pressure change ΔP [PSI]

- solute partial specific molar volume $\overline{V}$ [mL/g]
- cell volume V [mL] (for the instrument used in Glasgow = 0.5161)

The software also asks for confirmation of the coefficients of the 2nd order fits to the reference scans, and then proceeds to perform the calculations of thermal expansion coefficient as a function of temperature and plots the data in the final graph.

Step 3 – Calculating the volume change.

If the process under study undergoes a transition with increase in the temperature, and that transition produces a peak in the plot of the coefficient of thermal expansion vs. temperature, then the fractional volume change of that transition can be calculated by integrating the area under the curve. The area under the curve equals

$$\int \alpha_P dT = \int \frac{1}{V}\left(\frac{dV}{dT}\right) dT \qquad (3.32)$$

If we assume ΔV^o is small compared to V^o, and that V^o is essentially constant over the integration range, then

$$\int \alpha_P dT = \frac{\Delta V^0_{unf}}{V^0} \qquad (3.33)$$

The value of ΔV^o can be expressed as a percent of the partial volume of the studied solute V^o. If the value of V^o is known, then the absolute value of the volume change ΔV^o can be calculated by multiplying the fractional volume change by the V^o value.

The integration is carried out in the temperature region where the transition occurs. For protein thermal unfolding (and also for some other processes) this can be determined from the DSC scan, in which the transition peak usually correlates well with the peak in the PPC scan (it was the case in all the samples studied so far).

Troubleshooting 4: Defining the beginning of an unfolding transition.

In cases where the DSC scan is not available, the beginning and the end of the transition region needs to be determined from the PPC trace alone and this can sometimes be difficult. An example of this is shown in the Figure 3.11.

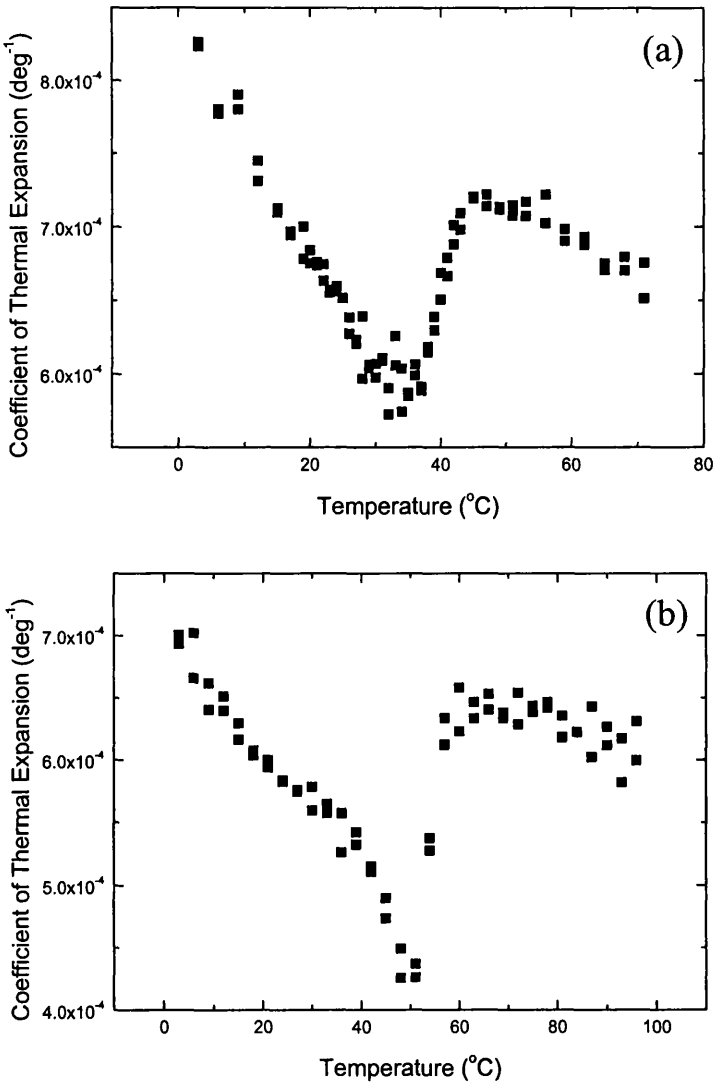

Figure 3.11 It is hard to define where the unfolding transition begins from the PPC measurement alone. (a) PPC of ribonuclease A unfolding at pH = 2.0 (b) PPC of lysozyme unfolding at pH=2

The baseline is assigned by projecting the pre-transition and post-transition baselines into the transition region and using these extended lines to from a progress baseline, as shown by the dashed line in the Figure 3.12.

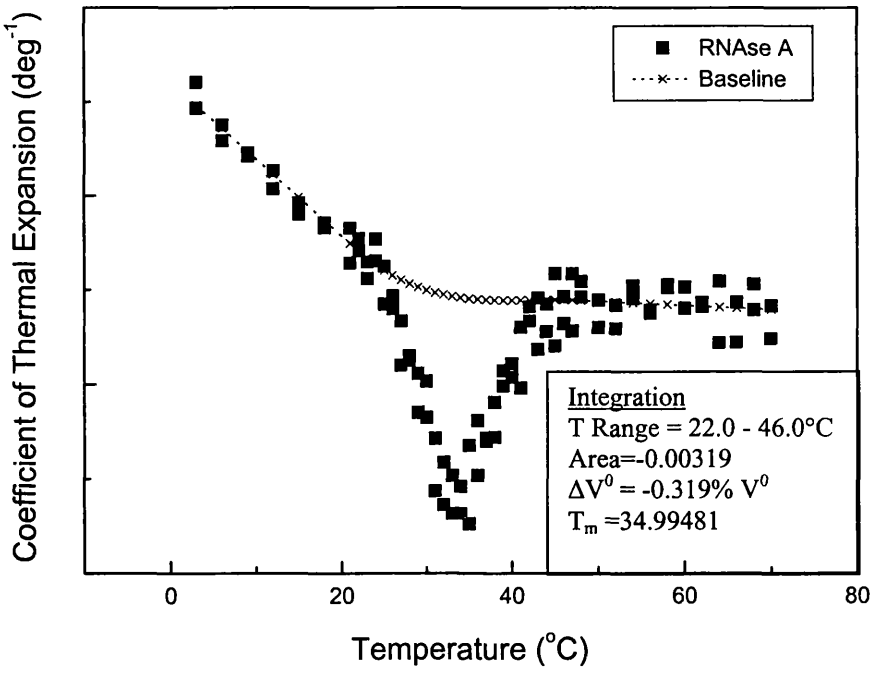

Figure 3.12 Baseline assignment and integration results for the thermal unfolding of the protein ribonuclease A in 20% methanol/water at pH=2.0.

The integration is performed to the baseline that is assigned arbitrarily and thus there may be some variation on the values depending on the choice of the baseline. It is best to try a few different baselines and compare and/or average the resulting area values.

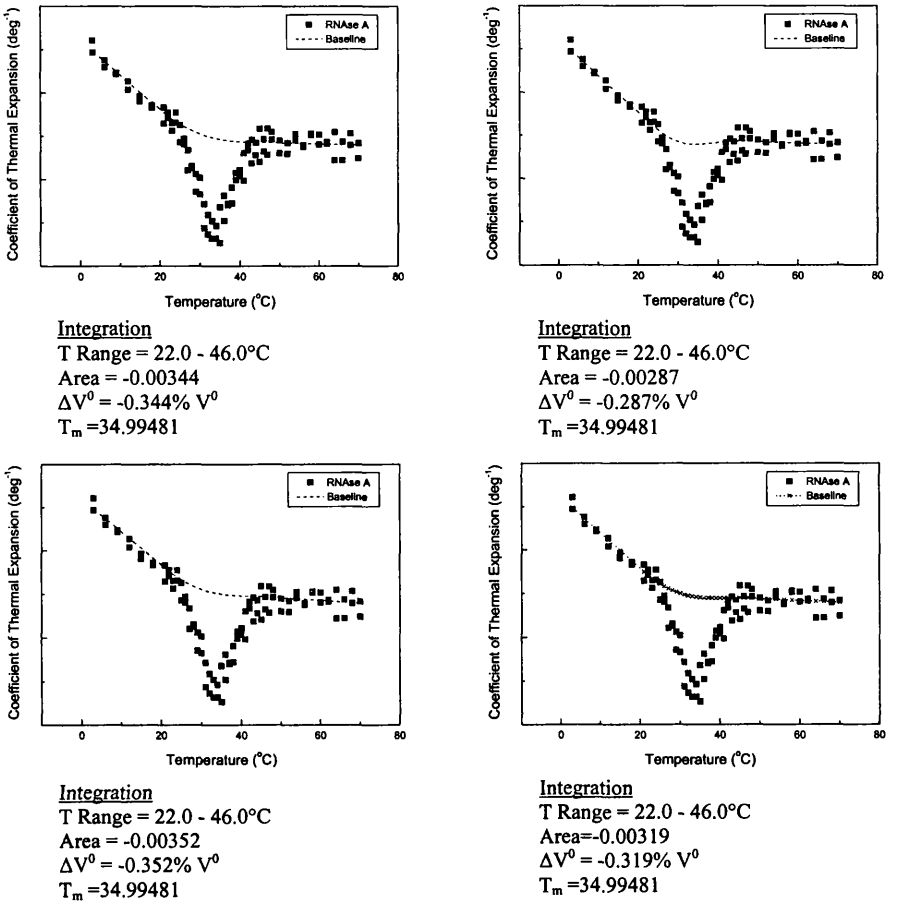

Integration
T Range = 22.0 - 46.0°C
Area = -0.00344
$\Delta V^0 = -0.344\% V^0$
$T_m = 34.99481$

Integration
T Range = 22.0 - 46.0°C
Area = -0.00287
$\Delta V^0 = -0.287\% V^0$
$T_m = 34.99481$

Integration
T Range = 22.0 - 46.0°C
Area = -0.00352
$\Delta V^0 = -0.352\% V^0$
$T_m = 34.99481$

Integration
T Range = 22.0 - 46.0°C
Area=-0.00319
$\Delta V^0 = -0.319\% V^0$
$T_m = 34.99481$

Figure 3.13 Thermal unfolding of the protein ribonuclease A in 20% methanol/water at pH=2.0. Four different baselines assigned for integration resulted in four different values of fractional volume change: -0.344%, -0.287%, -0.352% and -0.319%.

In the Figure 3.13 the same transition was assigned the baseline for integration four times, each time yielding different value of the area under the curve - 0.00319, -0.00344, -0.00287 and -0.00352. Based on these four results the average area is -0.00325 ± 0.00025 (with 8% error) and that gives the volume change of the process (in this case of protein unfolding) is -0.33 ± 0.03% of the total (partial molar) volume of the molecule (of the protein ribonuclease A in this case).

Here the volume change for unfolding of ribonuclease A is small and negative, indicating that the partial volume of the protein decreases only slightly upon unfolding.

The values of fractional volume change from work on other processes studies by PPC were somewhat higher, for example between 1.0 and 1.5% for phase transition of poly(n-isopropylacrylamide) polymers (Kujawa and Winnik 2001) or around 3.0% of lipid bilayers phase transitions (Heerklotz and Seelig 2002) and for both of these processes they are positive, indicating volume increase upon phase transition.

3.5 Error values associated with PPC measurement

Stemming from the observation that there might be a large error introduced by automatic software integration in the determination of heat values for the individual PPC cycles (see Troubleshooting 2 in section 3.4.2; see also Figure 3.9), the study of the errors associated with the technique was designed. The evaluation of the resulting error in thermal expansion coefficient (α) by error propagation analysis was done and is presented here.

3.5.1 *Repeatability*

As some variability in PPC measurements was noticed both in my measurements and of my colleagues (Cameron 2001) (Nöllmann 2001) I made a series of measurements that aimed to estimate the error of the measurements introduced by this variability and the extent by which changes in volumes of the cells influence the changes in net heat.

All measurements were done at the same temperature (25°C), ten PPC cycles of decompression/compression were executed, then the cells were reloaded and the series of ten measurements was repeated. I carried out five such series of ten measurements.

Then the heat values were analyzed statistically to check the significance of the observed variability. All statistical analysis and statistical tests were carried out using computer program Minitab.

Water vs. Water measurements

For each series of ten PPC cycles with equal cell volumes the average heat, its standard deviation and standard error of the mean were calculated. The results are presented in Table 3.2.

Series	Mean (μcal)	Standard Deviation (μcal)	Standard Error of the Mean (μcal)
a	-5.628	0.626	0.140
b	-5.560	0.618	0.138
c	-6.118	0.742	0.166
d	-5.806	0.559	0.125
e	-5.879	0.618	0.138

Table 3.2 Average heats, standard deviations and standard errors of the mean for water -water PPC measurements.

To determine if there is a significant difference between the five dataset the Analysis of Variance (ANOVA) test was performed.

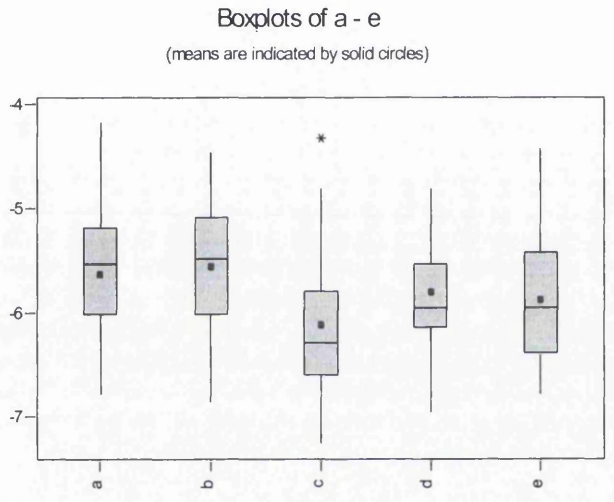

Figure 3.14 Graphical representation of datasets for heats of water-water PPC experiment (means are indicated by solid dots) used for ANOVA test.

The results of the test confirm that all five datasets are identical at 95% confidence level, it means that there is no significant difference in average heat and its standard deviation when cells are reloaded.

Buffer vs. Buffer

As the experimental variability was mostly observed for buffer vs. buffer PPC measurements, the above series of measurements and analysis were repeated for the buffer vs. buffer system. The buffer used was 50 mM glycine buffer at pH=2.5. All measurements were carried out at 25°C, ten PPC cycles of decompression/compression were executed, then the cells were reloaded and the

series of ten measurements was repeated. Six such series of ten measurements were carried out.

For each series of ten PPC cycles with equal cells' volumes the average heat, its standard deviation and standard error of the mean were calculated. The results are presented in Table 3.3.

Series	Mean (μcal)	Standard Deviation (μcal)	Standard Error of the Mean (μcal)
a	-5.966	1.185	0.265
b	-5.672	0.445	0.099
c	-9.879	5.457	1.220
d	-5.584	0.376	0.084
e	-5.820	0.248	0.055
f	-5.787	0.215	0.048

Table 3.3 Average heats, standard deviations and standard errors of the mean for buffer-buffer PPC measurements.

To determine if there is a significant difference between the five dataset the Analysis of Variance (ANOVA) test was performed.

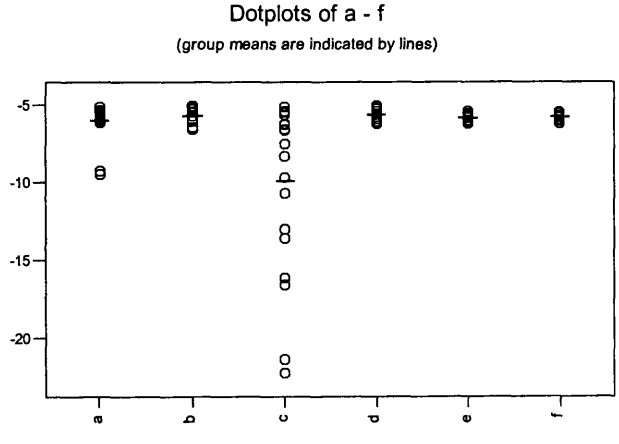

Figure 3.15 Graphical representation of datasets for heats of buffer-buffer PPC experiment (means are indicated by lines) used for ANOVA test.

The results of the test show that datasets are not identical at 95% confidence level, as it can be seen from the graphical representation: dataset c is clearly different.

There was a variability in PPC signal not usually observed for buffer vs. buffer scan at the same temperature.

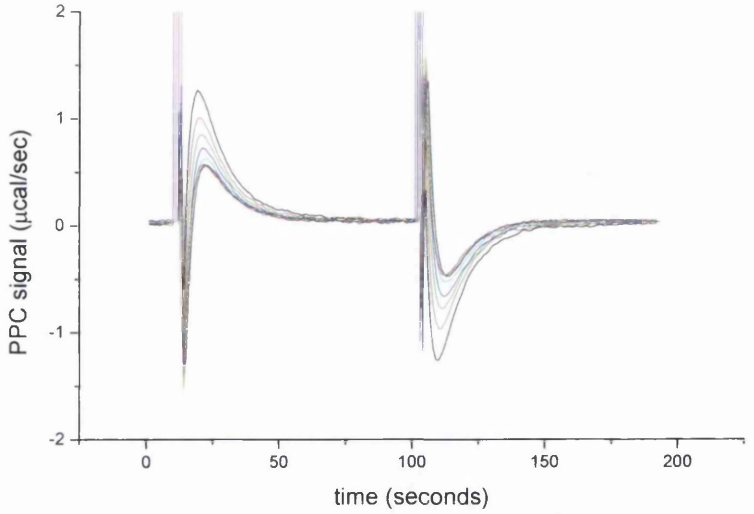

Figure 3.16 Changes in PPC signal in dataset c.

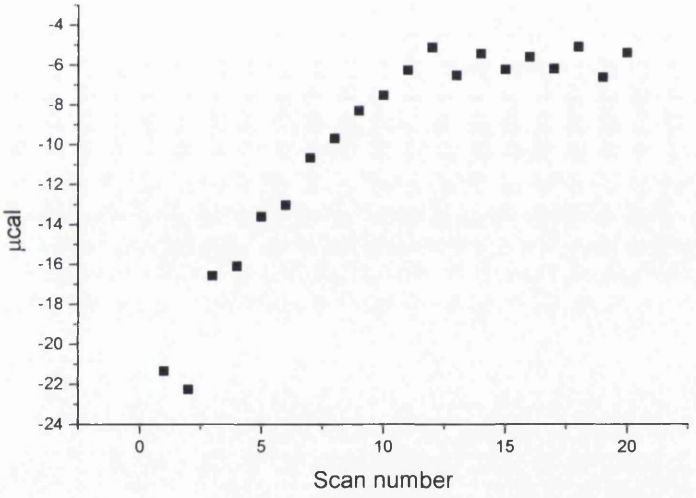

Figure 3.17Changes in ΔQ in dataset c.

ΔQ starts very low (-22 µcal) and after few PPC cycles it reaches a mean value (as seen in other datasets) for buffer vs. buffer system (about -6 µcal). There is something causing this odd behaviour, with the main suspect being a bubble in the cell, which is removed with subsequent pressure changes.

One useful conclusion from this preliminary study was drawn for the future measurements – in order to prevent air bubbles influencing the PPC measurement,

several compressions and decompressions over the loaded sample were carried out in order to remove the potential air trapped in the cells.

After eliminating dataset c the results of the ANOVA test confirm that all five datasets are identical at 95% confidence level.

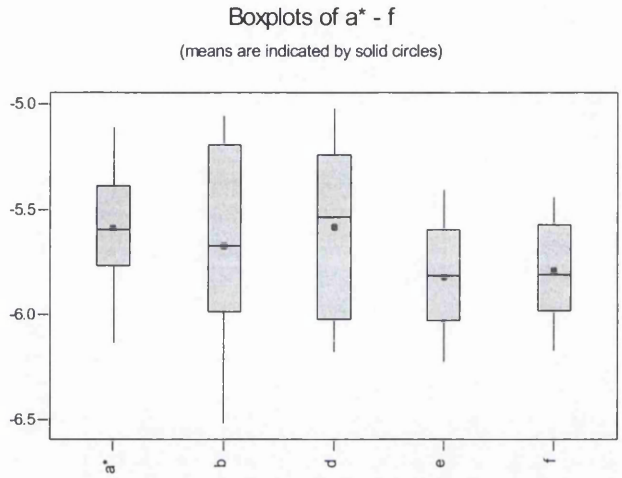

Figure 3.18 Graphical representation of datasets for heats of buffer -buffer PPC experiment (means are indicated by solid dots) used for ANOVA test.

Concluding from the statistical analysis, there is relatively large error for heat measurements with PPC – the standard deviation is about 12% of the measured value for water-water scans (at 25°C). The observed errors for buffer-buffer scans range from 5 to 26%, where the high value of 26% is probably caused by the air bubble in the cell.

Such a big error for water measurement results from the very small differential heats if both cells are loaded with the same substance. Both water-water and buffer-buffer are in fact the reference measurements, the heats of which are subtracted later from much larger heats obtained from the sample-buffer.

In order to evaluate whether such large error values for the reference measurements increase the error in α of the solute the full error propagation calculations had to be carried out.

3.5.2 *Theoretical error propagation.*

Thermal expansion coefficient (α) is calculated from the following formula:

$$\alpha = -\frac{Q_{SB} - Q_{BB} - C \cdot \overline{V} \cdot (Q_{BW} - Q_{WW} + E(T) \cdot V \cdot P)}{T \cdot C \cdot \overline{V} \cdot V \cdot P} \tag{3.34}$$

This is the same equation as Eq. 3.27, however for simplicity the symbols for heat differences for reference scans are in the Q_{XX} form here, instead of ΔQ_{XX}; their meaning and definition is the same. All the symbols are explained earlier in this chapter (section 3.3.2).

For the error analysis unit conversion factors (from input unit to SI units) have been omitted to simplify the equations.

Five auxiliary functions (X, Y, U, W and Z) have been defined for error propagation analysis.

Let's define X and Y as

$$X = Q_{SB} - Q_{BB} + C \cdot \overline{V} \cdot (Q_{BW} - Q_{WW} + E(T) \cdot V \cdot P) \tag{3.35}$$

$$Y = T \cdot C \cdot \overline{V} \cdot V \cdot P \tag{3.36}$$

Let's also define the following auxiliary functions for calculating the error in function X:

$$U = C \cdot \overline{V} \cdot (Q_{BW} - Q_{WW} + E(T) \cdot V \cdot P) \tag{3.37}$$

$$W = Q_{BW} - Q_{WW} + E(T) \cdot V \cdot P \tag{3.38}$$

and

$$Z = E(T) \cdot V \cdot P \tag{3.39}$$

The functions 3.35, 3.37 and 3.38 can also be simplified in the following way

$$X = Q_{SB} - Q_{BB} + U \tag{3.40}$$

$$U = C \cdot \overline{V} \cdot W \tag{3.41}$$

$$W = Q_{BW} - Q_{WW} + Z \tag{3.42}$$

To calculate error in thermal expansion coefficient (α), it can be conveniently represented by the Eq. 3.43.

$$\alpha = -\frac{X}{Y} \tag{3.43}$$

and the uncertainty in α determination (S_α) (standard deviation in α) can be calculated from

$$S_\alpha = \alpha \cdot \sqrt{\left(\frac{S_X}{X}\right)^2 + \left(\frac{S_Y}{Y}\right)^2} \tag{3.44}$$

where S_X and S_Y are standard deviations in X and Y determination, respectively:

$$S_X = \sqrt{S_{Q_{SB}}^2 + S_{Q_{BB}}^2 + S_U^2} \tag{3.45}$$

$$S_Y = Y \cdot \sqrt{\left(\frac{S_T}{T}\right)^2 + \left(\frac{S_C}{C}\right)^2 + \left(\frac{S_{\overline{V}}}{\overline{V}}\right)^2 + \left(\frac{S_V}{V}\right)^2 + \left(\frac{S_P}{P}\right)^2} \tag{3.46}$$

where S_U is the uncertainty in function U (3.37, 3.41), which is defined as follows:

$$S_U = U \cdot \sqrt{\left(\frac{S_C}{C}\right)^2 + \left(\frac{S_{\overline{V}}}{\overline{V}}\right)^2 + \left(\frac{S_W}{W}\right)^2} \tag{3.47}$$

Standard deviation S_W of function W (3.38, 3.42) is represented by Eq. 3.48

$$S_W = \sqrt{S_{Q_{BW}}^2 + S_{Q_{WW}}^2 + S_Z^2} \tag{3.48}$$

where S_Z is the uncertainty in function Z (3.39):

$$S_Z = Z \cdot \sqrt{\left(\frac{S_{E(T)}}{E(T)}\right)^2 + \left(\frac{S_{V_0}}{V_0}\right)^2 + \left(\frac{S_P}{P}\right)^2} \tag{3.49}$$

After using the equations 3.45 to 3.49 for S_Z, S_W, S_U, S_Y and S_X, and evaluating Eq. 3.44 for uncertainty in α we obtain:

$$S_\alpha = \alpha \cdot \phi \tag{3.50}$$

where

$$\phi = \left(\frac{S_T}{T}\right)^2 + \left(\frac{S_C}{C}\right)^2 + \left(\frac{S_{\overline{V}}}{\overline{V}}\right)^2 + \left(\frac{S_{V_0}}{V_0}\right)^2 + \left(\frac{S_P}{P}\right)^2 + \frac{1}{X^2}\left(S_{Q_{SB}}^2 + S_{Q_{BB}}^2\right) +$$
$$+ \frac{W^2}{X^2}\left(S_C^2 \cdot \overline{V}^2 + S_{\overline{V}}^2 \cdot C^2\right) + \frac{C^2\overline{V}^2}{X^2}\left\{S_{Q_{BW}}^2 + S_{Q_{WW}}^2 + Z^2\left[\left(\frac{S_{E(T)}}{E(T)}\right)^2 + \left(\frac{S_V}{V}\right)^2 + \left(\frac{S_P}{P}\right)^2\right]\right\} \tag{3.51}$$

where values for X, U, W and Z are calculated from equations 3.35, 3.37, 3.38 and 3.39 as defined above.

In the determination of α of the sample, instead of using measured heat values of Q_{BB}, Q_{BW} and Q_{WW}, the temperature dependence of these heats is fitted to a second order polynomial function of temperature and fitted values used in place of experimental values.

$$Q_{XY} = A_{XY} + B_{XY} \cdot T + C_{XY} \cdot T^2 \tag{3.52}$$

where A_{XY}, B_{XY} and C_{XY} are fit coefficients of buffer vs. buffer (BB), buffer vs. water (BW) and water vs. water (WW) scans, respectively.

For the use in equation 3.51 the errors of determination of each of the reference heats (S_Q) from the polynomial fit are calculated from the errors of the fit coefficients using the following equation (derived from standard error propagation rules):

$$S_Q = \sqrt{S_Q^2} \tag{3.53}$$

$$S^2_Q = S^2_A + S^2_B T^2 + S^2_C T^4 + S^2_D T^6 + S^2_T(B^2+4C^2T^2+9D^2T^4) \tag{3.54}$$

where S_A, S_B, S_C and S_D are the errors of the coefficients, and S_T is the error associated with the temperature measurement.

E(T) is a function of temperature given by Eq. 3.19. From the error propagation rules is has been calculated that the error in E(T) ($S_{E(T)}$) could be represented by a function of temperature (T) and standard deviation in temperature (S_T):

$$S_{E(T)} = \sqrt{S^2_{E(T)}} \tag{3.55}$$

$$S^2_{E(T)} = (0.00476)^2 S^2_T + (1.050252\times10^{-4})^2 S^2_T T^2 + (1.999536\times10^{-6})^2 S^2_T T^4 + (1.783224\times10^{-8})^2 S^2_T T^6 + (6.325\times10^{-11})^2 S^2_T T^8 \tag{3.56}$$

3.5.3 *Error evaluation*

The next step in error analysis that was carried out was construction of a spreadsheet based on the derived equation 3.51, and determination of error values of α, from given error values of heats and of other variables.

The errors were evaluated for the PPC scan of ribonuclease A unfolding in 30% v/v methanol at pH = 2.0. The values used for calculation of α according to the equation 3.27 and their errors that were used here for calculation of error in α (S_α) are presented in Table 3.4. The resulting errors in α are plotted against temperature in Figure 3.19. The calculated values of error in α were between 5.5×10^{-5} K^{-1} (at 3°C) and 9.5×10^{-5} K^{-1} (at 72°C), which constitutes 15-20% of the calculated value of α.

Variable	Value used	Variable's error	Value used
Concentration (C / mg mL^{-1})	2.6966	S_C	0.13
Partial Specific Volume ($\overline{V}$ / mL mg^{-1})	0.703	$S_{\overline{V}}$	0.01
Cell volume (V / mL)	0.5161	S_V	0.0001
Pressure change (P / PSI)	69.81	S_P	1
Temperature (T / K)	variable	S_T	0.02
E(T)	variable	$S_{E(T)}$	variable

Table 3.4 Values used for calculation of error in α for ribonuclease A unfolding.

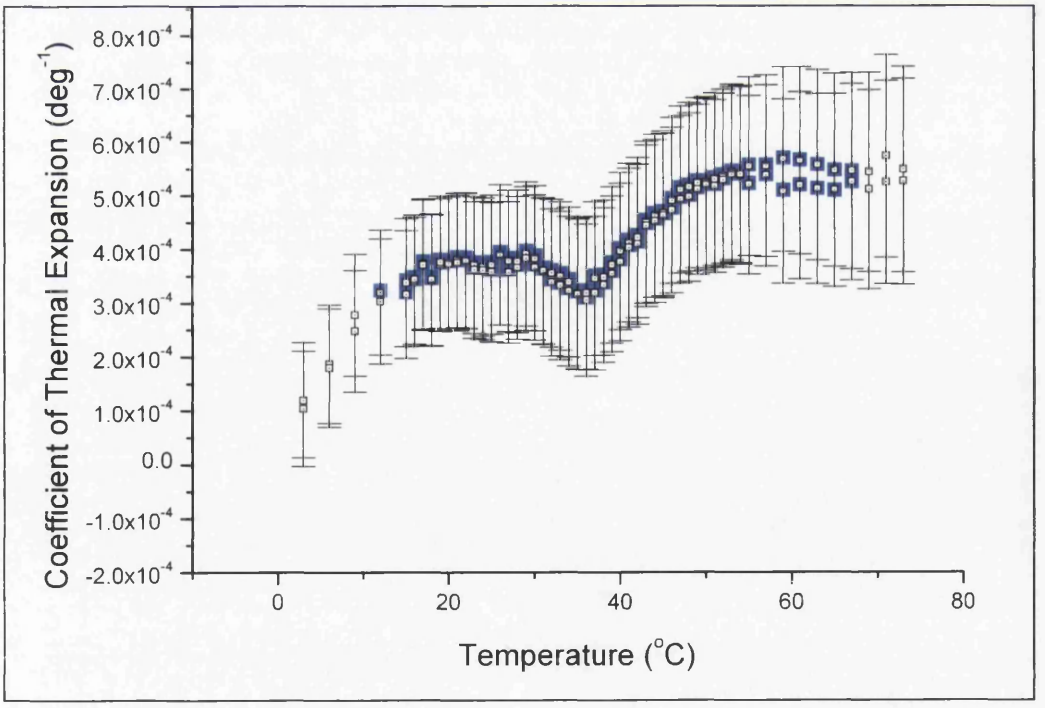

Figure 3.19 The values of error in α calculated from theoretical error propagation for ribonuclease A unfolding in 30% v/v methanol solution.

Because it was suggested that the errors in temperature determination (S_T) have the huge effect on the value of α (Wang and Epand 2004), the effect on change in the temperature standard deviation (S_T) on the value of S_α was investigated. In the calculations above the value of 0.02°C was used for error associated with temperature variation during the isothermal PPC scan (decompression/compression cycle), because this is the value that the manufacturers give for the VP-DSC instrument (MicroCal LCC 2000b). The value of S_T of 0.01 and 0.03°C have been used in calculation of the error in α (S_α) causing the decrease by 20% or the increase by 20% in S_α when compared to the S_α value at S_T=0.02°C. With the S_T set to 0.01 and 0.03°C the error in α increased or decreased only slightly.

To check if there are indeed big temperature changes induced by the pressure jumps during the PPC measurement, 10 raw data files were investigated to look for the recorded temperature changes as a function of time (see Figure 3.7 for the data recorded in the raw PPC files). A variety of conditions were chosen, both PPC cycles at low and at high temperature, and with aqueous buffers, protein samples and methanolic solutions.

The average "jump" in temperature induced by pressure change recorded during the PPC cycle was between 0.01 and 0.02°C. The only conditions where the temperature variation induced by pressure jump that was higher than that was for 40% v/v methanolic buffer vs. water. The change in T was 0.03°C in this case.

This shows that the instrument is reliable to keep the temperature within the 0.02°C error and the concern of Wang and Epand (2004) about this factor introducing huge errors in determination of thermal expansion coefficient are unnecessary.

The error for protein scans in water has not been analyzed due to the time constraints, but it could be safely assumed that in water the errors should be smaller than in the case of aqueous methanolic solutions.

having the spreadsheet for error calculations available, such analysis should be quick and straightforward.

This is especially important for methanol solutions, which give very large heats in PPC measurements (for example 40% v/v methanol in water against water yields from -9500 to -6500 μcal compared to -10 to -6 μcal for water against water scans). It is important to determine what effect the errors associated with these heats has on the error of final α values.

Chapter 4

STRUCTURE MAKING AND STRUCTURE BREAKING BY PPC: AMINO ACIDS AS MODEL SYSTEMS

Outline

Chapter 4 covers

- Two-state mixture model of water
- Theory of structure making and structure breaking properties of solutes
- Amino acids and their side-chains structure making and structure breaking properties (from PPC measurements)
- Amino acids side-chains structure making and structure breaking properties from tripeptides and N-acetyl amino systems (data analysis from densitometry measurements)
- Amino acids in modified aqueous solvents

4.1 Introduction

The interaction between the solvent and the various constituent groups of proteins, such as amino acid side-chains and the backbone peptide group, play a crucial role in the structure and function of proteins in aqueous solutions (Murphy et al. 1998; Sorenson et al. 1999).

As these interactions are complex in the protein molecules, one useful approach is to study the thermodynamics and hydration of small molecular compounds that model the different constituent groups of proteins.

Amino acids, as proteins' building blocks, are one of such model systems. The hydration of amino acids has been studied by PPC by Lin et al. (2002) and have been repeated here. The data for volumes and α for amino acids are also compared to values obtained from densitometric measurements in literature.

Additionally, the data derived for amino acids side-chains from PPC are compared to data for the side-chains derived from densitometric measurements of other compounds: tripeptides and N-acetyl amino acids amides.

It is also shown that changes in solvent environment cause changes in the volumetric properties of the amino acids. In aqueous methanolic solutions the characteristic structure breaking and structure making properties of the amino acids are reduced, and hence this approach of solvent modifications is used in the later chapters for studying solvation of proteins.

4.2 Structure making and structure breaking properties of solutes

Pure water - two-state mixture model

There have been many attempts to explain the thermodynamic properties of liquid water based on the notion of cooperative, "ice-like", "flickering cluster" models (Frank and Evans 1945; Kauzmann 1959; Nemethy and Scheraga H.A. 1962). None of them has been completely successful, but the overall picture seems valid and useful when trying to interpret experimental data. Most recently, Urquidi et al. (1999) have shown that water can be modelled as a mixture of two rapidly inter-converting species: the first one, a bulky form similar to that in ice-Ih that is more structured and less dense, and the other that is less structured and more dense form such as that found in ice-II (Urquidi et al. 1999).

The two-state mixture model of water has been criticized for its simplicity already in 1980 (Endo), however since then the theory has been considerably developed by Professor G.W. Robinson's group (Bassez et al. 1987; Cho et al. 2002; Urquidi et al. 1999; Vedamuthu et al. 1994).

The two-state mixture model has been successful in explaining all the physical anomalies of water (such as refractive index, viscosity, density, isothermal compressibility) as well as such biological phenomena as thermal and cold protein unfolding. It also is useful for understanding of volumetric properties of solutions (Chalikian 2001)

The two-state mixture model of water was originally described by Loren Hepler in 1969. According to this model increasing either the temperature or the pressure of the pure water increases the fraction of the more dense, less structured species at the expense of the other species (Hepler 1969; Urquidi et al. 1999).

Solute hydration in the two-state mixture model of water: structure making and structure breaking properties

A solution is different from water as a pure liquid, because the water molecules that are in the direct proximity of the solute have different properties than the bulk of the solvent. Hence in the model of a solute hydration there is a distinction between two "types" of water in solution: the bulk water, and the solvation water. The solvation water usually has different properties from the bulk water, such as different density and altered hydrogen bonding that result from the close interaction with the solute.

The properties of water in the solvation layer depend on the nature of the solute. There are broadly two types of solutes, hydrophobic and hydrophilic, and they interact with water differently. They promote different type of behaviour of the water molecules in the solvation layer. In the two-state mixture model of water the differences between bulk water and hydration water arise from shifting the ratio of the more dense to the less dense of water species (Chalikian 2001).

$$(H_2O)_b \rightleftharpoons (H_2O)_d$$

$(H_2O)_b$ here represents the bulky, less dense iceIh-like water and $(H_2O)_d$ signifies the denser form of water.

A useful conceptual model is based on the extent to which an added solute might enhance or decrease the amount of residual structure in water. A structure-making solute increases the fraction of the less dense species at the expense of the more dense species in the solute's hydration water, whereas the structure-breaking solute has the opposite effect. It is usually assumed that the hydrophobic solutes are structure-makers and the hydrophilic solutes are structure-breakers.

This is based on the models of hydrophobic interaction that suggest that in the presence of non-polar groups water molecules re-arrange themselves into ice-like "clathrate" structures around the group in order to best satisfy their H-bonding requirements. This is supported experimentally by the observed increase in heat capacity (positive ΔC_p) on the exposure of such groups to water, and by volumetric changes (e.g. Kauzmann 1959).

Kosmotropes and chaotropes

One potential difficulty with such simple conceptual models is that different researchers sometimes use different terms and definitions in slightly different ways. One example of this is in the terms "kosmotrope" (order-maker) and "chaotrope" (disorder-maker). They originally denoted the empirical effect that different solutes had on the stability of proteins and membranes.

Unfortunately, they started to be widely used to describe the property of increasing, or decreasing respectively, the structuring of water, which was assumed to correlate to the effect these solutes have on the protein stability. For example Moelbert et al. (2003) developed a two state computational model for water to study a "chaotropic effect" where chaotropic substances are shown to induce alterations in hydrogen bonding between solvent molecules.

Bachelor et al. (2004) have shown recently that the effect solutes have on protein stability does not correlate to the structure-making or breaking properties, thus this terminology should not be used interchangeably as it may sometimes be misleading.

Is $\left(\partial C_p / \partial P\right)_T$ diagnostic of structure making and structure breaking properties?

Using the two state mixture model of water, the change in heat capacity with pressure will be connected to structure breaking and structure making properties of the solutes, hence it can be used as a useful diagnostic parameter or predictor of such features.

To derive the formulas, let's consider the case where the pressure is increased over a pure water. According to Le Chatelier's principle the equilibrium shifts towards the more dense, less structured water with ice-II-type bonding. Because it takes heat to break the structure, a decrease in structure will decrease the heat capacity, C_p of the pure water, thus C_p is inversely related to pressure at constant temperature

$$\left(\frac{\partial C_p}{\partial P}\right)_T < 0 \qquad (4.1)$$

Increasing the pressure can be considered theoretically in the same way for the water of solvation around the solute. In the case of the structure-making solute increasing the pressure shifts the equilibrium of the hydration water towards denser, less structured species (ice-II-type). This shift decreases the solute's heat capacity C_p, making $\left(\partial C_p / \partial P\right)_T$ negative. Conversely, if the pressure is increased over the solution of the structure-breaking solute, it leaves less of the structured water (ice-Ih-type) structure to break, increasing the solute's C_p and making $\left(\partial C_p / \partial P\right)_T$ positive.

Thus the sign of the specific heat's pressure derivative at the constant T $\left(\partial C_p / \partial P\right)_T$ indicates whether the solute has "structure-making" or "structure-breaking" properties.

It is easier to relate $\left(\partial C_p / \partial P\right)_T$ to the partial molar volume of the solute V° and to the temperature T than to the heat capacity C_p, as volumetric and calorimetric data are more accessible experimentally. This was first derived by Hepler (1969) as shown below.

One begins with fundamental thermodynamic relation

$$dH = TdS + VdP \qquad (4.2)$$

Differentiation the above equation by P at constant T gives

$$\left(\frac{\partial H}{\partial P}\right)_T = T\left(\frac{\partial S}{\partial P}\right)_T + V \qquad (4.3)$$

Substituting Maxwell relation $\left(\frac{\partial S}{\partial P}\right)_T = -\left(\frac{\partial V}{\partial T}\right)_P$ into Eq. 4.3 gives

$$\left(\frac{\partial H}{\partial P}\right)_T = V - T\left(\frac{\partial V}{\partial T}\right)_P \qquad (4.4)$$

Differentiating Eq. 4.4 by T at constant P gives

$$\left(\frac{\partial C_p}{\partial P}\right)_T = \left(\frac{\partial V}{\partial T}\right)_P - \left(\frac{\partial V}{\partial T}\right)_P - T\left(\frac{\partial^2 V}{\partial T^2}\right)_P = -T\left(\frac{\partial^2 V}{\partial T^2}\right)_P \qquad (4.5)$$

Differentiating Eq. 4.5 with respect to the moles of solute, at a low concentration where V° is partial molar volume and C_p° is partial heat capacity of the solute at infinite dilution, and using the definition of $\alpha = (1/V^\circ)(\partial V^\circ / \partial T)_P$ gives

$$\left(\frac{\partial C_p^\circ}{\partial P}\right)_T = -T\left(\frac{\partial^2 V^\circ}{\partial T^2}\right)_P = -T\left(\frac{\partial(\alpha V^\circ)}{\partial T^2}\right)_P \qquad (4.6)$$

This equation conveniently relates $(\partial C_p / \partial P)_T$ to the partial molar volume of the solute V° that is available from density measurements, or to thermal expansion coefficient α that is available from PPC, thus making the prediction of structure making and breaking properties more accessible experimentally.

Heat and cold thermal unfolding of proteins in two-state mixture model of water

Robinson and Cho (1999) showed that the curvature in the total free-energy function for protein unfolding can be attributed to the steep change with temperature of the proportions of ice-Ih-type and ice-II-type bonding in the liquid.

In this paper, following the work on the two-state outer neighbour mixed bonding model of water, it was proposed that non-polar groups promote the formation of the low density ice Ih-type bonding in their neighbourhood, whereas polar groups tend to promote the higher density ice II-type structure. In a protein, because of the large numbers of exposed polar and non-polar groups, large changes in the neighbouring water structure can occur. These changes, of course, depend on whether the protein is in the native or the unfolded state. It was shown to have a direct impact on the thermodynamics of protein unfolding at both high and low temperatures. For example, it is known that the non-polar hydration entropies become rapidly more negative with increasing temperature (Robinson and Cho 1999). This very unusual behaviour can be directly related to the promotion in the outer bulk liquid of the more stable Ih-type bonding at the expense of II-type bonding by non-polar groups of the protein. In contrast, polar groups have an opposite effect on the thermodynamics. It is the subtle balance created by these outer hydration contributions, mixed with ordinary thermodynamic contributions

from the inner hydration shell and those from hydrogen-bond and van der Waals forces within the protein molecule itself that is responsible for both heat and cold denaturation of proteins.

This theory, which depends on transformations with increasing temperature or pressure, is consistent with all the properties of this substance, including the ten or so "anomalies", and has been recently used to explain the effect that surrounding water has on proteins. Robinson et al. (2001) discussed this outer neighbour two-state structural theory for liquid water, the role it plays in explaining water's anomalous properties and its description of protein denaturation both as a function of temperature and pressure.

Other authors also developed very similar two-state mixture theories (Chalikian 2001; Tanaka 2000).

How to measure solvation layer properties?

The solvation layer waters are hard to distinguish from the bulk water macroscopically and the question arises how their properties can be studied separately from the bulk water.

Since it is impossible to observe the solvation layer in isolation, we must find methods in which the properties of the solute layer affect the measured properties of the bulk solution. A good candidate for such measurements are volumetric properties of solutes, such as partial molar volume or its derivative, thermal expansivity that is described by the thermal expansion coefficient (for more detailed description see chapter 3). Such measurements of the solute properties incorporate the volume of the solvation water in them so can give us an insight in how the solvation layer water differs for the bulk water. The volumetric properties of the solutes can be obtained from thermodynamic analysis of calorimetric data obtained on aqueous solutions of different solutes. Data on amino acids and other solutes are presented here.

4.3 Amino acids structure making and structure breaking properties

As the structure making and structure breaking properties of solutes can be extracted from the second derivative of the solute's volume, measuring the first derivative of this volume simplifies the process of obtaining this information as compared with tedious density measurements.

Shortly after introducing the PPC method, the manufacturers (MicroCal) came up with an idea to apply the method to study proteins' building blocks – amino acids (Lin et al. 2002). They are the suitable small molecule models for exposed protein side chains and protein hydration. The study conducted at the manufacturer's site was published (Lin et al. 2002), presenting among others the study of the amino acids properties by PPC.

As a preliminary to my work on proteins, and to test the new instrument and procedures, I chose to repeat some of these measurements in Glasgow for comparison. Interestingly, this has exposed some apparent discrepancies in the published data.

Differences in α between hydrophobic and hydrophilic amino acids

It has been previously argued that the differences between hydrophobic and hydrophilic solutes are reflected in the temperature dependence of thermal expansion coefficient (α) (Hepler 1969; Lin et al. 2002).

In the work of Lin et al. (2002) it has been observed that solutes that increase the amount of structure in water have large positive $(\partial\alpha/\partial T)_p$ (i.e. at low temperature the value of α is small or even negative and it is increasing with temperature) and solutes that decrease the amount of structure in water have large negative $(\partial\alpha/\partial T)_p$ (i.e. at low temperature value of α is large and positive and

decreases with temperature) (Lin et al. 2002). The authors have claimed that this trend applies to aqueous solutions of amino acids side chains (Lin et al. 2002).

The results published by Lin et al. (2002) are presented below, in Figure 4.1.

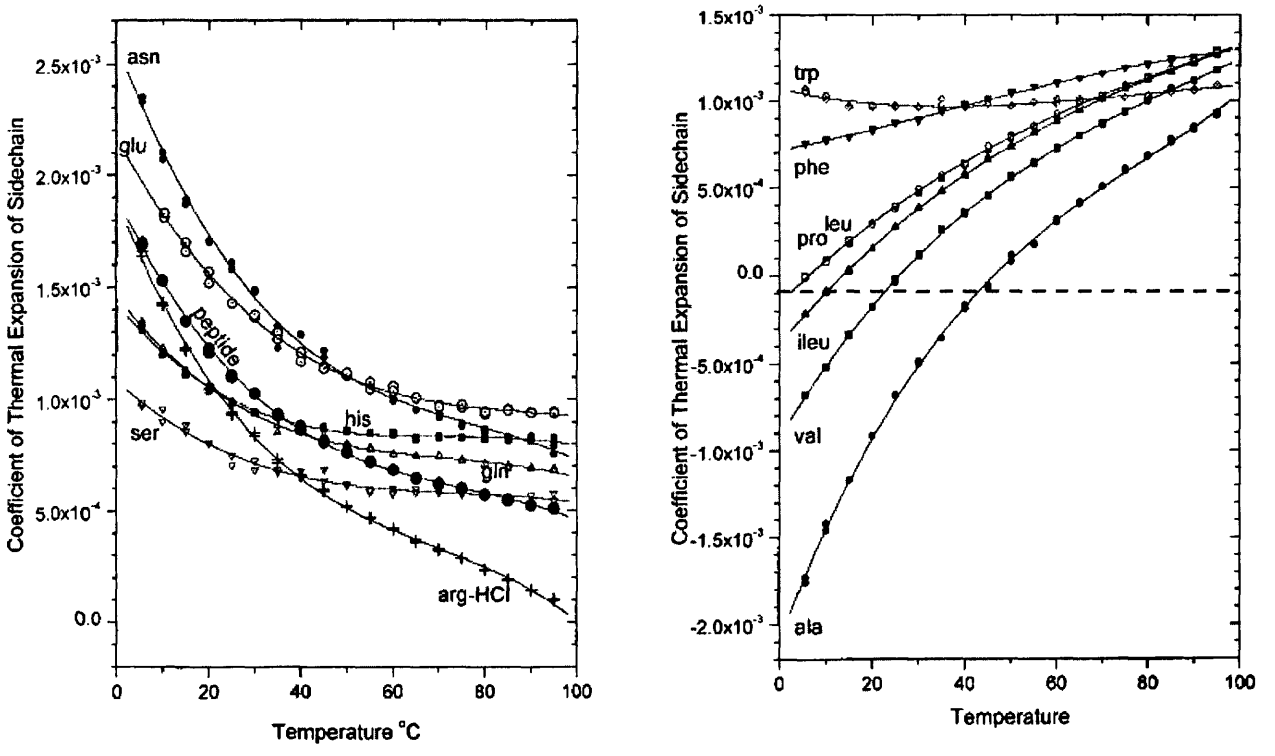

Figure 4.1 Huge differences between hydrophilic and hydrophobic amino acid side chains observed by PPC (Lin et al. 2002). Here thermal expansion coefficient α was calculated "relative to glycine", i.e. the heats given out by glycine solution at the same concentration were subtracted from the amino acid heat, to yield the side chain only contribution to the thermal expansion coefficient.

This amino acid model could be very useful for deciphering protein solvation in the small molecule scale, and for studying the effects of solvents modifications on small solutes' and in later phases also proteins solvation. To use this amino acid model for studying solvents effects on solvation I have tried to replicate the results obtained by Lin et al. (2002) in water. The amino acids chosen for the PPC study were: alanine and valine as representatives of the apolar side chain group, asparagine, glutamine, serine and histidine as representatives of the polar side chain group.

For ease of comparison with the results of the Brandts' group I have used the volumes of the amino acid side chains published therein, as they generally agree

well and there are only slight differences with the values obtained from density data from literature (see Table 4.1).

I have used the same method of calculating alpha contribution of the side chain only, subtracting heats of glycine from the heats of the whole amino acid molecule, both obtained directly from PPC experiment.

$$\alpha = -\frac{\Delta Q_{S/W} - \Delta Q_{W/W}}{T\Delta P m_S \bar{V}} \tag{4.7}$$

In the above equation the heat of sample vs. water (Q_{SW}) is obtained by subtracting heats of glycine vs. water experiment from amino acid vs. water experiment:

$$Q_{S/W} = Q_{AA/W} - Q_{GLY/W} \tag{4.8}$$

$Q_{AA/W}$ and $Q_{GLY/W}$ were obtained at the same concentration and pressure, and the slight experimental differences in concentration and pressure were corrected by multiplying by ratio X_{NEW}/X_{OLD} where X was either pressure or concentration.

This correction was possible as the heat Q is directly proportional to both concentration and pressure. The experimental amino acid concentrations were between 9 and 11 mg/ml and standardized to 10 mg/ml. The experimental pressures were between 69 and 72 psi and standardized to 70 psi. The heat of glycine vs. water experiment were fitted to the 3rd order polynomial of temperature to allow subtraction of glycine heats at exactly the same temperatures as the amino acid data points in the PPC measurement – as described in Chapter 3.

Amino acid	V_{SC} used by Lin et al. (2002) / $cm^3\ g^{-1}$	V_{SC} from density measurements of tripeptides and N-acetyl amino acid amides / $cm^3\ g^{-1}$	V_{SC} from density measurements of amino acids, compiled by Harpaz et al. (1994) / $cm^3\ g^{-1}$
Ala	1.220	1.215[a] 1.134[b]	1.158
Val	1.140	1.120[a] 1.112[b]	1.103
Ile	1.140	1.141[a] 1.101[b]	1.093
Leu	1.140	1.129[a] 1.139[b]	1.128
Ser	0.576	0.580[a]	0.563
Thr	0.763	0.755[a]	0.747
Asn	0.607	0.655[a]	0.588
Gln	0.708	0.698[a]	0.704
Phe	0.863	0.888[a]	0.863
Trp	0.778	0.760[a]	0.774
His	0.698	0.734[a]	0.685
Cys	0.630	0.669[a]	0.644
Met	0.833	0.867[a]	0.827
Pro	0.939	0.806[a]	0.960
Arg-HCl	0.634	1.123406[a] (data for Arg Ac^-)	0.728
Glu	0.653	0.666[a]	0.572
Peptide	0.632		

[a] – data from Hackel et al. (1999)

[b] – data from Hakin and Hedwig (2000)

Table 4.1 Partial specific volumes for the amino acid side chains at 25°C.

In contrast to the published data, the results obtained here show that thermal expansion coefficients for all side chains, irrespective of their polarity, look very similar, as shown in Figure 4.2.

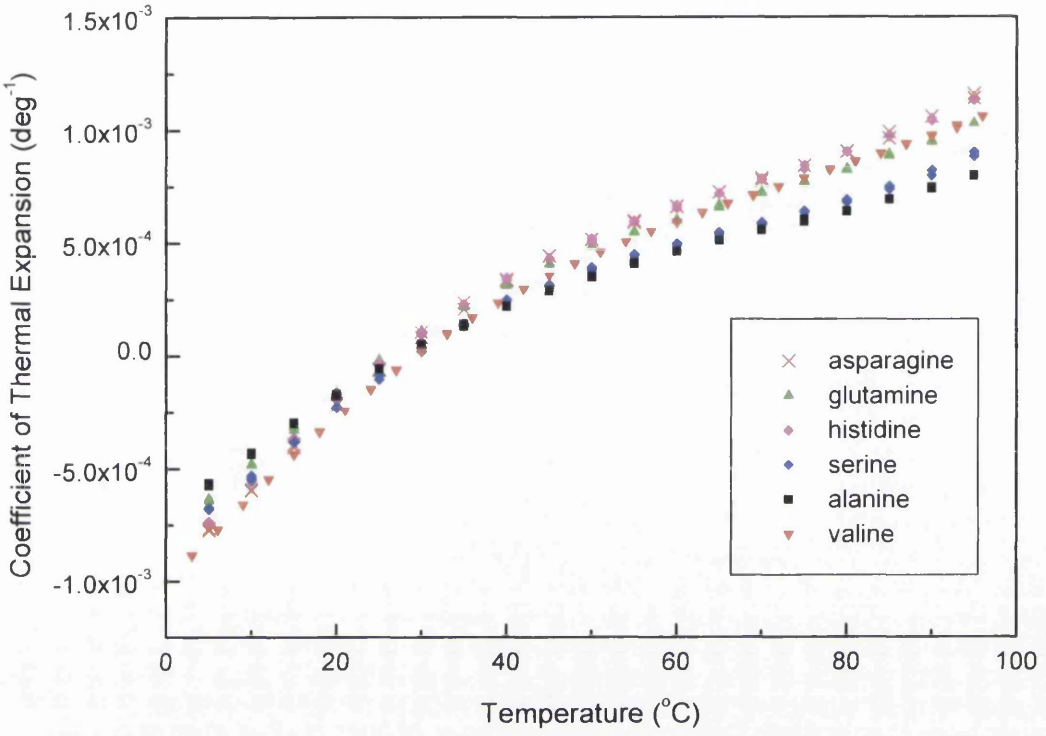

Figure 4.2 Thermal expansion coefficients for the amino acid side-chains obtained from PPC. Calculated from amino acids in water "relative to glycine" as described in text and as determined in Glasgow.

There is a good agreement of the shape and values of α(T) obtained with the data from Lin et al. (2002) for the hydrophobic side chains of alanine and valine. However all the hydrophilic side chains studied (asparagine, glutamine, serine and histidine) overlap with the hydrophobic ones and do not agree with the data published by Lin et al. (2002).

In order to explain this disagreement, the calculations were carried out manually in the Microsoft Excel spreadsheet, instead of using the MicroCal software, confirming the experimental results.

During the close scrutiny of the calculation and data analysis process, it was found that the experimental data can produce the same values as in the paper of Lin et al. (2002), but only if the step of subtracting glycine heats is omitted.

It would appear, therefore, that the previous workers (Lin et al. 2002) have inadvertently omitted to make the appropriate corrections for one set of data.

This suggests that the two amino acids groups have been subject to different procedures for calculating alpha, the hydrophobic one have been indeed calculated "relative to glycine", whereas the hydrophilic one was not, hence the two datasets should not be compared to each other.

When the approach of subtracting glycine heats is used, it is difficult to see any differences between hydrophobic and hydrophilic amino acids side chains. Hence this approach is impracticable to distinguish between the two amino acids groups. Most importantly, this seems to invalidate the significant difference between hydrophobic and hydrophilic side chains contribution claimed by Lin et al. (2002).

Some slight differences between them can be seen when comparing α for the whole amino acids molecules (see Figure 4.3). Thus a better approach would be not to subtract glycine heats, as this entirely obscures the picture and makes it impossible to distinguish between hydrophobic and hydrophilic amino acids.

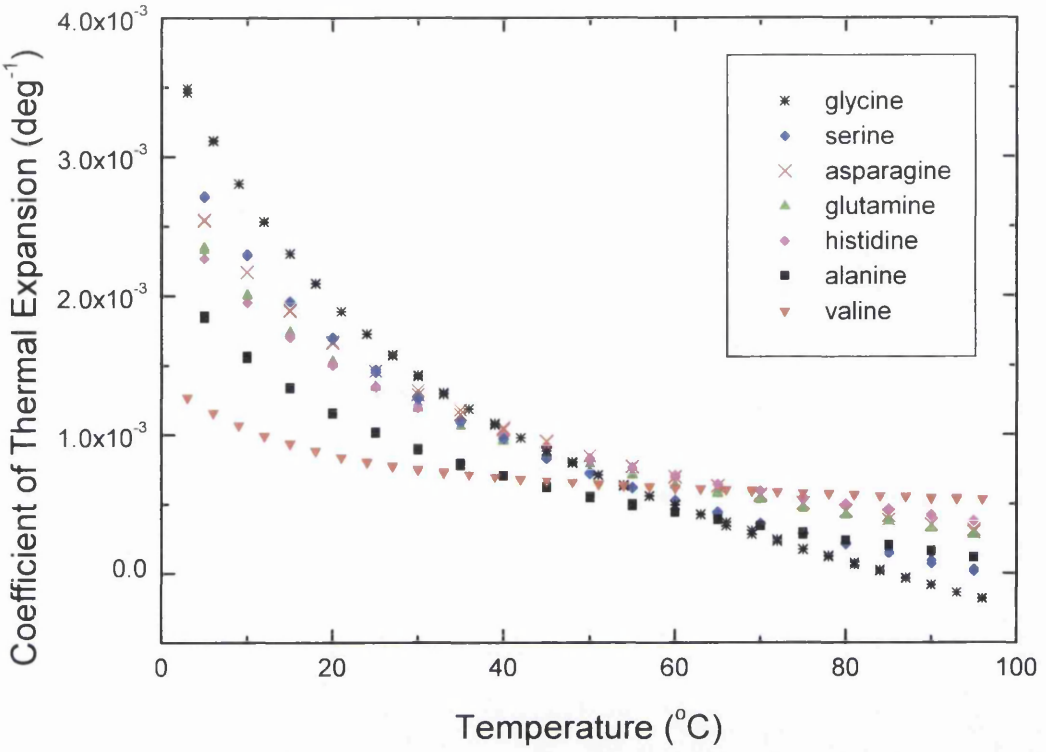

Figure 4.3 Comparison of thermal expansion coefficient for amino acids in water obtained from PPC as a function of temperature.

As can be seen from Figure 4.3 and Figure 4.6 all amino acids have structure breaking properties (as indicated by positive $\left(\partial C_p / \partial P\right)_T$ values), presumably dominated by their charged amino and carboxyl groups. They thus display volumetric properties that are characteristic for electrolytes. Side-chains on the other hand (Figure 4.2 and Figure 4.6) all seem to be structure making (apolar characteristic). The inability to distinguish between polar and apolar side-chains in Figure 4.2 suggests that subtracting glycine heats from the heats of the whole amino acids molecules may not be the best approach to obtain α that is indicative of side chains properties.

Validation of α data obtained from PPC for amino acids

For further validation of the thermal expansion coefficient data for amino acids obtained here, PPC data have been compared to data derived directly from density measurements available from the literature (Kikuchi et al. 1995).

Partial molar volumes obtained at temperatures of 5, 15, 25, 35 and 45 °C were fitted to the quadratic function of temperature

$$V°(T) = a + b\,(T-273.15) + c\,(T-273.15)^2 \qquad (4.9)$$

and a derivative of V°(T) function was used for calculating the thermal expansion coefficient:

$$\alpha = \frac{1}{V^o}\left[b + 2c(T - 273.15)\right] \qquad (4.10)$$

α obtained in this way from densitometric measurements (Kikuchi et al. 1995) is in excellent agreement with data obtained here from PPC (see Figure 4.4).

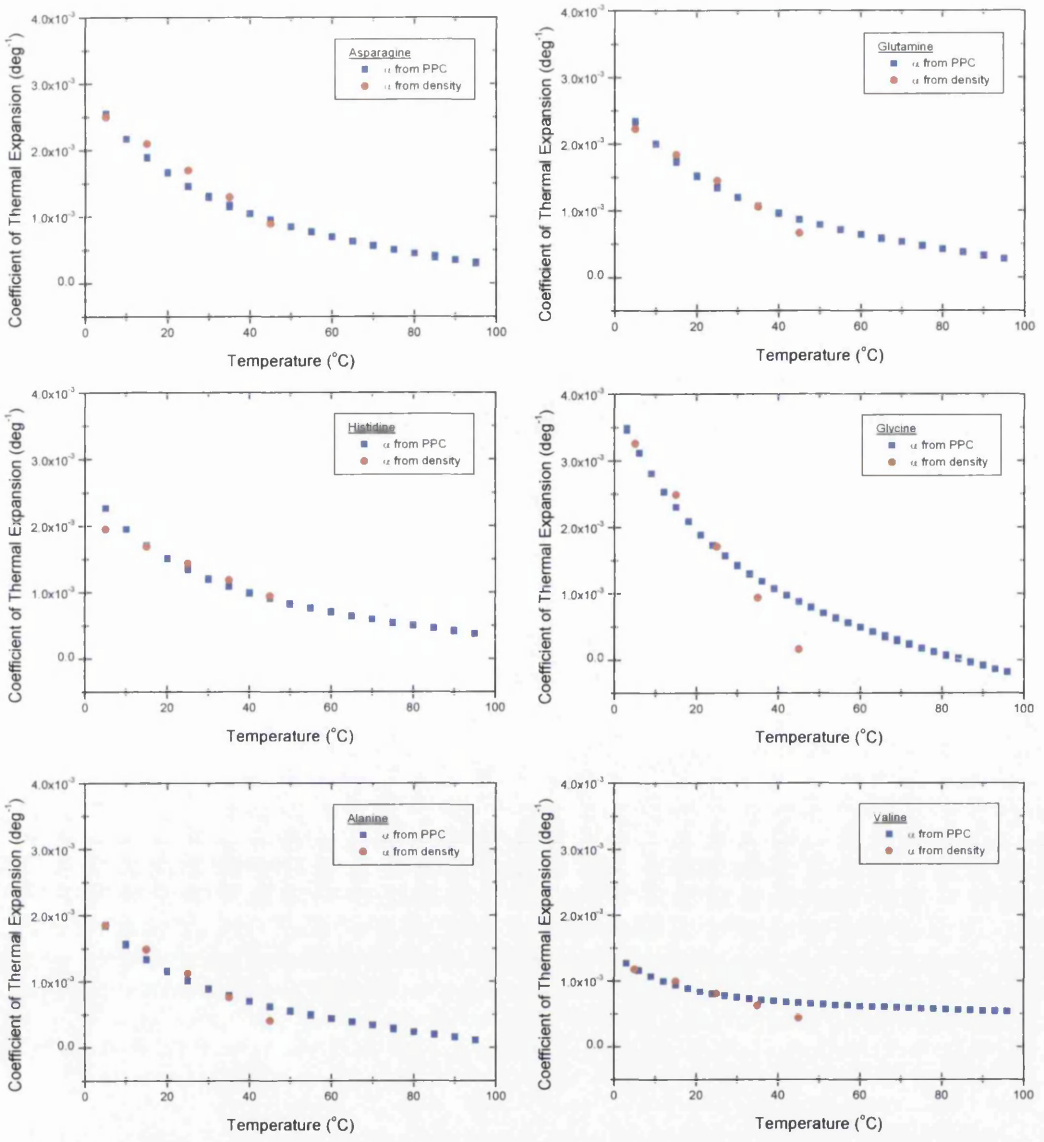

Figure 4.4 Thermal expansion coefficient for amino acids – values obtained from PPC measurement compared to values obtained as the derivative of partial molar volume from density measurements of Kikuchi et al. (1995).

Here the data in the Figure 4.3 for the whole amino acids are confirmed by data obtained from density measurements, thus proving that indeed one data set (for hydrophilic groups) in Lin et al. (2002) was treated differently in data analysis and the step of subtracting glycine heats was omitted. This means that their proposed differences in α for hydrophobic versus hydrophilic side-chains groups are most likely no longer valid.

$(\partial C_p / \partial P)_T$ obtained from α for whole amino acids and their side-chains

The values of $(\partial C_p / \partial P)_T$ for the amino acids and their side-chains can be calculated from the second derivative of volume, hence also from a derivative of thermal expansion coefficient measured by PPC. When the thermal expansion coefficient is fitted to the third order polynomial function of temperature

$$\alpha(T) = A + B \cdot T + C \cdot T^2 + D \cdot T^3 \qquad (4.11)$$

where A, B, C and D are the coefficients fitted using least-squares method.
The derivative of (αV°) is then

$$\left(\frac{\partial(\alpha V^\circ)}{\partial T}\right)_P = V^\circ \cdot \left(B + 2C \cdot T + 3D \cdot T^2\right) \qquad (4.12)$$

For the above equation it was assumed that V° is constant with temperature, in the same way as it is assumed in calculations of α by the PPC software (see Chapter 3 for detailed discussion). This assumption introduces error in the $(\partial C_p / \partial P)_T$ values that is smaller than 5%, thus making it a good approximation. The values of V° at 25 °C were used in the calculations.

Substituting the above into equation 4.6, one obtains the formula used to obtain $(\partial C_p / \partial P)_T$ from experimental α values from PPC

$$\left(\frac{\partial C_p^\circ}{\partial P}\right)_T = -T \cdot V^\circ \cdot \left(B + 2C \cdot T + 3D \cdot T^2\right) \qquad (4.13)$$

The values of $(\partial C_p / \partial P)_T$ that have been calculated from PPC results for the studied amino acids are shown in Figure 4.5 and Table 4.2

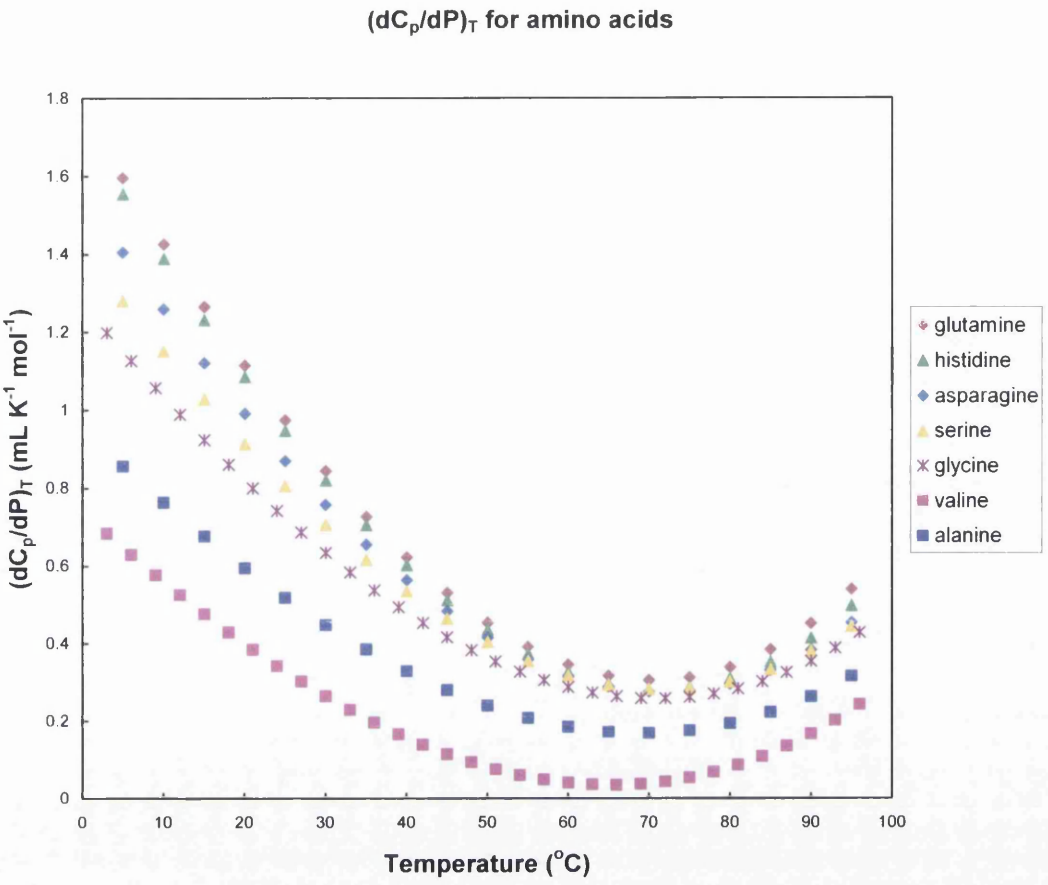

Figure 4.5 $\left(\partial C_p / \partial P\right)_T$ for amino acids (calculated from α obtained from the heats of whole amino acids molecules in water measured by PPC).

Amino acid	$\left(\partial C_p / \partial P\right)_T$ at 25°C (mL K^{-1} mol^{-1})	Side-chain Hydropathy
Gln	0.975	-3.5
His	0.948	-3.2
Asn	0.870	-3.5
Ser	0.806	-0.8
Gly	0.724	-0.4
Ala	0.518	1.8
Val	0.329	4.2

Table 4.2 The values of $\left(\partial C_p / \partial P\right)_T$ at 25°C for the amino acids measured by PPC.

Additionally, in Table 4.2, the data for $\left(\partial C_p / \partial P\right)_T$ of amino acids are compared to the hydropathy Kyte-Doolittle scale (Kyte and Doolittle 1982), which has assigned a hydropathy index to each amino acid, based on its relative hydrophobicity (positive value) or hydrophilicity (negative value). The trend in $\left(\partial C_p / \partial P\right)_T$ values correlates well with side-chain hydrophobicity described by the hydropathy plot.

Although $\left(\partial C_p / \partial P\right)_T$ for all amino acid is positive and it does not distinguish between polar and apolar side-chains, it can nevertheless be compared between the amino acids, and slight differences between polar and apolar ones can be seen. The general trend here is that the structure breaking properties for polar side-chains add to the structure breaking properties of the charged ends, and $\left(\partial C_p / \partial P\right)_T$ for polar side-chains is higher that that of glycine, and $\left(\partial C_p / \partial P\right)_T$ of apolar side-chains are lower. If instead of calculating α "relative to glycine" by subtracting heat values of glycine from that of the whole amino acid molecules, the amino acids $\left(\partial C_p / \partial P\right)_T$ values are compared to glycine $\left(\partial C_p / \partial P\right)_T$ values, then the polar and apolar characteristics of amino acids can be distinguished using data derived from the PPC measurements.

Figure 4.6 shows the values of $\left(\partial C_p / \partial P\right)_T$ derived from α for the side-chains groups that were obtained by subtracting the glycine heats from the whole molecules heats, the approach proposed by Lin et al. (2002) and discussed earlier in this section.

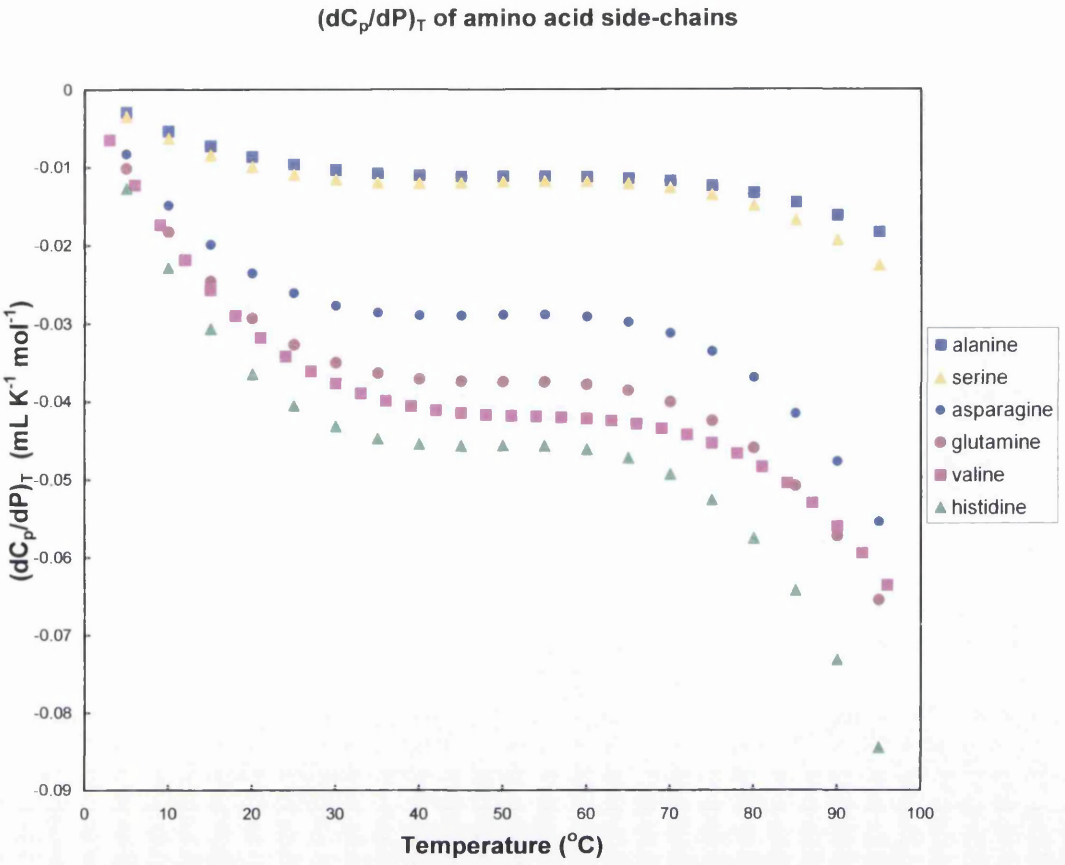

Figure 4.6 $\left(\partial C_p / \partial P\right)_T$ for amino acid side-chains (calculated from α obtained from the heats of amino acids in water "relative to glycine" measured by PPC)

All amino acids side-chains in Figure 4.6 have negative $\left(\partial C_p / \partial P\right)_T$ values and thus display structure making properties (apolar characteristics) even though serine, asparagine, glutamine and histidine are obviously polar. Failure to distinguish between structure making and structure breaking properties here may result from the proximity of the amino acid and carboxyl groups charged ends and the effect of electrostriction (Kikuchi et al. 1995). Thus subtracting glycine properties in the amino acid model seems to be inappropriate for modelling the side chains properties.

Thermal expansion coefficient α for the whole amino acids is more sensitive a measure though to structure making and structure breaking properties and slightly different behaviour can be noticed for polar and apolar amino acids in Figure 4.3.

Side-chains properties obtained from tripeptides model

Though experiments on amino acids provide the most complete data for side chain volumes in solution, these side chain volumes are not exactly comparable with those in proteins. This is because, in amino acids, the electrostriction around charged amino and carboxyl groups affects the solvation of side chains so as to reduce their volumes. This effect can be diminished by separating the side chains from these charged groups.

Thus, more accurate data on volumes of amino acids side-chains are given by the work of Reading and Hedwig (Hackel et al. 1998; Hedwig 1992; Reading and Hedwig 1990; Schwitzer and Hedwig 1998), who determined the volumes in solution of tripeptides of the form Gly-X-Gly, where X is one of the naturally occurring amino acids. The tripeptides should therefore be a better model, because the single side-chain is flanked by two peptide groups which mimic the situation in a polypeptide or a protein. This can be seen on the example of the solution side-chain volumes at 25°C – the ones calculated from the tripeptide density measurements are 0.6–2.9 $Å^3$ larger than those calculated from amino acids (Harpaz et al. 1994).

More recently, the partial molar volumes of the various Gly–X–Gly tripeptides were determined in aqueous solution over the temperature range 10–90 °C using a differential scanning densitometry (DSD) method (Hackel et al. 1999). Although the results obtained using DSD are not as precise as those determined isothermally, the advantage of this method is that in a single scan, partial molar volume data are obtained across a wide temperature range. Precise density measurements at 25 °C have also been made for aqueous solutions of most of the tripeptides (Reading and Hedwig 1990; Schwitzer and Hedwig 1998). They are in excellent agreement, within the combined uncertainties, between the partial molar volumes at 25 °C derived from these density data and those obtained using DSD (Hackel et al. 1999).

The quantities $V^{o}(R)$, which give the volume changes on replacing hydrogen atoms of the backbone glycyl group by the various side chains, were calculated from the partial molar volume data for the tripeptides using Eq. 4.13

$$V^{o}(R) = V^{o}(Gly\text{-}X\text{-}Gly) - V^{o}(GlyGlyGly) \quad (4.14)$$

These $V^{o}(R)$ results for each side chain were analysed using the quadratic function of temperature:

$$V^{o}(R) = a + b\,(T-273.15) + c\,(T-273.15)^2 \quad (4.15)$$

where a, b and c are the coefficients fitted using least-squares method. The values of these coefficients for 19 amino-acid side chains were published by Hackel et al. (1999).

For comparison with the PPC measurements here, I derived thermal expansion coefficient values for the six amino acids studied by PPC. α was calculated as a derivative of $V^{o}(R)$

$$\alpha = \frac{1}{V^{o}}\left[b + 2c\cdot(T-273.15)\right] \quad (4.16)$$

V^{o} was assumed to be temperature independent as was discussed earlier in this chapter and in chapter 3.

Additionally, I have obtained $\left(\partial C_p / \partial P\right)_T$ values from the second derivative of $V^{o}(R)$ function according to Eq. 4.6

$$\left(\frac{\partial C_p^{o}}{\partial P}\right)_T = -T\cdot 2c \quad (4.17)$$

The values for α are presented in Figure 4.7and the values for $\left(\partial C_p / \partial P\right)_T$ in Figure 4.8.

Side chains properties obtained from N-acetyl amino acid amides model

A possible alternative to tripeptides as a set of compounds that realistically model the amino acid side-chains of proteins are N-acetyl amino acid amides. They are neutral amino acid derivatives that have one secondary and one primary amide functional group adjacent to the side-chain. This is structurally similar to that in a

polypeptide. N-acetyl amino acid amides have been shown to be good model compounds for peptides and proteins as the partial molar heat capacities and volumes of the glycyl group over the wide range of temperature have been shown to be in excellent agreement to those derived from thermodynamic data for the series of peptides alanyl(glycyl)$_x$glycine, where x=1-3 (Hackel et al. 1998).

Hakin and Hedwig (2000) reported partial molar volumes (V^o) at the infinite dilution of aqueous solutions of N-acetylglycinamide, N-acetylalaninamide, N-acetylvalinamide, N-acetylleucinamide and N-acetylisoleucinamide at the temperatures of 15, 25, 40 and 55°C.

The authors used the data for these model compounds to estimate the volumes for alanine, valine, leucine and isoleucine side-chains according to the equation

$$V^o(R) = V^o(AcXNH_2) - V^o(AcglyNH_2) \quad (4.18)$$

where $V^o(AcXNH_2)$ and $V^o(AcglyNH_2)$ are, respectively, the partial molar volumes at the infinite dilution of the compounds $AcXNH_2$ and $AcglyNH_2$.

Each of the compounds V^o data were also fitted to the function of temperature of the form

$$V^o(AcXNH_2) = a + b\,(T-308.15) + c\,(T-308.15)2 \quad (4.19)$$

where a, b and c are the coefficients fitted using least-squares method. The quantity of (T-308.15) was used by the authors as an independent variable, because the temperature 308.15K was the mid-point of the temperature range studied.

I have used the equations 4.18 and 4.19 to calculate the temperature dependence of the volume of alanine and valine side-chains

$$V^o(R) = (a_x-a_{gly}) + (b_x-b_{gly})\,(T-308.15) + (c_x-c_{gly})\,(T-308.15)^2 \quad (4.20)$$

Using the coefficients a_x, a_{gly}, b_x, b_{gly}, c_x, c_{gly} from Hakin and Hedwig (2000), I have derived the temperature dependence of thermal expansion coefficient α for alanine and valine side-chains. α was calculated as a derivative of $V^o(R)$

$$\alpha = \frac{1}{V^o}\left[b + 2c\cdot(T-308.15)\right] \quad (4.21)$$

V^{o} was assumed to be temperature independent as was discussed earlier in this chapter and in chapter 3.

I have also obtained $\left(\partial C_p / \partial P\right)_T$ values from the second derivative of $V^{o}(R)$ function according to Eq. 4.6, which is identical as in equation 4.17. The values for α are presented in Figure 4.7 and the values for $\left(\partial C_p / \partial P\right)_T$ in Figure 4.8 together with the values obtained from the tripeptides model system.

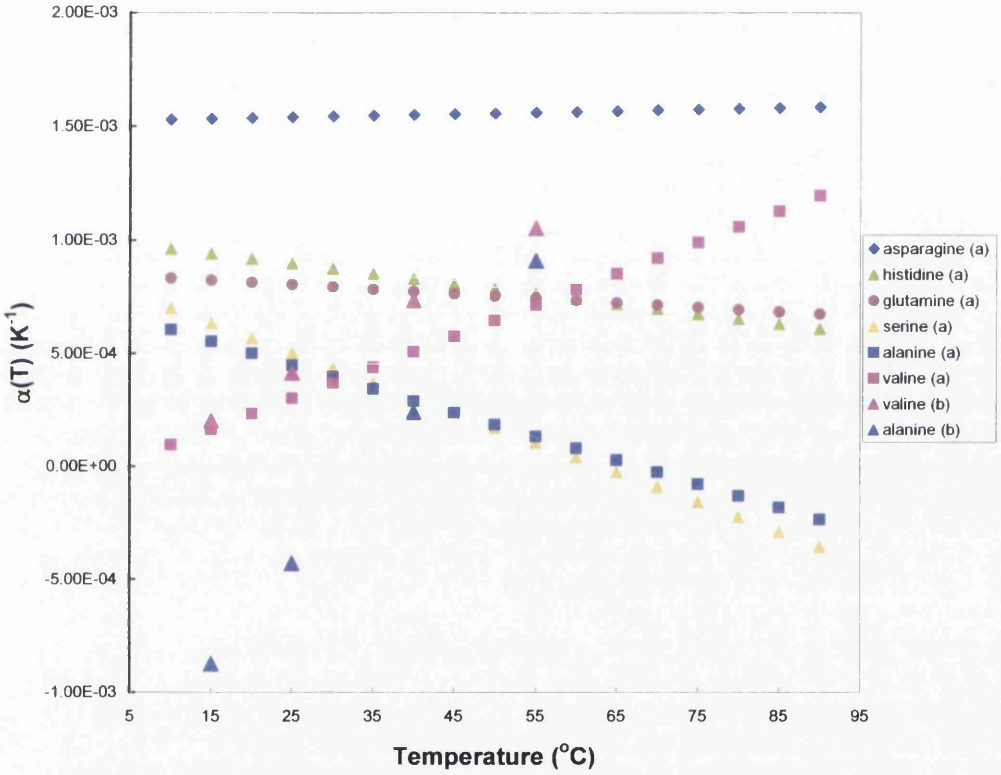

Figure 4.7 α(T) derived from density measurements: (a) from DSD for tripeptides Hackel et al. (1999), (b) from isothermal densitometry for N-acetyl amino acid amides Hakin and Hedwig (2000)

Thermal expansion coefficient values of the side-chains derived from tripeptides and N-acetyl amino acid amides are in the same range ($-1x10^{-3}$ – $1.5x10^{-3}$) as the α values for side-chains obtained from amino acids by PPC. α derived from tripeptides and N-acetyl amino acid amides shows, however, more variation than the α data from PPC, where temperature dependence of α for all studied amino acid side-chains looks almost identical.

Contrary to α derived from PPC (Figure 4.2), α for three side-chains, histidine, glutamine and serine, is decreasing with temperature in Figure 4.7. Positive $\left(\partial C_p / \partial P\right)_T$ associated with this trend agrees with the polar, structure breaking character of these amino acids.

α(T) for valine from the tripeprides model increases with temperature (negative $\left(\partial C_p / \partial P\right)_T$ indicates hydrophobic character), however α(t) for alanine does not. But in the data derived from N-acetyl amino acid amides α(T) for both of the hydrophobic amino acids, valine and alanine, increases with temperature and has positive $\left(\partial C_p / \partial P\right)_T$, indicating their structure breaking properties. Moreover, data for valine derived from the two model systems agree very well.

The data for alanine and asparagine obtained from tripeptides are dubious, as they don't agree with the apolar and polar, respectively, characters of these side-chains. The errors here may result from the technique used, as differential densitometry (DSD) is not as precise as isothermal densitometry. Moreover, Hackel et al. (1999) have measured the apparent molar volumes and assumed it equals to the partial molar volume at the infinite dilution, V^o, and that approximation may also be a source of errors.

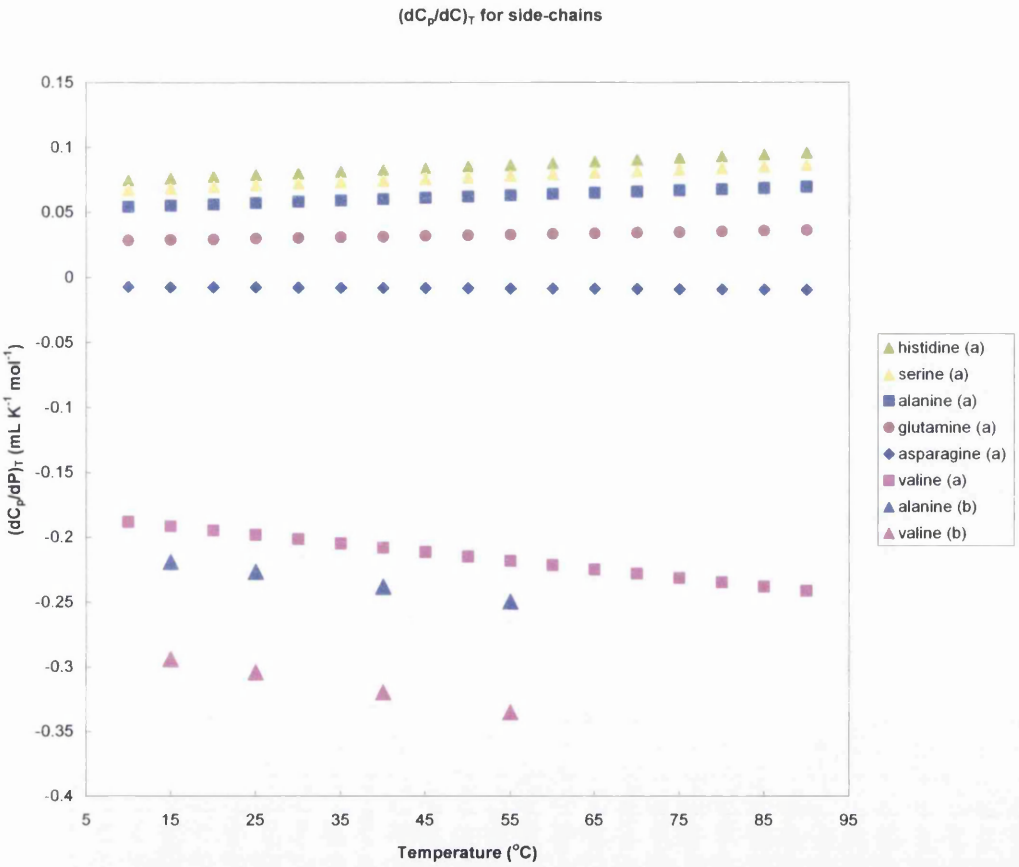

Figure 4.8 $\left(\partial C_p / \partial P\right)_T$ for amino acid side-chains derived from density measurements: (a) from DSD for tripeptides Hackel et al. (1999), (b) from isothermal densitometry for N-acetyl amino acid amides Hakin and Hedwig (2000)

Amino acid	$\left(\partial C_p / \partial P\right)_T$ for amino acid model system (mL K^{-1} mol^{-1})	$\left(\partial C_p / \partial P\right)_T$ for tripeptides model system (mL K^{-1} mol^{-1})	$\left(\partial C_p / \partial P\right)_T$ for N-acetyl amino acid model system (mL K^{-1} mol^{-1})
Asn	-0.026	-0.008	-
Gln	-0.033	0.030	-
His	-0.040	0.079	-
Ser	-0.011	0.071	-
Ala	-0.010	0.057	-0.227
Val	-0.034	-0.198	-0.304

Table 4.3 The values of $\left(\partial C_p / \partial P\right)_T$ at 25°C for the amino acids side-chains calculated.

Figure 4.8 and Table 4.3 show the $\left(\partial C_p / \partial P\right)_T$ values for the side-chains derived from the two model systems studied. The sign of $\left(\partial C_p / \partial P\right)_T$ agrees with the side-chains hydrophobicity, except from the two values, for Ala and Asn derived from tripetides.

The values obtained from the amino acid model system by PPC have negative values of $\left(\partial C_p / \partial P\right)_T$ for all the studies side-chains, and, as opposed to the data for the whole amino acids molecules, there is not even a trend here that would agree with the side-chain hydrophobicity (see Figure 4.6).

The overall conclusion is that subtracting the heats of glycine from the heats of whole amino acids from calorimetric PPC measurements results in values for both α and $\left(\partial C_p / \partial P\right)_T$ that do not reproduce hydrophobicity of the side-chains. This is most probably due to electrostriction caused by the charged amino and carboxyl groups in the direct proximity of the side-chain and amino acid model system being inappropriate for such subtraction.

The other two model systems for evaluating side-chain properties give better results in α and $\left(\partial C_p / \partial P\right)_T$, which mainly agree with side-chains hydrophobicity. The other two systems were however studied by densitometry, and it was the volume of the reference compound that was subtracted from the compounds studied to obtain the side-chain properties, not the heat of the reference compound as in the case of PPC. Density measurement results actually should not be compared to the calorimetric measurements results.

PPC proves to be a useful technique, when the whole amino acids molecules are considered – the trends in α and $\left(\partial C_p / \partial P\right)_T$ agree well with the trend in hydrophobicity of the side-chains. The problem with differentiating between the

structure making and structure breaking properties seem to come mostly from the model system chosen and not from the technique.

PPC shows good potential for discriminating between structure making and structure breaking properties of solutes by obtaining $\left(\partial C_p / \partial P\right)_T$ easily as have been shown by Batchelor et al. (2004). It would be advantageous to apply this technique to the other model compounds systems and evaluate their structure making and structure breaking properties from PPC, a calorimetric method, for comparison with the existing densitometric data.

4.4 Amino acids in modified aqueous solvents

If we consider the two-state mixture model of water again, the balance between the more dense and less dense forms, and hence water properties as a solvent, can be changed in a variety of ways, either by changing absolute variables such as temperature or pressure, or by adding solutes or other solvents to water and creating a solution with modified properties as a solvent. The solution's hydrogen-bonded structure in such an aqueous solution is different if we compare it to the pure water at the same conditions (temperature and pressure). The two-state mixture model of water describes the changes in water's hydrogen-bonded structure in all of the above cases.

Here, the focus is on modifying the water structure by addition of different solutes / solvents. It has long been observed the effect some substances have on protein stability. The terms 'kosmotrope' (order-maker) and 'chaotrope' (disorder-maker) refer to the property of increasing, or decreasing respectively, the hydrogen-bonded structure of water. It has been recently shown that although some of protein stabilisers and destabilisers work by the indirect mechanism of changing the water structure, some work by other mechanisms such as possibly preferential interaction, excluding volume effects or by increasing or decreasing the solubility of a protein's hydrophobic core (Batchelor et al. 2004).

Methanol addition to water changes water structure in an interesting way. At low concentrations is enhances H-bonded structure in water, due to forming clathrate cages around the hydrophobic methyl group (Sato et al. 2000). This structure making properties are also confirmed by the negative values of $\left(\partial C_p / \partial P\right)_T$ determined from the PPC measurement of 2% methanol solution in water (see Figure 4.9).

However, above 30% concentration v/v "abrupt breakage of the saturated hydration structure" takes place (Sato et al. 2000). Water becomes hydrogen bonded with methanol hydroxyl group, which decreases its hydrogen bonded structure. At these concentrations methanol becomes a structure breaker. The

values of $\left(\partial C_p / \partial P\right)_T$ determined from PPC for 40% methanol concentration are positive (in the room temperature region), indicating structure breaking properties. At the higher temperature these values become negative, probably because with increasing temperature there is less structuring in water that can be "broken" by methanol molecules.

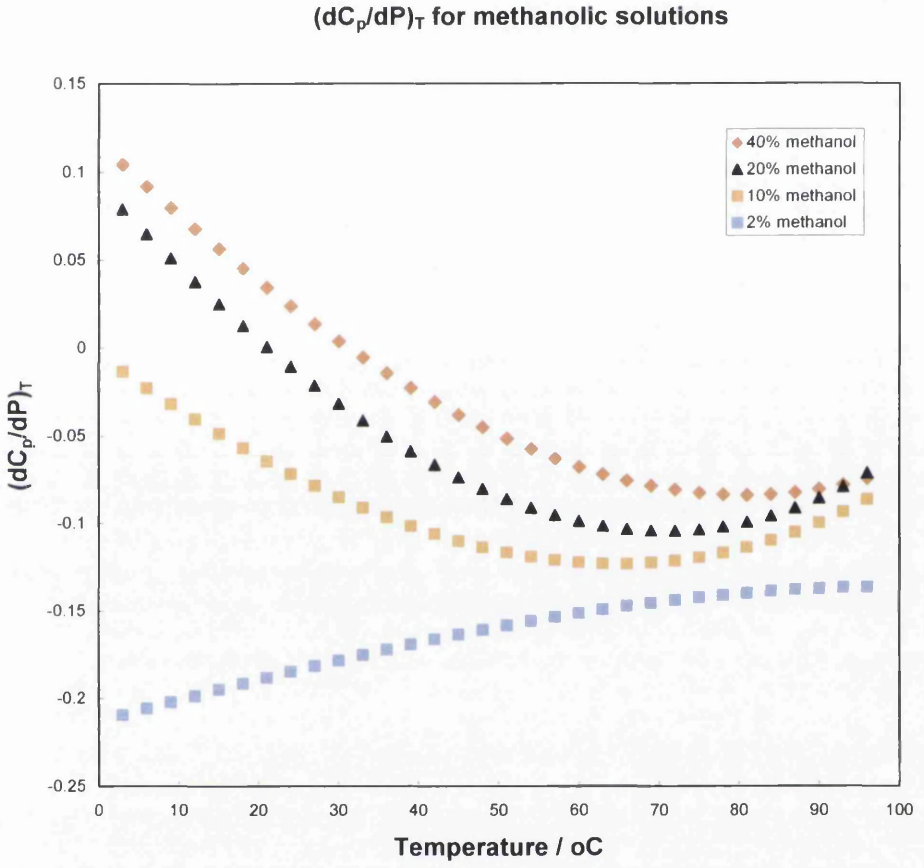

Figure 4.9 $\left(\partial C_p / \partial P\right)_T$ for methanol in water– calculated from α obtained by PPC from the heats of methanol solutions in water

Calculations of $\left(\partial C_p / \partial P\right)_T$ values for methanolic solutions were carried out in the same way as for the amino acids, as described earlier in this chapter.

On the other hand, D_2O is known to have stronger hydrogen bonding than water. Thus in this solvent the structure making and structure breaking properties should be enhanced.

The two above solvents were chosen to investigate their effects on properties of the model solutes – amino acids. Three amino acids, glycine, valine and asparagine, were chosen for the study of the effects of modifying the water's H-bonded structure on their structure breaking properties.

The results are presented in the Figures 4.10, 4.11 and 4.12.

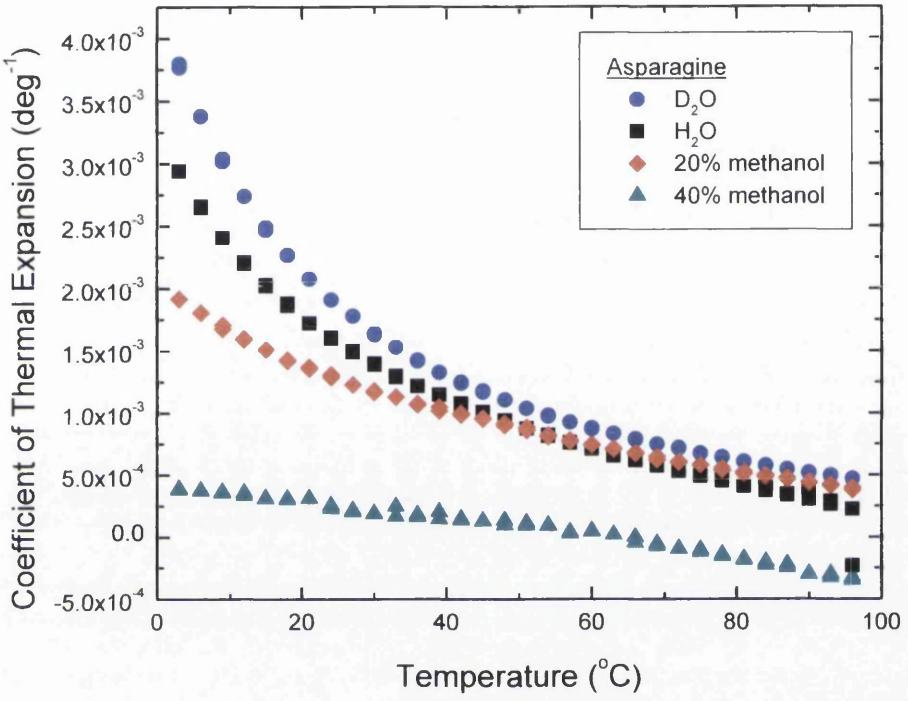

Figure 4.10 The thermal expansion coefficient obtained by PPC for asparagine in water, D_2O, 20% and 40% (v/v) methanol solutions.

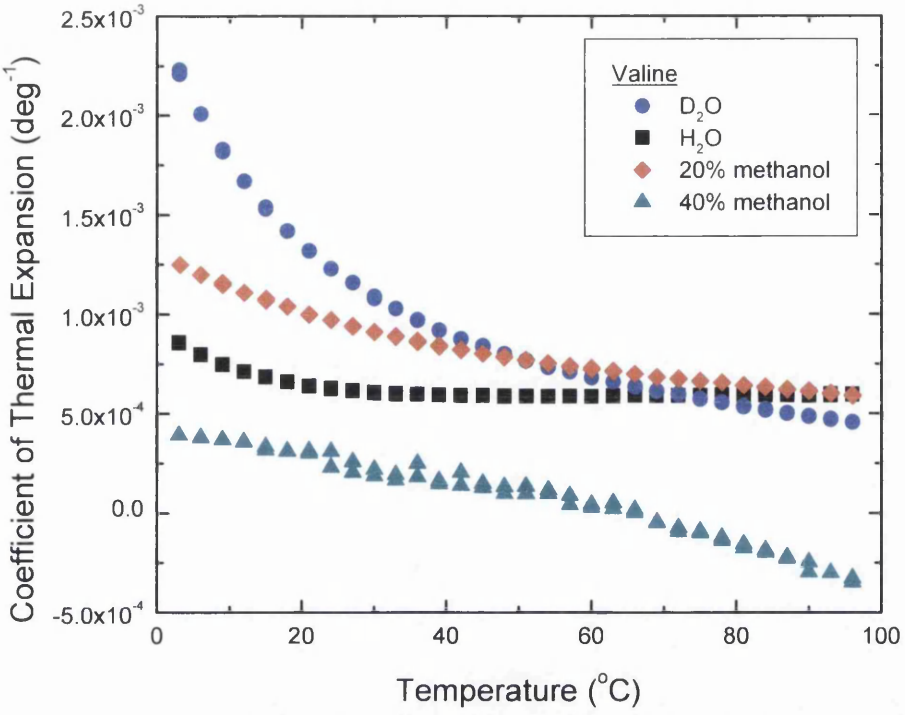

Figure 4.11 The thermal expansion coefficient obtained by PPC for valine in water, D_2O, 20% and 40% (v/v) methanol solutions.

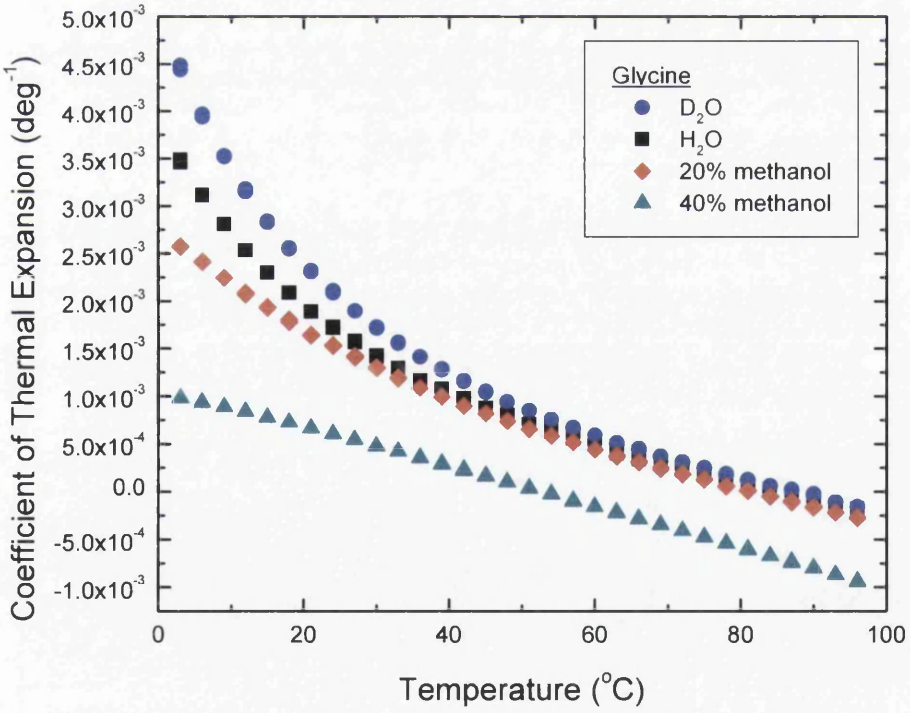

Figure 4.12 The thermal expansion coefficient obtained by PPC for glycine in water, D_2O, 20% and 40% (v/v) methanol solutions.

The general trend in the temperature dependence of thermal expansion coefficient α seen in the figures 4.10 – 4.12 is higher α values in D_2O as compared to H_2O and lower α in 20% methanol solution and even lower in 40% methanol.

As well, the curvature of the $\alpha(T)$ function is enhanced in D_2O in comparison to water, whereas it is decreased in methanolic solutions. The curvature of $\alpha(T)$ corresponds to its derivative, which is used for $\left(\partial C_p / \partial P\right)_T$ evaluation. Enhanced curvature is equivalent to increase in $\left(\partial C_p / \partial P\right)_T$, which indicates enhanced structure breaking properties. Again, decreased curvature in 20% and 40% methanol indicates lower $\left(\partial C_p / \partial P\right)_T$ than in water, and thus decreased structure breaking properties.

The results thus confirm that the stronger H-bonding D_2O as compared to water enhances solute's structure breaking properties, whereas the addition of methanol to water decreases these properties with increasing methanol concentrations.

4.5 Discussion

Though amino acids are protein building blocks, they are not the best small molecular model compounds for studying protein solvation. In proteins the exposed surface amino acid side-chains are neighbouring with peptide groups and the other side-chains, whereas in the amino acid molecule they are flanked by two charged groups and that is a different environment from the protein molecule.

This study shows, however, that the PPC is a more useful technique to study structure making and breaking properties than densitometric measurements. Firstly, because isothermal measurements at several temperatures can be easily automated in PPC and not in densitometry. Secondly, because $\left(\partial C_p / \partial P\right)_T$, a predictor of structure breaking and making properties, is a first derivative from α obtained from PPC, and a second derivative of V° obtained from densitometry. In the case of data obtained from densitometry as compared to the PPC, this increases the error associated with fitting temperature dependent functions to experimental data and then calculating their derivatives.

Conceptually, tripeptides and N-acetyl amino acids amides should be better models for volumetric properties of amino acid side-chains, however due to obtaining data through densitometry and later calculating the second derivative of the temperature dependence function of V°, the predictions of the structure making and breaking properties are not always accurate.

Though there is very little difference in the thermal expansion coefficient for amino acids and α for side-chains are almost identical, PPC is still useful for following the changes of structure making and breaking properties that occur when amino acids are transferred to a different solvent.

D_2O was shown to intensify structure making properties of both amino acids, valine and asparagine. On the contrary, methanolic solutions decrease these properties with increasing concentration of methanol.

As these solvents were shown to have an effect on the solvation of amino acids, they were chosen for the study of solvation of proteins. Modifying the solvent influences the solvation of exposed amino acid side-chains on the protein surface and hence modifies the hydrophobic effect that arises from solvation.

Chapter 5

ΔC_P OF PROTEIN UNFOLDING IN METHANOL WATER MIXTURES

Outline

Chapter 5 covers

- Previous studies of protein unfolding and stability in methanol water mixtures
- Lysozyme unfolding in methanol water mixtures studied by DSC
- Ribonuclease A unfolding in methanol water mixtures studied by DSC
- Structural studies of the three proteins in methanol water mixtures by circular dichroism

5.1 Introduction

The change in heat capacity (C_p) that is observed by DSC during thermal protein unfolding comes from melting of ordered water solvating non-polar residues exposed during the unfolding process (Privalov and Gill 1988). Thus large positive ΔC_p for unfolding of proteins is believed to be the "signature" of the hydrophobic effect that stabilises native structures of proteins.

It was shown previously that the change in the water H-bonded structure upon adding methanol as a cosolvent influences the extent of the ΔC_p value of unfolding of a model protein, bovine ubiquitin (Woolfson et al. 1993). The previous studies on ubiquitin are described below.

Additionally, it was shown previously that ubiquitin and lysozyme at low temperature are folded into native-like structures in methanol/water mixtures. Supporting structural information for ubiquitin and lysozyme from literature studies using NMR and CD in methanolic solutions is also presented in this chapter.

The intention here is to extend the study of ΔC_p changes to other proteins, and to complete the picture by later comparing this with volumetric information obtained from PPC for the same proteins (in the next chapter).

This chapter presents the investigation of the effect an increase in methanol concentration has on the ΔC_p value of unfolding of two other model proteins, lysozyme and ribonuclease A. As the structural information for ribonuclease A is not available from literature, the research into the ribonuclease A structure by circular dichroism is presented to complete the picture.

5.2 Previous research on protein structure and unfolding in methanolic solutions

5.2.1 *Ubiquitin thermal unfolding in methanolic solutions*

The unfolding of bovine ubiquitin has been studied in aqueous solutions of methanol of concentrations between 0 to 50% v/v (Woolfson et al. 1993). The change in heat capacity (ΔC_p) for each methanol concentration was determined there by series of DSC experiments in buffers of varying pH by the method described in chapter 2. Their findings were that as addition of methanol decreases the ordering of water, the ΔC_p also decreases, disappearing altogether at the concentration of alcohol above 30% v/v.

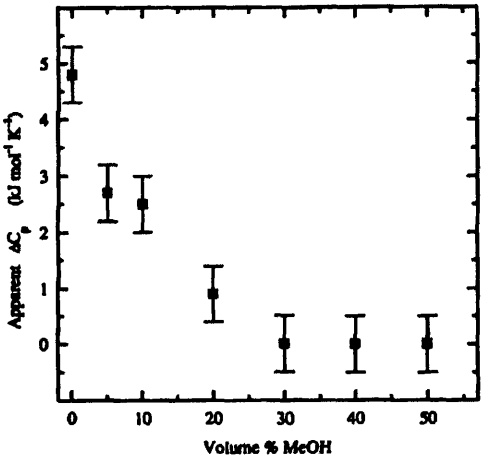

Figure 5.1 The effect of increasing methanol concentration on the heat capacity change of ubiquitin unfolding. (Woolfson et al. 1993)

ΔC_p for ubiquitin in water (with no methanol added) was 4.8 ± 0.5 $kJ \cdot K^{-1} \cdot mol^{-1}$and it was shown to decrease by more than by half by addition of 20% v/v methanol to water (Woolfson et al. 1993). The results from my preliminary work also confirm this effect of methanol concentration increase on the decrease in ubiquitin ΔC_p, the values obtained for ΔC_p of ubiquitin unfolding were 1.0 ± 0.17 $kJ \cdot K^{-1} \cdot mol^{-1}$ in 20% aqueous methanol, 0.80 ± 0.12 $kJ \cdot K^{-1} \cdot mol^{-1}$ in 30% and 0.0 ± 0.22 $kJ \cdot K^{-1} \cdot mol^{-1}$ in 40% aqueous methanol.

ΔC_p of ubiquitin unfolding for different methanol concentrations has also been determined from NMR analysis of chemical shifts (Jourdan and Searle 2001) confirming the close to zero ΔC_p above 30% v/v methanol in water. At low pH, the partial unfolding of ubiquitin to the A state was monitored by NMR through the appearance of a new set of resonances slightly displaced from those of the N state (Figure 5.2a). This was most clearly visible for the signal of His 68 at 8.8 ppm. The coexistence of two sets of signals shows the two conformations to be in slow exchange, which enabled the thermodynamics (ΔC_p, ΔH and ΔG) of the N to A state transition to be determined from the temperature dependence of the relative populations.

The data in Figure 5.2b show that the N to A transition has a noticeable temperature dependence in methanol water mixtures. ΔG vs. T shows significant curvature in 20% methanol, the plots become, however, essentially linear in 30-50% methanol, indicating that ΔC_p is significantly diminished under these conditions, in agreement with the conclusions of Woolfson et al. (1993).

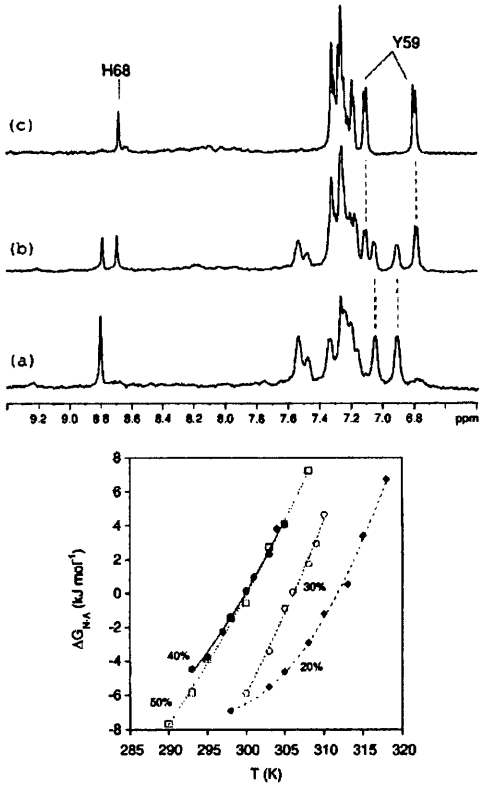

Figure 5.2 (top) 1H NMR spectra (500 MHz) of the native to A state transition in 40% methanol at pH 2.0; (a) N state at 288 K; (b) N and A state equally populated at 300 K; and (c) A state fully populated at 318 K. (bottom) Temperature-stability

profiles (ΔG vs. T) for the N to A transition at various concentrations of methanol (20, 30, 40, and 50% v/v). Linear lines of best fit indicate ΔC_p that is close to zero for 30, 40 and 50% methanol in water (from Jourdan and Searle 2001).

By NMR only two clearly resolved states in slow exchange can be seen. This demonstrated that that ubiquitin folds cooperatively to the native state, even thought in methanol water mixtures the solvent-ordering effects of the hydrophobic interactions are significantly diminished (Jourdan and Searle 2001).

5.2.2 *Ubiquitin - structural information in methanolic solutions*

High resolution structures of ubiquitin have been determined by both X-ray and NMR (DiStefano and Wand 1987; Vijay-Kumar et al. 1987; Weber et al. 1987). Alcoholic cosolvents (both TFE and methanol) have been shown to induce a partially unfolded state at low pH (A state) in which a high proportion of secondary structure (both native and non-native) is stabilized in the absence of significant tertiary interactions (Brutscher et al. 1997; Harding et al. 1991; Stockman et al. 1993). The A state of ubiquitin in 60% methanol at pH=2.3 is represented by three loosely coupled segments of secondary structure with enhanced internal mobility (see Figure 5.3) (Brutscher et al. 1997)

Figure 5.3 (left) Structure of the N state of ubiquitin from the X-ray coordinates (1ubq) (Vijay-Kumar et al. 1987)); (right) model of the A state of ubiquitin in 60% methanol at low pH (Brutscher et al. 1997). (Figure adapted from Jourdan and Searle 2001)

However, the A state of ubiquitin was only shown to exist in the methanol concentrations of above 50% and at low pH. Jourdan and Searle (2001) in their

studies of ubiquitin unfolding in methanol and urea mixtures probed ubiquitin structure with circular dichroism at various methanol concentrations in water (see Figure 5.4).

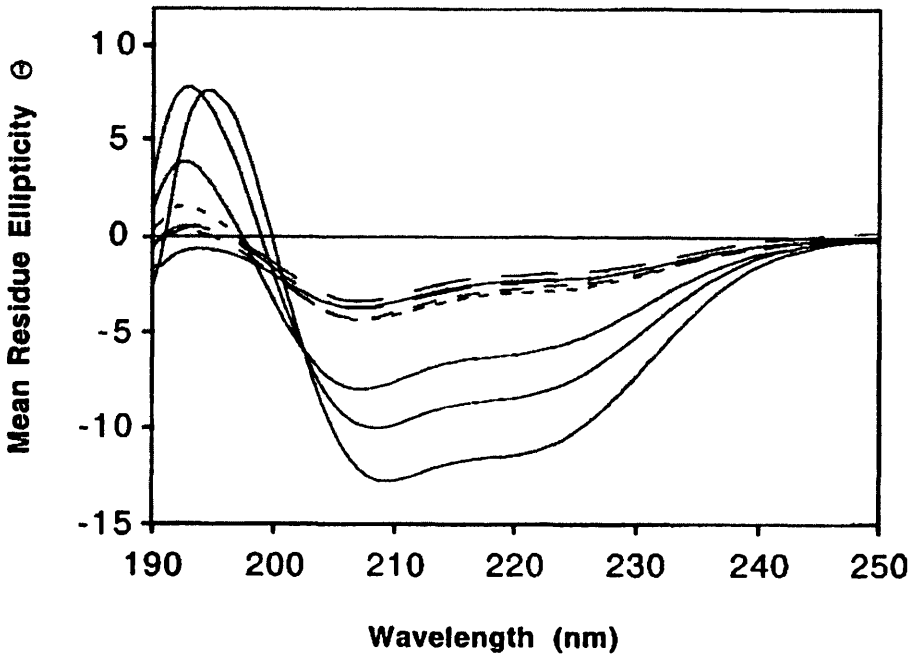

Figure 5.4 CD spectra of ubiquitin collected at 290K and pH 2.0 at various concentrations of methanol (0, 10, 20, 30, 40, 50, 60, and 100% in order of increasing ellipticity at 222 nm). (Jourdan and Searle 2001)

In the Figure 5.4 the transition from native (N) to the A state above 50% v/v methanol is evident from the large increase in ellipticity at 208 and 222 nm. The CD measurements of ubiquitin demonstrate that in the range of methanol concentrations where ΔC_p of ubiquitin thermal unfolding was studied by Woolfson et al. (1993) (up to 50% v/v) ubiquitin was natively folded at the temperature of 290K (16.85°C).

Taking the unfolding and structural data for ubiquitin together, Jourdan and Searle (2001) concluded that at methanol concentrations between 30 - 50% van der Waals interactions in the packing of the nonpolar protein core, which is common to both the N -> U and the N -> A transitions, appear to be the folding drive force in the absence of entropic effects associated with release of ordered solvent (hydrophobic effect). Their data demonstrated that the hydrophobic effect is not a prerequisite for stabilization of the native state or the A state and that van der

Waals packing of the nonpolar core appears to be the dominant factor in stabilization of the native state (Jourdan and Searle 2001).

5.2.3 *Lysozyme - structural information in methanolic solutions*

Similarly to ubiquitin, a small model protein lysozyme has also been shown to undergo the transition to A state in methanolic solutions (Kamatari et al. 1998). This transition also appears above 50% v/v methanol in water and is highly cooperative (no intermediates of molten globule characteristics were detected). Figures 5.5 and 5.6 below show the transition from N to A state with increasing methanol concentration monitored by NMR and CD respectively.

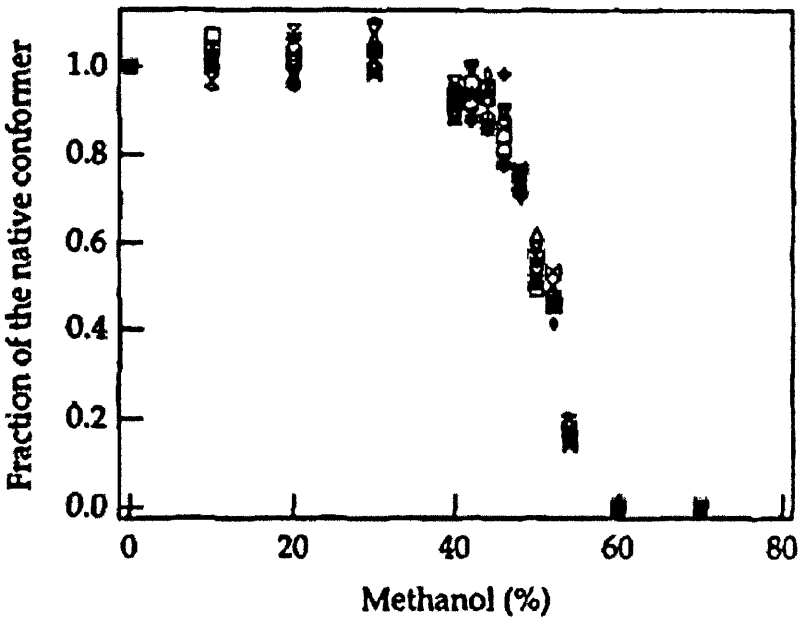

Figure 5.5 Fractions of the native state conformation versus methanol concentration, obtained from ^{1}H NMR signal intensities of several individual protons. The NMR measurements were made at pH* 1.9 and 25°C. (from Kamatari et al. 1998)

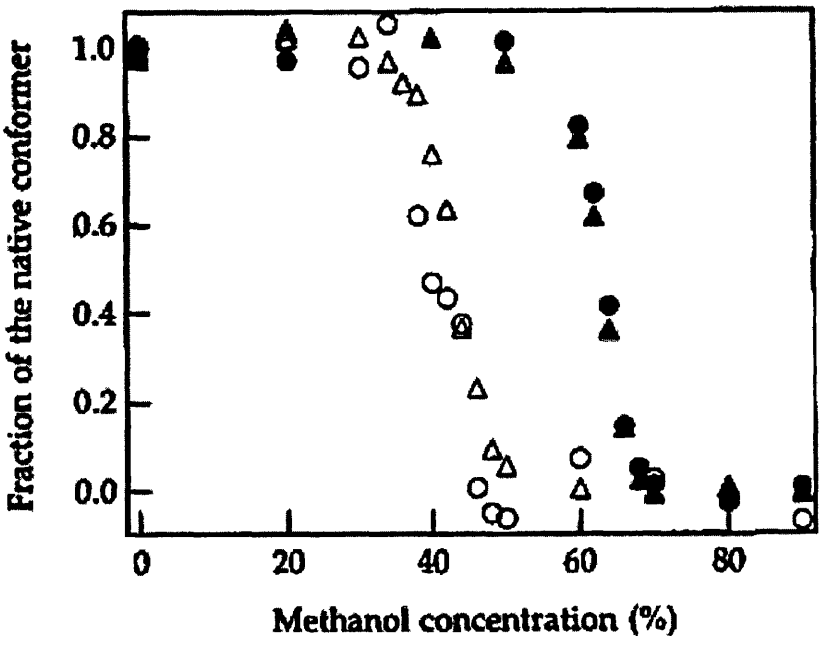

Figure 5.6 Fractions of the native state conformation versus methanol concentration, obtained from the ellipticity change at 222nm (circle) and 288 nm (triangle). The measurements were made at pH 1.9 (open) and pH 3.0 (filled) at 25°C. (from Kamatari et al. 1998)

Because there was structural information available for lysozyme in methanolic solutions, it was the first protein chosen here for investigating the effect of increasing methanol concentrations on the heat capacity change of unfolding.

Moreover, since these structural studies confirm that ubiquitin and lysozyme retain their native-like structures below 50% methanol, it seems reasonable to suppose that any effects on the thermodynamics of unfolding measured by DSC relate mainly to solvent interaction with the unfolded polypeptide, providing the methanol concentration is not too high.

5.3 Lysozyme – ΔC_p of unfolding in methanolic solutions

ΔC_p for lysozyme unfolding in water (with no methanol added) was calculated from data from Kovrigin and Potekhin (2000) where the thermal unfolding of lysozyme was monitored by DSC over a pH range in aqueous acetonitrile solutions. The enthalpies of unfolding (ΔH) together with temperature of unfolding (T_m) data were used to calculate ΔC_p in water using the method described in chapter 2. ΔC_p in water was calculated to be 5.80 ± 0.13 kJ·K^{-1}·mol^{-1}. The effect of methanol addition to water on ΔC_p of lysozyme unfolding has not been investigated previously.

Surprisingly in comparison to the ubiquitin studies, the results obtained for ΔC_p for lysozyme unfolding in 40% methanol in water are not close to zero. The enthalpy vs. temperature plots for water and 40% methanol (Figure 5.7) show that lysozyme is destabilized in 40% methanol as compared to pure water - the unfolding temperatures are lower. However, the correlation between enthalpy and temperature of unfolding yields ΔC_p of value 4.03 ± 0.33 kJ·K^{-1}·mol^{-1}, which is only 30% decrease as compared to ΔC_p for protein unfolding in water.

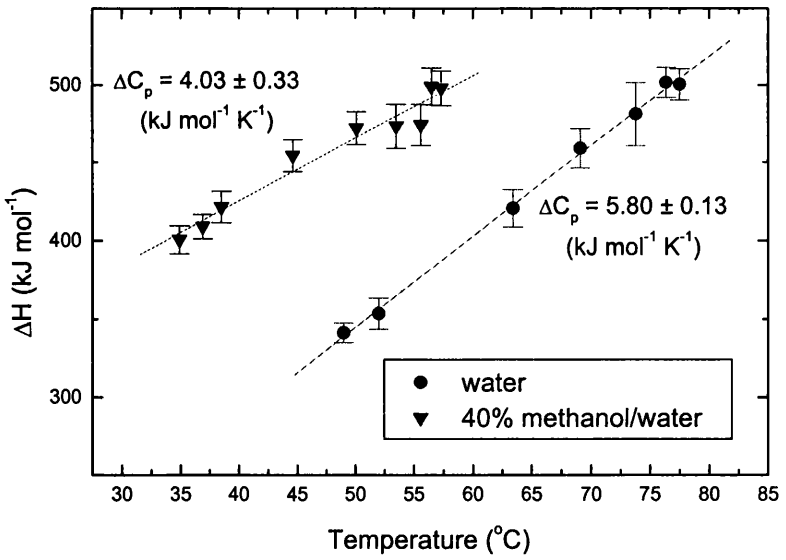

Figure 5.7 Comparison of unfolding enthalpies versus temperature plots in water and 40% aqueous methanol. Lysozyme unfolding for 40% methanol was monitored by DSC in the pH range 2.0 – 4.5; ΔC_p for unfolding in water was calculated from data from Kovrigin and Potekhin (2000)

Lysozyme unfolding was also analysed in 30% and 50% of methanol in water, showing further decrease in ΔC_p to the value of 3.13 ± 0.67 kJ·K^{-1}·mol^{-1}, which is about 50% of the ΔC_p of lysozyme unfolding in water (see Figure 5.8).

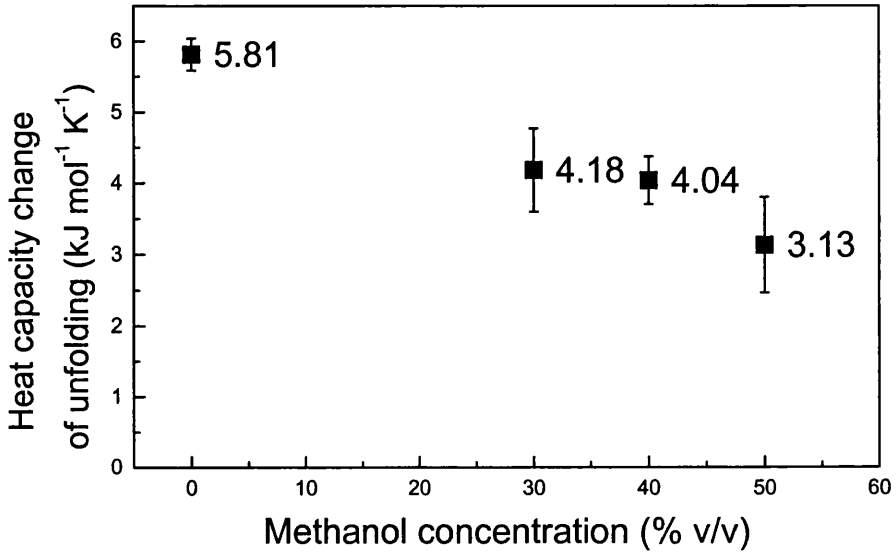

Figure 5.8 Change in ΔCp of lysozyme unfolding with increasing methanol concentration

5.4 Ribonuclease A - ΔC_p of unfolding in methanolic solutions

Data for ribonuclease A unfolding in water were obtained from the thermal unfolding study of ribonuclease and its mutants by DSC over a pH range published by Catanzano et al. (1997). Here, the enthalpies of unfolding (ΔH) and the temperature of unfolding (T_m) data from Catanzano et al. (1997) were used to calculate ΔC_p in water using the method described in chapter 2. ΔC_p in water was calculated to be 8.24 ± 0.82 kJ·K^{-1}·mol^{-1}. The effect of methanol addition to water on ΔC_p of ribonuclease A unfolding has not been investigated previously.

From the DSC results obtained in this study the value of ΔC_p of RNase A in 40% methanol that was determined was 10.08 kJ $\pm$ 0.82 mol^{-1} K^{-1}. This was even more unexpected than the values for lysozyme, as here the value of ΔC_p in 40% methanol increases by 22% when compared to that in water without methanol.

Ribonuclease A unfolding was also calculated from DSC measurements in 20% and 30% methanol concentrations, showing lowering of ΔC_p by 16% in 20% methanol , and in methanol concentration of 30% the increase of ΔC_p to the same value as in water (see Figure 5.9).

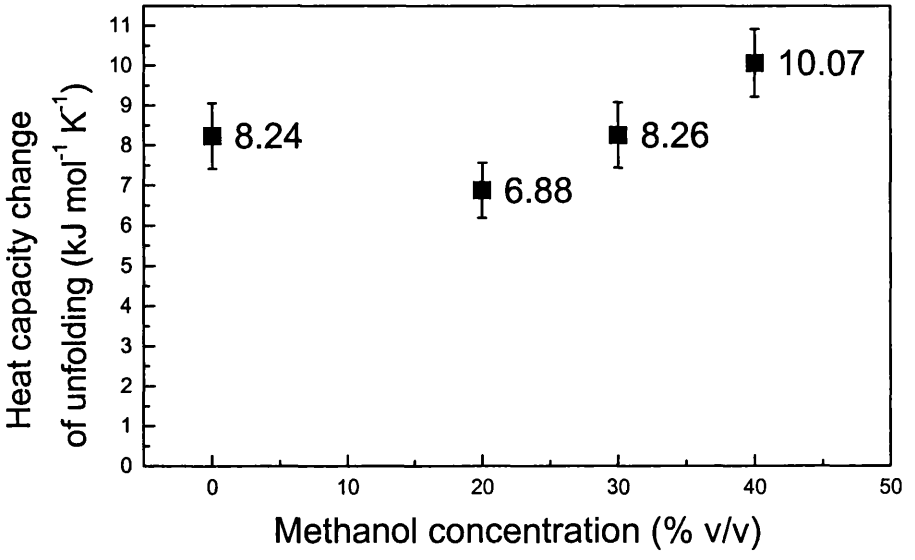

Figure 5.9 Change in ΔCp of ribonuclease A unfolding with increasing methanol concentration

As ribonuclease A has not been characterized structurally in methanolic solutions, it is possible that it undergoes a transition to the A state (expanded α-helical state, that lysozyme and ubiquitin adopt above 50% v/v methanol concentration) or some other structural change. The conformation of ribonuclease A was therefore studied with circular dichroism to check if the protein is in its native conformation in these conditions.

5.5 Structural studies in methanolic solutions by circular dichroism

To investigate why the behaviour of ΔC_p of unfolding with increasing methanol concentration differs between ubiquitin, lysozyme and ribonuclease A, the structure of these proteins was probed by circular dichroism in water, and in methanol concentrations of 30 and 40% v/v.

Because the pH variation method used for determination of ΔC_p requires DSC measurements to be carried out at the range of different pH conditions, CD spectra for the proteins were acquired at the extremity pH conditions, pH = 2.0 and pH=7.0.

To look for differences both in the folded and in unfolded state, CD measurements were carried out at two temperatures, at 10°C (for the folded state) and at 80°C (for the unfolded state). It has to be noted, however, that at pH = 7 the proteins are not unfolded at 80°C in water (0% methanol), and ubiquitin may not be fully unfolded at this temperature even at 30% methanol. In fact, ubiquitin in water at pH=7 most probably has not started unfolding at 80°C, as at pH = 4 its T_m is 90°C (Wintrode et al. 1994), thus it is most likely higher at pH=7. In the case of pH = 2 the proteins should be fully unfolded (denatured) in all the conditions.

For lysozyme and ribonuclease A the CD spectra were recorded in both far (190-260nm) and near-UV (260-340nm) region, for ubiquitin in the far-UV region only, as ubiquitin has not give enough signal in the near-UV region.

All the CD spectra are included in Appendix A.

5.5.1 *Circular Dichroism spectra obtained at pH = 2*

When looking at the far-UV spectra of ribonuclease A, it can be noted that the spectra at different methanol concentrations at the low temperature (10°C) do not overlap. There seem to be significant differences between different methanol concentration for ribonuclease A, when compared to the spectra of lysozyme and ubiquitin, which overlap at 10°C at different methanol concentrations. The most

significant difference for ribonuclease A is between spectra for 0% and 20% methanol, where the intensity at 222nm increases by 14%. The spectra for 0% and 10% methanol overlap, suggesting the structural change takes place between 10% and 20% methanol. The spectra for 20% and 40% overlap as well.

When a near-UV spectra of ribonuclease A are considered, the spectra for 0% and 10% overlap again, and spectra for 30% and 40% overlap as well, but are different from the 0 and 10% ones, with 8% difference in intensity at 276nm. Overall this picture suggests that there is some change in the structure of ribonuclease A, where above 20% methanol the protein conformer seems to be significantly different from that between 0% and 10% methanol.

Near-UV spectra for lysozyme at 10°C also show the difference between the spectrum in water, and overlapping spectra for 30 and 40% methanol. However, at far-UV the spectra at low temperature overlap, thus the differences in near-UV spectra may merely come from the modified solvent environment around more exposed residues that produce signal in near-UV region (cysteines, aromatic amino acids).

Near-UV spectra for ubiquitin are not available as the signal for this protein is too weak in this UV region.

The high temperature (80°C) spectra in near-UV for both lysozyme and ribonuclease show that the tertiary structure is diminished in the unfolded protein. The far-UV structures for ribonuclease show structural differences between different methanol concentrations, similarly to the low temperature far-UV spectra for this protein. The high temperature spectra for lysozyme and ubiquitin do not show such significant differences.

5.5.2 *Circular Dichroism spectra obtained at pH = 7*

At low temperature (10°C) at pH = 7 the far-UV spectra of ribonuclease A do not show much significant variation at different methanol concentrations as they do at pH = 2.

The far-UV spectra of lysozyme at pH = 7, however, shows more variation at different methanol concentrations than at pH = 2, but they do not seem to be hugely significant. The difference between lysozyme in water and in 30 – 40% methanol seem to be significant in near-UV, similarly to the pH=2 spectra.

At high temperature (80°C) the near-UV spectra of ribonuclease A and lysozyme show diminished tertiary structure in the unfolded proteins. The far-UV spectra don't show much variation with methanol concentration for these two proteins. The high temperature far-UV spectra for ubiquitin are inconclusive, as at the temperature of 80% ubiquitin in water is not unfolded, thus making it impossible to compare unfolded spectra across the methanol concentration.

Both spectra of ubiquitin in water and 30% methanol at pH = 7 were also acquired at 95°C and show further unfolding as compared with the spectra at 80°C (see Figure A.7 in Appendix A) but the protein in water cannot be assumed fully unfolded even at the temperature of 95°C making the comparisons impossible, as the unfolded spectrum of ubiquitin in water at pH = 7 is inaccessible experimentally.

5.6 Conclusions

Based on the previous studies on ubiquitin unfolding in aqueous methanolic solutions, it was expected that the trend in the decrease of ΔC_p with increase in methanol concentration applies to other proteins as well. However for both lysozyme and ribonuclease, the significant decrease of ΔC_p above 30% methanol was not observed.

There is a decreasing trend in ΔC_p for lysozyme, but only half of the ΔC_p is diminished, with methanol concentration as high as 50% v/v. The decreasing trend can also be noted for ribonuclease between 0% to 20% methanol concentrations, where ΔC_p decreases by 16%. The possibility is that these two proteins cannot unfold into the same state as ubiquitin does in methanolic solutions.

It has been argued by Jourdan and Searle (2001) that ubiquitin forms the A-state at high temperatures, thus its unfolded state is different from unfolded state in water. There is still cooperative folding taking place in methanolic solutions, even though the unfolded state is somewhat different. It is possible that lysozyme and ribonuclease A only form the A-state partially in the unfolded state, as both proteins have four disulfide bridges each, restricting the possibility of such conformational change. Thus the unfolded form may be quite different in lysozyme and ribonuclease A when compared to ubiquitin.

The ΔC_p for ribonuclease A starts increasing again at the concentrations of methanol above 20%, reaching ΔC_p values at 40% methanol that are higher than that for ribonuclease A unfolding in water. Concluding from the circular dichroism study, there are some structural differences in the protein conformation below and above 20% methanol concentration, which may signify that above 20% methanol we are observing different folded and unfolded states than in water, making the comparisons across the methanol concentration range impossible.

Traditionally, the hydrophobic effect was considered to be the main source of the ΔC_p effect for protein unfolding. ΔC_p in such model would originate from

exposing hydrophobic residues upon protein unfolding and melting of the water's H-bonding structure in solvation layer of those amino acids.

Addition of methanol diminishes this contribution of hydrophobic interactions to ΔC_p of unfolding, as have been shown in the case of ubiquitin. However, it is recently been argued, that there are additional contributions to ΔC_p effect of protein unfolding (Cooper 2005). One of such contributions could be for example cooperative melting of hydrogen bonding within the protein natively folded structure upon the unfolding.

Such other contributions to ΔC_p of unfolding could explain why, whereas ΔC_p for ubiquitin unfolding in methanolic solutions is almost completely diminished, it decreased only slightly for lysozyme and ribonuclease A unfolding. The remaining ΔC_p of unfolding of lysozyme and ribonuclease A in methanolic solutions could possibly come from such other contributions to ΔC_p.

Chapter 6

PPC OF PROTEIN UNFOLDING IN METHANOL WATER MIXTURES

Outline

Chapter 6 covers

- Thermal expansion coefficient α determined for protein unfolding of ubiquitin, lysozyme and ribonuclease A in methanolic solutions, water and D_2O
- Structure making and structure breaking properties of protein surface
- Variation in ΔV_{unf} with increasing methanol concentration

6.1 Introduction

Pressure Perturbation Calorimetry technique was developed with studying protein solvation in mind, as volumetric properties (thermal expansion coefficient measured by PPC amongst them) are sensitive to changes in the volume of the molecules together with their solvation (hydration) layers.

As such, this technique perfectly suits studying protein unfolding in water-methanol mixtures, a system that is aimed at investigating the hydrophobic interactions' role in protein unfolding and stability. If the volumes of the folded and unfolded forms of a protein are assumed to be similar in water to the methanolic solutions, the results obtained from this technique should be mostly sensitive to the changes in the solvation layer water at the protein surface.

In methanolic solutions, both because of the disruption caused by the methanolic –OH groups and by the more "organic" solvent-like nature of methanol, there should be less "clathrate-like" structure formation around non-polar amino acids; the so-called "solvent ordering effect" is decreased. The structure making properties of non-polar solutes should be diminished in such solvent systems, as the hydrogen bonded structure of water is decreased upon addition of methanol. Using this system for PPC study thus gives further insight into protein solvation under these specific conditions and the importance of hydrophobic interaction in stabilizing protein folded states.

If less structuring around such solutes is induced in water by methanol addition, the solvation layer should have a smaller volume in the folded state at lower temperature. On the contrary, with the use of D_2O instead of water, a solvent where the hydrogen bonds are stronger and more structuring should be induced by structure making solutes, the hydration volume might be expected to be larger. The expected volume changes upon protein unfolding would as a result be smaller in methanolic solutions than in water (there is less solvent structuring to be lost upon unfolding) and larger in D_2O (there is more H-bonded structuring in the solvation layer to lose upon unfolding).

Since the ΔV_{unf} is expected to be different for the proteins in different solvents, PPC is a perfect method to gain further insight into protein unfolding in such modified solvents systems.

At first experiments were designed to repeat the protein unfolding studies at different concentrations of methanol cosolvent that were carried out to obtain information on ΔC_p. Here, information, additional to previous studies, on ΔV of unfolding of model proteins of ubiquitin, lysozyme and ribonuclease A is obtained by PPC and the information on ΔC_p and ΔV are compared.

The protein unfolding of the three proteins has also been studied in D_2O in order to determine if this solvent has opposite effects on structure making and breaking properties to methanolic solutions, and thus on volumetric properties of the studied proteins.

6.2 Protein unfolding transition observed in PPC corresponds to the one observed in DSC

The unfolding reaction in water and in 10% aqueous methanol for the three model proteins was monitored by DSC under the same conditions as the ones used for PPC unfolding in order to confirm that the transition monitored by both techniques is exactly the same (the same starting points, melting points and end points of the transition visible by both methods).

In order to see the full unfolding transition for the proteins in the PPC experimental range (0-95°C), the melting temperature (T_m) had to be decreased by lowering the pH. With the T_m for ubiquitin unfolding at 90°C at pH = 4 (Wintrode et al. 1994), 79°C for lysozyme at pH = 4.6 (Velicelebi and Sturtevant 1979) and 62°C for ribonuclease A at pH = 6 (Catanzano et al. 1997), the end of the unfolding transition and the post-transition baseline necessary to estimate ΔV_{unf} would not be possible to see in the PPC experiment. Thus all the unfolding experiments were carried out at the pH = 2.

The unfolding transition can be clearly seen for all three proteins (see Figures in Appendix B). The unfolding temperatures agree with the T_m determined from DSC experiments under the same conditions.

What needs to be noted however, is that the DSC experiments were carried out at the constant scan rates of 60 °C per hour (1°C/min), whereas in the PPC experiment the rate with which the temperature increases varies. The rate can be estimated after the scan is finished, by dividing the time taken by the experiment, by the range of temperatures between the lowest and highest points measured. It has been determined that if the PPC scan is carried out with temperature intervals of every 3°C (with automatic baseline determination) it corresponds to the DSC scan rate of 32°C per hour. These were the standard conditions for the temperature PPC scan, and the average scan rate here is twice slower than for the typical DSC experiment.

Various "scan rates" have been used for different experiments, and it has been shown in several cases that the transition temperature for protein unfolding in PPC was scan rate independent for the studied proteins. This can be seen on the example of ubiquitin unfolding in 10% methanol at pH=2 in Figure 6.1. This is expected for the relatively reversible thermal transition in these single globular proteins.

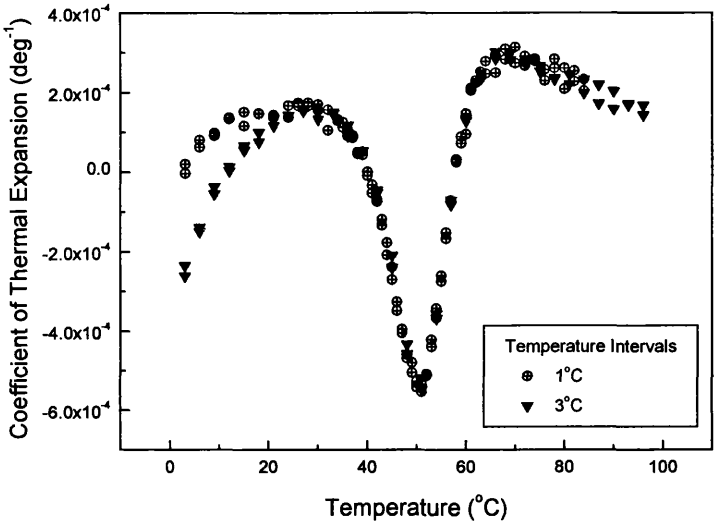

Figure 6.1 Ubiquitin unfolding in 10% methanol, pH=2, monitored at two different "scan rates" in PPC: with temperature intervals of 1°C and 3°C.

It should be noted that for some proteins the T_m of unfolding is dependent on the scan rate and in such conditions the average temperature increase "scan rate" of the PPC scan should be estimated, and if needed, the DSC experiment should be carried out with the same scan rate.

Temperature intervals	Experimental Scan Rate in PPC
3°C	32 °C/hour
2°C	20 °C/hour
1°C	13 °C/hour

Table 6.1 Average experimental scan rates in the PPC experiments.

It needs to be remembered however that these are just rough comparisons, as the constant scan rate of the DSC experiment is not equivalent to the step-wise increments of temperature in PPC that are separated by periods of isothermal pressure scans.

6.3 Structure making and structure breaking properties of protein surface

Here, the summary for temperature dependence of α is presented in different methanol concentration, in water and in D_2O in Figures 6.2 – 6.4.

Apart from the expected decrease of T_m with increase in methanol concentration, the interesting general trend may be seen in the values of α – at higher methanol concentrations they become lower, and often negative with increase of methanol content to 30-40% v/v.

The other interesting fact to notice on the summary figures is that the shape of the α(T) curve before the unfolding transition begins varies considerably with solvent conditions (the individual figures for each protein and solvent conditions are presented in Appendix B). Usually the pre-transitional baseline has negative slope (coefficient $(\partial\alpha/\partial T)_P$) in water and D_2O, whereas the slope of α(T) becomes positive in methanolic solutions.

The slope of α(T) function is represented by its derivative $(\partial\alpha/\partial T)_P$ that can in turn be used to estimate the sign of $(\partial C_p/\partial P)_T$, which is indicative of structure making or structure breaking properties. In water and D_2O the slope of α(T) is negative, which gives positive $(\partial C_p/\partial P)_T$ - indicating structure breaking properties of the protein surface before the unfolding transition begins. This is intuitive, as the exposed amino acid residues on the protein surface are mostly polar as the protein has to be soluble in water.

In the case of methanolic solutions the situation is reverse, the positive slope of α(T) indicates negative $(\partial C_p/\partial P)_T$ and thus structure making properties of the

protein surface. Being aware that the structure of the studied proteins does not change with methanol additions to water up to 40% in the case of ubiquitin and lysozyme (see Chapter 5) and the residues on the protein surface are still the same as in the case of protein in water, this leads to conclusion that the polar amino acids lose some of their structure breaking properties in the methanol water mixtures. This signifies and further confirms the effect that the methanol addition to water has on the solvent-ordering effect of the residues (both polar and non-polar) on the protein surface.

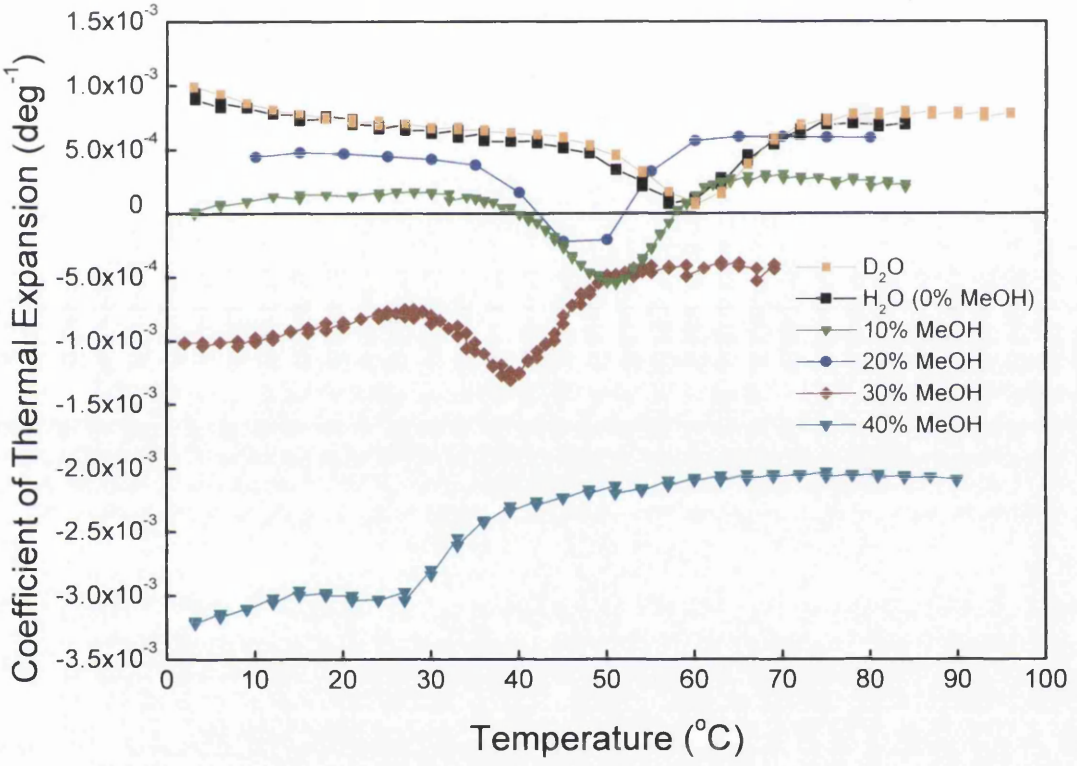

Figure 6.2 Ubiquitin unfolding - Changes in α in different methanol concentration, in water and in D_2O.

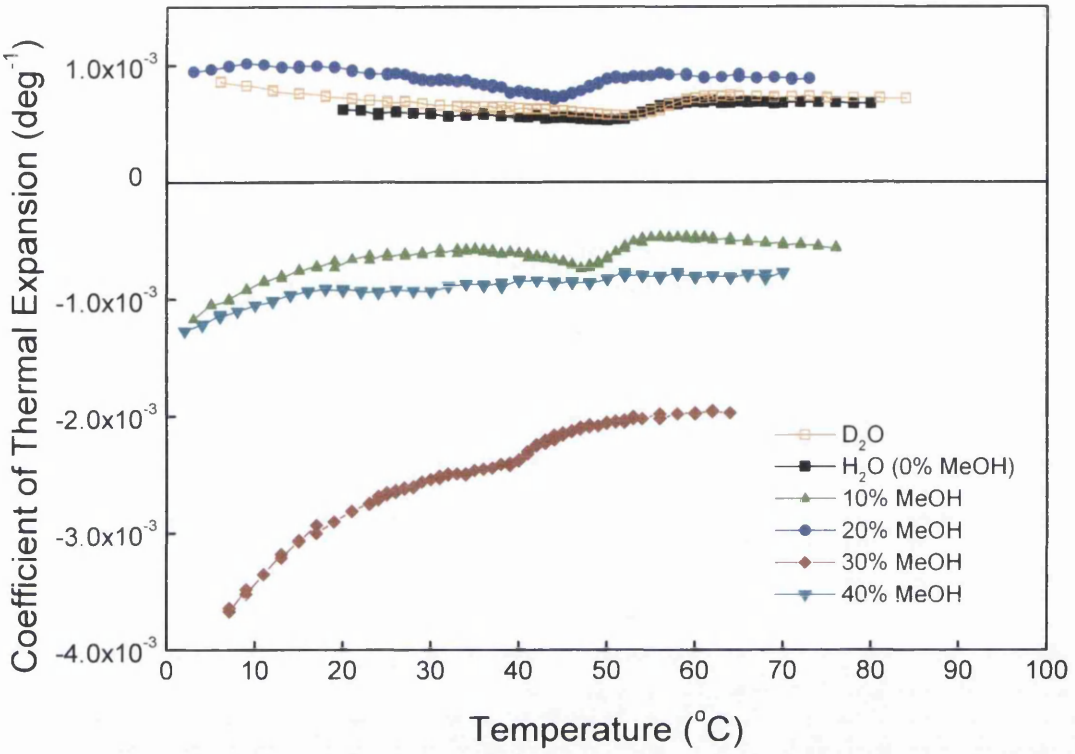

Figure 6.3 Lysozyme unfolding - Changes in α in different methanol concentration, in water and in D_2O.

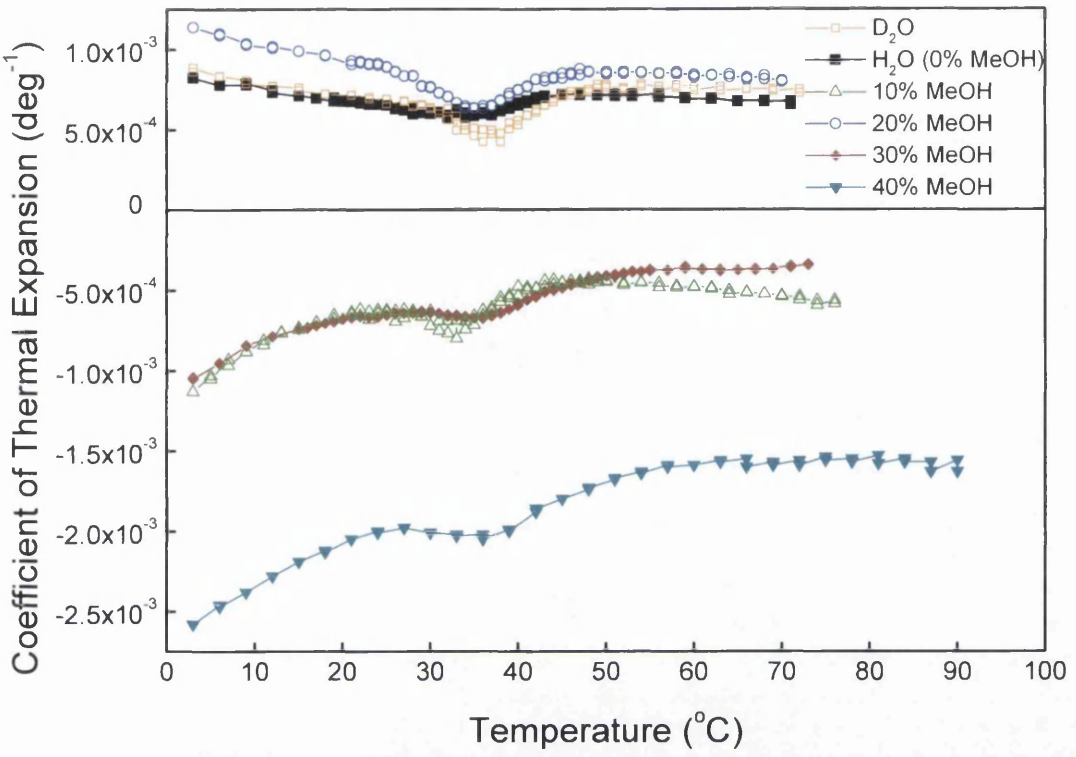

Figure 6.4 Ribonuclease A unfolding - Changes in α in different methanol concentration, in water and in D_2O.

Lin et al. (2002) propose the difference in α between the temperatures of 5 and 40°C ($\Delta\alpha_{5\text{-}40}$) as a useful predictor of the solvation effects associated with the accessible surface of the native proteins, since expansion of the intrinsic volume of a protein should not exhibit a large temperature dependence. The authors showed that the values of $\Delta\alpha_{5\text{-}40}$ correlated with the amino acid composition of the six proteins studied, they did however show that there is lack of correlation of $\Delta\alpha_{5\text{-}40}$ with the amino acid composition of the solvent accessible surface of the proteins.

I would like to propose the slope of the pre-transitional baseline in the plot of α(T) as an indicator of solvation effects at the protein surface rather than $\Delta\alpha_{5\text{-}40}$. Firstly, it is indicative of the structure making and structure breaking properties of the solutes as it is directly related to $\left(\partial C_p / \partial P\right)_T$. Secondly, comparing $\Delta\alpha_{5\text{-}40}$ is only a valid approach if the unfolding transition does not start below 40°C, and could not

be used here as for most of the conditions studied in this thesis the unfolding transition starts as low as 20°C.

Both approaches aim to determine the sign of the slope of the pre-transitional baseline, the determination of the α derivative $(\partial\alpha / \partial T)_P$ seems however a more flexible approach than comparing the differences in α at the two selected temperatures.

6.4 Volume changes upon unfolding (ΔV_{unf}) varies with increasing methanol concentration

Here, the volume change upon protein unfolding was determined from the temperature dependence of thermal expansion coefficient (α) for the three proteins studied in this thesis at various methanol concentrations in water.

The aim was to investigate if the ΔV_{unf} change with the change in solvent conditions, and if such changes correlate with the changes observed earlier in ΔC_p.

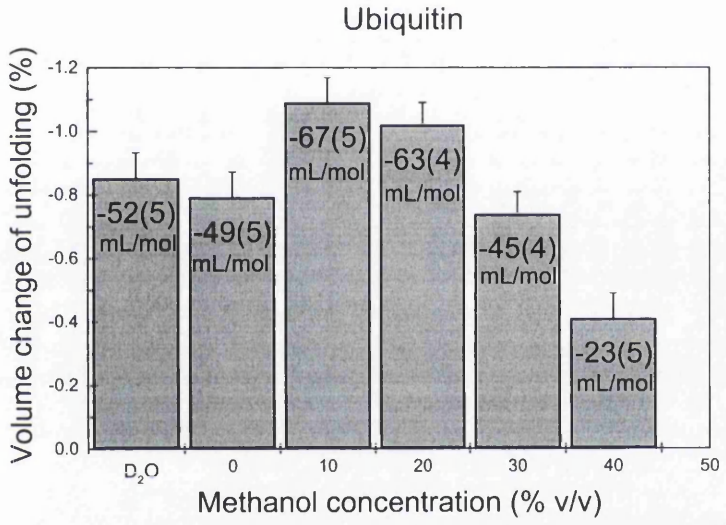

Figure 6.5 Change in ΔV_{unf} with increasing methanol concentration for ubiquitin unfolding.

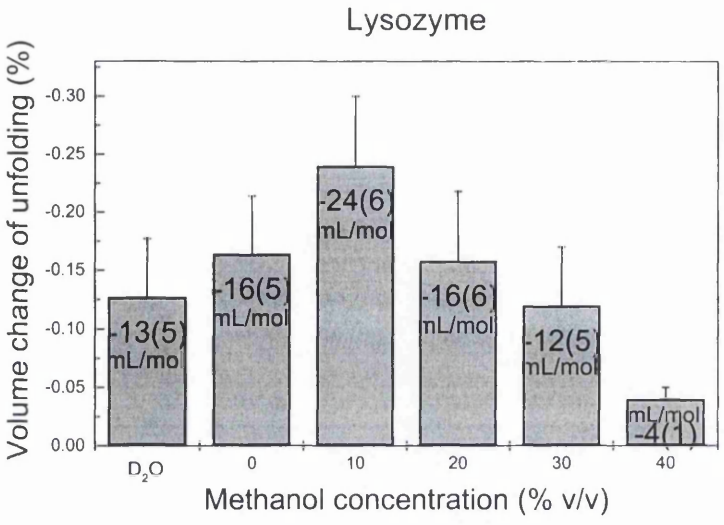

Figure 6.6 Change in ΔV_{unf} with increasing methanol concentration for lysozyme unfolding.

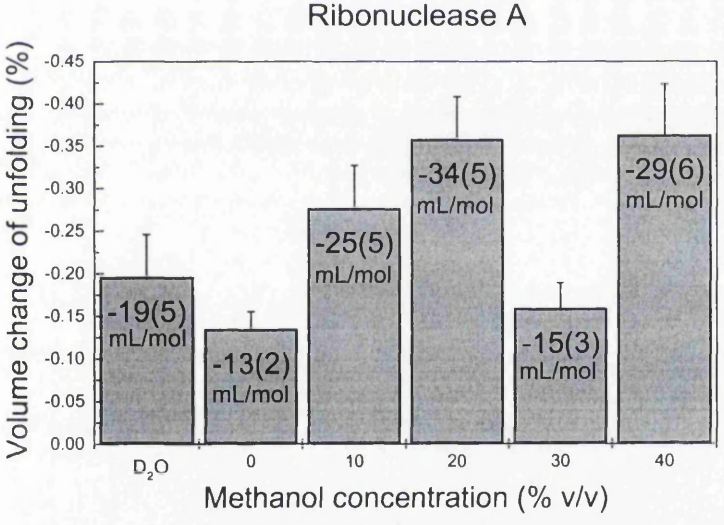

Figure 6.7 Change in ΔV_{unf} with increasing methanol concentration for ribonuclease A unfolding.

The volume change of unfolding (ΔV_{unf}) was determined from the temperature dependence of α measured by PPC as described in the Chapter 3. The volume change was calculated as the percent of the total partial molar volume of the protein.

The molar volume change upon unfolding in mL mol^{-1} presented in the Figures 6.5 – 6.7 was calculated by multiplying the known values of the partial molar volumes of the proteins (below) by the percent change determined from the calculations.

V^{o} (ubiquitin) = 6160 mL /mol
V^{o} (lysozyme) = 10 039 mL /mol
V^{o} (ribonuclease A) = 9620 mL /mol
(from Squire and Himmel 1979)

The volume change upon unfolding (ΔV_{unf}) that was determined for all the proteins and conditions in this study was always negative, i.e. the partial volume of the protein is lower of the unfolded state than that of the folded state.

The negative volume change can arise from the solvation effects of the protein surface, or melting out the H-bonded structure in the protein solvation layer with increasing temperature.

However, the extent of the decrease in volume (ΔV_{unf}) was observed to change with changing solvent conditions.

For lysozyme and ubiquitin there is a trend in ΔV_{unf} becoming less negative with increasing methanol concentration, which means smaller volume change upon unfolding. That could possibly come from the decreased structuring of water in methanolic solutions that decreases the volume of the solvation shell in the folded state. Assuming that the volumes of the unfolded protein solvation shell is similar in different methanol concentrations this could contribute to the decrease in ΔV_{unf}.

There is no trend in the ΔV_{unf} values of ribonuclease A with increasing methanol concentration. This could arise from the structural changes within the protein molecule that would largely influence its intrinsic volume. If the observed volume changes do not come mainly from the solvent effects it is impossible to separate the solvent contribution to the protein intrinsic volume contribution to the volume changes upon unfolding.

6.5 Conclusions

Overall, PPC proves to be useful technique for investigating the solvation effects of the protein.

The shape of the $\alpha(T)$ function in the pre-transitional baseline may be indicative of the extent of structure breaking properties of the protein surface, and may in future be a useful tool to estimate for example the effects the mutations in protein have on the solvation properties at the protein surface.

The protein unfolding transition is associated with smaller volume changes in methanolic solutions than in water. The unfolding in D_2O does not seem to have a significant effect on the volume change though. This may arise from the differences between water and D_2O being too small to be visible in the case of macromolecules such as proteins investigated here.

For ubiquitin and lysozyme the decrease in ΔV_{unf} that is seen above 20% methanol concentration correlates with the decrease in ΔC_p of the thermal unfolding reaction in the same solvent conditions. This may be indicative that the decreased solvent ordering effect in methanolic solutions indeed causes the decrease in the volume of the protein solvation shell in the natively folded state.

Chapter 7

PPC OF CYTOCHROME C CONFORMATIONAL TRANSITIONS

Outline

Chapter 7 covers

- Previous studies of cytochrome c structural transitions by high pressure spectroscopy

- PPC and DSC study of cytochrome c thermal unfolding at atmospheric pressure

7.1 Introduction

Cytochrome c is a small (12.4 kDa), single-chain globular protein that is an interesting model for studying protein unfolding, because it may adopt the native (N), unfolded (U) and molten globule (MG) conformation, depending on solution temperature, pH and ionic strengths (Arai and Kuwajima 2000; Goto et al. 1993). At room temperature and acidic pH (around pH = 2) the conformational state of cytochrome c is determined by the ionic strength – at low salt the protein is unfolded, while at high salt it adapts the MG conformation (Goto et al. 1993). Molten globule was also shown to be the intermediate state between native and unfolded forms in the acid unfolding of cytochrome c (Goto et al. 1993).

In contrast to many other proteins that are capable of adopting the molten globule states, cytochrome c exhibits a cooperative thermal unfolding from the molten globule state (MG-to-U transition) (Potekhin and Pfeil 1989).

Recently, the volume change for cytochrome c thermal unfolding was evaluated at different pH conditions (both for native and molten globule unfolding) and at different pressures by monitoring thermal unfolding using Soret absorption spectroscopy (Dubins et al. 2003).

Soret absorption spectroscopy measures optical absorbance of the heme group in the vicinity of 400 nm and reflects the spin state of the iron, and is hence sensitive to the conformational state of the protein. The native protein (low spin state) has a maximum at 409nm with an extinction coefficient of 106 mM^{-1} cm^{-1}, while the molten globule state at pH = 2 (high spin state) has a maximum at 400nm and with an extinction coefficient of 115 mM^{-1} cm^{-1} (Goto et al. 1990).

Dubins et al. (2003) studied the thermal unfolding of cytochrome c for a MG-to-U transition (molten globule to unfolded state) at pH = 2 and N-to-U (native to unfolded state) at the pH range from 3.4 to 4.3. The denaturation profiles were obtained at increasing pressures from 50 to 2200 bar and extrapolated to obtain these parameters at the atmospheric pressure (data for 50bar were used to estimate

the atmospheric pressure thermodynamic parameters as the difference between them could be neglected in this study).

Each denaturation profile was analysed using the two-state approximation to obtain the transition temperature, T_m, and van't Hoff enthalpy, ΔH_{vH}.
The volume changes of unfolding (ΔV_{unf}) were obtained from temperature dependence of T_m and ΔH_{vH} by using the Clapeyron equation:

$$\Delta V(T_m, P) = \left(\frac{\Delta T_m}{\Delta P}\right)\left(\frac{\Delta H_{vH}}{T_m}\right) \qquad (8.1)$$

Two important observations about ΔV_{unf} were made. Firstly, the change in the volume upon unfolding for natively folding cytochrome c is positive under all experimental conditions, i.e. the protein partial volume (the intrinsic volume plus its hydration shell) increase upon unfolding. Secondly, the unfolding of the molten globule conformation was observed to have the negative volume of unfolding, i.e. its partial volume decreases upon unfolding, at the pressures up to 1500 bar.

The data on volume changes at atmospheric pressure are readily accessible by PPC and the experiment here was designed to compare the volumetric data obtained from this high pressure spectroscopic study and from calorimetric measurements by PPC and DSC.

The measurements were carried out at exactly the same conditions as in the published article, at the series of pH of 2.0, 3.4, 3.6, 4.0 and 4.3, at the salt concentration of 200mM NaCl (the salt stabilising effect is necessary for molten globule formation at pH = 2, cytochrome c with no salt would be otherwise acid-unfolded at that pH and the MG-to-U transition could not have been studied). The protein concentration used though were larger than 0.3 mg/mL used by Dubins et al. (2003), because PPC requires protein concentrations above 3mg/mL. Here 5-7mg/mL concentrations were used for PPC and about 1 mg/mL for DSC. The temperature scanning rate in DSC (and the approximated temperature rate in PPC) was 0.5°C/min, the same as in the experiment by Dubins et al. (2003).

7.2 Comparison of thermodynamic data obtained from high pressure spectroscopy and calorimetry

The PPC experiments were carried out with the temperature intervals of every 3°C so that the experimental rate of temperature increase is comparable to that of Dubins et al. (2003). Obtaining data points at smaller intervals would make the integrations of temperature dependence of α and hence the ΔV_{unf} determinations more precise, but as the protein unfolding parameters sometimes display scanrate dependence (unlike ubiquitin example in Figure 6.1), the conditions were kept in agreement with the previous study to ease the comparison.

Instead of obtaining the data points at closer intervals, two scans were carried out at each pH and the resulting ΔV_{unf} were averaged. The percentage change in volumes upon unfolding obtained was -0.27% for MG-to-U transition at pH = 2 and between 0.40 and 0.70% for the N-to-U transition. The difference in ΔV_{unf} obtained from the two scans was 0.05-0.1%. The volume change percentage is relative to protein partial molar volume, and the value of $V^o = 8855$ cm^3 mol^{-1} was used to calculate the molar volume change upon unfolding for comparison to that obtained by Dubins et al. (2003). The results are presented below (Table 7.1).

pH	ΔV_{unf} from optical melting[a] (cm^3 mol^{-1})	ΔV_{unf} from PPC (cm^3 mol^{-1})	T_m from optical melting[a] (°C)	T_m from PPC (°C)
MG-to-U				
2.0	-36 ± 3	-24 ± 3	39.4 ± 0.3	46 ± 1
N-to-U				
3.4	15 ± 2	42 ± 3	62.8 ± 0.3	71.5 ± 0.5
3.6	24 ± 3	45 ± 4	62.3 ± 0.3	71 ± 1
4.0	34 ± 4	60 ± 3	69.2 ± 0.3	73 ± 1
4.3	48 ± 6	57 ± 3	69.5 ± 0.3	74.5 ± 0.5

Table 7.1 Comparison of volumes of unfolding (ΔH_{vH}) obtained from high pressure study([a]) by Dubins et al. (2003) and PPC of cytochrome c unfolding at the same conditions.

The DSC experiments were carried out with the same buffers as the PPC experiments, though with smaller concentration of the protein. The thermal denaturation profiles from DSC were used to determine the start and the end of the unfolding transition, to aid baseline determination for ΔV_{unf} calculation from the temperature dependence of α from PPC.

Additionally, the enthalpies of unfolding (ΔH) were evaluated for comparison with the data obtained previously in the high pressure study (Dubins et al. 2003). The thermal unfolding transition of both native and molten globule were both cooperative, with the $\Delta H_c/\Delta H_{vH}$ ratio close to 1 (between 0.97 and 1.25). Data for ΔH_{vH} are presented in the Table 7.2 below.

pH	ΔH_{vH} from optical melting[a] (kcal mol^{-1})	ΔH_{vH} from DSC (kcal mol^{-1})	T_m from optical melting[a] (°C)	T_m from DSC (°C)
MG-to-U				
2.0	31	39.6	39.4 ± 0.3	43.5 ± 0.3
N-to-U				
3.4	46	67.3	62.8 ± 0.3	73.6 ± 0.3
3.6	43	67.7	62.3 ± 0.3	67.3 ± 0.3
4.0	50	85.2	69.2 ± 0.3	71.4 ± 0.3
4.3	59	87.7	69.5 ± 0.3	73.6 ± 0.3

Table 7.2 Comparison of enthalpies of unfolding (ΔHvH) obtained from high pressure study(a) by Dubins et al. (2003) and DSC of cytochrome c unfolding at the same conditions.

7.3 Discussion

Generally, data from PPC and DSC agree qualitatively with the data obtained from the high pressure study (Dubins et al. 2003).The most important finding that ΔV_{unf} has a different sign for the MG-to-U and N-to-U transitions was confirmed by the data obtained from PPC.

However, the data obtained here from PPC and DSC have systematically higher values than that reported in the paper by Dubins et al. (2003). ΔV_{unf} values measured here are bigger by 9-27 cm^3 mol^{-1} (the difference at pH = 3.4 is quite

substantial). These differences result from slightly less pH dependence of ΔV_{unf} obtained from PPC than that obtained from high pressure spectroscopy.

This should be noted, however, that the volumes of unfolding measured by PPC for the transitions with similar T_m (pH 3.4 and 3.6 have T_m close to 71°C) yield similar values of ΔV_{unf}, 42 and 45 cm^3 mol^{-1}, respectively, whereas the high pressure study gives two different ΔV_{unf} of 15 and 24 cm^3 mol^{-1} at those pH conditions, even though the T_m values are very similar (62.8 and 62.3°C respectively).

The same is the case of the pH of 4.0 and 4.3. The results from PPC have similar T_m values (73 and 74.5°C) and similar ΔV_{unf} values (60 and 57 cm^3 mol^{-1}, respectively), whereas the ΔV_{unf} values obtained from the high pressure study are quite different (34 and 48 cm^3 mol^{-1}, respectively) though the T_m temperatures are almost identical (69.2 and 69.5°C).

The similarities between pH 3.4 and 3.6 are also visible from DSC results, with similar T_m values and ΔH between the two pH conditions obtained by both methods (DSC and high pressure study). The unfolding transitions at pH 4.0 and 4.3 are also described by the very similar thermodynamic parameters, again confirmed by both methods.

The systematic error with ΔV_{unf} and ΔH having bigger values in the study here than in the high pressure study by Dubins et al. (2003) may result from up to 20 times higher concentrations used here (in the case of PPC) and up to 10 times higher concentrations in the case of DSC. For example, the buffer used here was 10mM acetate (pH 3.4 – 4.3) or 10mM glycine - HCl (pH 2.0) in order to keep the same experimental conditions, but perhaps a buffer with higher concentration should have been used as the systematically slightly higher Tm here suggests that the pH monitored here may be slightly higher than that studied by Dubins et al. (2003) . Another source of disparities may lay in inaccuracies of both methods. In particular, it may be that changes in the Soret band do not necessarily reflect directly the conformational state of the protein.

Another conclusion drawn in the paper by Dubins et al. (2003) is also confirmed here. Based on the ΔV_{unf} for the MG-to-U and N-to-U transitions, the authors evaluated the value for ΔV for N-to-MG transition at 40°C ($\Delta V = 4 \pm 47$ cm^3 mol^{-1} or expressed in specific terms (per grams rather than per mol) $\Delta v = (0 \pm 4) \times 10^{-3}$ cm^3 g^{-1}) and compared it with Δv for this transition at 25°C (8×10^{-3} cm^3 g^{-1}) (from Chalikian et al. 1995). Based on these two values the authors evaluated the expansibility change, Δe, accompanying the N-to-MG transition to be $-(5 \pm 3) \times 10^{-4}$ cm^3 g^{-1} K^{-1}.

Here, it was possible to estimate this result directly from differences in α obtained for MG and N states at 25°C from PPC measurements.

α(N) = 5.7×10^{-4} K^{-1} (pH = 4.3)
α(N) = 6.1×10^{-4} K^{-1} (pH = 4.0)
α(N) = 5.4×10^{-4} K^{-1} (pH = 3.6)
α(N) = 5.4×10^{-4} K^{-1} (pH = 3.4)

α(MG) = 8.0×10^{-4} K^{-1} (pH = 2, scan 1)
α(MG) = 9.2×10^{-4} K^{-1} (pH = 2, scan 2)

Calculated from these values, the average difference in α between native (N) and molten globule (MG) states at 25°C is $-(2.9 \pm 0.6) \times 10^{-4}$ K^{-1}, which corresponds to Δe of $-(2.1 \pm 0.4) \times 10^{-4}$ cm^3 g^{-1} K^{-1}, the value with the same sign, at the same order of magnitude and within the error of the value estimated by Dubins et al. (2003).

It is remarkable that the values obtained indirectly from comparison of ΔV of cytochrome thermal unfolding at elevated pressures and ΔV of acid-induced folding at room temperature yield the expansibility of N-to-MG transition that is directly comparable to that obtained from PPC.

7.4 Conclusions

The finding of Dubins et al. (2003) that the volumes of unfolding have opposite sign for the transitions from native to unfolded and from molten globule to unfolded state was confirmed here.

This is the first comparison of volumetric data obtained from such different experimental techniques and approaches. The data on volumes and enthalpies of cytochrome c unfolding from high pressure spectroscopy has been shown here to be in good experimental agreement with data from calorimetry at atmospheric pressure.

Moreover, the value for specific expansibility change, Δe, of N-to-MG transition obtained indirectly from estimating ΔV of N-to-MG transition at two temperatures is shown to be in excellent agreement with the value of Δe for this transition obtained from the difference between the thermal expansion coefficients values of the protein at two conformations measured by PPC.

Here is has been shown that Pressure Perturbation Calorimetry has a potential to obtain the same volumetric parameters that so far were only available indirectly from high pressure studies and by monitoring the pressure dependence of protein unfolding thermodynamic parameters. Further study is needed to resolve what was the source of the small differences in results between the two techniques for cytochrome c unfolding and if such differences for other proteins occur as well.

Chapter 8

CONCLUSIONS AND FUTURE WORK

Outline

Chapter 8 covers

- General conclusions
- Suggested future work

8.1 General conclusions

As a result of the work described here, the following conclusions can be made:

1. PPC is a viable method for studying volume changes of protein transitions.

2. Expansibility in particular can be related to volume changes of the solvation layer at the protein surface.

3. Expansibility data can be correlated with structure making and structure breaking properties of the solutes.

4. There appears to be serious discrepancy in published data and interpretation of expansibility values for amino acid side-chains, which has been identified here.

5. The effects on methanol on ΔC_p and volumetric parameters of protein unfolding show some trends that might be related to structure making and breaking properties of methanol.

6. The PPC data of structural transitions of cytochrome c compare well with those obtained by others using more indirect spectroscopic techniques.

8.2 Suggested future work

The results obtained in this thesis open several possibilities for a new research.

First of all, the PPC measurements of amino acids need to be extended to include all twenty four naturally occurring amino acids, as only a small group has been studied in this work. Further verification of the thermal expansion coefficient in the published data could be carried out (e.g. on the aromatic amino acids).

The study of volumetric properties of amino acids and their side chains could also include other systems for studying side-chains properties in an environment that resembles proteins more closely, such as tripeptides and N-acetyl amino acids. These have been extensively studied by densitometry and PPC volumetric data could complete the picture of their characterisation. In addition this could further prove the viability of the PPC technique.

Protein transitions other than thermal unfolding (such as for example acid denaturation or guanidium/urea denaturation) could be examined by PPC as an extension of studying cytochrome c structural transitions. Proteins that form intermediate states (such as for example molten globule) on their folding/unfolding pathways could be chosen for such studies. Evaluation of volumetric properties of such folding intermediates could bring new insights into the protein folding problem.

As well as studying protein volumetric properties (α and ΔV) in the presence of denaturants, the same could be investigated for the proteins in the presence of protein stabilising solutes to evaluate their effects on the properties of the solvation shell at the protein surface.

The use of methanol as a cosolvent that perturbs the water hydrogen bonded structure could be extended to study other model proteins, provided that they can be shown to be natively folded at concentrations of methanol up to 40% v/v. Small, stable proteins should be chosen for such studies, preferably without

disulfide bonds in their structure, for comparison with previous results for ubiquitin, as both lysozyme and ribonuclease A differ from ubiquitin in that they do have disulfide bonds.

Acetonitrile, another cosolvent that decreases water hydrogen bonded structure similarly to methanol, has been previously used for studies of lysozyme unfolding and evaluation of ΔC_p in acetonitrile-water mixtures (Kovrigin and Potekhin 2000). This study could be extended by adding PPC measurement to evaluate if the acetonitrile effects on ΔV_{unf} and the ΔC_p correlate with each other. Additionally, this could be later extended to other proteins similarly to the methanol-water system.

The above are just a few new directions to be taken on the road to fuller understanding of thermodynamics of protein solvation, stability and structural transitions.

APPENDIX A

STRUCTURAL STUDIES IN METHANOLIC SOLUTIONS BY CIRCULAR DICHROISM

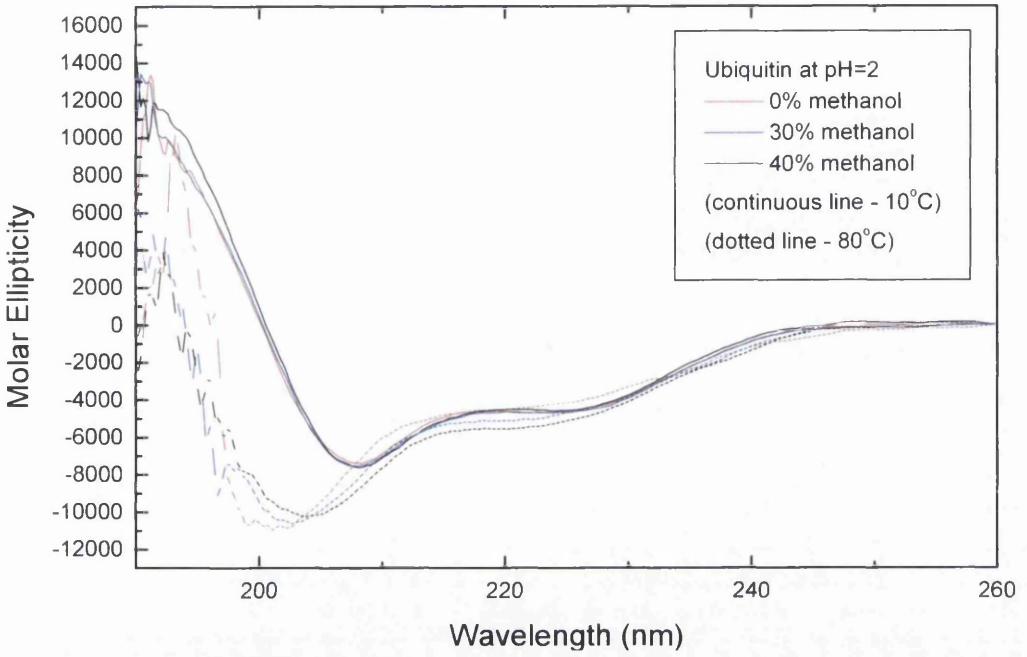

Figure A.1 Far-UV CD spectra of ubiquitin at pH=2, at various methanol concentrations and at temperatures of 10 and 80°C.
(Molar Ellipticity in all figures is expressed in the units of [deg m^{-1} M^{-1}] or [deg cm^2 $dmol^{-1}$] as explained in the section 2.3.3).

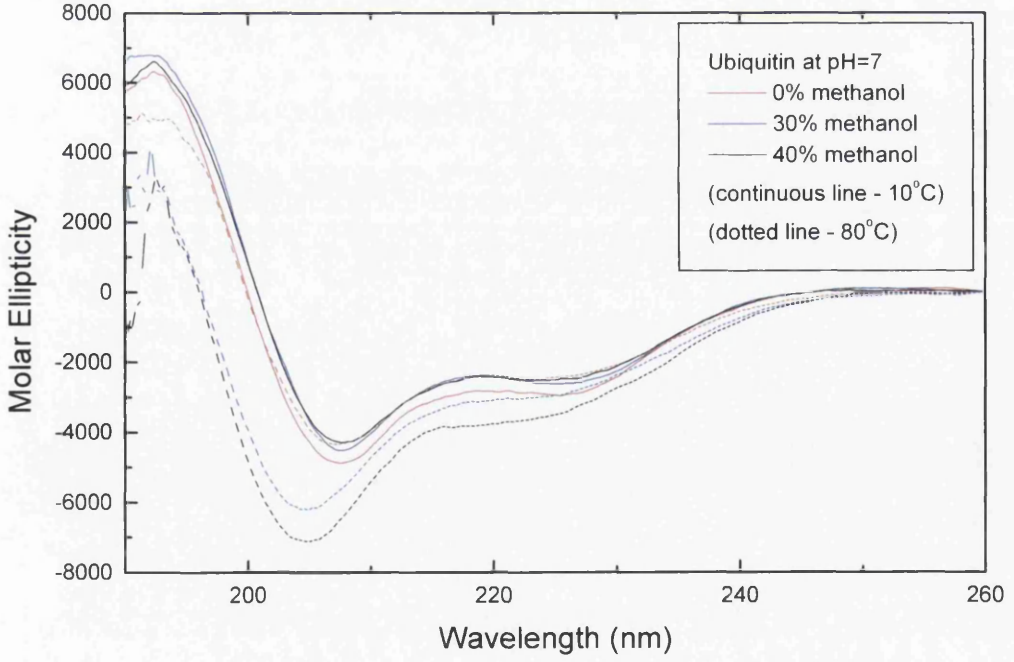

Figure A.2 Far-UV CD spectra of ubiquitin at pH=7, at various methanol concentrations and at temperatures of 10 and 80°C.

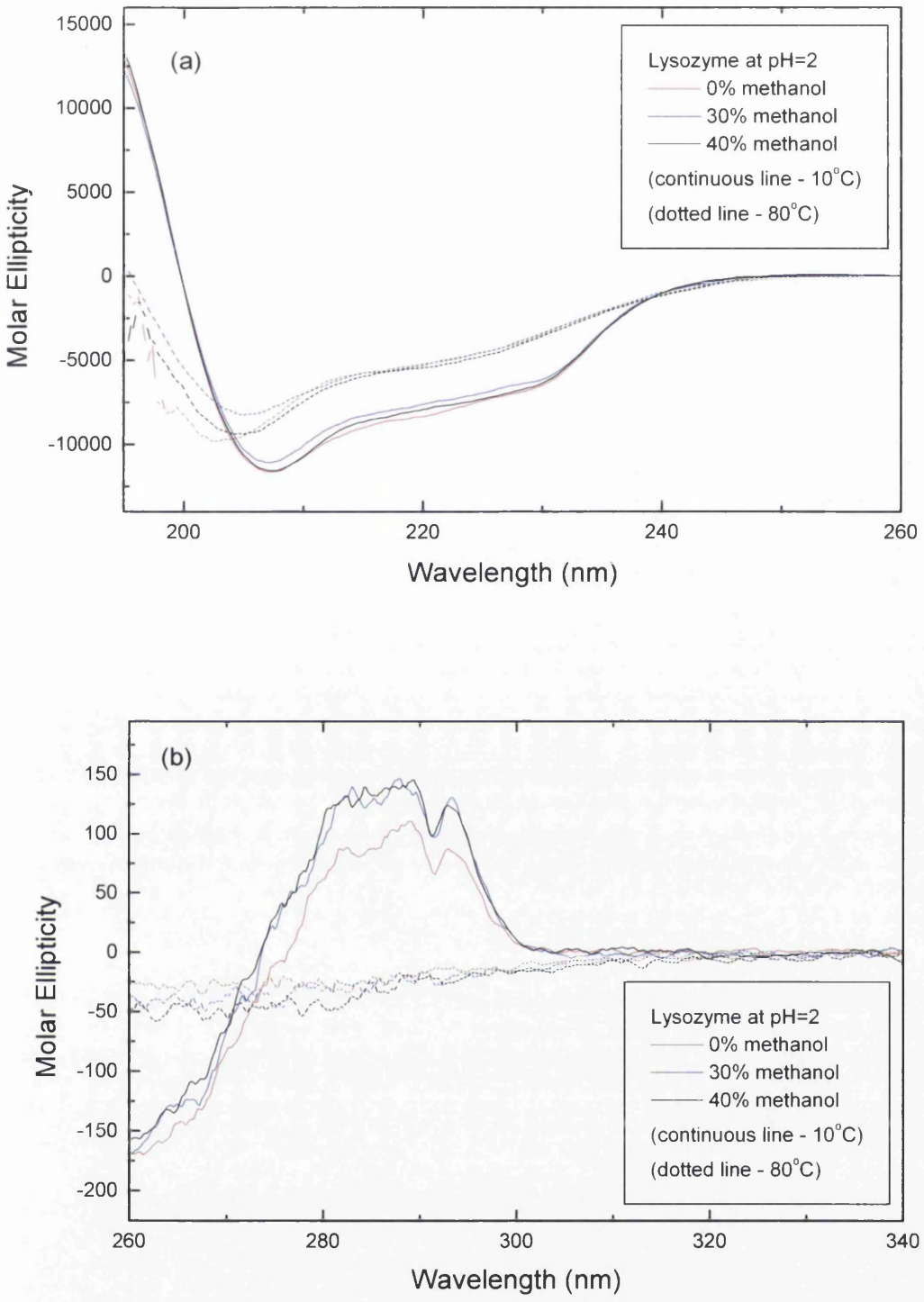

Figure A.3 CD spectra of lysozyme at pH=2, at various methanol concentrations and at temperatures of 10 and 80°C. (a) Far-UV (b) Near-UV

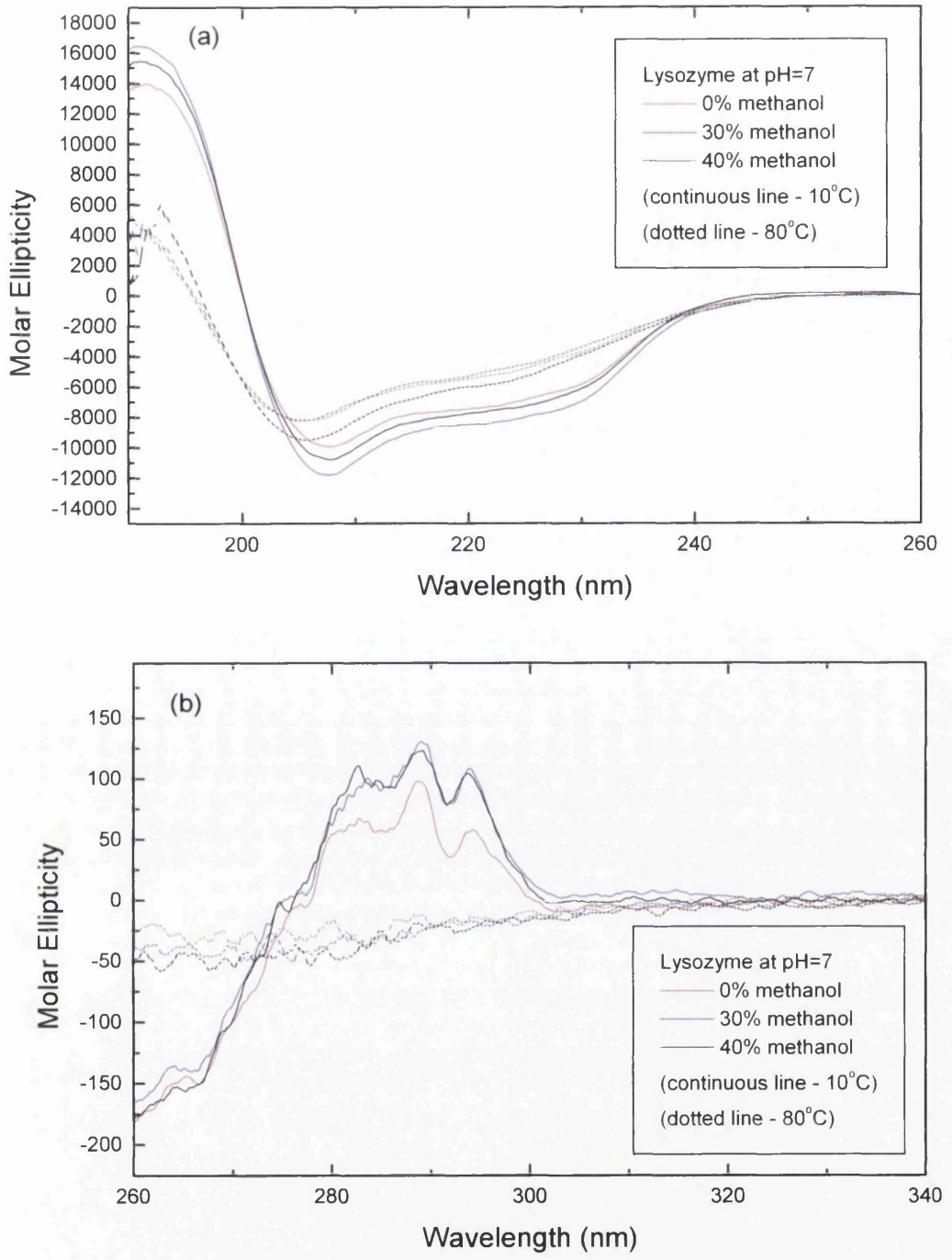

Figure A.4 CD spectra of lysozyme at pH=7, at various methanol concentrations and at temperatures of 10 and 80°C. (a) Far-UV (b) Near-UV

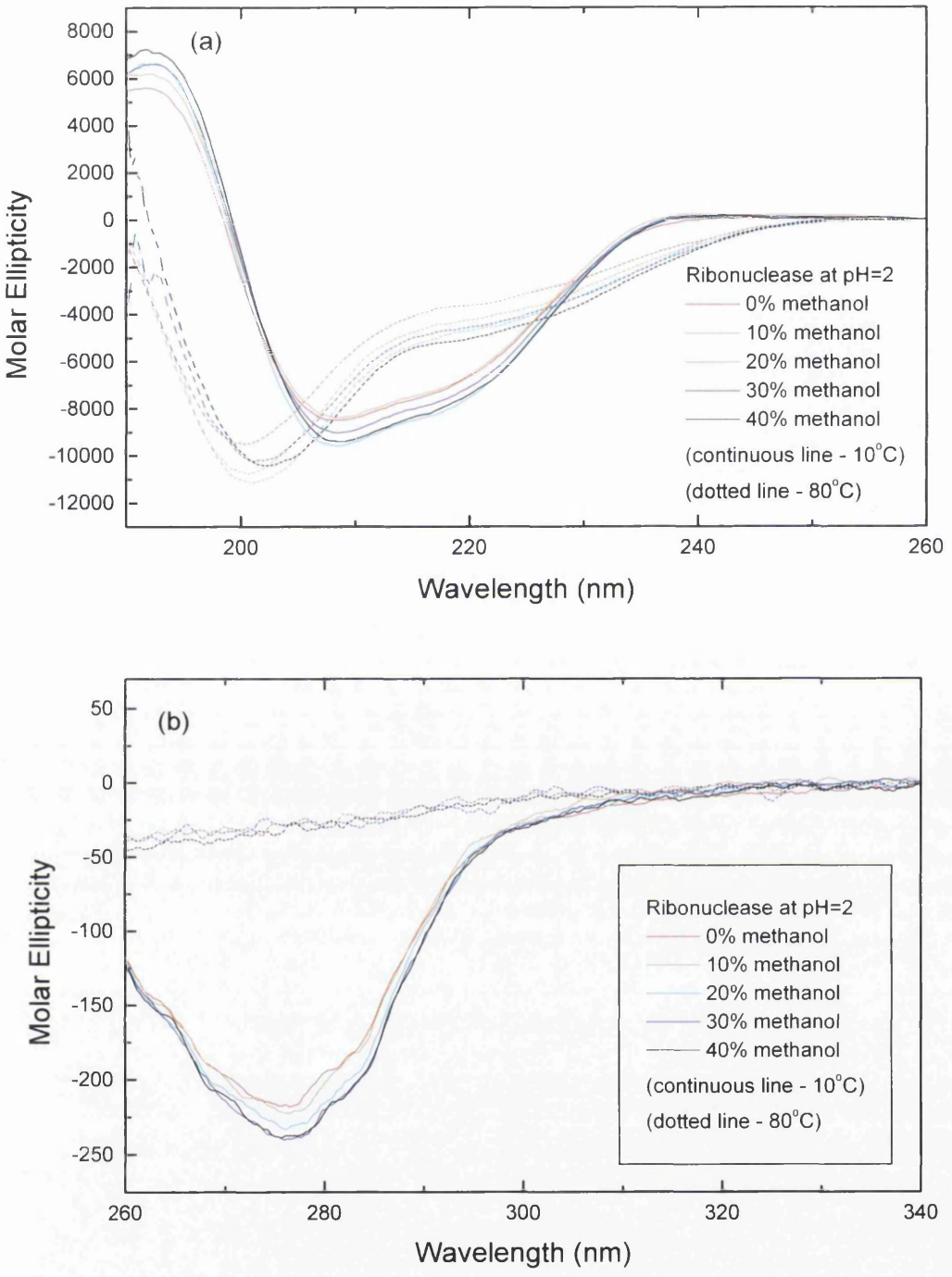

Figure A.5 CD spectra of ribonuclease A at pH=2, at various methanol concentrations and at temperatures of 10 and 80°C. (a) Far-UV (b) Near-UV

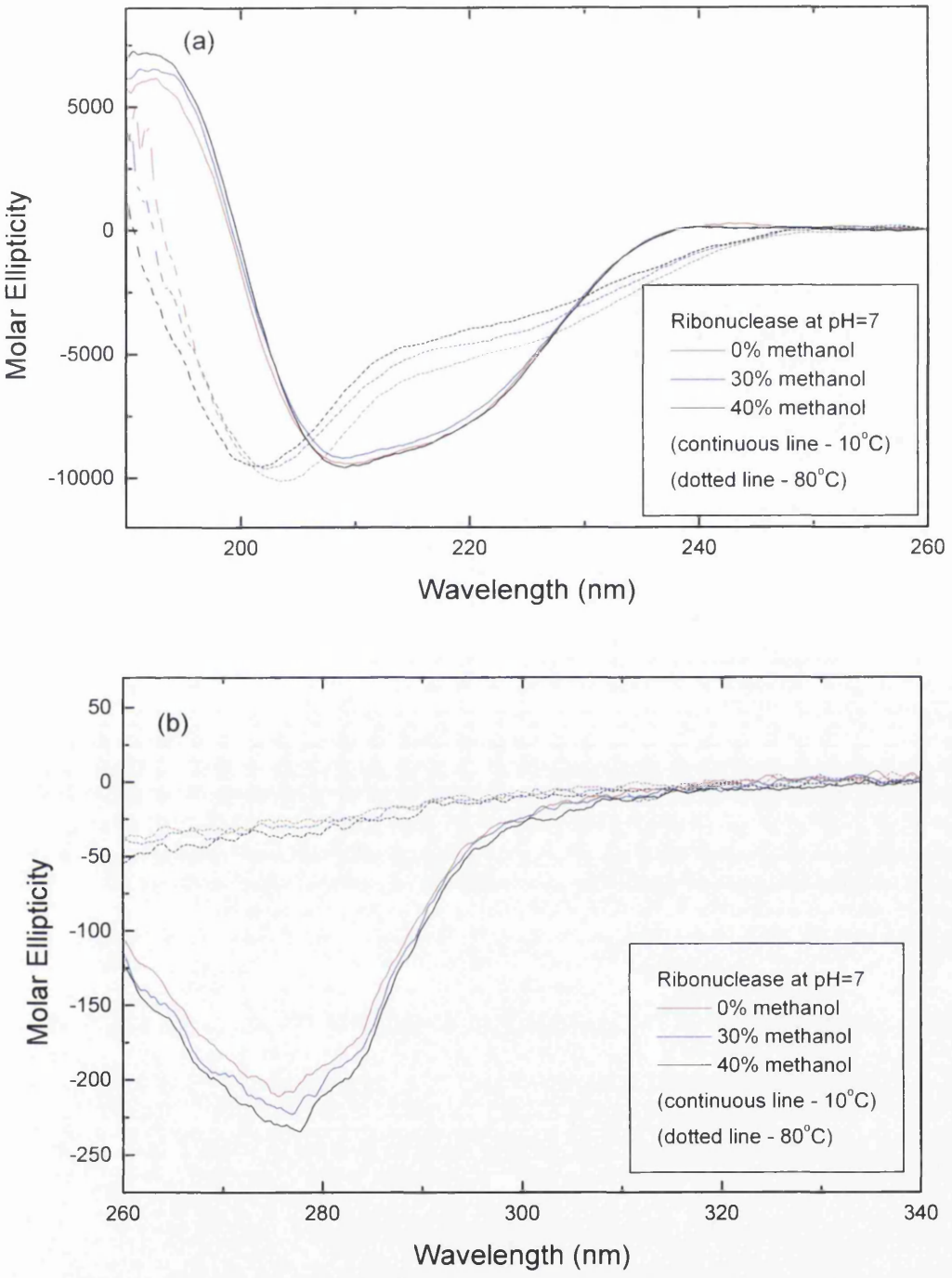

Figure A.6 CD spectra of ribonuclease A at pH=7, at various methanol concentrations and at temperatures of 10 and 80°C. (a) Far-UV (b) Near-UV

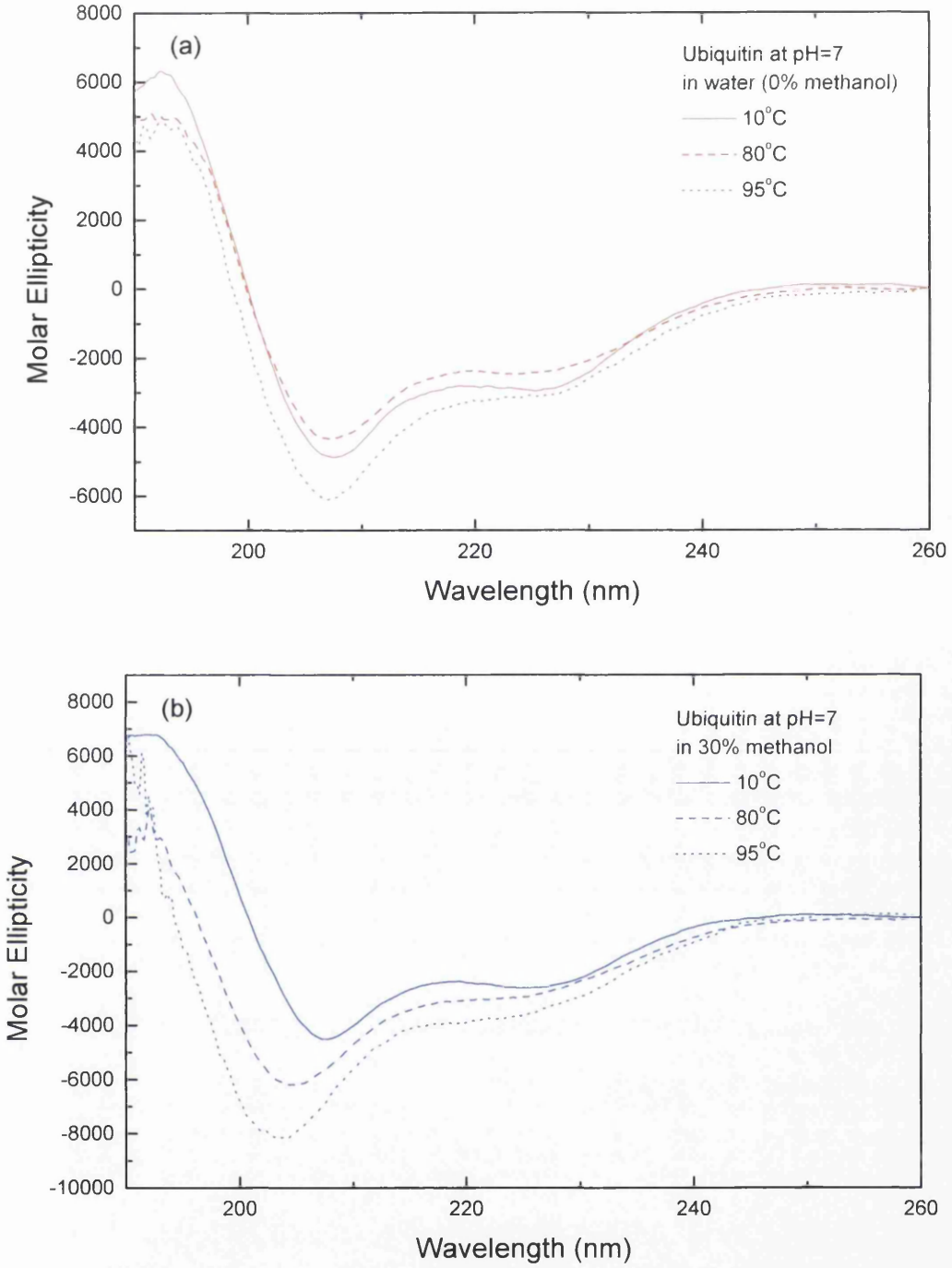

Figure A.7 Evidence that at temperature of 80° ubiquitin in water and 30% methanol at pH = 7 is still not in its unfolded form – the spectra of ubiquitin acquired at 95°C show further unfolding.

APPENDIX B

PPC SCANS OF PROTEIN UNFOLDING IN WATER, METHANOLIC SOLUTIONS AND D_2O.

WATER - UBIQUITIN

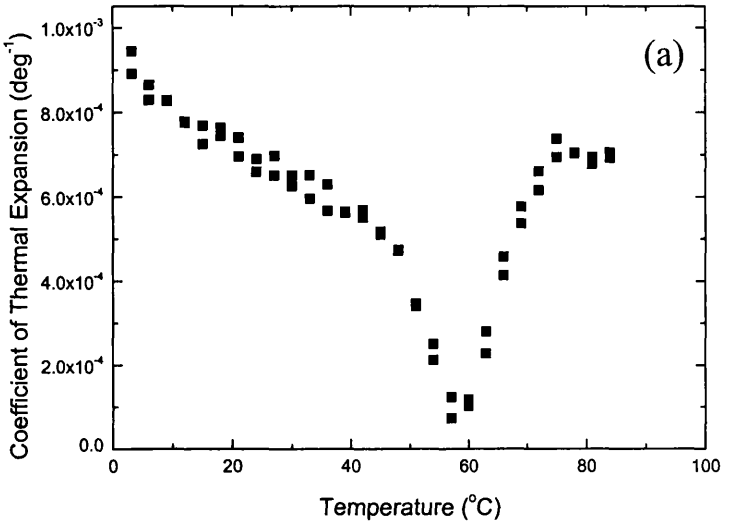

Integration:

Temperature Range = 39 - 78°C

Area = -0.00793

ΔV_{unf} = -0.793%

T_m = 57°C

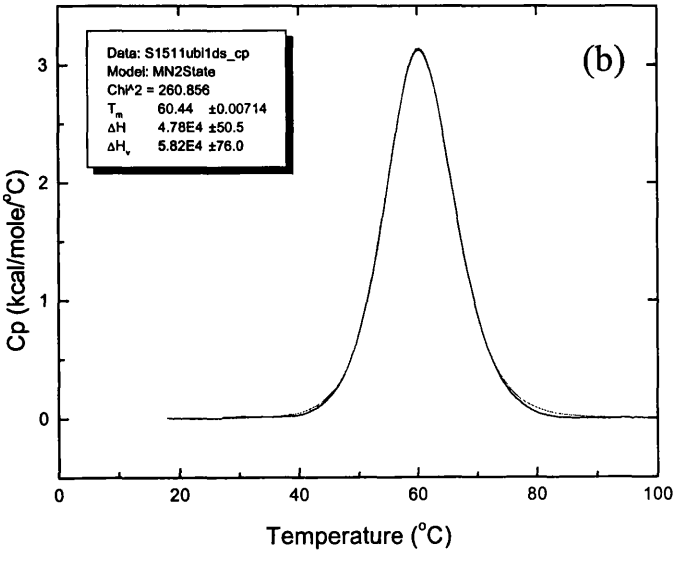

Figure B.1 Ubiquitin thermal unfolding in water at pH = 2, monitored by: (a) PPC; (b) DSC.

WATER - LYSOZYME

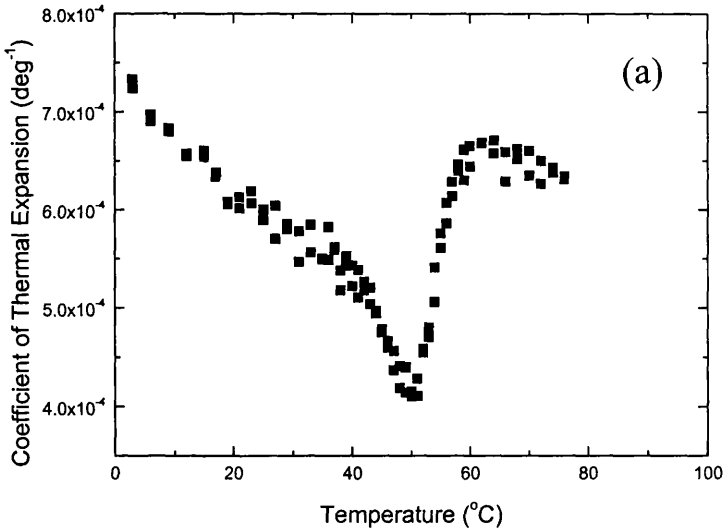

Integration:

Temperature Range = 40 - 62°C

Area = -0.00164

ΔV_{unf} = -0.164%

T_m = 51°C

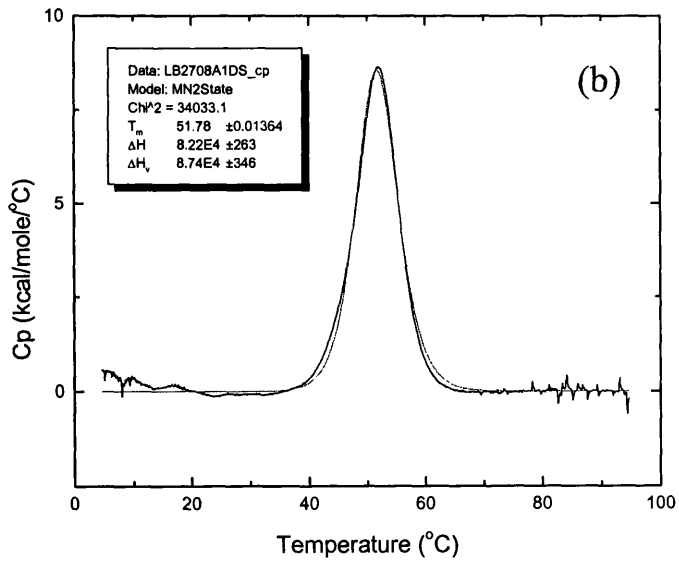

Figure B.2 Lysozyme thermal unfolding in water at pH = 2, monitored by: (a) PPC; (b) DSC.

WATER - RIBONUCLEASE A

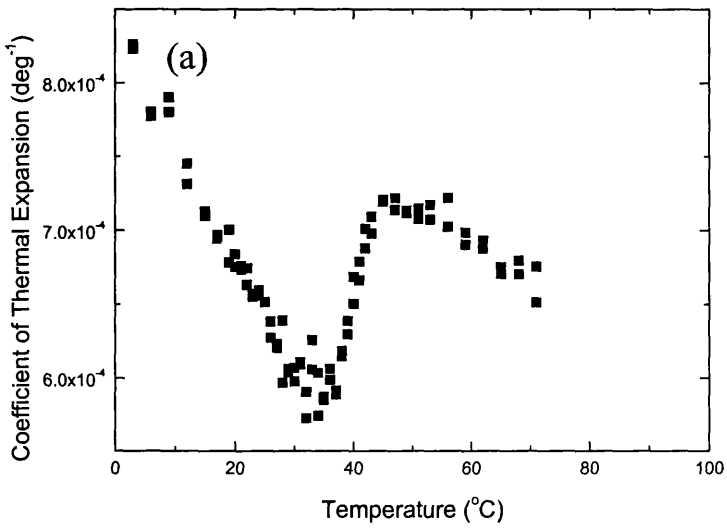

Integration:

Temperature Range = 20 - 47°C

Area = -0.00135

ΔV_{unf} = -0.135%

T_m = 37°C

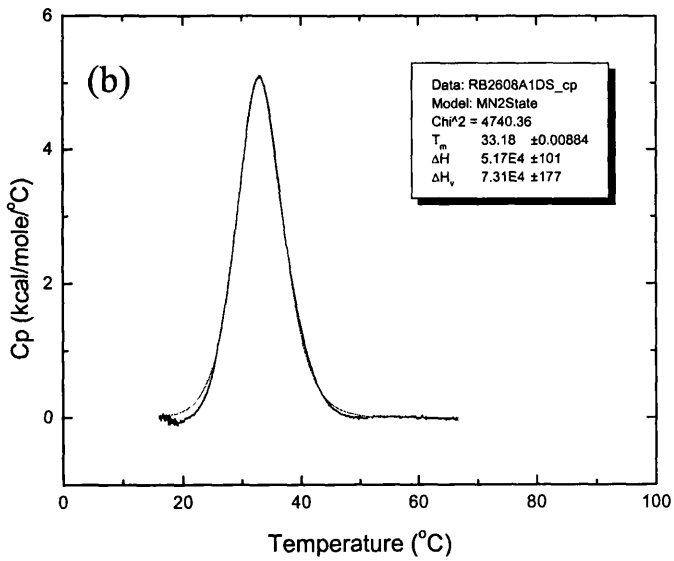

Figure B.3 Ribonuclease A thermal unfolding in water at pH = 2, monitored by: (a) PPC; (b) DSC.

D_2O – UBIQUITIN, LYSOZYME AND RIBONUCLEASE A

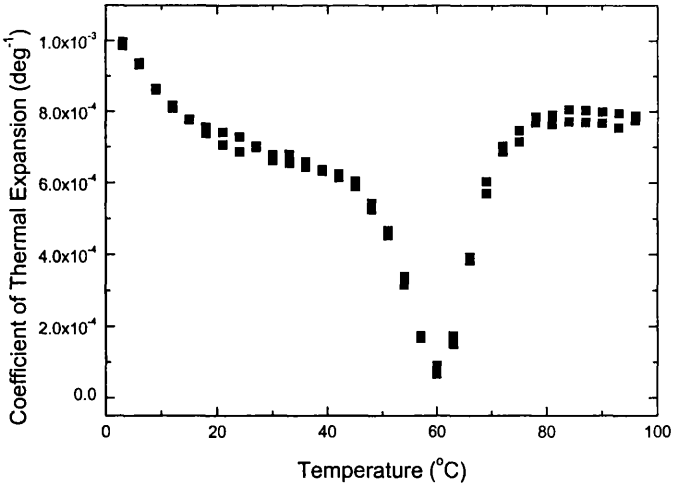

Integration:

Temperature Range = 39 - 78°C

Area = -0.00853

ΔV_{unf} = -0. 853%

T_m = 60°C

Figure B.4 Ubiquitin thermal unfolding in D2O at pH = 2, monitored by PPC.

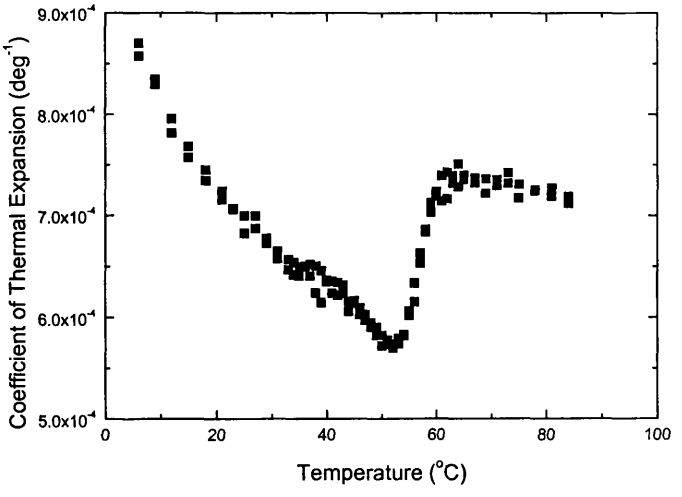

Integration:

Temperature Range = 40 - 64°C

Area = -0.00127

ΔV_{unf} = -0.127%

T_m = 53°C

Figure B.5 Lysozyme thermal unfolding in D2O at pH = 2, monitored by PPC.

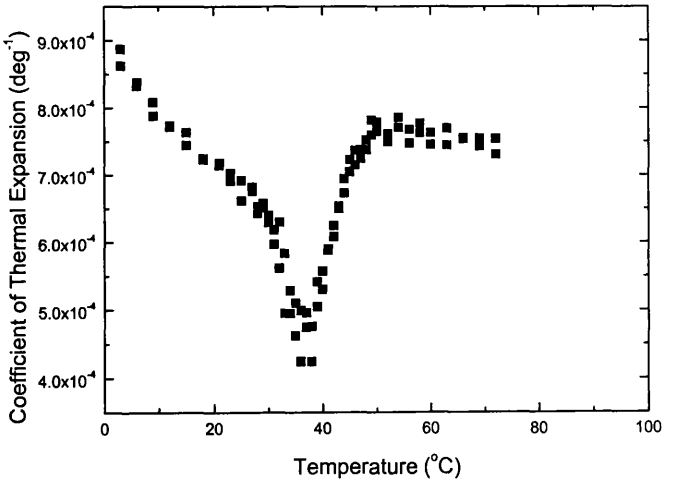

Integration:

Temperature Range = 28 - 50°C

Area = -0.00196

ΔV_{unf} = -0.196%

T_m = 38°C

Figure B.6 Ribonuclease A thermal unfolding in D_2O at pH = 2, monitored by PPC.

10% AQUEOUS METHANOL - UBIQUITIN

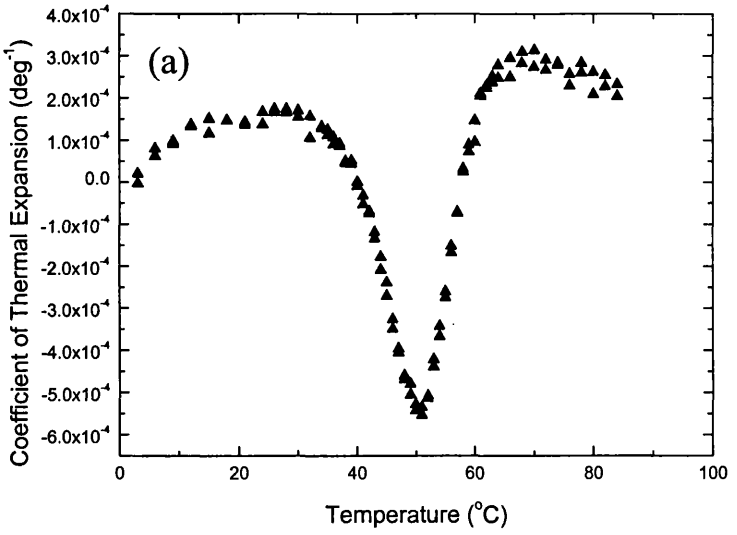

Integration:

Temperature Range = 30 - 68°C

Area = -0.00109

ΔV_{unf} = -0.109%

T_m = 51°C

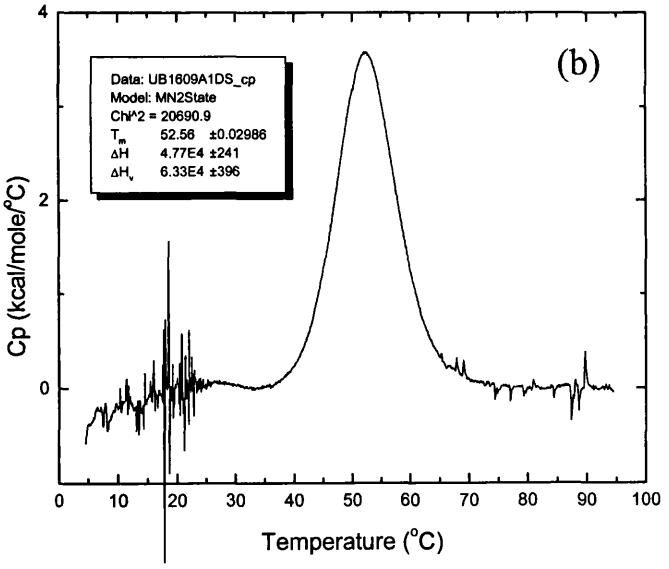

Figure B.7 Ubiquitin thermal unfolding in 20% aqueous methanol at pH = 2, monitored by: (a) PPC; (b) DSC.

10% AQUEOUS METHANOL – LYSOZYME

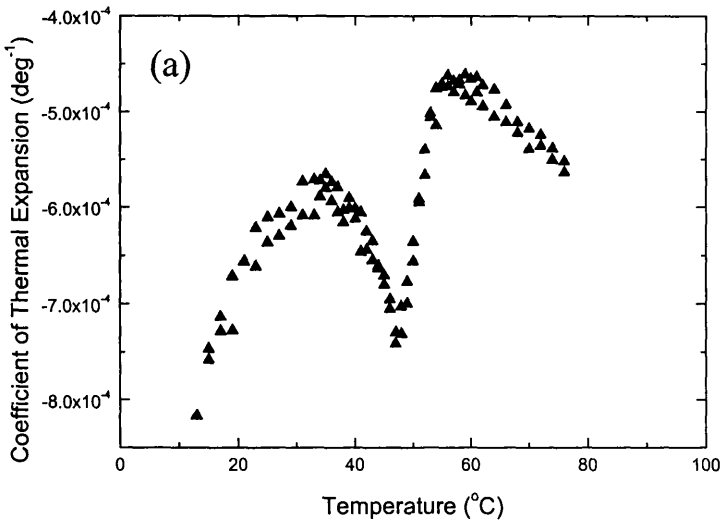

Integration:

Temperature Range = 35 - 56°C

Area = -0.0024

ΔV_{unf} = -0.24%

T_m = 47°C

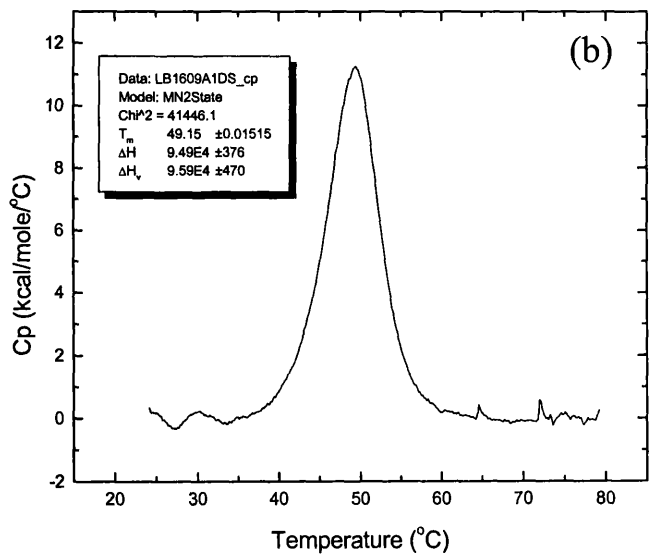

Figure B.8 Lysozyme thermal unfolding in 20% aqueous methanol at pH = 2, monitored by: (a) PPC; (b) DSC.

10% AQUEOUS METHANOL - RIBONUCLEASE A

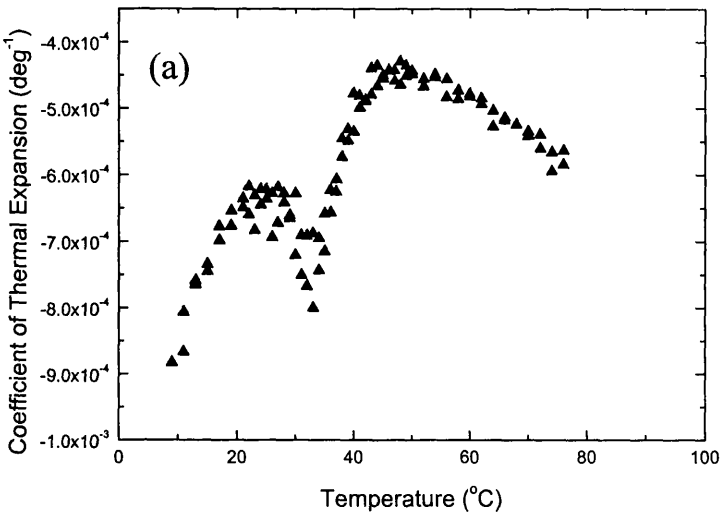

Integration:

Temperature Range = 19 - 46°C

Area = -0.00277

ΔV_{unf} = -0.277%

T_m = 33°C

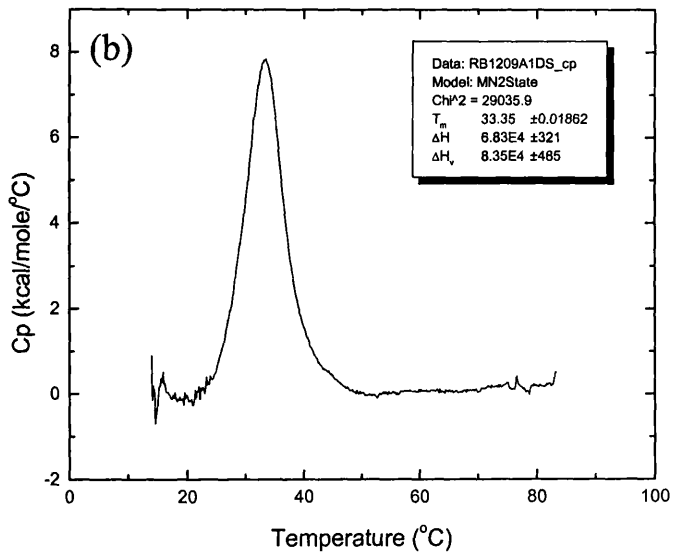

Figure B.9 Ribonuclease A thermal unfolding in 20% aqueous methanol at pH = 2, monitored by: (a) PPC; (b) DSC.

20% AQUEOUS METHANOL

UBIQUITIN, LYSOZYME AND RIBONUCLEASE

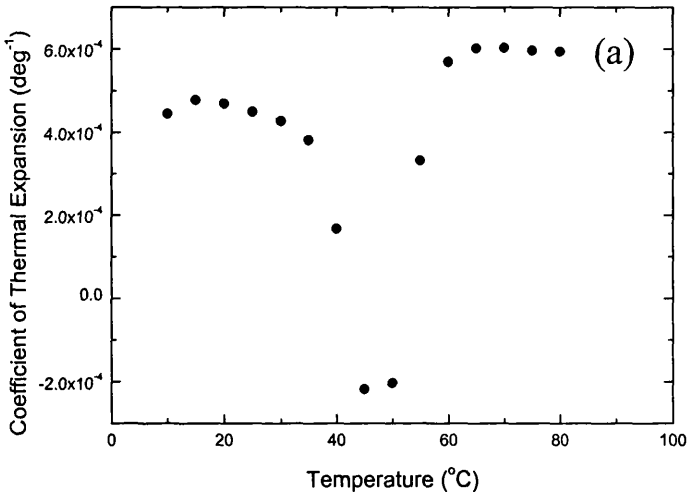

Integration:

Temperature Range = 25 - 60°C

Area = -0.01029

ΔV_{unf} = -1.029%

T_m = 50°C

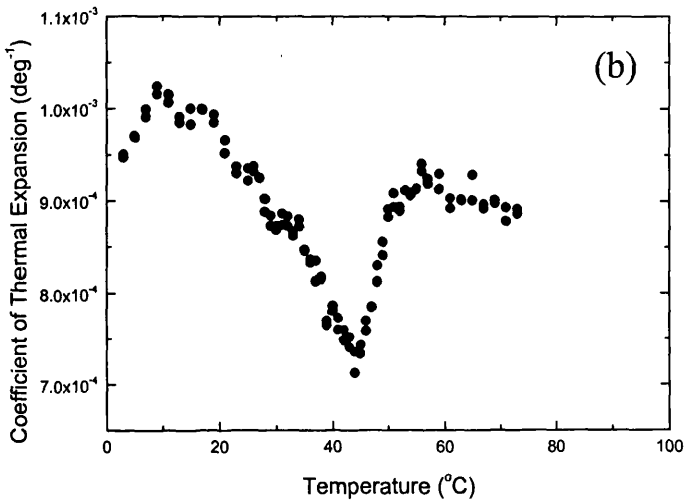

Integration:

Temperature Range = 27 - 56°C

Area = -0.00158

ΔV_{unf} = -0.158%

T_m = 44°C

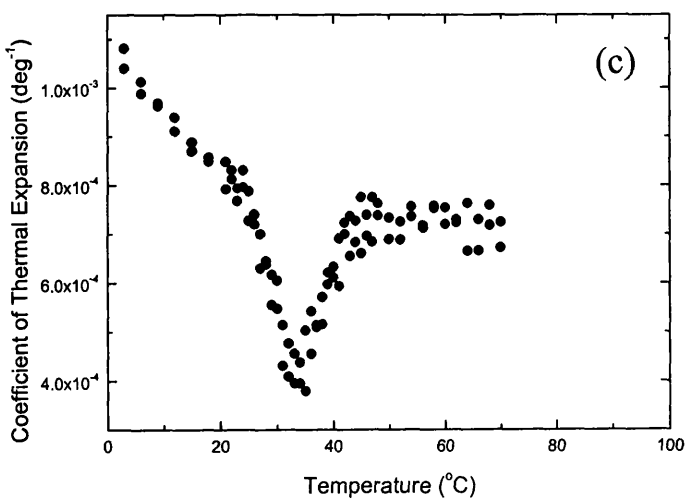

Integration:

Temperature Range = 39 - 78°C

Area = -0.00358

ΔV_{unf} = -0.358%

T_m = 35°C

Figure B.10 Thermal unfolding of (a) ubiquitin, (b) lysozyme, (c) ribonuclease A in 20% aqueous methanol at pH = 2, monitored by PPC.

30% AQUEOUS METHANOL

UBIQUITIN, LYSOZYME AND RIBONUCLEASE

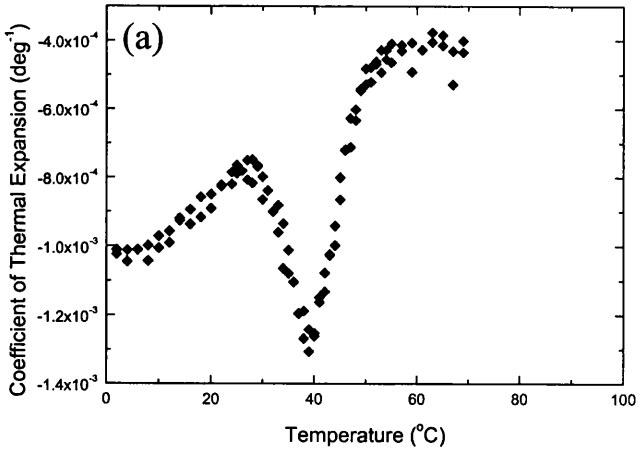

Integration:

Temperature Range = 26 - 52°C

Area = -0.0074

ΔV_{unf} = -0.74%

T_m = 38°C

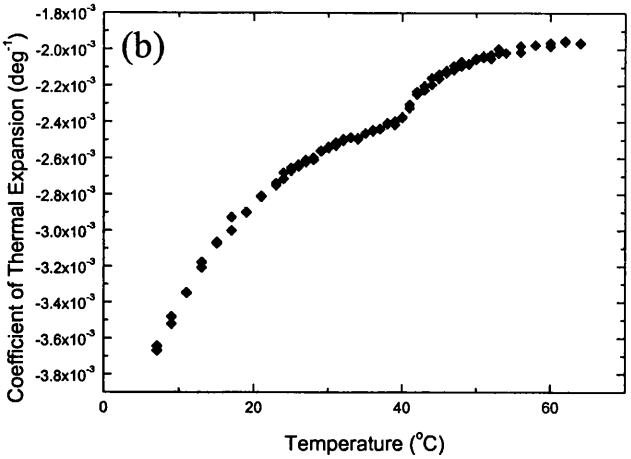

Integration:

Temperature Range = 26 - 48°C

Area = -0.00093

ΔV_{unf} = -0.093%

T_m = 39°C

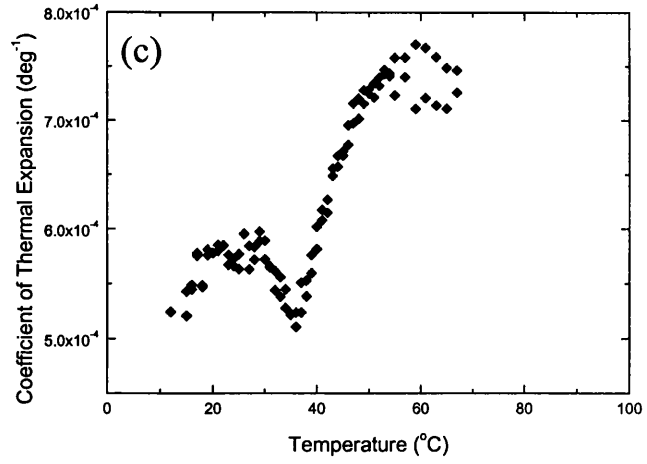

Integration:

Temperature Range = 26 - 52°C

Area = -0.00158

ΔV_{unf} = -0.158%

T_m = 36°C

Figure B.11 Thermal unfolding of (a) ubiquitin, (b) lysozyme, (c) ribonuclease A in 20% aqueous methanol at pH = 2, monitored by PPC.

40% AQUEOUS METHANOL

UBIQUITIN, LYSOZYME AND RIBONUCLEASE

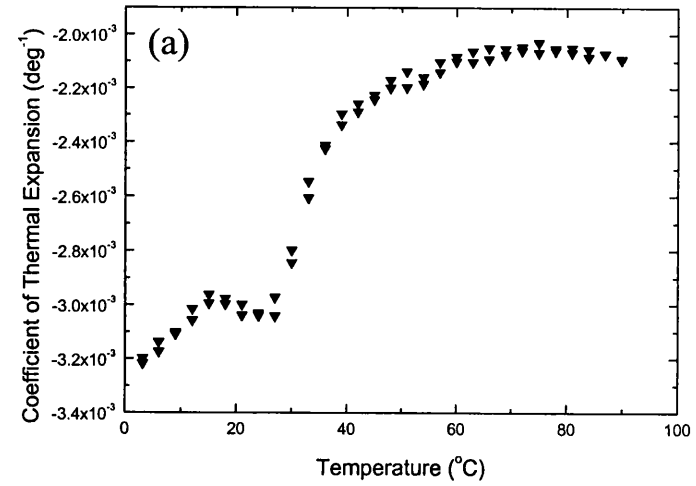

Integration:

Temperature Range = 12 - 42°C

Area = -0.00408

ΔV_{unf} = -0.408%

T_m = 27°C

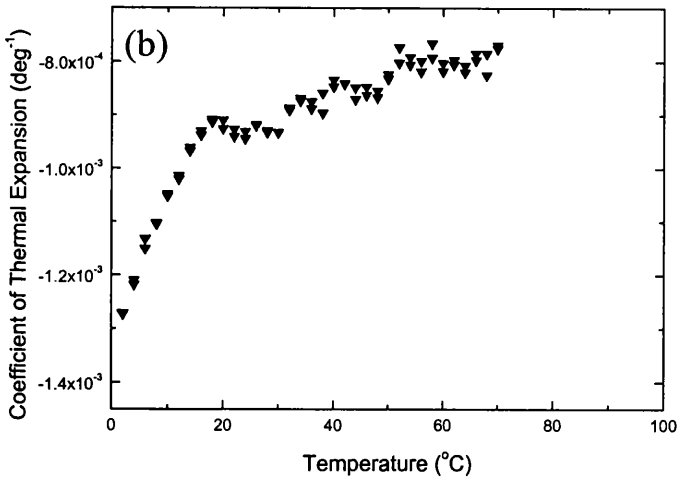

Integration:

Temperature Range = 16 - 52°C

Area = -0.00082

ΔV_{unf} = -0. 082%

T_m = 30°C

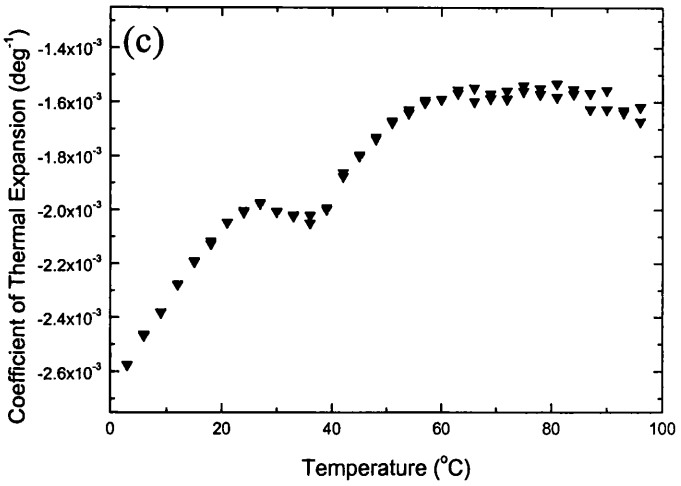

Integration:

Temperature Range = 21 - 57°C

Area = -0.00363

ΔV_{unf} = -0.363%

T_m = 36°C

Figure B.12 Thermal unfolding of (a) ubiquitin, (b) lysozyme, (c) ribonuclease A in 40% aqueous methanol at pH = 2, monitored by PPC.

APPENDIX C

PPC AND DSC SCANS OF CYTOCHROME C UNFOLDING

MG-to-U TRANSITION (pH = 2.0)

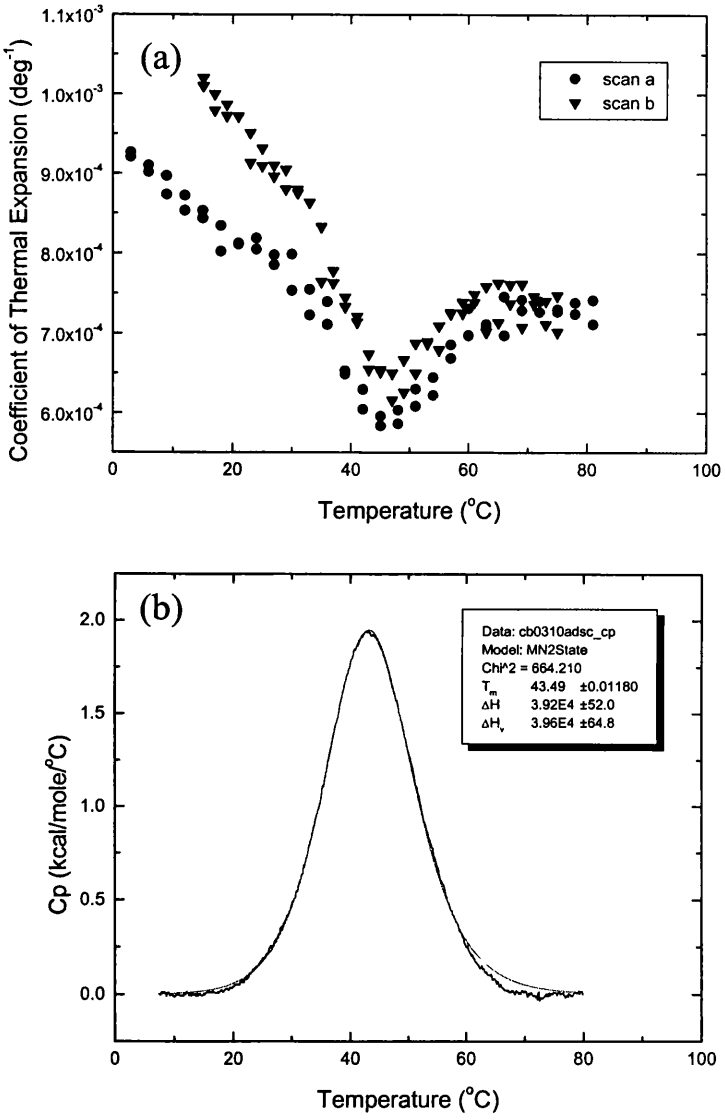

Figure C.1 Thermal unfolding of cytochrome c at pH = 2 (MG-to-U transition) monitored by (a) PPC (b) DSC

N-to-U TRANSITION (pH = 3.4)

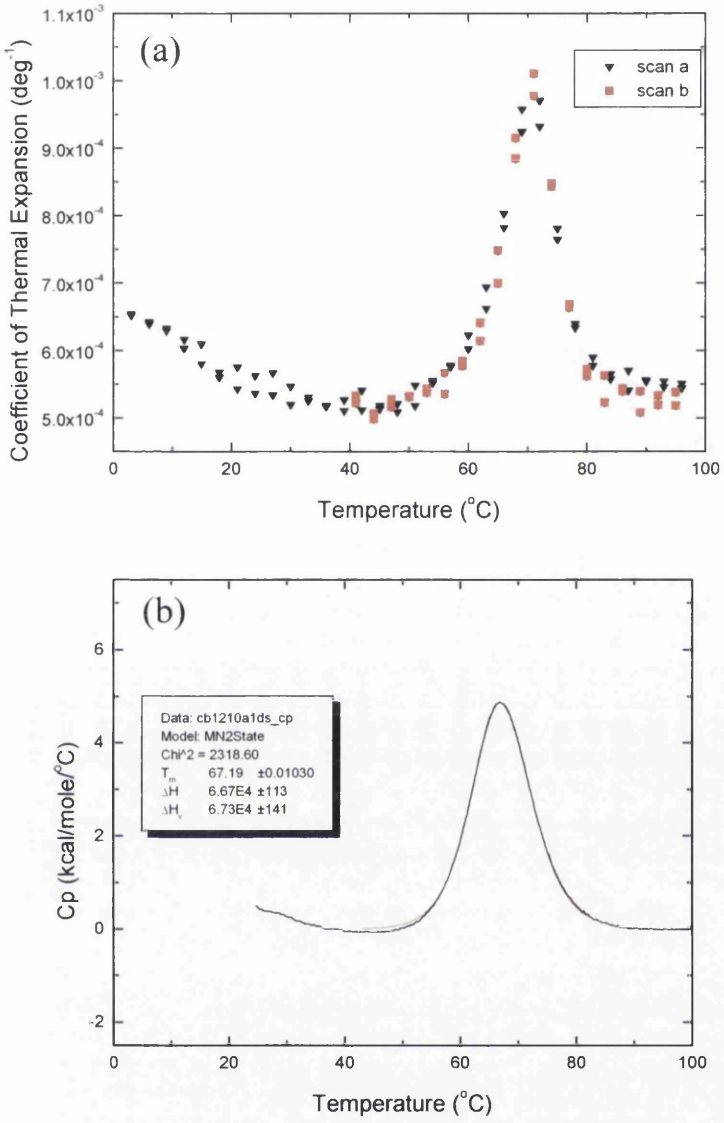

Figure C.2 Thermal unfolding of cytochrome c at pH = 3.4 (N-to-U transition) monitored by (a) PPC (b) DSC

N-to-U TRANSITION (pH = 3.6)

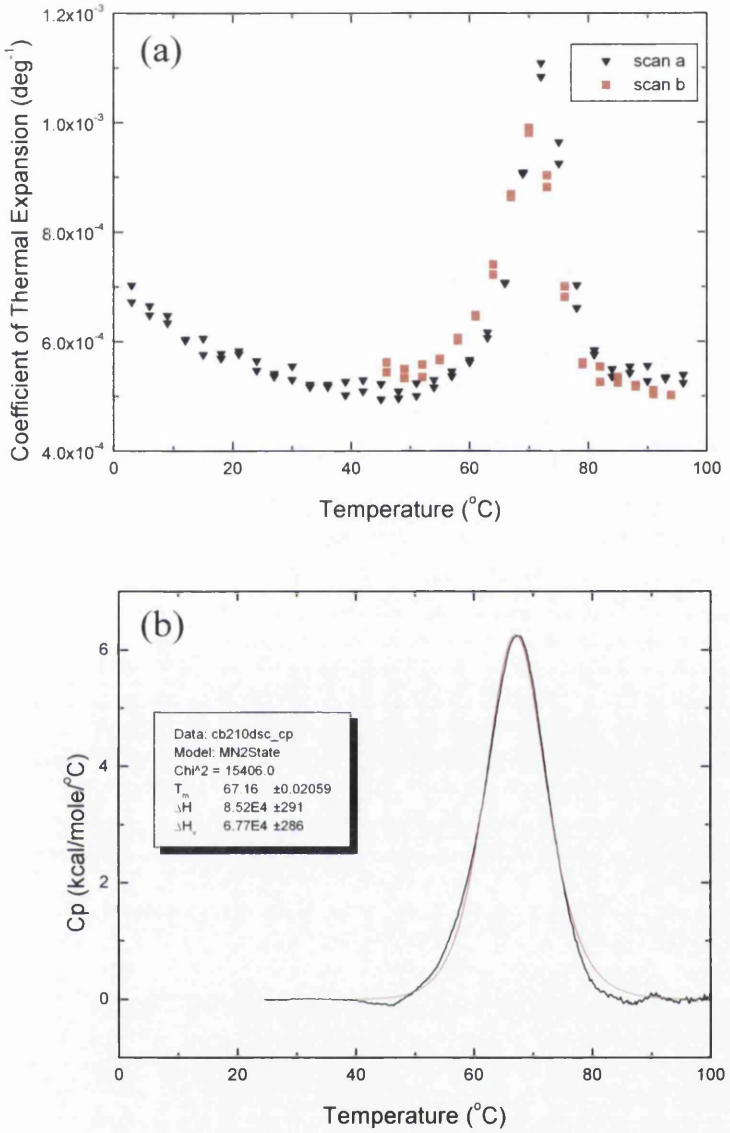

Figure C.3 Thermal unfolding of cytochrome c at pH = 3.6 (N-to-U transition) monitored by (a) PPC (b) DSC

N-to-U TRANSITION (pH = 4.0)

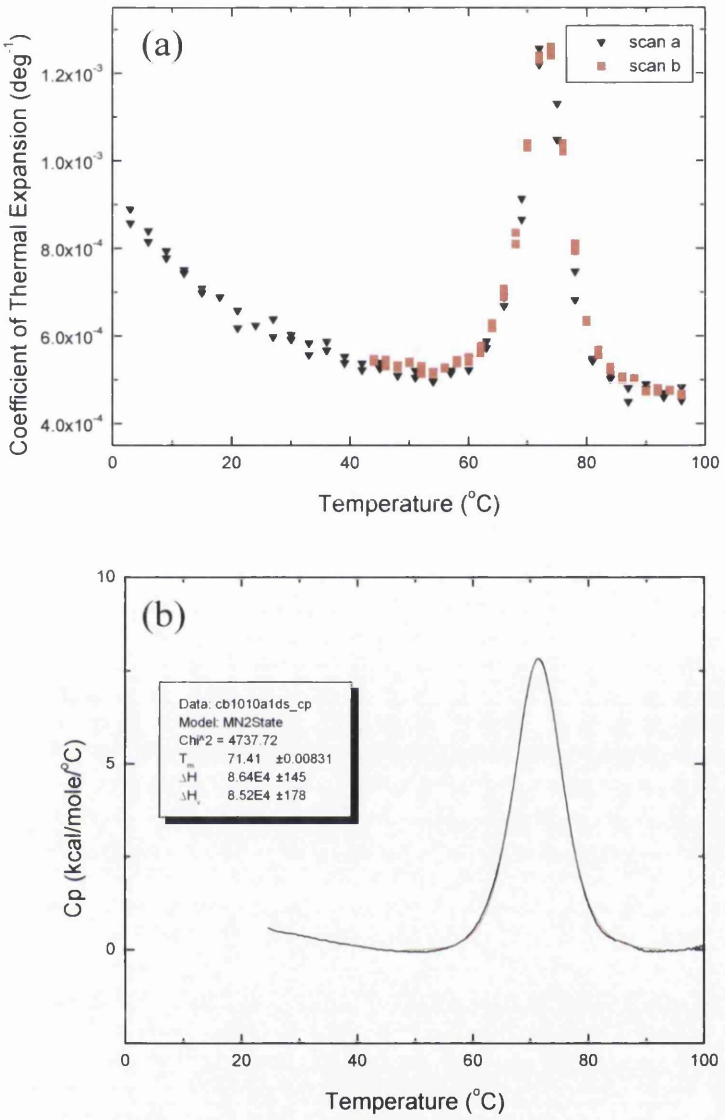

Figure C.4 Thermal unfolding of cytochrome c at pH = 4.0 (N-to-U transition) monitored by (a) PPC (b) DSC

N-to-U TRANSITION (pH = 4.3)

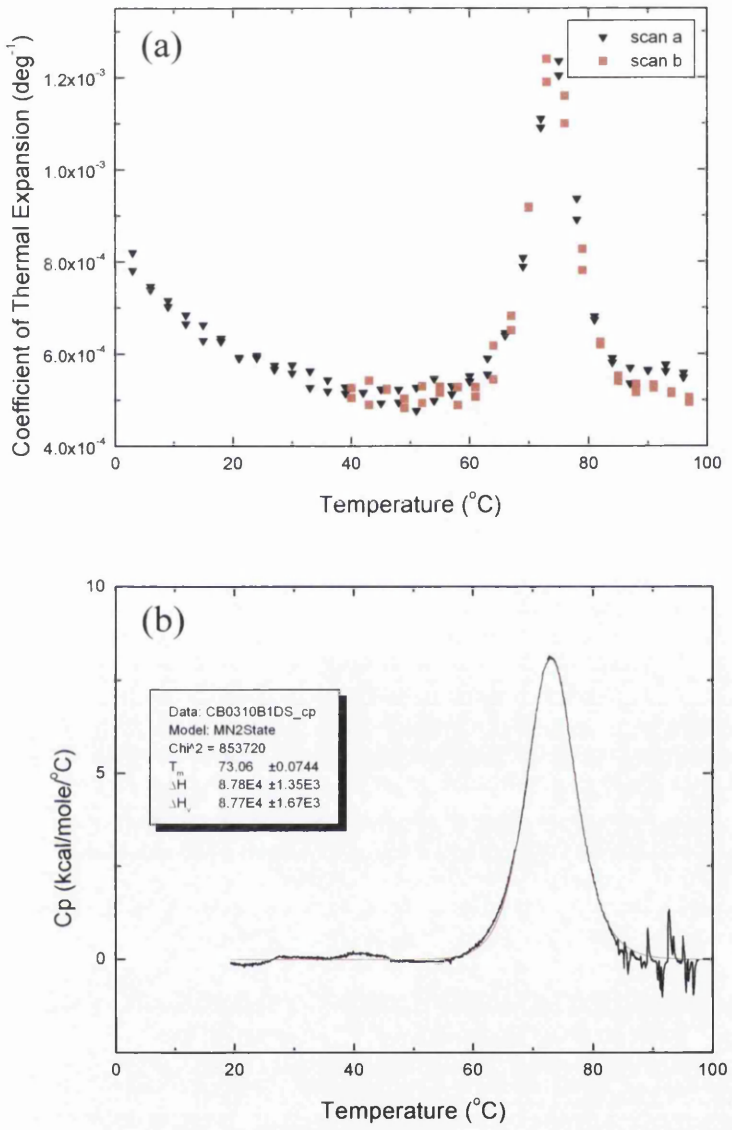

Figure C.5 Thermal unfolding of cytochrome c at pH = 4.3 (N-to-U transition) monitored by (a) PPC (b) DSC

APPENDIX D

CONVERSION TABLE FOR METHANOL/WATER MIXTURES CONCENTRATIONS AT 25°C

% v/v	%wt	x_A	molar ratio	molalilty (M_A)
423.6882	533.5828	**0.75**	**1 : 0.333333**	166.526
282.4588	355.7218	0.666667	**1 : 0.5**	111.0174
141.2294	177.8609	**0.5**	**1 : 1**	55.50868
100	125.9376	0.414543	1 : 1.412294	39.30391
94.15293	118.5739	**0.4**	1 : 1.5	37.00579
79.4044	**100**	0.359892	1: 1.778609	31.20904
70.6147	88.93046	0.333333	**1 : 2**	27.75434
60.52688	76.22611	**0.3**	1 : 2.333333	23.78943
60	75.56256	0.298167	1 : 2.353823	23.58235
50	62.9688	0.261466	1 : 2.824588	19.65196
47.07647	59.28697	**0.25**	**1 : 3**	18.50289
47.64264	**60**	0.252248	1 : 2.964349	18.72542
40	50.37504	0.220715	1 : 3.530735	15.72157
39.7022	**50**	0.219432	1 : 3.557218	15.60452
35.30735	44.46523	**0.2**	**1 : 4**	13.87717
31.76176	**40**	0.183603	1 : 4.446523	12.48362
30	37.78128	0.175204	1 : 4.707646	11.79118
28.24588	35.57218	0.166667	**1 : 5**	11.10174
23.82132	**30**	0.144327	1 : 5.928697	9.362712
20	25.18752	0.124047	1 : 7.06147	7.860783
17.65367	22.23261	0.111111	**1 : 8**	6.938585
15.88088	**20**	0.101081	1 : 8.893046	6.241808
15.69216	19.76232	**0.1**	**1 : 9**	6.167631
14.12294	17.78609	0.090909	**1 : 10**	5.550868
11.76912	14.82174	0.076923	**1 : 12**	4.625723
10	12.59376	0.066125	1 : 14.12294	3.930391
8.826837	11.11631	0.058824	**1 : 16**	3.469293
7.94044	**10**	0.053231	1 : 17.78609	3.120904
7.433126	9.361101	**0.05**	1 : 19	2.92151
5	6.29688	0.034193	1 : 28.24588	1.965196
4.413419	5.558154	0.030303	**1 : 32**	1.734646
3.97022	**5**	0.027343	1 : 35.57218	1.560452
2.544276	3.2042	0.017696	1 : 55.50868	**1**
1.908207	2.40315	0.013331	1 : 74.01158	**0.75**
1.272138	1.6021	0.008927	1 : 111.0174	**0.5**
0.636069	0.80105	0.004484	1 : 222.0347	**0.25**

Table D.1 Conversion table for methanol/water mixtures concentrations at 25°C. Values commonly used are in bold.

Symbols and definitions used for methanol concentration in Table D.1:

% v/v – percentage of volume ratios

$\% v/v = V_{MeOH}/V_{H2O} \times 100\%$

%wt - weight percentage

$\%wt = m_{MeOH}/m_{H2O} \times 100\%$

x_A - molar fraction of methanol

$x_A = n_{MeOH}/(n_{MeOH}+n_{H2O})$

molar ratio

$n_{MeOH} : n_{H2O}$

molalilty (M_A)

$M_A = n_{MeoH}*1000/m_{H2O}$

Where:

m_{H2O} – mass of water

m_{MeOH} – mass of methanol

n_{H2O} – number of moles of water

n_{MeOH} – number of moles of methanol

V_{H2O} - volume of water

V_{MeOH} - volume of methanol

REFERENCES

Arai, M. and Kuwajima, K. 2000, "Role of the molten globule state in protein folding", *Advances in Protein Chemistry*, vol. 53, pp. 209-282.

Aune, K. C. and Tanford, C. 1969, "Thermodynamics of the denaturation of lysozyme by guanidine hydrochloride. I. Dependence on pH at 25 degrees", *Biochemistry*, vol. 8, no. 11, pp. 4579-4585.

Babul, J. and Stellwagen, E. 1972, "Participation of the protein ligands in the folding of cytochrome c", *Biochemistry*, vol. 11, no. 7, pp. 1195-1200.

Banipal, P. K., Banipal, T. S., Lark, B. S., and Ahluwalia, J. C. 1997, "Partial molar heat capacities and volumes of some mono-, di- and tri-saccharides in water at 298.15, 308.15 and 318.15 K", *Journal of the Chemical Society-Faraday Transactions*, vol. 93, no. 1, pp. 81-87.

Bassez, M. P., Lee, J., and Robinson, G. W. 1987, "Is liquid water really anomalous", *Journal of Physical Chemistry*, vol. 91, no. 22, pp. 5818-5825.

Batchelor, J. D., Olteanu, A., Tripathy, A., and Pielak, G. J. 2004, "Impact of protein denaturants and stabilizers on water structure", *Journal of the American Chemical Society*, vol. 126, no. 7, pp. 1958-1961.

Blandamer, M. J. and Hoiland, H. 1999, "Volumetric properties of solutions: A novel method of data analysis yielding partial molar volumes and partial molar expansions of solutes", *Physical Chemistry Chemical Physics*, vol. 1, no. 8, pp. 1873-1875.

Brandts, J. F. 1964, *Journal of the American Chemical Society*, vol. 86, pp. 4291-4301.

Brandts, J. F. and Hunt, L. 1967, "The thermodynamics of protein denaturation. 3. The denaturation of ribonuclease in water and in aqueous urea and aqueous ethanol mixtures", *Journal of the American Chemical Society*, vol. 89, no. 19, pp. 4826-4838.

Brandts, J. F. and Lin, L. N. 2004, "Rebuttal to communication critical of the use of pressure perturbation calorimetry for measuring volumetric properties of solutes [Thermochim. Acta (2003) 75-80]", *Thermochimica Acta*, vol. 414, no. 1, pp. 95-100.

Brutscher, B., Brüschweiler, R., and Ernst, R. R. 1997, "Backbone dynamics and structural characterization of the partially folded A state of ubiquitin by 1H, 13C, and 15N nuclear magnetic resonance spectroscopy", *Biochemistry*, vol. 36, pp. 13043-13053.

Bull, H. B. and Breese, K. 1973, "Temperature dependence of partial volumes of proteins", *Biopolymers*, vol. 12, pp. 2351-2358.

Cameron, D. 2001. Personal Communication

Catanzano, F., Graziano, G., Capasso, S., and Barone, G. 1997, "Thermodynamic analysis of the effect of selective monodeamidation at asparagine 67 in ribonuclease A", *Protein Science*, vol. 6, no. 8, pp. 1682-1693.

Chalikian, T. V. 2003, "Volumetric properties of proteins", *Annual Review of Biophysics and Biomolecular Structure* p. 110601.

Chalikian, T. V. 2001, "Structural thermodynamics of hydration", *Journal of Physical Chemistry B*, vol. 105, no. 50, pp. 12566-12578.

Chalikian, T. V. and Breslauer, K. J. 1996, "Compressibility as a means to detect and characterize globular protein states", *Proceedings of the National Academy of Sciences of the United States of America*, vol. 93, no. 3, pp. 1012-1014.

Chalikian, T. V. and Breslauer, K. J. 1998, "Thermodynamic analysis of biomolecules: a volumetric approach", *Current Opinion in Structural Biology*, vol. 8, no. 5, pp. 657-664.

Chalikian, T. V. and Filfil, R. 2003, "How large are the volume changes accompanying protein transitions and binding?", *Biophysical Chemistry*, vol. 104, no. 2, pp. 489-499.

Chalikian, T. V., Gindikin, V. S., and Breslauer, K. J. 1995, "Volumetric characterizations of the native, molten globule and unfolded states of cytochrome-c at acidic pH", *Journal of Molecular Biology*, vol. 250, no. 2, pp. 291-306.

Chalikian, T. V., Gindikin, V. S., and Breslauer, K. J. 1996a, "Spectroscopic and volumetric investigation of cytochrome c unfolding at alkaline pH: Characterization of the base-induced unfolded state at 25 degrees C", *FASEB Journal*, vol. 10, no. 1, pp. 164-170.

Chalikian, T. V., Sarvazyan, A. P., and Breslauer, K. J. 1994, "Hydration and partial compressibility of biological compounds", *Biophysical Chemistry*, vol. 51, no. 2-3, pp. 89-109.

Chalikian, T. V., Totrov, M., Abagyan, R., and Breslauer, K. J. 1996b, "The hydration of globular proteins as derived from volume and compressibility measurements: cross correlating thermodynamic and structural data", *Journal of Molecular Biology*, vol. 260, pp. 588-603.

Chalikian, T. V., Volker, J., Anafi, D., and Breslauer, K. J. 1997, "The native and the heat-induced denatured states of alpha- chymotrypsinogen A: Thermodynamic and spectroscopic studies", *Journal of Molecular Biology*, vol. 274, no. 2, pp. 237-252.

Cho, C. H., Urquidi, J., Singh, S., Park, S. C., and Robinson, G. W. 2002, "Pressure effect on the density of water", *Journal of Physical Chemistry A*, vol. 106, no. 33, pp. 7557-7561.

Cooper, A. 1976, "Thermodynamic fluctuations in protein molecules", *Proceedings of the National Academy of Sciences of the United States of America*, vol. 73, no. 8, pp. 2740-2741.

Cooper, A. 2005, "Heat capacity effects in protein folding and ligand binding: a re-evaluation of the role of water in biomolecular thermodynamics", *Biophysical Chemistry*, vol. In Press, Corrected Proof.

Cooper, A. 1999a, "Thermodynamics analysis of biomolecular interactions", *Current Opinion in Chemical Biology*, vol. 3, pp. 557-563.

Cooper, A. 1999b, "Thermodynamics of protein folding and stability," in *Protein: A comprehensive treatise*, vol. 2 G. Allen, ed., JAI Press Inc., pp. 217-270.

Cooper, A. 2000, "Heat capacity of hydrogen-bonded networks: an alternative view of protein folding thermodynamics", *Biophysical Chemistry*, vol. 85, pp. 25-39.

Cooper, A. and Johnson, C. M. 1994, "Differential scanning calorimetry.," in *Methods in molecular biology: Microscopy, optical spectroscopy and macroscopic techniques.*, B. M. a. A. H. T. C.Jones, ed., Humana Press, New York, pp. 125-135.

Cooper, A., Johnson, C. M., Lakey, J. H., and Nollmann, M. 2001, "Heat does not come in different colours: entropy-enthalpy compensation, free energy windows, quantum confinement, pressure perturbation calorimetry, solvation and the multiple causes of heat capacity effects in biomolecular interactions", *Biophysical Chemistry*, vol. 93, no. 2-3, pp. 215-230.

Creighton, T. E. 1993, "Proteins: Structures and molecular properties", 2nd ed. W.H. Freeman and Company, New York.

Danielewicz-Ferchmin, I., Banachowicz, E., and Ferchmin, A. R. 2003, "Protein hydration and the huge electrostriction", *Biophysical Chemistry*, vol. 106, no. 2, pp. 147-153.

de la Torre, G. J. 2001, "Building hydrodynamic bead-shell models for rigid bioparticles of arbitrary shape", *Biophysical Chemistry*, vol. 94, no. 3, pp. 265-274.

Dill, K. A. 1990, "Dominant forces in protein folding", *Biochemistry*, vol. 29, no. 31, pp. 7133-7155.

DiStefano, D. L. and Wand, A. J. 1987, "Two-dimensional H-1-NMR study of human ubiquitin - a main chain directed assignment and structure-analysis", *Biochemistry*, vol. 26, no. 23, pp. 7272-7281.

Dubins, D. N., Filfil, R., Macgregor, R. B., and Chalikian, T. V. 2003, "Volume and compressibility changes accompanying thermally- induced native-to-unfolded and molten globule-to-unfolded transitions of cytochrome c: A high pressure study", *Biochemistry*, vol. 42, no. 29, pp. 8671-8678.

Dunitz, J. D. 1995, "Win some, lose some: enthalpy-entropy compensation in weak intermolecular interactions", *Chemical Biology*, vol. 2, pp. 709-712.

Ebbing, D. D. 1993, "General Chemistry" Houghton Mifflin Company, Boston.

Endo, H. 1980, "Is a 2-state model approach applicable to liquid water", *Journal of Chemical Physics*, vol. 72, no. 8, pp. 4324-4326.

Frank, H. S. and Wen, W.-Y. 1957, "Structural aspects of ion-solvent interactions in aqueous solutions: a suggested picture of water structure". *Discussions of Faraday Society,* vol. 24, pp. 133-140.

Frank, H. S. and Evans, M. W. 1945, "Free volume and entropy in condensed systems. III. Entropy in binary liquid mixtures; partial molal entropy in dilute solutions; structure and thermodynamics in aqueous electrolytes.", *Journal of Chemical Physics*, vol. 13, pp. 507-532.

Frauenfelder, H., Hartmann, H., Karplus, M., Kuntz, I. D., Kuriyan, J., Parak, F., Petsko, G. A., Ringe, D., Tilton, R. F., Connolly, M. L., and Max, N. 1987, "Thermal-expansion of a protein", *Biochemistry*, vol. 26, no. 1, pp. 254-261.

Gallagher, K. R. and Sharp, K. A. 2003, "A new angle on heat capacity changes in hydrophobic solvation", *Journal of the American Chemical Society*, vol. 125, no. 32, pp. 9853-9860.

Goto, Y., Hagihara, Y., Hamada, D., Hoshino, M., and Nishii, I. 1993, "Acid-induced unfolding and refolding transitions of cytochrome c - a 3-state mechanism in H_2O and D_2O", *Biochemistry*, vol. 32, no. 44, pp. 11878-11885.

Goto, Y., Takahashi, N., and Fink, A. L. 1990, "Mechanism of acid-induced folding of proteins", *Biochemistry*, vol. 29, no. 14, pp. 3480-3488.

Graziano, G. 1999, "Hydration thermodynamics of aliphatic alcohols", *Physical Chemistry Chemical Physics*, vol. 1, pp. 3567-3576.

Graziano, G., Catanzano, F., Riccio, A., and Barone, G. 1997, "A reassessment of the molecular origin of cold denaturation", *Journal of Biochemistry*, vol. 122, no. 2, pp. 395-401.

Hackel, M., Hedwig, G. R., and Hinz, H. J. 1998, "The partial molar heat capacity and volume of the peptide backbone group of proteins in aqueous solution", *Biophysical Chemistry*, vol. 73, no. 1-2, pp. 163-177.

Hackel, M., Hinz, H. J., and Hedwig, G. R. 1998, "Tripeptides in aqueous solution: Model compounds for the evaluation of the partial molar heat capacities of amino acid side-chains in proteins", *Thermochimica Acta*, vol. 308, no. 1-2, pp. 23-34.

Hackel, M., Hinz, H. J., and Hedwig, G. R. 1999, "Partial molar volumes of proteins: amino acid side-chain contributions derived from the partial molar volumes of some tripeptides over the temperature range 10-90 degrees C", *Biophysical Chemistry*, vol. 82, no. 1, pp. 35-50.

Hakin, A. W. and Hedwig, G. R. 2000, "The partial molar heat capacities and volumes of some N-acetyl amino acid amides in aqueous solution over the temperature range 288.15 to 328.15 K", *Physical Chemistry Chemical Physics*, vol. 2, no. 8, pp. 1795-1802.

Harding, M. M., Williams, D. H., and Woolfson, D. N. 1991, "Characterization of a partially denatured state of a protein by 2-dimensional NMR - reduction of the hydrophobic interactions in ubiquitin", *Biochemistry*, vol. 30, no. 12, pp. 3120-3128.

Harpaz, Y., Gerstein, M., and Chothia, C. 1994, "Volume changes on protein-folding", *Structure*, vol. 2, no. 7, pp. 641-649.

Hedwig, G. R. 1992, "Partial molar volumes of the amino-acid side-chains of proteins in aqueous-solution - some comments on their estimation using partial molar volumes of amino-acids and small peptides", *Biopolymers*, vol. 32, no. 5, pp. 537-540.

Heerklotz, H. and Seelig, J. 2002, "Application of Pressure Perturbation Calorimetry to lipid bilayers", *Biophysical Journal*, vol. 82, no. 3, pp. 1445-1452.

Hepler, L. G. 1969, "Thermal expansion and structure in water and aqueous solutions", *Canadian Journal of Chemistry*, vol. 47, pp. 4613-4617.

Hinz, H. J. Pressure modulation calorimetry (PMC). Online . http://www.uni-muenster.de/Chemie.pc/Hinz/Methoden/PMC_eng.html Last Updated: 18-12-2003. Last Accessed: 5-10-2004.

Hinz, H. J., Vogl, T., and Meyer, R. 1994, "An alternative interpretation of the heat-capacity changes associated with protein unfolding", *Biophysical Chemistry*, vol. 52, no. 3, pp. 275-285.

Hoshino, M., Hagihara, Y., Hamada, D., Kataoka, M., and Goto, Y. 1997, "Trifluoroethanol-induced conformational transition of hen egg- white lysozyme studied by small-angle X-ray scattering", *FEBS Letters*, vol. 416, no. 1, pp. 72-76.

Ibarra-Molero, B., Loladze, V. V., Makhatadze, G. I., and Sanchez-Ruiz, J. M. 1999, "Thermal versus guanidine-induced unfolding of ubiquitin. An analysis in terms of the contributions from charge-charge interactions to protein stability", *Biochemistry*, vol. 38, pp. 8138-8149.

Jourdan, M. and Searle, M. S. 2001, "Insights into the stability of native and partially folded states of ubiquitin: Effects of cosolvents and denaturants on the thermodynamics of protein folding", *Biochemistry*, vol. 40, no. 34, pp. 10317-10325.

Kamatari, Y. O., Konno, T., Kataoka, M., and Akasaka, K. 1998, "The methanol-induced transition and the expanded helical conformation in hen lysozyme", *Protein Science*, vol. 7, pp. 681-688.

Kamatari, Y. O., Konno, T., Kataoka, M., and Akasaka, K. 1996, "The methanol-induced globular and expanded denatured states of cytochrome c: A study by CD fluorescence, NMR and small-angle X-ray scattering", *Journal of Molecular Biology*, vol. 259, no. 3, pp. 512-523.

Kamatari, Y. O., Ohji, S., Konno, T., Seki, Y., Soda, K., Kataoka, M., and Akasaka, K. 1999, "The compact and expanded denatured conformations of apomyoglobin in the methanol-water solvent", *Protein Science*, vol. 8, no. 4, pp. 873-882.

Kauzmann, W. 1959, "Some factors in the interpretation of protein denaturation", *Advances in Protein Chemistry*, vol. 14, pp. 1-63.

Kell, G. S. 1967, "Precise representation of volume properties of water at one atmosphere", *Journal of Chemical and Engineering Data*, vol. 12, no. 1, pp. 66-69.

Kelly, S. M. and Price, N. C. 1997, "The application of circular dichroism to studies of protein folding and unfolding", *Biochimica et Biophysica Acta*, vol. 1338, pp. 161-185.

Kharakoz, D. P. and Bychkova, V. E. 1997, "Molten globule of human alpha-lactalbumin: Hydration, density, and compressibility of the interior", *Biochemistry*, vol. 36, no. 7, pp. 1882-1890.

Kharakoz, D. P. and Sarvazyan, A. P. 1993, "Hydrational and intrinsic compressibilities of globular- proteins", *Biopolymers*, vol. 33, no. 1, pp. 11-26.

Kiefhaber, T. 1995, "Proten folding kinetics," in *Protein stability and folding*, B. A. Shirley, ed., Humana Press, Totova, New Jersey.

Kikuchi, M., Sakurai, M., and Nitta, K. 1995, "Partial molar volumes and adiabatic compressibilities of amino- acids in dilute aqueous-solutions at 5, 15, 25, 35, and 45- Degrees-C", *Journal of Chemical and Engineering Data*, vol. 40, no. 4, pp. 935-942.

Konishi, Y. and Scheraga, H. A. 1980, "Regeneration of ribonuclease A from the reduced protein. 1. Conformational analysis of the intermediates by measurements of enzymatic activity, optical density, and optical rotation", *Biochemistry*, vol. 19, no. 7, pp. 1308-1316.

Kovrigin, E. L. and Potekhin, S. A. 2000, "On the stabilizing action of protein denaturants: acetonitrile effect on stability of lysozyme in aqueous solutions", *Biophysical Chemistry*, vol. 83, pp. 45-59.

Kujawa, P. and Winnik, F. M. 2001, "Volumetric studies of aqueous polymer solutions using pressure perturbation calorimetry: A new look at the temperature-induced phase transition of poly(N-isopropylacrylamide) in water and D_2O", *Macromolecules*, vol. 34, pp. 4130-4135.

Kumar, S. and Nussinov, R. 1999, "Salt bridge stability in monomeric proteins", *Journal of Molecular Biology*, vol. 293, no. 5, pp. 1241-1255.

Kyte, J. and Doolittle, R. F. 1982, "A simple method for displaying the hydropathic character of a protein", *Journal of Molecular Biology*, vol. 157, no. 1, pp. 105-132.

Laaksonen, A., Kusalik, P. G., and Svishchev, I. M. 1997, "Three-dimensional structure in water-methanol mixtures", *Journal of Physical Chemistry A*, vol. 101, no. 33, pp. 5910-5918.

Li, H., Yamada, H., and Akasaka, K. 1998, "Effect of pressure on individual hydrogen bonds in proteins. Basic pancreatic tripsin inhibitor", *Biochemistry*, vol. 37, no. 5, pp. 1167-1173.

Lin, L. N., Brandts, J. F., Brandts, J. M., and Plotnikov, V. 2002, "Determination of the volumetric properties of proteins and other solutes using pressure perturbation calorimetry", *Analytical Biochemistry*, vol. 302, no. 1, pp. 144-160.

Loladze, V. V., Ermolenko, D. N., and Makhatadze, G. I. 2001, "Heat capacity changes upon burial of polar and nonpolar groups in proteins", *Protein Science*, vol. 10, pp. 1343-1352.

Loladze, V. V., Ibarra-Molero, B., Sanchez-Ruiz, J. M., and Makhatadze, G. I. 1999, "Engineering a thermostable protein via optimalization of charge-charge interactions on the protein surface", *Biochemistry*, vol. 38, pp. 16419-16423.

Makhatadze, G. I., Medvedkin, V. N., and Privalov, P. L. 1990, "Partial molar volumes of polypeptides and their constituent groups in aqueous-solution over a broad temperature-range", *Biopolymers*, vol. 30, no. 11-12, pp. 1001-1010.

Makhatadze, G. I. and Privalov, P. L. 1990, "Heat-capacity of proteins .1. Partial molar heat-capacity of individual amino-acid-residues in aqueous-solution - hydration effect", *Journal of Molecular Biology*, vol. 213, no. 2, pp. 375-384.

Merzel, F. and SMITH, J. C. 2002, "Is the first hydration shell of lysozyme of higher density than bulk water?", *Proceedings of the National Academy of Sciences of the United States of America*, vol. 99, no. 8, pp. 5378-5383.

MicroCal LCC 2000a, *Pressure Perturbation Calorimetry (PPC) application note.*

MicroCal LCC 2000b, *VP-DSC Microcalorimeter User's Manual.*

MicroCal LCC 2000c, *United States Patent* 6,513,969 B2 (patent).

MicroCal LCC 2001, *PPC Data Analysis in Origin(TM): Tutorial Guide.*

Moelbert, S. and De Los Rios, P. 2003, "Chaotropic effect and preferential binding in a hydrophobic interaction model", *Journal of Chemical Physics*, vol. 119, no. 15, pp. 7988-8001.

Murphy, K. P. and Freire, E. 1992, "Thermodynamics of structural stability and cooperative folding behavior in proteins", *Advances in Protein Chemistry*, pp. 313-361.

Murphy, L. R., Matubayasi, N., Payne, V. A., and Levy, R. M. 1998, "Protein hydration and unfolding - insights from experimental partial specific volumes and unfolded protein models", *Folding and Design*, vol. 3, no. 2, pp. 105-118.

Myers, J. K. and Pace, C. N. 1996, "Hydrogen bonding stabilizes globular proteins", *Biophysical Journal*, vol. 71, no. 4, pp. 2033-2039.

Nemethy, G. and Scheraga H.A. 1962, "Structure of water and hydrophobic bonding in proteins. A model for the thermodynamic properties of liquid water.", *Journal of Chemical Physics*, vol. 36, p. 3382.

Nöllmann, M. 2001. Personal Communication

Pace, C. N. 2001, "Polar group burial contributes more to protein stability than nonpolar group burial", *Biochemistry*, vol. 40, pp. 310-313.

Pace, C. N., Shirley, B. A., McNutt, M., and Gajiwala, K. 1996, "Forces contributing to the conformational stability of proteins", *FASEB Journal*, vol. 10, pp. 75-83.

Plotnikov, V., Brandts, J. M., Brandts, J. F., Lin, L.-N., and Frasca, V. 2000, "Pressure Perturbation Calorimetry: A novel technique to measure volumetric and solvation properties of proteins and biopolymers in solution" In: Biocalorimetry 2001 Conference: Current Trends in Microcalorimetry, Philadelphia, PA, July 26-28, 2001

Potekhin, S. and Pfeil, W. 1989, "Microcalorimetric studies of conformational transitions of ferricytochrome c in acidic solution", *Biophysical Chemistry*, vol. 34, no. 1, pp. 55-62.

Prehoda, K. E., Mooberry, E. S., and Markley, J. L. 1998, "Pressure denaturation of proteins: evaluation of compressibility effects", *Biochemistry*, vol. 37, pp. 5785-5790.

Privalov, P. L. 1990, "Cold denaturation of proteins", *Biochemistry and Molecular Biology*, vol. 25, no. 4, pp. 281-305.

Privalov, P. L. and Gill, S. J. 1988, "Stability of protein structure and hydrophobic interaction", *Advances in Protein Chemistry*, vol.39, pp. 191-234.

Randzio, S. L. 2000, "Transitiometry - Towards a global virtual instrument control and a virtual link between experiment and modelling", *Thermochimica Acta*, vol. 355, no. 1-2, pp. 107-113.

Randzio, S. L. 2003, "Comments on "volumetric studies of aqueous polymer solutions using pressure perturbation calorimetry..." [Macromolecules 34 (2001) 4130]", *Thermochimica Acta*, vol. 398, no. 1-2, pp. 75-80.

Reading, J. F. and Hedwig, G. R. 1990, "Thermodynamic properties of peptide solutions .6. the amino- acid side-chain contributions to the partial molar volumes and heat-capacities of some tripeptides in aqueous-solution", *Journal of the Chemical Society-Faraday Transactions*, vol. 86, no. 18, pp. 3117-3123.

Reis, J. C. R., Blandamer, M. J., Davis, M. I., and Douheret, G. 2001, "The concepts of non-Gibbsian and non-Lewisian properties in chemical thermodynamics", *Physical Chemistry Chemical Physics*, vol. 3, no. 8, pp. 1465-1470.

Robertson, A. D. and Murphy, K. P. 1997, "Protein structure and the energetics of protein stability", *Chemical Reviews*, vol. 97, pp. 1251-1267.

Robinson, G. W. and Cho, C. H. 1999, "Role of hydration water in protein unfolding", *Biophysical Journal*, vol. 77, pp. 3311-3318.

Robinson, G. W., Urquidi, J., Singh, S., and Cho, C. H. 2001, "Protein denaturation described by a two-state structural model of liquid water", *Cellular and Molecular Biology*, vol. 47, no. 5, pp. 757-765.

Rontgen, W. K. 1892, *Phys. Chim. (Wied)*, vol. 45, p. 91.

Rosgen, J., Beerman, B., and Hinz, H. J. 2002, "The importance of being 'global' or "how to get full information on protein stability"", In: Applications of Biocalorimetry (ABC III), August 27-30, 2002, Dublin, Ireland.

Sanchez-Ruiz, J. M. and Makhatadze, G. I. 2001, "To charge or not to charge?", *Trends in Biotechnology*, vol. 19, no. 4, pp. 132-135.

Sasahara, K. and Nitta, K. 1999, "Pressure-induced unfolding of lysozyme in aqueous guanidinium chloride solution", *Protein Science*, vol. 8, pp. 1469-1474.

Sasahara, K., Sakurai, M., and Nitta, K. 2001, "Pressure effect on denaturant-induced unfolding of hen egg white lysozyme", *Proteins-Structure Function and Genetics*, vol. 44, no. 3, pp. 180-187.

Sato, T., Chiba, A., and Nozaki, R. 2000, "Hydrophobic hydration and molecular association in methanol- water mixtures studied by microwave dielectric analysis", *Journal of Chemical Physics*, vol. 112, no. 6, pp. 2924-2932.

Schwitzer, M. A. and Hedwig, G. R. 1998, "Thermodynamic properties of peptide solutions. 16. Partial molar heat capacities and volumes of some tripeptides of sequence gly-X-gly in aqueous solution at 25 degrees C", *Journal of Chemical and Engineering Data*, vol. 43, no. 3, pp. 477-481.

Seemann, H., Winter, R., and Royer, C. A. 2001, "Volume, expansivity and isothermal compressibility changes associated with temperature and pressure unfolding of Staphylococcal Nuclease", *Journal of Molecular Biology*, vol. 307, pp. 1091-1102.

Sharp, K. A. and Madan, B. 1997, "Hydrophobic effect, water structure, and heat capacity changes", *Journal of Physical Chemistry B*, vol. 101, pp. 4343-4348.

Shortle, D. 1999, "Protein folding as seen from water's perspective", *Nature Structural Biology*, vol. 6, no. 3, pp. 203-205.

Sorenson, J. M., Hura, G., Soper, A. K., Pertsemlidis, A., and Head-Gordon, T. 1999, "Determining the role of hydration forces in protein folding", *Journal of Physical Chemistry B*, vol. 103, no. 26, pp. 5413-5426.

Spolar, R. S., Livingstone, J. R., and Record, M. T. 1992, "Use of liquid hydrocarbon and amide transfer data to estimate contributions to thermodynamic functions of protein folding from the removal of nonpolar and polar surface from water", *Biochemistry*, vol. 31, pp. 3947-3955.

Squire, P. G. and Himmel, M. E. 1979, "Hydrodynamics and protein hydration", *Archives of Biochemistry and Biophysics*, vol. 196, no. 1, pp. 165-177.

Stockman, B. J., Euvrard, A., and Scahill, T. A. 1993, "Heteronuclear 3-Dimensional NMR-Spectroscopy of a partially denatured protein - the A-State of human ubiquitin", *Journal of Biomolecular NMR*, vol. 3, no. 3, pp. 285-296.

Svergun, D. I., Richard, S., Koch, M. H., Sayers, Z., Kuprin, S., and Zaccai, G. 1998, "Protein hydration in solution: Experimental observation by x-ray and neutron scattering", *Proceedings of the National Academy of Sciences of the United States of America*, vol. 95, no. 5, pp. 2267-2272.

Takano, K., Tsuchimori, K., Yamagata, Y., and Yutani, K. 2000, "Contribution of salt bridges near the surface of a protein to the conformational stability", *Biochemistry*, vol. 39, no. 40, pp. 12375-12381.

Takano, K., Yamagata, Y., Funahashi, J., Hioki, Y., Kuramitsu, S., and Yutani, K. 1999, "Contribution of intra- and intermolecular hydrogen bonds to the conformational stability of human lysozyme", *Biochemistry*, vol. 38, pp. 12698-12708.

Tanaka, H. 2000, "Simple physical model of liquid water", *Journal of Chemical Physics*, vol. 112, no. 2, pp. 799-809.

Torres, A. M., Grieve, S. M., and Kuchel, P. W. 1998, "NMR triple-quantum filtered relaxation analysis of ^{17}O-water in insulin solutions: an insight into the aggregation of insulin and the properties of its bound water", *Biophysical Chemistry*, vol. 70, no. 3, pp. 231-239.

Tsai, C. J., Maizel, J. V., and Nussinov, R. 2002, "The hydrophobic effect: A new insight from cold denaturation and a two-state water structure", *Critical Reviews in Biochemistry and Molecular Biology*, vol. 37, no. 2, pp. 55-69.

Urquidi, J., Cho, C. H., Singh, S., and Robinson, G. W. 1999, "Temperature and pressure effects on the structure of liquid water", *Journal of Molecular Structure*, vol. 485-486, pp. 363-371.

Uversky, V. N., Narizhneva, N. V., Kirschstein, S. O., Winter, S., and Lober, G. 1997, "Conformational transitions provoked by organic solvents in beta-lactoglobulin: Can a molten globule like intermediate be induced by the decrease in dielectric constant?", *Folding and Design*, vol. 2, no. 3, pp. 163-172.

Vedamuthu, M., Singh, S., and Robinson, G. W. 1994, "Properties of liquid water - origin of the density anomalies", *Journal of Physical Chemistry*, vol. 98, no. 9, pp. 2222-2230.

Velicelebi G. and Sturtevant J.M. 1979, "Thermodynamics of the denaturation of lysozyme in alcohol-water mixtures.", *Biochemistry*, vol. 18, no. 7, pp. 1180-1186.

Vijay-Kumar, S., Bugg, C. E., and Cook, W. J. 1987, "Structure of ubiquitin refined at 1.8 A resolution*1", *Journal of Molecular Biology*, vol. 194, no. 3, pp. 531-544.

Voet, D. and Voet, J. G. 1995, "Biochemistry" John Wiley and Sons,Inc., New York.

Voet, D., Voet, J. G., and Pratt, C. W. 1998, "Fundamentals of biochemistry" John Wiley and Sons,Inc., New York.

Wang, S. L. and Epand, R. M. 2004, "Factors determining pressure perturbation calorimetry measurements: evidence for the formation of metastable states at lipid phase transitions", *Chemistry and Physics of Lipids*, vol. 129, no. 1, pp. 21-30.

Weber, P. L., Brown, S., Mueller, L., Marsh, J. A., Butt, T. R., and Ecker, D. J. 1987, "NMR-studies of ubiquitin and engineered ubiquitin mutants", *Journal of Cellular Biochemistry* p. 220.

Wintrode, P. L., Makhatadze, G. I., and Privalov, P. L. 1994, "Thermodynamics of ubiquitin unfolding", *Proteins: Structure, Function and Genetics*, vol. 18, pp. 246-253.

Woolfson, D. N., Cooper, A., Harding, M. M., Williams, D. H., and Evans, P. A. 1993, "Protein folding in the absence of the solvent ordering contribution to the hydrophobic interaction", *Journal of Molecular Biology*, vol. 229, pp. 502-511.